Contract NAS8-28144
DPD No. 282
DR No. MA-04

Final Report

Volume III

September 1972

Book 2
Appendix

Astronomy Sortie Missions Definition Study

(NASA-CR-124044) ASTRONOMY SORTIE MISSIONS DEFINITION STUDY. VOLUME 3, BOOK 2: APPENDIX: DESIGN ANALYSIS AND TRADE STUDIES Final Report (Martin Co.) 383 p HC $21.25 CSCL 22A G3/30

N73-29871
Unclas
63477

MARTIN MARIETTA

Itek

Bendix

AM 1002-1004

Contract NAS8-28144
DPD No. 282
DR No. MA-04

Astronomy Sortie Missions Definition Study
Final Report

VOLUME III
BOOK 2

ASTRONOMY SORTIE PROGRAM
TECHNICAL REPORT
APPENDIX

DESIGN ANALYSIS AND TRADE STUDIES

SEPTEMBER 1972

Prepared for:

National Aeronautics and Space Administration
George C. Marshall Space Flight Center
Huntsville, Alabama

Martin Marietta Aerospace
Denver Division
Denver, Colorado 80201

Bendix Corporation
Navigation and Control Division
Denver, Colorado 80201

Itek Corporation
Optical Systems Division
Lexington, Massachusetts 02173

PREFACE

This document is submitted in accordance with the Data Procurement Document Number 282, Data Requirement Number MA-04 under the George C. Marshall Space Flight Center Contract NAS8-28144. This is Book 2, an Appendix to Volume III of the Astronomy Sortie Missions (ASM) Definition Study Final Report. It contains the detailed tables, charts and studies which support the mission and system analyses, subsystem analyses and the preliminary design tasks of Volume III, Book 1.

Comments or requests for additional information should be directed to:

Dale J. Wasserman/PD-MP-A
Astronomy Sortie Missions Definition Study
Contracting Officer's Representative
George C. Marshall Space Flight Center
Marshall Space Flight Center, Alabama 35812

William P. Pratt/8102
Astronomy Sortie Missions Definition Study
Martin Marietta Denver Division Study Manager
Denver, Colorado 80201

FOREWORD

The primary purpose of the Astronomy Sortie Mission Definition Study was to provide NASA with an overview of the Astronomy Sortie Mission requirements. The specific objectives of the study were to:

1. Evaluate the responsiveness of the sortie mission concept to stated scientific objectives.

2. Develop conceptual designs and interfaces for sortie missions including telescopes, mounts, controls, displays and support equipment.

3. Develop a system concept encompassing the Sortie Mission from mission planning through post-flight engineering and scientific documentation.

4. Provide development schedules and supporting research and technology requirements for Shuttle Sortie hardware.

The approach that was utilized in performing the study consisted of the following sequence:

1. Analyzing and conceptual designing the alternative candidate astronomy sortie mission program that maximized the utilization of common features.

2. Analyzing the astronomy sortie mission program to ensure compatibility between interfacing systems, evaluating overall performance and ensuring mission responsiveness, and developing a complete mission profile.

3. Analyzing the support subsystems to a depth which was sufficient to establish feasibility, compatibility with other subsystems, adequate performance, physical characteristics, interface definition, reliability level, and compatibility with manned operations.

4. Conceptually designing the selected astronomy sortie mission program which included defining the significant design features, dimensions and interfaces on layout drawings, and defining the telescope system physical characteristics and support requirements.

5. Providing development schedules and supporting research and technology requirements.

The final report of the study is contained in four volumes, of which this volume is Book 2 of Volume III. The four volumes of the report are:

Volume I - Astronomy Sortie Missions Definition Study Final Report: Executive Summary

This volume summarizes the significant achievements and activities of the study effort.

Volume II - Astronomy Sortie Missions Definition Study Final Report:
- Book 1 - Astronomy Sortie Program Technical Report

Book 1 of this volume includes the definition of telescope requirements, preliminary mission and systems definition, identification of alternative sortie programs, definition of alternative sortie programs, the evaluation of the alternative sortie programs and the selection of the recommended astronomy sortie mission program. This volume identifies the various concepts approached and documents the rationale for the concept and approaches selected for further consideration.

Volume II - Astronomy Sortie Missions Definition Study Final Report:
- Book 2 - Appendix

Book 2 of this volume contains the Baseline Experiment Definition Documents (BEDD's) that were prepared for each of the experiments considered during the study.

Volume III - Astronomy Sortie Missions Definition Study Final Report:
- Book 1 - Design Analyses and Trade Studies

Book 1 of this volume includes the results of the design analyses and trade studies conducted on candidate concepts during the

selection of recommended configurations as well as the design analyses and trade studies conducted on the selected concept.

Volume III - Astronomy Sortie Missions Definition Study Final Report

- Book 2 - Appendix

Book 2 of this volume contains the backup or supporting data for the design analyses and trade studies that are summarized in Volume III, Book 1

Volume IV - Astronomy Sortie Missions Definition Study Final Report: Program Development Requirements

This volume contains the planning data for subsequent phases and includes the gross project planning requirements; schedules; milestones and networks; and supporting research and technology.

CONTENTS

Appendix A1

STUDY OF CANDIDATE SHUTTLE ORBITER STABILIZATION SYSTEM

The shuttle orbiter model used in this study is the Grumman version shown in figure A1-1. The inertias and mass properties associated with this configuration are:

a. Inertias:

$$I_{xx}=1.41x10^6 kg\text{-}m^2 (1.04x10^6 \text{ slug-ft}^2)$$

$$I_{yy}=8.22x10^6 kg\text{-}m^2 (6.05x10^6 \text{ slug-ft}^2)$$

$$I_{zz}=8.55x10^6 kg\text{-}m^2 (6.30x10^6 \text{ slug-ft}^2)$$

$$I_{xy}=I_{xz}=I_{yz}=0$$

b. Orbiter mass:

$$M=91x10^3 kg \ (6.2x10^3 \text{ slugs})$$

The shuttle orbiter is assumed to be stabilized in a 500 km (270 NM) circular orbit.

This appendix comprises five major completely independent sections and a list of references.

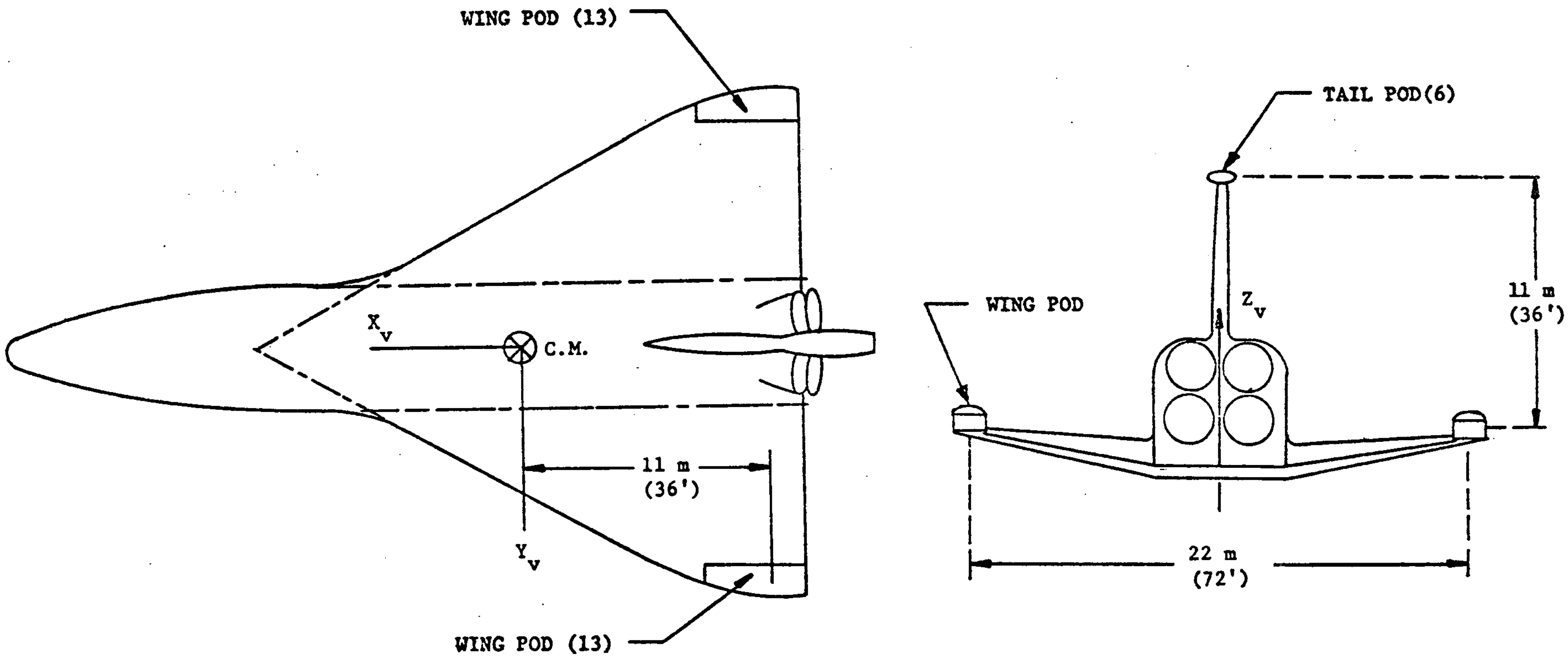

Figure A1-1. Grumman Shuttle Orbiter Configuration

A1.1. DETERMINATION OF SHUTTLE ORBITER BASELINE ATTITUDE CONTROL PROPULSION SYSTEM (ACPS) ON-ORBIT FUEL CONSUMPTION

The shuttle orbiter baseline ACPS consists of 32 engines (13 mounted in each of the two wing pods and six in the one tail pod). Figure A1-1 is a sketch of the orbiter showing the location of these three pods. Table A1-1 lists the functions of the various thrusters located in each pod. The wing pods control yaw and roll, while the wing pods in conjunction with the tail pod control pitch. To produce a pure uncoupled yaw or roll torque only two thrusters, one from each wing pod, are required.

The following shuttle orbiter baseline ACPS control parameters used in this study are:

a. Vehicle control moment arms (distance between appropriate engines):

1) pitch (Y_v axis): ℓ_y=11m (36 ft)

2) yaw (Z_v axis): ℓ_z=22m (72 ft)

3) roll (X_v axis): ℓ_x=22m (72 ft)

b. Attitude deadband: $\pm\theta_o$, θ_o=8.75 mrad(0.5 degree)

c. Propellant: monopropellant N_2H_4

d. I_{sp}=230 sec

e. Engine thrust level: F=1.8 kN (400 lbf)

f. Minimum firing time, t_f=100 msec

To compute the fuel consumed by the ACPS, the number of thruster actuations per orbit must be determined. The shuttle orbiter torque environment is assumed to comprise only gravity gradient torques. The ACPS stabilizes the shuttle orbiter by counteracting these disturbance torques. The resultant counteracting control torques are generated by the ACPS by expelling gas at a rate proportional to the rectified gravity gradient torques acting on the orbiter. The maximum average rectified gravity gradient torques that can exist about the orbiter X_v, Y_v, and Z_v axes are:

Table A1-1. On-Orbit ACPS Thruster Functions

Location	Firing Direction (number of engines)	Function
Wing Pod	Side (3)	$\pm$Y Translation
	Forward (3)	-X Translation, Pitch and Yaw Attitude Control
	Aft (3)	+X Translation, Pitch and Yaw Attitude Control
	Down (2)	+Z Translation, Roll Attitude Control
	Up (2)	-Z Translation, Roll Attitude Control
Tail Pod	Forward (3)	Pitch Attitude Control
	Aft (3)	Pitch Attitude Control

$$T_{gx}\big|_{ra}=\frac{3}{\pi}\omega_o^{\,2}(I_{zz}-I_{yy}) \tag{1}$$

$$T_{gy}\big|_{ra}=\frac{3}{\pi}\omega_o^{\,2}(I_{zz}-I_{xx}) \tag{2}$$

$$T_{gz}\big|_{ra}=\frac{3}{\pi}\omega_o^{\,2}(I_{yy}-I_{xx}) \tag{3}$$

where

$$\omega_o^{\,2}=\frac{gR}{r^3} \tag{4}$$

ω_o is the shuttle orbital rate, g is the gravitational acceleration of the earth, R is the mean radius of the earth, R=6.44 Mm (R=4 000 statute miles), and r is the distance between the center of the earth and orbiter center of mass.

For a 500 km (270 NM) circular orbit,

$$\omega_o^{\,2}=\frac{(32.2)(4000)^2(5280)^2}{[4000+270(1.15)]^3(5280)^3}=1.22\text{x}10^{-6}\ \frac{1}{\text{sec}^2}$$

$$\omega_o=1.10\text{x}10^{-3}\frac{1}{\text{sec}} \tag{5}$$

$T_{gx}\big|_{ra}$, $T_{gy}\big|_{ra}$, and $T_{gz}\big|_{ra}$ equals

$$T_{gx}\big|_{ra}=0.384\text{ N-m (0.291 ft-lb)} \tag{6}$$

$$T_{gy}\big|_{ra}=8.31\text{ N-m (6.12 ft-lb)} \tag{7}$$

$$T_{gz}\big|_{ra}=7.94\text{ N-m (5.84 ft-lb)} \tag{8}$$

The minimum angular momentum impulse bit (MIB) that can be imparted to the orbiter due to firing the ACPS is the same for each control axis. MIB equals

$$MIB=F\ell_x t_f=F\ell_z t_f=(2F)\ell_y t_f$$

$$=3\ 960 \text{ N-m-sec } (2\ 880 \text{ ft-lb-sec}) \qquad (9)$$

Although the moment arm for pitch ℓ_y is half of those for yaw ℓ_z and roll ℓ_x, the number of engine firings for pitch is double those required for either yaw or roll, thus making an MIB for pitch equal to those for yaw and roll.

The vehicle body rates about the X_v, Y_v, and Z_v due to one MIB equals

$$\omega_i=\frac{MIB}{I_{ii}} \quad (i=x,\ y,\ z) \qquad (10)$$

where

ω_i is the angular rate about the i^{th} axis, radians per second, (deg/sec)

I_{ii} is the orbiter inertia about the i^{th} axis, kg-m^2, (slug-ft^2)

ω_x, ω_y, ω_z equal

$$\omega_x=2.81 \text{ mrad/sec } (0.161 \text{ deg/sec}) \qquad (11)$$

$$\omega_y=0.482 \text{ mrad/sec } (27.6\text{x}10^{-3} \text{ deg/sec}) \qquad (12)$$

$$\omega_z=0.463 \text{ mrad/sec } (26.6\text{x}10^{-3} \text{ deg/sec}) \qquad (13)$$

Assume that the vehicle is in a torque-free environment. In this environment, the orbiter will limit cycle between the limits of the attitude deadband $\pm\theta_o$. Figure A1-2 is a sketch of the ACPS deadband. The lower limit $-\theta_o$, is designated state a, and the upper limit, $+\theta_o$, is designated state b. Assume the i^{th} vehicle axis is at state a. At this point, the ACPS thrusters will fire one MIB sending the i^{th} axis towards state b. As the i^{th} axis traverses the deadband from a to b, the axis angular velocity ω_{ab} equals

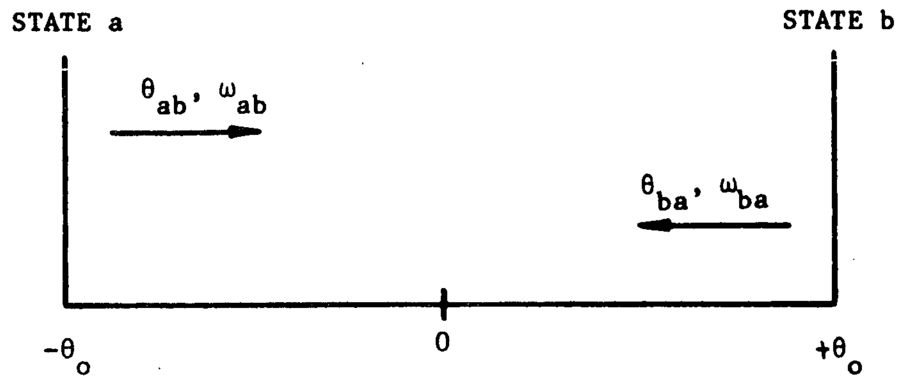

Figure A1-2. Sketch of ACPS Attitude Deadband

$$\omega_{ab}=\omega_i+\omega_{ab}(0) \tag{14}$$

The position of the axis θ_{ab} equals

$$\theta_{ab}=[\omega_i+\omega_{ab}(0)]t-\theta_o \tag{15}$$

When the axis reaches state b, the thrusters fire once more sending the vehicle back towards a. The angular velocity ω_{ba} and position θ_{ba} as the axis travels back towards a equal

$$\omega_{ba}=-\omega_i+\omega_{ba}(0) \tag{16}$$

$$\theta_{ba}=[-\omega_i+\omega_{ba}(0)]t+\theta_o \tag{17}$$

From equation 15, the time t_{ab} for the axis to traverse the dead-band from state a to state b equals

$$\theta_{ab}=\theta_o=[\omega_i+\omega_{ab}(0)]t_{ab}-\theta_o$$

$$t_{ab}=\frac{2\theta_o}{\omega_i+\omega_{ab}(0)} \tag{18}$$

From equation 17, the time t_{ba} to return to state a equals

$$\theta_{ba}=-\theta_o=[-\omega_i+\omega_{ba}(0)]t_{ba}+\theta_o$$

$$t_{ba}=\frac{2\theta_o}{\omega_i-\omega_{ba}(0)} \tag{19}$$

Under steady state conditions

$$t_{ab}=t_{ba} \tag{20}$$

Therefore, using equations 18, 19, and 20,

$$\omega_{ab}(0)=-\omega_{ba}(0) \tag{21}$$

Since the angular velocity of the i^{th} axis cannot change instantaneously at either boundary of the deadband, the following expressions can be written using equations 14 and 16.

$$\omega_{ba}(0)=\omega_i+\omega_{ab}(0) \tag{22}$$

$$\omega_{ab}(0)=-\omega_i+\omega_{ba}(0) \tag{23}$$

Using equations 21, 22, and 23, the following expressions for $\omega_{ab}(0)$ and $\omega_{ba}(0)$ can be written

$$\omega_{ab}(0)=-\frac{\omega_i}{2} \tag{24}$$

$$\omega_{ba}(0)=\frac{\omega_i}{2} \tag{25}$$

Substituting the above expressions into either equation 18 or 19 results in the time, t_{Ti}, required to traverse the attitude deadband, $2\theta_o$

$$t_{Ti}=t_{ab}=t_{ba}=\frac{4\theta_o}{\omega_i} \qquad (i=x,y,z) \tag{26}$$

For the orbiter ACPS, θ_o equals 8.75 mrad (0.5 degree). Substituting the values of ω_i given in equations 11 through 13 into 26 yields the times that it takes to traverse the X_v, Y_v, and Z_v axis deadbands, respectively.

$$t_{TX}=12.4 \text{ seconds} \tag{27}$$

$$t_{TY}=72.7 \text{ seconds} \tag{28}$$

$$t_{TZ}=75.6 \text{ seconds} \tag{29}$$

The assumption that the orbiter is in a torque-free environment is valid if the actual gravity gradient torques acting on the orbiter are unable to prevent the ACPS from limit cycling with every ACPS actuation. The gravity gradient decelerating angular momentum impulse, H_{gi}, for the above deadband transit times, t_{Ti}, equal

$$H_{gi}=(T_{gi}|_{ra})t_{Ti} \qquad (i=x,y,z) \qquad (30)$$

Using equations 6, 7, 8, 27, 28, and 29, H_{gi} for the X_v, Y_v, and Z_v axes equal

$$H_{gx}=4.76 \text{ N-m-sec } (3.61 \text{ ft-lb-sec}) \qquad (31)$$

$$H_{gy}=604 \text{ N-m-sec } (445 \text{ ft-lb-sec}) \qquad (32)$$

$$H_{gz}=600 \text{ N-m-sec } (441 \text{ ft-lb-sec}) \qquad (33)$$

Note that the maximum value of H_{gi} is less than one-sixth the value of one MIB indicating that the gravity gradient torque environment cannot prevent the ACPS from limit cycling. The assumption that the shuttle orbiter is in a torque-free environment is valid. The consequences of this valid assumption is that the fuel consumption rate is independent of the stabilized orbiter attitude and only depends on the average time, t_{Ti}, it takes to traverse the ACPS deadbands.

The number of engine firings per orbit equals

$$\text{NEF/orbit}=2T_o\left(\frac{1}{t_{Tx}} + \frac{2}{t_{Ty}} + \frac{1}{t_{Tz}}\right) \qquad (34)$$

where T_o is the period in seconds of one orbit.

$$T_o = \frac{2\pi}{\omega_o}$$

$$= \frac{2\pi}{1.10\text{x}10^{-3}} = 5\ 700 \text{ seconds}$$

Substituting equations 10 and 26 into equation 34,

$$\text{NEF/orbit} = \frac{(\text{MIB})T_o}{2\theta_o}\left(\frac{1}{I_{xx}} + \frac{2}{I_{yy}} + \frac{1}{I_{zz}}\right) \tag{36}$$

The weight of fuel per orbit (kgf/orbit) equals

$$\text{WOF/orbit} = 0.102\ (\text{NEF/orbit})\frac{Ft_f}{I_{sp}} \tag{37}$$

Substituting equation 36 into 37,

$$\text{WOF/orbit} = \frac{0.102(\text{MIB})T_o Ft_f}{2\theta_o I_{sp}}\left(\frac{1}{I_{xx}} + \frac{2}{I_{yy}} + \frac{I}{I_{zz}}\right) \tag{38}$$

For the baseline orbiter ACPS,

$$\text{WOF/orbit}=110 \text{ kgf/orbit (242 lb/orbit)} \tag{39}$$

The weight of fuel per day equals

$$\text{WOF/day} = \frac{(24)(3\ 600)}{T_o}\ \text{WOF/orbit} = 1\ 670 \text{ kgf/day}$$

$$\text{(3 660 lb/day)} \tag{40}$$

This ACPS fuel consumption is too large. As an alternative, assume that only one thruster instead of multiple thruster pairs are fired when an attitude deadband limit $\pm\theta_o$ is reached. This modified ACPS system reduces the fuel consumption by decreasing the magnitude of one MIB by a factor of two, thus increasing the time it takes to traverse the attitude deadband. But since only one thruster is fired instead of oppositely directed thruster pairs a translational force F is produced. The change in the orbiter's velocity ΔV due to this translational force equals

$$\Delta V = \frac{F}{m}t_f = \frac{1.8\text{x}10^3}{91\text{x}10^3}(0.1) = 1.98\text{x}10^{-3}\text{m/sec } (6.5\text{x}10^{-3}\text{ft/sec}) \tag{41}$$

Since this modified ACPS will still limit cycle back and forth through the attitude deadbands thus, producing a force F with alternately opposite directions, the net result of these small ΔV's on the orbiter's orbit should be negligible.

Assume that the forward and aft firing tail pod thrusters are used to control pitch, the forward and aft firing wing pod thrusters are used to control yaw, and the up and down ($\pm Z$ axis) firing wing pod thrusters are used to control the roll axis. Note that from figure A1-1, the wing pods are located 11 meters (36 feet) aft of the orbiter center of mass ($\ell_{C.M.}=11_m$). Also note that it is impossible to produce a roll control torque without producing a large pitch component due to the location of the roll thrusters with respect to the orbiter's center of mass. The resulting MIB's about the three control axes due to firing these three types of thrusters are:

a. Pitch control thrusters (forward and aft firing tail pod engines):

1) $(MIB)_X=(MIB)_Z=0$

2) $(MIB)_Y=F\ell_y t_f=1\ 980$ N-m-sec (1 440 ft-lb-sec)

b. Yaw control thrusters (forward and aft firing wing pod engines):

1) $(MIB)_X=(MIB)_Y=0$

2) $(MIB)_Z=0.5\ F\ell_z t_f=1\ 980$ N-m-sec (1 440 ft-lb-sec)

c. Roll control thrusters (up and down firing wing pod thrusters):

1) $(MIB)_Z=0$

2) $(MIB)_Y=F\ell_{C.M.} t_f= 1\ 980$ N-m-sec (1 400 ft-lb-sec)

3) $(MIB)_X=0.5\ F\ell_x t_f=1\ 980$ N-m-sec (1 440 ft-lb-sec)

Depending on how this system's firing logic is instrumented and the initial conditions of the pitch axis when the first roll axis thruster firing occurs, the additional pitch MIB caused by the roll axis thrusters can either cause fewer or additional pitch axis thruster firings, thus increasing or decreasing fuel consumption. To estimate the fuel consumption for this modified ACPS system, assume that the pitch coupling moment due to a roll thruster firing is zero. The resultant weight of fuel consumed per orbit equals

$$WOF/orbit = \frac{0.102(MIB)T_o Ft_f}{4\theta_o I_{sp}} \left(\frac{1}{I_{xx}} + \frac{1}{I_{yy}} + \frac{1}{I_{zz}}\right) \qquad (42)$$

For this modified orbiter ACPS system,

$$WOF/orbit = 24.4 \text{ kgf/orbit } (53.8 \text{ lb/orbit}) \qquad (43)$$

The weight of fuel per day equals

$$WOF/day = \frac{(24)(3\ 600)}{T_o} WOF/orbit = 370 \text{ kgf/day}$$

$$(815 \text{ lb/day}) \qquad (44)$$

The use of either the baseline or modified ACPS system would also make the problem of meeting the final stabilization requirements of the ASM experiments more difficult as shown in appendix B3.4. Due to the firing of these large ACPS thrusters, any slight offset of the experiment center of mass from the center of rotation of its fine stabilization system will result in a large disturbance torque being coupled through the isolation system to the experiments. For a detailed discussion of this problem the reader is referred to Appendix B3.4.

The conclusions of this analysis are:

a. For both the baseline and modified ACPS systems, the fuel consumption is independent of the stabilized orbiter orientation. The fuel consumption for the baseline ACPS is 1 670 kgf/day (3 660 lb/day) and for the modified ACPS, it is 370 kgf/day (815 lb/day).

b. For the baseline ASM mission duration of 7 days, these large fuel consumption rates would result in a heavy orbiter stabilization system.

c. The combustion by-products due to these large fuel consumptions are a source of experiment contamination which could degrade the experiments or cause them to be shut down.

d. Using either the baseline or modified ACPS system makes the problems of meeting the final stabilization requirements of the ASM experiments more difficult. (See appendix B3.4.

A1.2. SIZING OF X-POP SHUTTLE ORBITER CMG STABILIZATION SYSTEM

This CMG system was sized based on the gravity gradient momentum that must be stored per orbit. The following assumptions were used to size the CMG system.

a. The desired shuttle orbiter attitude is the X-POP attitude shown in figure A1-3.

b. The shuttle orbiter is inertially held in its desired orientation during the primary experimentation period θ_E denoted in the figure. The length of this period, t, is 3 550 seconds.

c. The CMG's are desaturated during the secondary experimentation period also denoted in the figure.

d. The CMG system is assumed to have a shuttle orbiter maneuver capability ω_{MAN} of 2.91×10^{-4} radians per second (1 degree per minute).

For a shuttle orbiter stabilized in the X-POP attitude shown in figure A1-3, the gravity gradient torques acting on the orbiter are

$$T_{gx} = 3\omega_o^2 \, a_y a_z \, (I_{zz} - I_{yy}) \tag{1}$$

$$T_{gy} = 3\omega_o^2 \, a_x a_z \, (I_{xx} - I_{zz}) \tag{2}$$

$$T_{gz} = 3\omega_o^2 \, a_x a_y \, (I_{yy} - I_{xx}) \tag{3}$$

where a_x, a_y, and a_z are the components of the local vertical vector shown in the figure and ω_o is the orbital rate. For a 270 NM circular orbit, ω_o equals 1.10×10^{-3} radians per second. From figure A1-3, the vector $\hat{a}$ equals

$$\hat{a} = \begin{bmatrix} a_x \\ a_y \\ a_z \end{bmatrix} = \begin{bmatrix} 0 \\ \cos\omega_o t \\ \sin\omega_o t \end{bmatrix} \tag{4}$$

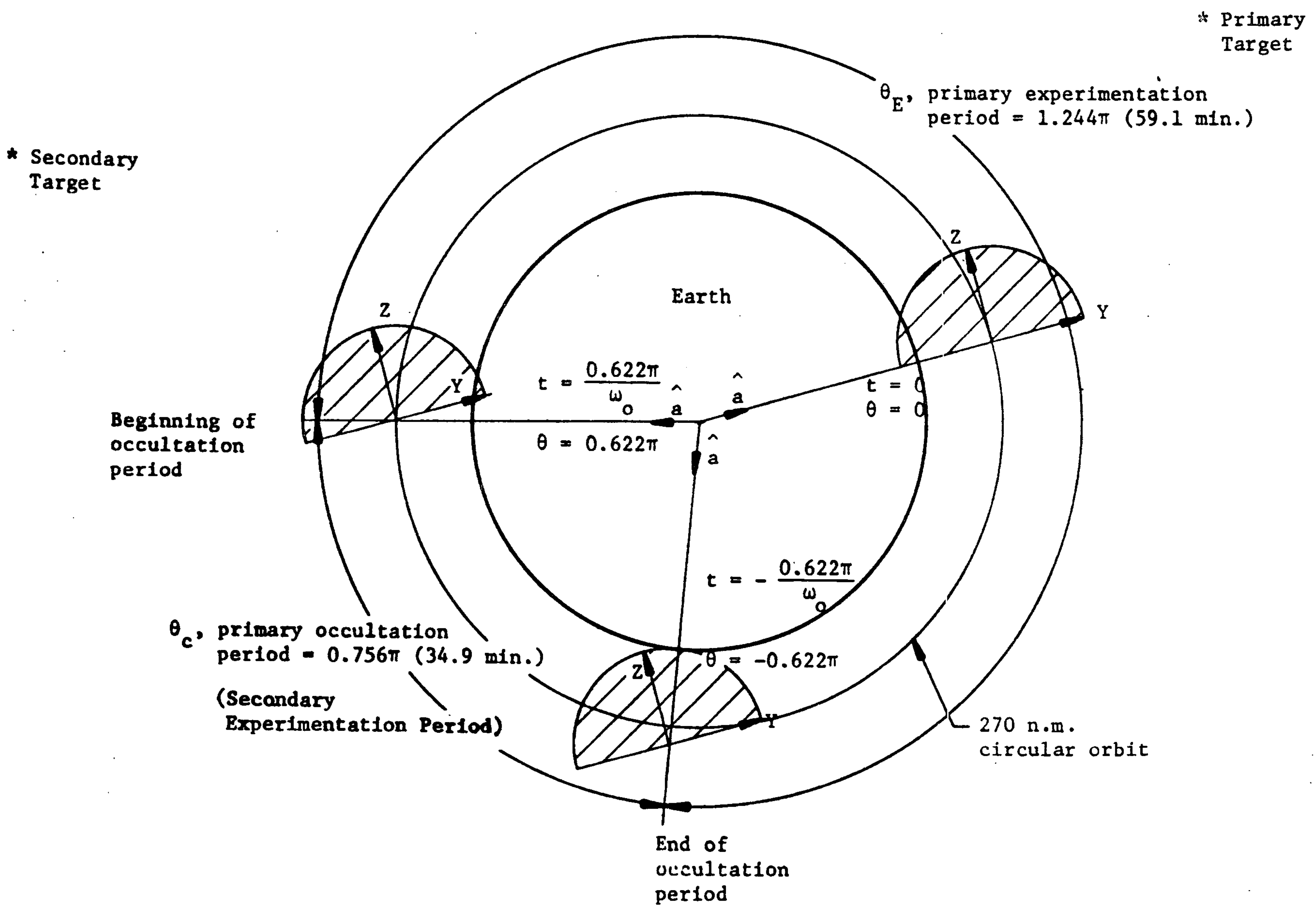

Figure A1-3. Sketch of X-POP Stabilized Shuttle Orbiter With a Double Gimbal ASM Experiment Pointing System

Assume the orbiter is misaligned from the true X-POP attitude by two small rotational angles ε_y and ε_z about the Y and Z axes, respectively. The resultant local vertical vector $\hat{a}'$ equals

$$\hat{a}' = \begin{bmatrix} a_x' \\ a_y' \\ a_z' \end{bmatrix} = \begin{bmatrix} 1 & \varepsilon_z & -\varepsilon_y \\ -\varepsilon_z & 1 & 0 \\ \varepsilon_y & 0 & 1 \end{bmatrix} \begin{bmatrix} a_x \\ a_y \\ a_z \end{bmatrix}$$

$$\hat{a}' = \begin{bmatrix} \varepsilon_z \cos\omega_o t - \varepsilon_y \sin\omega_o t \\ \cos\omega_o t \\ \sin\omega_o t \end{bmatrix} \qquad (5)$$

Assume that ε_y and ε_z are equal ($\varepsilon_y=\varepsilon_z=\varepsilon$). The resultant gravity gradient torques are

$$T_{gx}' = \frac{3\omega_o^2}{2} (I_{zz}-I_{yy}) \sin 2\omega_o t \qquad (6)$$

$$T_{gy}' = \frac{3\omega_o^2}{2_2} (I_{zz}-I_{xx}) \varepsilon [1-\cos 2\omega_o t - \sin 2\omega_o t] \qquad (7)$$

$$T_{gz}' = \frac{3\omega_o}{2} (I_{yy}-I_{xx}) \varepsilon [1+\cos 2\omega_o t - \sin 2\omega_o t] \qquad (8)$$

Integrating the above torque equations results in the gravity gradient momentum that the CMG's must store.

$$H_{gx} = \int T_{gx}' dt = -\frac{3\omega_o}{4} (I_{zz}-I_{yy}) \cos 2\omega_o t \qquad (9)$$

$$H_{gy} = \int T_{gy}' dt = \frac{3\omega_o}{4} (I_{zz}-I_{xx}) \varepsilon [2\omega_o t - \sin 2\omega_o t + \cos 2\omega_o t] \qquad (10)$$

$$H_{gz} = \int T_{gz}' dt = \frac{3\omega_o}{4} (I_{yy}-I_{xx}) \varepsilon [2\omega_o t + \sin 2\omega_o t + \cos 2\omega_o t] \qquad (11)$$

The gravity gradient momentum that is stored in the CMG's has two components; they are (1) the accumulated momentum $\vec{H}_a$ due to the constant axial gravity gradient torque biases and (2) the cyclic momentum $\vec{H}_c$ due to the cyclic gravity gradient torques. The axial components of $\vec{H}_a$ and $\vec{H}_c$ are

$$\text{X axis:}\quad H_{ax}=0 \tag{12}$$

$$H_{cx}=-\frac{3\omega_o}{4}(I_{zz}-I_{yy})\cos 2\omega_o t \tag{13}$$

$$\text{Y axis:}\quad H_{ay}=\frac{3\omega_o^2}{2}(I_{zz}-I_{xx})\varepsilon t \tag{14}$$

$$H_{cy}=\frac{3\omega_o}{4}(I_{zz}-I_{xx})\varepsilon[\cos 2\omega_o t-\sin 2\omega_o t] \tag{15}$$

$$\text{Z axis:}\quad H_{az}=\frac{3\omega_o^2}{2}(I_{yy}-I_{xx})\varepsilon t \tag{16}$$

$$H_{cz}=\frac{3\omega_o}{4}(I_{yy}-I_{xx})\varepsilon[\sin 2\omega_o t+\cos 2\omega_o t] \tag{17}$$

The magnitude of the accumulated momentum $\vec{H}_a$ equals

$$|\vec{H}_a|=\sqrt{H_{ax}^2+H_{ay}^2+H_{az}^2}=\frac{3\omega_o^2}{2}\varepsilon t\sqrt{(I_z-I_x)^2+(I_y-I_x)^2} \tag{18}$$

Assume that ε equals 1.745×10^{-2} radian (1 degree). The momentum $|\vec{H}_a|$ accumulated during the primary experimentation period (t = 3 550 seconds) equals

$$|\vec{H}_a|=1\ 200\ \text{N-m-sec (882 ft-lb-sec)} \tag{19}$$

The magnitude of the cyclic momentum $\vec{H}_c$ equals

$$|\vec{H}_c|=\sqrt{H_{cx}^2+H_{cy}^2+H_{cz}^2} \tag{20}$$

Since the shuttle orbiter inertias I_{yy} and I_{zz} are approximately equal, $|\vec{H}_c|$ can be approximated by

$$|\vec{H}_c| = \frac{3\omega_o}{4} \{[(I_{zz}-I_{yy})^2 + \epsilon^2 (I_{zz}-I_{xx})^2 + \epsilon^2 (I_{yy}-I_{xx})^2]\cos^2 2\omega_o t$$

$$+\epsilon^2 [(I_{zz}-I_{xx})^2 + (I_{yy}-I_{xx})^2]\sin^2 2\omega_o t\}^{1/2} \quad (21)$$

The peak cyclic momentum $|\vec{H}_c|_p$ corresponds to t equal to zero.

$$|\vec{H}_c|_p = \frac{3\omega_o}{4} [(I_{zz}-I_{yy})^2 + \epsilon^2 (I_{zz}-I_{xx})^2 + \epsilon^2 (I_{yy}-I_{xx})^2]^{1/2} \quad (22)$$

$$|\vec{H}_c|_p = 314 \text{ N-m-sec } (231 \text{ ft-lb-sec}) \quad (23)$$

The CMG system besides storing the gravity gradient momentum must also store the momentum due to aerodynamic torques, H_{aero}. Assume H_{aero} equals

$$H_{aero} = 0.05(|\vec{H}_a| + |\vec{H}_c|_p) \quad (24)$$

$$H_{aero} = 75.7 \text{ N-m-sec } (55.6 \text{ ft-lb-sec}) \quad (25)$$

To meet the shuttle orbiter maneuvering requirement of 2.91×10^{-4} radians per second (1 degree per minute), the CMG system must impart the following angular momentum to the orbiter in order to maneuver it about its axis of maximum inertia (i.e., Z axis) at the above rate:

$$H_{MAN} = I_{zz}\omega_{MAN} = 2\ 490 \text{ N-m-sec } (1\ 830 \text{ ft-lb-sec}) \quad (26)$$

After the shuttle orbiter is placed in its X-POP attitude by the baseline orbiter ACPS system, the CMG system takes over control by absorbing the remaining residual momentum left by the baseline system. Assume that the shuttle orbiter is in a torque-free environment. For the shuttle orbiter baseline ACPS, this assumption was shown to be valid in section A1-1. Each vehicle axis will limit cycle between the limits of the ACPS attitude deadband $\pm\theta_o$. Figure A1-2 is a sketch of this ACPS attitude deadband. The lower limit, $-\theta_o$, is designated state a, and the upper limit is designated state b. Assume that the i^{th} vehicle axis is at state a. The appropriate ACPS thrusters will fire sending the i^{th} axis towards state b, the axial angular velocity ω_{ab} equals

$$\omega_{ab}=\omega_i+\omega_{ab}(0) \quad (27)$$

where ω_i is the change in angular rate about the i^{th} axis due t
a single ACPS firing. The position of the axis θ_{ab} equals

$$\theta_{ab}=[\omega_i+\omega_{ab}(0)]t-\theta_o \quad (28$$

When the axis reaches state b, the thrusters fire once more sen
the i^{th} axis back towards state a. The angular velocity, θ_{ba},
the axis travels back towards a equals

$$\omega_{ba}=-\omega_i+\omega_{ba}(0) \quad (2$$

$$\theta_{ba}=[-\omega_i+\omega_{ba}(0)]t+\theta_o \quad (3$$

From equation 28, the time t_{ab} for the axis to traverse the de
from state a to state b equals

$$\theta_{ab}=\theta=[\omega_i+\omega_{ab}(0)]t_{ab}-\theta_o$$

$$t_{ab}=\frac{2\theta_o}{\omega_i+\omega_{ba}(0)}$$

From equation 30, the time t_{ba} to return to state a equals

$$\theta_{ba}=-\theta_o=[-\omega_i+\omega_{ba}(0)]t_{ba}+\theta_o$$

$$t_{ba}=\frac{2\theta_o}{\omega_i-\omega_{ba}(0)}$$

Under steady state conditions

$$t_{ab}=t_{ba}$$

Therefore, using equations 31, 32, and 33,

$$\omega_{ab}(0)=-\omega_{ba}(0)$$

Since the angular velocity of the i^{th} axis cannot change instantaneously at either boundary of the deadband, the following expressions can be written using equations 27 and 29.

$$\omega_{ba}(0)=\omega_i+\omega_{ab}(0) \tag{35}$$

$$\omega_{ab}(0)=-\omega_i+\omega_{ba}(0) \tag{36}$$

Using equations 34, 35, and 36, the following expressions for $\omega_{ab}(0)$ and $\omega_{ba}(0)$ can be written

$$\omega_{ab}(0)=-\frac{\omega_i}{2} \tag{37}$$

$$\omega_{ba}(0)=\frac{\omega_i}{2} \tag{38}$$

The residual momentum that the CMG's must absorb equals

$$H_{tran}=\sqrt{\sum_i I_{ii}^2\omega_{ba}^2(0)}=0.5\sqrt{\sum_i I_{ii}^2\omega_i^2} \tag{39}$$

From section A1.1., ω_i equals

ω_x=2.81 mrad/sec (0.161 deg/sec)

ω_y=0.482 mrad/sec ($27.6\text{x}10^{-3}$ deg/sec)

ω_z=0.463 mrad/sec ($26.6\text{x}10^{-3}$ deg/sec)

Substituting the above values of ω_i into equation 39, H_{tran} equals

H_{tran}=3 390 N-m-sec (2 500 ft-lb-sec)

The CMG system for stabilizing the shuttle orbiter in a X-POP attitude is sized in table A1-2. The total CMG angular momentum storage requirement is 9 060 N-m-sec (6 668 ft-lb-sec). This momentum storage requirement can be met by three Skylab ATM CMG's. The total CMG momentum capability of three ATM CMG's is 9 350 N-m-sec. (6 900 ft-lb-sec) which exceeds the required momentum storage capability by 290 N-m-sec (232 ft-lb-sec).

Table A1-2. Sizing of a CMG System for a X-POP Stabilized Shuttle Orbiter

$\lvert\vec{H}_a\rvert$	1 200 N-m-sec	(882 ft-lb-sec)
$\lvert\vec{H}_c\rvert_p$	314 N-m-sec	(231 ft-lb-sec)
H_{aero}	76 N-m-sec	(56 ft-lb-sec)
Sub Total	1 590 N-m-sec	(1 169 ft-lb-sec)
Safety Factor	x2	
	3 180 N-m-sec	(2 338 ft-lb-sec)
Maneuver H_{MAN}	2 490 N-m-sec	(1 830 ft-lb-sec)
Transitional Momentum (from ACPS to CMG control)	3 390 N-m-sec	(2 500 ft-lb-sec)
Total CMG Momentum Storage Requirement	9 060 N-m-sec	(6 668 ft-lb-sec)

A1.2.1. CMG Momentum Desaturation System - When CMGs are used to control and stabilize the attitude of a spacecraft, an additional torquing system is required to prevent the CMGs from becoming saturated. This additional torquing system is referred to as a momentum desaturation system. For the CMG stabilized shuttle orbiter, there exists three feasible methods of performing desaturation; they are reaction control, magnetic, and gravity gradient desaturation.

An RCS desaturation system generates the required desaturation torques by employing mass expulsion thrusters. This system has a high torque capability and therefore, can readily desaturate the CMGs. The resulting large desaturation torques preclude the use of this system during experimentation because it would significantly disturb the experiments' attitude control system and prevent it from meeting its desired pointing and stabilization performance. The system's principal disadvantage is that the mass expelled by an RCS is a probable source of experiment contamination that could degrade or cause the experiment to be shut down. This RCS contamination problem is the driving force behind the rationale for selecting a CMG system instead of an RCS to stabilize and control the attitude of the shuttle orbiter. For this reason, an RCS desaturation system is eliminated as a candidate.

A magnetic desaturation system generates a magnetic dipole moment $\vec{M}$ onboard the vehicle which interacts with the earth's magnetic $\vec{B}$ field to produce the required desaturation torques. The magnetic moment $\vec{M}$ is generated by energizing electromagnets or flat magnetic air coils. A three-axis magnetometer is needed to measure the earth's $\vec{B}$ field in order to compute the required $\vec{M}$. This system's major problem is that the large magnetic field produced by a system large enough to desaturate the shuttle orbiter CMGs is a severe source of ASM experiment magnetic contamination. Like the RCS desaturation system, the magnetic desaturation system is eliminated as a candidate because of experiment contamination.

A gravity gradient CMG desaturation system utilizes the natural gravitational forces between the spacecraft and the earth to generate the desaturation torques. In order to take advantage of these torques, the spacecraft must be maneuvered to a favorable gravity gradient orientation. This method of desaturating the CMGs requires no additional equipment or fuel and only depends on the ability of the CMGs to maneuver the vehicle. For an X-POP stabilized shuttle orbiter, the required gravity gradient desaturation maneuvers are small and could be performed at the beginning and the end of the primary occultation period while the telescope is being slewed to the secondary and primary targets, respectively. A gravity gradient desaturation system unlike an RCS or a magnetic system is not a source of experiment contamination. This is the main reason for selecting a gravity gradient desaturation system.

Ideally, if the shuttle orbiter is stabilized in a true X-POP attitude and the torque environment is due only to the gravitational pull of the earth, the momentum stored in the CMGs would be cyclic and thus, no desaturation system would be needed. Such an idealization is not realistic. Assume that the orbiter is misaligned from a true X-POP attitude by two small rotational errors ε about both the Y and Z axes. The resultant gravity gradient torque equations are

$$T_{gx}=\frac{3\omega_o^2}{2}(I_{zz}-I_{yy})\sin 2\theta \tag{40}$$

$$T_{gy}=\frac{3\omega_o^2}{2}(I_{zz}-I_{xx})\varepsilon[1-\cos 2\theta-\sin 2\theta] \tag{41}$$

$$T_{gz}=\frac{3\omega_o^2}{2}(I_{yy}-I_{xx})\varepsilon[1+\cos 2\theta-\sin 2\theta] \tag{42}$$

where θ equals $\omega_o t$. These gravity gradient torque equations correspond to the primary experimentation period θ_E in figure A1-3. At the beginning of the occultation period θ_c, assume that the following desaturation maneuvers ε_{xd}, $\varepsilon_{yd}-\varepsilon$, and $\varepsilon_{zd}-\varepsilon$ are performed about the X, Y, and Z axes, respectively. Assume these maneuvers are made instantaneously. The resultant local vertical vector $\hat{a}_d$ equals

$$\hat{a}_d=\begin{bmatrix} a_{xd} \\ a_{yd} \\ a_{zd} \end{bmatrix}=\begin{bmatrix} 1 & \varepsilon_{zd} & -\varepsilon_{yd} \\ -\varepsilon_{zd} & 1 & \varepsilon_{xd} \\ \varepsilon_{yd} & -\varepsilon_{xd} & 1 \end{bmatrix}\begin{bmatrix} 0 \\ \cos\theta \\ \sin\theta \end{bmatrix}$$

$$\hat{a}_d=\begin{bmatrix} \varepsilon_{zd}\cos\theta-\varepsilon_{yd}\sin\theta \\ \cos\theta+\varepsilon_{xd}\sin\theta \\ -\varepsilon_{xd}\cos\theta+\sin\theta \end{bmatrix} \tag{43}$$

Substitute $\hat{a}_d$ into the gravity gradient torque equations 1 through 3 and assume that any products or squares of ε_{xd}, ε_{yd}, and ε_{zd} equal zero ($\varepsilon_{xd}^2=\varepsilon_{yd}^2=\varepsilon_{zd}^2=\varepsilon_{xd}\varepsilon_{yd}=\varepsilon_{xd}\varepsilon_{zd}=\cdots=0$). The resultant gravity gradient desaturation torque equations are

$$T_{gx}^{(d)} = \frac{3\omega_o^2}{2}(I_{zz}-I_{yy})[\sin 2\theta - 2\varepsilon_{xd}\cos 2\theta] \tag{44}$$

$$T_{gy}^{(d)} = \frac{3\omega_o^2}{2}(I_{zz}-I_{xx})[\varepsilon_{yd}(1-\cos 2\theta) - \varepsilon_{zd}\sin 2\theta] \tag{45}$$

$$T_{gz}^{(d)} = \frac{3\omega_o^2}{2}(I_{yy}-I_{xx})[\varepsilon_{zd}(1+\cos 2\theta) - \varepsilon_{yd}\sin 2\theta] \tag{46}$$

To desaturate the CMGs completely, the net accumulated angular momentum during one orbit must be zero. To compute representative desaturation maneuvers, assume that the shuttle orbiter is stabilized as shown in figure A1-3. Since the net accumulated momentum must be zero, the following equations must be satisfied.

$$H_x = \int_{\frac{-0.622\pi}{\omega_o}}^{\frac{0.622\pi}{\omega_o}} T_{gx}\,dt + \int_{\frac{0.622\pi}{\omega_o}}^{\frac{1.378\pi}{\omega_o}} T_{gx}^{(d)}\,dt$$

$$= \frac{1}{\omega_o}\int_{-0.622\pi}^{0.622\pi} T_{gx}\,d\theta + \frac{1}{\omega_o}\int_{0.622\pi}^{1.378\pi} T_{gx}^{(d)}\,d\theta = 0 \tag{47}$$

$$H_y = \int_{\frac{-0.622\pi}{\omega_o}}^{\frac{0.622\pi}{\omega_o}} T_{gy}\,dt + \int_{\frac{0.622\pi}{\omega_o}}^{\frac{1.378\pi}{\omega_o}} T_{gy}^{(d)}\,dt$$

$$= \frac{1}{\omega_o}\int_{-0.622\pi}^{0.622\pi} T_{gy}\,d\theta + \frac{1}{\omega_o}\int_{0.622\pi}^{1.378\pi} T_{gy}^{(d)}\,d\theta = 0 \tag{48}$$

$$H_z = \int_{\frac{-0.622\pi}{\omega_o}}^{\frac{0.622\pi}{\omega_o}} T_{gz}\,dt + \int_{\frac{0.622\pi}{\omega_o}}^{\frac{1.378\pi}{\omega_o}} T_{gz}^{(d)}\,dt$$

$$= \frac{1}{\omega_o}\int_{-0.622\pi}^{0.622\pi} T_{gz}\,d\theta + \frac{1}{\omega_o}\int_{0.622\pi}^{1.378\pi} T_{gz}^{(d)}\,d\theta = 0 \tag{49}$$

Substitute the expressions for T_{gi} and $T_{gi}^{(d)}$ $(i=x,y,z)$ into the above equations.

$$H_x = \frac{3\omega_o}{2}(I_{zz}-I_{yy})\{\int_{-0.622\pi}^{0.622\pi} \sin\theta d\theta$$

$$+\int_{0.622\pi}^{1.378\pi} (\sin 2\theta - 2\varepsilon_{xd}\cos 2\theta)d\theta\}=0 \tag{50}$$

$$H_y = \frac{3\omega_o}{2}(I_{zz}-I_{xx})\{\varepsilon\int_{-0.622\pi}^{0.622\pi} (1-\cos 2\theta-\sin 2\theta)d\theta$$

$$+\int_{0.622\pi}^{1.378\pi} [\varepsilon_{yd}(1-\cos 2\theta)-\varepsilon_{zd}\sin 2\theta]d\theta\}=0 \tag{51}$$

$$H_z = \frac{3\omega_o}{2}(I_{yy}-I_{xx})\{\varepsilon\int_{-0.622\pi}^{0.622\pi} (1+\cos 2\theta-\sin 2\theta)d\theta$$

$$+\int_{0.622\pi}^{1.378\pi} [\varepsilon_{zd}(1+\cos 2\theta)-\varepsilon_{yd}\sin 2\theta]d\theta\}=0 \tag{52}$$

Forming the integrations in equation 38 through 40,

$$H_x = -2.08\omega_o(I_{zz}-I_{yy})\varepsilon_{xd}=0 \tag{53}$$

$$H_y = 2.20\omega_o\ (I_{zz}-I_{xx})\pi(\varepsilon+0.365\varepsilon_{yd})=0 \tag{54}$$

$$H_z = 1.535\omega_o(I_{yy}-I_{xx})\pi(\varepsilon+0.955\varepsilon_{zd})=0 \tag{55}$$

From the above equations, ε_{xd}, ε_{yd}, and ε_{zd} equal

$$\varepsilon_{xd}=0 \tag{56}$$

$$\varepsilon_{yd}= -2.74\varepsilon \tag{57}$$

$$\varepsilon_{zd}= -1.05\varepsilon \tag{58}$$

The resulting desaturation maneuvers about the X, Y, and Z axes are 0, -3.74ε, and -2.05ε, respectively. The resultant eigen-axis desaturation maneuver ε_d equals

$$\varepsilon_d=\varepsilon\sqrt{(-3.74)^2+(-2.05)^2}=4.26\varepsilon \tag{59}$$

At the beginning of the desaturation interval θ_c, the desaturation maneuver ε_d is performed. Then, at the end of this interval, the orbiter is maneuvered back to its X-POP attitude that it was in just prior to desaturation. Assume that ε equals 1.745×10^{-2} radians (1 degree), the resultant eigenaxis maneuver ε_d equals 7.44×10^{-2} radians (4.26 degrees). This maneuver ε_d is relatively small and should not interfere with the pointing of the ASM experiments at a secondary target. If the orbiter has a maneuver capability of 2.91×10^{-4} radians per second (1 degree per minute), the desaturation maneuver ε_d will take approximately 4 minutes to perform.

By sampling the momentum stored in the CMGs during the primary experimentation period θ_E, the accumulated momentum $\vec{H}_a$ that the gravity gradient desaturation scheme must desaturate is determined. From $\vec{H}_a$, the appropriate gravity gradient desaturation maneuvers are then computed.

A1.2.2. Pseudo-Axis-of-Inertia Alignment Scheme - The pseudo-axis-of-inertia alignment scheme attempts to place the shuttle orbiter in an orientation where the average momentum stored in the CMGs during an orbit is minimized. By minimizing the average momentum stored in the CMGs, the required gravity gradient CMG desaturation maneuvers are also minimized. If this system operated perfectly, the average CMG momentum would be zero thus, eliminating the necessity of desaturating the CMGs. At the end of each desaturation interval, two maneuvers ε_{ya} and ε_{za} with respect to the desired X-POP attitude are performed about the orbiter Y and Z control axes, respectively. These maneuvers are performed in an attempt to minimize the accumulated momentum stored in the CMGs during the next orbit. To illustrate how this system operates, assume that the shuttle orbiter's principal and control axes are slightly misaligned. Assuming that the orbiter is stabilized in a X-POP attitude with its X control axis perpendicular to the orbital plane, these axial misalignments will produce a nonzero average momentum to be accumulated in the CMGs thus, necessitating a momentum dump. Also, the orbiter's products of inertia I_{xy}, I_{xz}, and I_{yz} are not zero due to the axial misalignments. The resultant gravity gradient torque equations are:

$$T_{gx}=3\omega_o^2\ \{a_y''a_z''(I_{zz}-I_{yy})+a_x''a_z''I_{xy}$$
$$-a_x''a_y''I_{xz}+[(a_z'')^2-(a_y'')^2]I_{yz}\} \qquad (60)$$
$$T_{gy}=3\omega_o^2\ \{a_x''a_z''(I_{xx}-I_{zz})+a_x''a_y''I_{yz}$$
$$-a_y''a_z''I_{xy}+[(a_x'')^2-(a_z'')^2]I_{xz}\} \qquad (61)$$
$$T_{gz}=3\omega_o^2\ \{a_x''a_y''(I_{yy}-I_{xx})+a_y''a_z''I_{xz}$$
$$-a_x''a_z''I_{yz}+[(a_y'')^2-(a_x'')^2]I_{xy}\} \qquad (62)$$

where the local vertical vector $\hat{a}''$ equals

$$\hat{a}''=\begin{bmatrix} a_x'' \\ a_y'' \\ a_z'' \end{bmatrix}=\begin{bmatrix} 1 & \varepsilon_{za} & -\varepsilon_{ya} \\ -\varepsilon_{za} & 1 & 0 \\ \varepsilon_{ya} & 0 & 1 \end{bmatrix}\begin{bmatrix} a_x \\ a_y \\ a_z \end{bmatrix} \qquad (63)$$

The local vertical vector $\hat{a}$ was defined in equation 4.

$$\hat{a}=\begin{bmatrix} a_x \\ a_y \\ a_z \end{bmatrix}=\begin{bmatrix} 0 \\ \cos\omega_o t \\ \sin\omega_o t \end{bmatrix} \qquad (4)$$

Substituting 4 into 63, $\hat{a}''$ equals

$$\hat{a}''=\begin{bmatrix} a_x'' \\ a_y'' \\ a_z'' \end{bmatrix}=\begin{bmatrix} \varepsilon_{za}\cos\omega_o t-\varepsilon_{ya}\sin\omega_o t \\ \cos\omega_o t \\ \sin\omega_o t \end{bmatrix} \qquad (64)$$

Compute the averages of $a_y''a_z''$, $a_x''a_z''$, $a_x''a_y''$, $(a_x'')^2$, $(a_y'')^2$, and $(a_z'')^2$ neglecting all terms that contain products or squares of ε_{ya} and ε_{za}

$$\overline{a_y''a_z''}=0 \tag{65}$$

$$\overline{a_x''a_z''}= -\frac{\varepsilon_{ya}}{2} \tag{66}$$

$$\overline{a_x''a_y''}= \frac{\varepsilon_{za}}{2} \tag{67}$$

$$\overline{(a_x'')^2} =0 \tag{68}$$

$$\overline{(a_y'')^2} = \frac{1}{2} \tag{69}$$

$$\overline{(a_z'')^2} = \frac{1}{2} \tag{70}$$

Substituting equations 65 through 70 into equations 60 through 62, the average gravity gradient torques are:

$$\overline{T}_{gx}= -\frac{3\omega_o^2}{2}\,[\varepsilon_{ya}I_{xy}+\varepsilon_{za}I_{xz}] \tag{71}$$

$$\overline{T}_{gy}= -\frac{3\omega_o^2}{2}\,[\varepsilon_{ya}(I_{xx}-I_{zz})-\varepsilon_{za}I_{yz}+I_{xz}] \tag{72}$$

$$\overline{T}_{gz}= \frac{3\omega_o^2}{2}\,[\varepsilon_{za}(I_{yy}-I_{xx})+\varepsilon_{ya}I_{yz}+I_{xy}] \tag{73}$$

By integrating the above average gravity gradient torques over one orbit, the resultant average gravity gradient angular momentum equals

$$\overline{H}_{gx}= -3\pi\omega_o[\varepsilon_{ya}I_{xy}+\varepsilon_{za}I_{xz}] \tag{74}$$

$$\overline{H}_{gy}= -3\pi\omega_o[\varepsilon_{ya}(I_{xx}-I_{zz})-\varepsilon_{za}I_{yz}+I_{xz}] \tag{75}$$

$$\overline{H}_{gz}= 3\pi\omega_o[\varepsilon_{za}(I_{yy}-I_{xx})+\varepsilon_{ya}I_{yz}+I_{xy}] \tag{76}$$

Since the orbiter's principal and control axes are only slightly misaligned, the orbiter's products of inertia can be approximated by

$$I_{xy}=\varepsilon_{oz}(I_{yy}-I_{xx}) \tag{77}$$

$$I_{xz}=\varepsilon_{oy}(I_{xx}-I_{zz}) \tag{78}$$

$$I_{yz}=\varepsilon_{ox}(I_{zz}-I_{yy}) \tag{79}$$

where ε_{ox}, ε_{oy}, and ε_{oz} are the misalignments between X, Y, and Z principal and control axes, respectively. By judiciously substituting the above approximations for I_{xy}, I_{xz}, and I_{yz} into equations 74 through 76 and by neglecting all terms that contain products of ε_{oz}, ε_{oy}, and ε_{ox} with ε_{ya} and ε_{za}, the average gravity gradient momentum equations are

$$\overline{H}_{gx}=0 \tag{80}$$

$$\overline{H}_{gy}= -3\pi\omega_o[\varepsilon_{ya}(I_{xx}-I_{zz})+I_{xz}] \tag{81}$$

$$\overline{H}_{gz}= 3\pi\omega_o[\varepsilon_{za}(I_{yy}-I_{xx})+I_{xy}] \tag{82}$$

If ε_{ya} and ε_{za} are zero, the momentum that the CMGs will accumulate during one orbit equals

$$\overline{H}_{x\ CMG}=0 \tag{83}$$

$$\overline{H}_{y\ CMG}= -3\pi\omega_o I_{xz} \tag{84}$$

$$\overline{H}_{z\ CMG}=3\pi\omega_o I_{xy} \tag{85}$$

Equations 80 through 82 can be written as

$$\overline{H}_{gx}=0 \tag{86}$$

$$\overline{H}_{gy}=K_1\varepsilon_{ya}+\overline{H}_{y\ CMG} \tag{87}$$

$$\overline{H}_{gz}=K_2\varepsilon_{za}+\overline{H}_{z\ CMG} \tag{88}$$

where

$$K_1 = 3\pi\omega_o (I_{zz} - I_{xx})$$

$$K_2 = 3\pi\omega_o (I_{yy} - I_{xx})$$

If the system operates perfectly, $\overline{H}_{gy}$ and $\overline{H}_{gz}$ will equal zero.

$$\overline{H}_{gy} = K_1 \varepsilon_{ya} + \overline{H}_{y\ CMG} = 0 \tag{89}$$

$$\overline{H}_{gz} = K_2 \varepsilon_{za} + \overline{H}_{z\ CMG} = 0 \tag{90}$$

From equations 89 and 90, the pseudo-axis alignment maneuvers ε_{ya} and ε_{za} equal

$$\varepsilon_{ya} = -\frac{\overline{H}_{y\ CMG}}{K_1} \tag{91}$$

$$\varepsilon_{za} = -\frac{\overline{H}_{z\ CMG}}{K_2} \tag{92}$$

$\overline{H}_{y\ CMG}$ and $\overline{H}_{z\ CMG}$ are determined by sampling the momentum stored in the CMGs. $\overline{H}_{y\ CMG}$ and $\overline{H}_{z\ CMG}$ were assumed to be due to principal and control axis misalignments, they could have also been partially or entirely due to aerodynamic torques acting on the orbiter; and the system would still have worked just as well. Depending on how well this pseudo-axis alignment scheme works, it may not be necessary to desaturate the CMGs every orbit.

A1.3. SIZING OF X-POP SHUTTLE ORBITER LOW THRUST RCS STABILIZATION SYSTEM

The sizing of this shuttle orbiter low thrust RCS stabilization system is broken into two parts. First, the RCS engine thrust level F as a function of the RCS attitude deadband is determined. Second, the total RCS impulse $\Sigma F\Delta t$ required to stabilize the shuttle orbiter during a 7-day ASM mission is computed. $\Sigma F\Delta t$ is directly proportional to the amount of RCS fuel required.

A1.3.1. Sizing of the Shuttle Orbiter RCS Stabilization System Engine Thrust Level - The proposed low thrust shuttle orbiter RCS stabilization system should have engines that are

a. Small enough to prevent excessive limit cycling between the limits of the attitude deadband.

b. Large enough to insure that the vehicle will not exceed the attitude deadband.

This RCS shuttle orbiter stabilization system was sized using the following assumptions:

a. The RCS engine impulse $F\Delta t$ is the same for all engines.

b. The effective RCS engine impulse duration Δt equals 80 msec. An impulse duration of 80 msec was selected to reduce the raw fuel loss per impulse to an acceptable level.

c. The engines are fired in pairs in order to produce a pure torque moment (no translational motion).

d. The RCS is decoupled such that an engine pair firing produces a torque about only one control axis.

e. The moment arm ℓ between engine pairs is 18.3 meters (60 feet).

Assume that the orbiter's i^{th} axis has just impinged on the upper deadband limit due to gravity gradient torques acting on the vehicle's i^{th} axis. A RCS engine pair is fired imparting a single momentum impulse bit, $MIB=F\Delta t\ell$, to the i^{th} axis sending it towards the lower deadband limit. The engine impulse $F\Delta t$ should be small enough to allow the gravity gradient torques to decelerate the i^{th} axis before it has traversed one quarter the width of the deadband. Figure A1-4 is a sketch of the RCS deadband. The i^{th} axis equations of motion are

$$\omega_i=\alpha_{gi}t-\omega_{oi} \tag{1}$$

$$\theta_i=\frac{1}{2}\alpha_{gi}t^2-\omega_{oi}t+\theta_o \tag{2}$$

where

ω_i is the i^{th} axis angular velocity

θ_i is the rotational displacement of the i^{th} axis

α_{gi} is the i^{th} axis acceleration due to the average rectified gravity gradient torque

ω_{oi} is the angular velocity imparted to the i^{th} axis due to one MIB firing

θ_o is the upper deadband limit (0.5 deg = 8.725 mrad)

t is the time from when the i^{th} axis impinged on the deadband's upper limit.

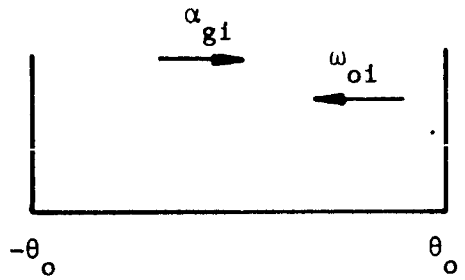

Figure A1-4. RCS Attitude Deadband for Computing Upper RCS Thrust Level

When θ_i reaches $\frac{\theta_o}{2}$, ω_i should equal zero. Substitute these values of θ_i and ω_i into equations (1) and (2).

$$0=\alpha_{gi}t-\omega_{oi} \tag{3}$$

$$\frac{\theta_o}{2}=\frac{1}{2}\alpha_{gi}t^2-\omega_{oi}t+\theta_o \tag{4}$$

From equation 3,

$$t=\frac{\omega_{oi}}{\alpha_{gi}} \tag{5}$$

Substitute equation 5 into 4 and solve for ω_{oi}

$$\frac{\theta_o}{2}=\frac{1}{2}\alpha_{gi}\left(\frac{\omega_{oi}}{\alpha_{gi}}\right)^2-\omega_{oi}\left(\frac{\omega_{oi}}{\alpha_{gi}}\right)+\theta_o \tag{6}$$

$$\omega_{oi}=(\alpha_{gi}\theta_o)^{1/2} \tag{7}$$

α_{gi} equals

$$\alpha_{gi}=\frac{T_{gi}|_{ra}}{I_{ii}} \tag{8}$$

where

$T_{gi}|_{ra}$ is the average worst case rectified gravity gradient torque acting on the i^{th} axis

I_{ii} is the moment of inertia for the i^{th} axis.

Substitute equation 8 into equation 7

$$\omega_{oi} = \left(\frac{T_{gi}|_{ra}\theta_o}{I_{ii}}\right)^{1/2} \tag{9}$$

One MIB equals

$$MIB = I_{ii}\omega_{oi} = F_i \Delta t \ \ell \tag{10}$$

From equations 9 and 10, the RCS engine thrust F_i equals

$$F_i = \frac{I_{ii}\omega_{oi}}{\ell \ \Delta t} = \frac{1}{\ell \ \Delta t}(T_{gi}|_{ra} I_{ii} \ \theta_o)^{1/2} \tag{11}$$

The average worst case rectified gravity gradient torques $T_{gi}|_{ra}$ acting on the three orbiter axes are

$$T_{gx}|_{ra} = \frac{3}{\pi}\omega_o^2 (I_{zz} - I_{yy}) \tag{12}$$

$$T_{gy}|_{ra} = \frac{3}{\pi}\omega_o^2 (I_{zz} - I_{xx}) \tag{13}$$

$$T_{gz}|_{ra} = \frac{3}{\pi}\omega_o^2 (I_{yy} - I_{xx}) \tag{14}$$

where ω_o is the shuttle orbiter's orbital rate. For a 270 NM circular orbit, ω_o equals

$$\omega_o = 1.10 \times 10^{-3} \ \frac{1}{sec} \tag{15}$$

$T_{gx}|_{ra}$, $T_{gy}|_{ra}$, and $T_{gz}|_{ra}$ equal

$$T_{gx}|_{ra} = 0.384 \text{ N-m } (0.291 \text{ ft-lb}) \tag{16}$$

$$T_{gy}|_{ra} = 8.31 \text{ N-m } (6.12 \text{ ft-lb}) \tag{17}$$

$$T_{gz}|_{ra} = 7.94 \text{ N-m } (5.84 \text{ ft-lb}) \tag{18}$$

Substituting the appropriate values of ℓ, Δt, I_{ii}, and $T_{gi}|_{ra}$ into equation 11, the RCS engine thrust F_i equal

$$F_x=5.10\times10^2\ \theta_o^{\ 1/2} \tag{19}$$

$$F_y=5.65\times10^3\ \theta_o^{\ 1/2} \tag{20}$$

$$F_z=5.62\times10^3\ \theta_o^{\ 1/2} \tag{21}$$

Since all the RCS engines are assumed to be identical the X axis determines the upper limit on engine thrust F.

$$F_{max}=5.10\times10^2\ \theta_o^{\ 1/2} \tag{22}$$

A RCS engine pair is commanded to fire when the i^{th} axis impinges on one of the attitude deadband limits. Assume that the RCS firing logic is governed by the following linear rate plus position law.

$$|K_R\omega_i+K_p\theta_i|=E \tag{23}$$

E is a positive constant scalar that corresponds to the attitude deadband limit. When the above equation is satisfied, a pair of RCS engines are fired.

Assume that the i^{th} axis has just impinged on the RCS upper deadband limit. This does not necessarily mean that θ_i equals θ_o, but only that equation 23 is satisfied. Since the i^{th} axis has impinged on the upper deadband limit, the absolute value brackets can be removed from equation 23.

$$K_R\omega_i+K_p\theta_i=E \tag{24}$$

An appropriate RCS engine pair is fired accelerating the i^{th} axis towards the lower deadband limit. Using figure A1-5, the following equations of motion for the i^{th} axis can be written.

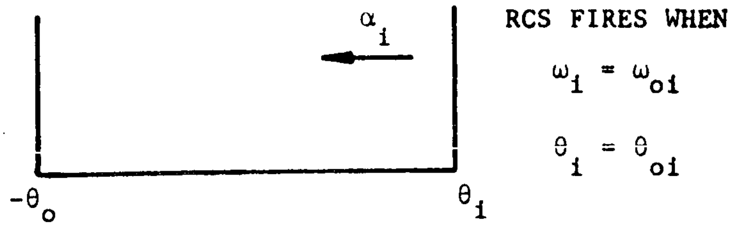

Figure A1-5. RCS Attitude Deadband for Computing Lower RCS Thrust Level

$$\omega_i = -\alpha_i\ t_i + \omega_{io} \tag{25}$$

$$\theta_i = -\frac{1}{2}\alpha_i t_i^2 + \omega_{io} t + \theta_{io} \tag{26}$$

where

α_i is the resultant acceleration due to gravity and the RCS engine pair firing

ω_{io} is the i^{th} axis angular velocity at the time of RCS firing

θ_{io} is the i^{th} axis rotational displacement at the time of RCS firing

t_i is the time from RCS firing

Substitute equations 25 and 26 into 24,

$$K_R[-\alpha_i t_i + \omega_{io}] + K_P[-\frac{1}{2}\alpha_i t_i^2 + \omega_{io} t + \theta_{io}] = E$$

or

$$K_R\omega_{io} + K_P\theta_{io} - K_R\alpha_i t_i + K_P[\omega_{io} t_i - \frac{1}{2}\alpha_i t_i^2] = E \tag{27}$$

Since $K_R\omega_{io} + K_P\theta_{io}$ equals E,

$$-K_R\alpha_i t_i + K_P[\omega_{io} t_i - \frac{1}{2}\alpha_i t_i^2] = 0 \tag{28}$$

Solving for t_i from equation 28,

$$t_i = 2[\frac{\omega_{io}}{\alpha_i} - \frac{K_R}{K_P}] \tag{29}$$

In order to prevent the i^{th} axis from exceeding the deadband E, the above expression for t_i must be zero or negative. If t_i is allowed to be positive, the i^{th} axis will exceed the attitude deadband causing the RCS to continue to fire for as long as the deadband is exceeded. From equation 29,

$$t_i = 2\left[\frac{\omega_{io}}{\alpha_i} - \frac{K_R}{K_P}\right] \leq 0$$

or

$$\alpha_i \geq \frac{K_P}{K_R}\,\omega_{io} \tag{30}$$

In order to solve for the minimum allowable value of α_i, ω_{io} must be computed. The following assumptions are made:

a. The RCS system fires when the i^{th} axis attitude error equals the upper attitude deadband limit, $K_P\theta_i = E$.

b. The RCS system imparts one MIB when the gravity gradient torque changes sign. The maximum average rectified gravity gradient $T_{gi}|_{ra}$ helps accelerate the i^{th} axis towards the lower attitude deadband limit.

The resulting equations of motion are

$$\omega_i = -\alpha_{gi}t - \alpha_{ji}\Delta t \tag{31}$$

$$\theta_i = -\frac{1}{2}\alpha_{gi}t^2 - (\alpha_{ji}\Delta t)t + \theta_o \tag{32}$$

where α_{ji} is the acceleration about the i^{th} axis due to one RCS engine pair firing for Δt seconds. When the i^{th} axis reaches the lower attitude deadband limit, θ_i equals $-\theta_o$ and ω_i equals $-\omega_{io}$.

$$-\omega_{io} = -\alpha_{gi}t - \alpha_{ji}\Delta t$$

or

$$\omega_{io} = \alpha_{gi}t + \alpha_{ji}\Delta t \tag{33}$$

$$-\theta_o = -\frac{1}{2}\alpha_{gi}t^2 - (\alpha_{ji}\Delta t)t + \theta_o \tag{34}$$

Using equation 34 to solve for t,

$$t=\frac{-\alpha_{ji}\Delta t+[(\alpha_{ji}\Delta t)^2+4\alpha_{gi}\theta_o]^{1/2}}{\alpha_{gi}} \tag{35}$$

Substituting equation 35 into 33, ω_{io} equals

$$\omega_{io}=[(\alpha_{ji}\Delta t)^2+4\alpha_{gi}]^{1/2} \tag{36}$$

Substitute equation 36 into 30,

$$\alpha_i \geq \frac{K_P}{K_R}[(\alpha_{ji}\Delta t)^2+4\alpha_{gi}]^{1/2} \tag{37}$$

Note that equation 30 was derived assuming that the RCS engines were fired to counteract gravity gradient torques that would have cause the i^{th} axis to exceed the attitude deadband limit, therefore

$$\alpha_i=\alpha_{ji}-\alpha_{gi} \tag{38}$$

Substitute equation 38 into 37,

$$\alpha_{ji}-\alpha_{gi}\geq\frac{K_P}{K_R}[(\alpha_{ji}\Delta t)^2+4\alpha_{gi}]^{1/2} \tag{39}$$

Solving equation 39 for α_{ji}, α_{ji} equals

$$\alpha_{ji}\geq\frac{\alpha_{gi}}{[1-(\frac{K_P}{K_R}\Delta t)^2]}+(\frac{K_P}{K_R})\left[\frac{4\alpha_{gi}\theta_o}{[1-(\frac{K_P}{K_R})\Delta t)^2]}+\frac{\alpha_{gi}{}^2\Delta t^2}{[1-(\frac{K_P}{K_R})\Delta t)^2]^2}\right]^{1/2} \tag{40}$$

Equation 40 can be approximated by

$$\alpha_{ji} \geq \left(\frac{K_P}{K_R}\right) \left[\frac{4\alpha_{gi}\theta_o}{1-\left(\frac{K_P}{K_R}\Delta t\right)^2}\right]^{1/2} \tag{41}$$

α_{ji} equals

$$\alpha_{ji} = \frac{T_{ji}}{I_{ii}} = \frac{F_i\ \ell}{I_{ii}} \tag{42}$$

where T_{ji} is the torque generated about the i^{th} axis due to one RCS engine pair firing. From equations 41 and 42, the lower limit on engine thrust F_i equals

$$F_i = \frac{2}{\ell}\left(\frac{K_P}{K_R}\right) \left[\frac{I_{ii}T_{gi}|_{ra}\theta_o}{1-\left(\frac{K_P}{K_R}\ \Delta t\right)^2}\right]^{1/2} \tag{43}$$

Assume that $\frac{K_P}{K_R}$ equals one. Substituting the appropriate values of ℓ, Δt, I_{ii}, and $T_{gi}|_{ra}$ into equation 43, F_i equals

$$F_x = 82\ \theta_o^{1/2} \tag{44}$$

$$F_y = 9.15\text{x}10^2\ \theta_o^{1/2} \tag{45}$$

$$F_z = 9.02\text{x}10^2\ \theta_o^{1/2} \tag{46}$$

Note that F_x is smaller than either F_y and F_z, and also note that F_y and F_z are almost twice as large as the maximum value of engine

thrust F given in equation 22. The above values of F_y and F_z were computed using the worst case average rectified gravity gradient torque $T_{gy}|_{ra}$ and $T_{gz}|_{ra}$, but the shuttle orbiter is stabilized in a X-POP attitude in order to minimize these torques. For the X-POP stabilized shuttle orbiter, $T_{gy}|_{ra}$ and $T_{gz}|_{ra}$ are due only to Y and Z axis attitude errors. The actual value of $T_{gy}|_{ra}$ and $T_{gz}|_{ra}$ are estimated to be approximately two orders of magnitude smaller than their worst case values, therefore the value of F_{max} given in equation 22 is valid and the minimum value of F, F_{min}, equals the above value of F_x.

$$F_{min} = F_x = 82\ \theta_o^{1/2} \tag{47}$$

The limits on the RCS engine thrust level F are

$$F_{min} < F < F_{max}$$

$$82\ \theta_o^{1/2} < F < 510\ \theta_o^{1/2} \tag{48}$$

Figure A1-6 is a plot of F_{max}, F_{min}, and a nominal thrust level F_{nom} as a function of the attitude deadband $\pm\theta_o$ The selected nominal value F_{nom} equals

$$F_{nom} = 260\ \theta_o^{1/2} \tag{49}$$

For an attitude deadband θ_o ranging from 0.291 mrad (1 min) to 8.7 mrad (0.5 degree), the nominal thrust level F_{nom} varies from 4.45 N (1 lbf) to 24.3 N (5.7 lbf), respectively.

A1.3.2. Sizing of the Shuttle Orbiter RCS Stabilization System Total Impulse $\Sigma F\Delta t$ Requirement - Assume that the shuttle orbiter is stabilized in the X-POP attitude shown in figure A1-7. The gravity gradient torques acting on the shuttle orbiter are:

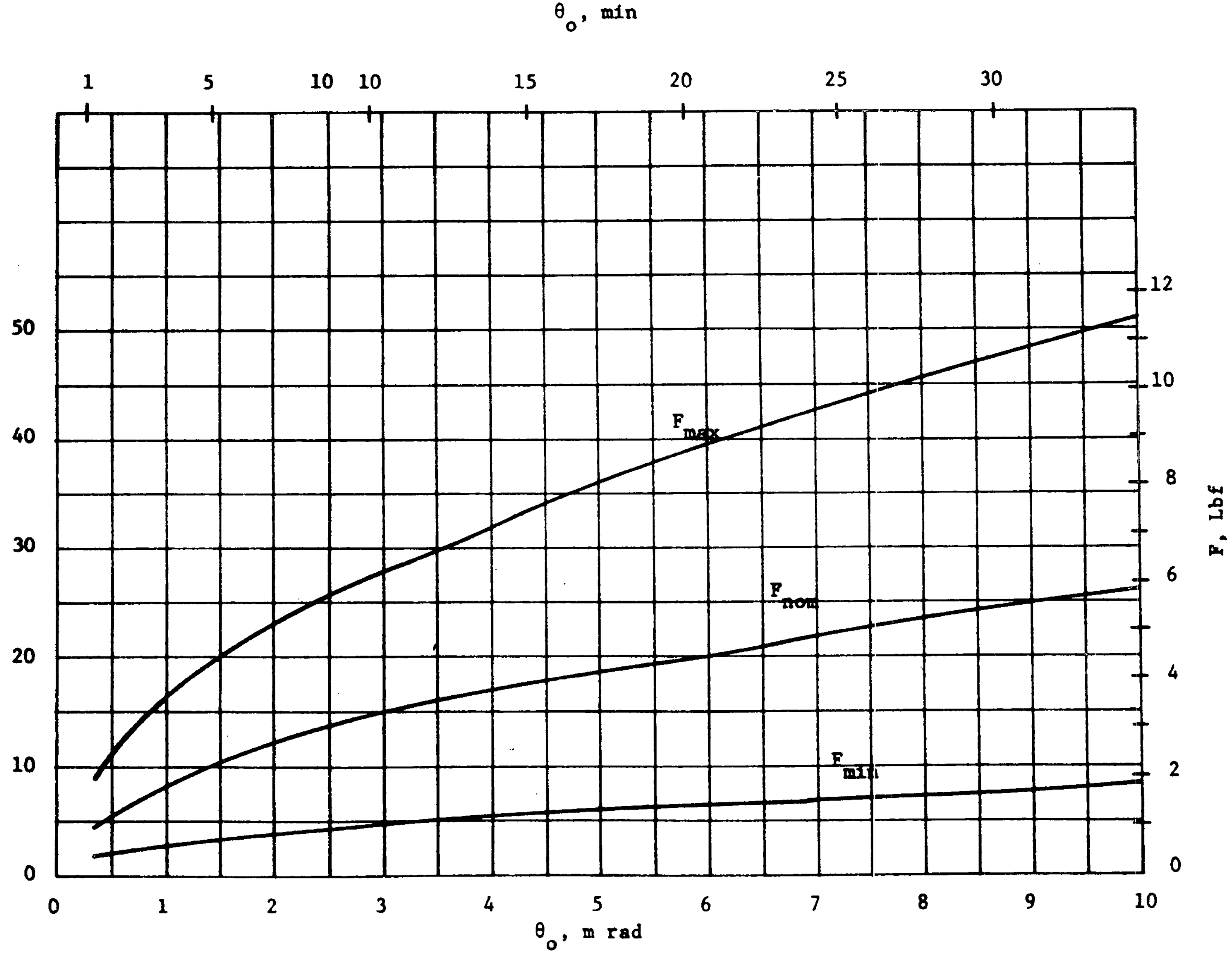

Figure A1-6. Shuttle Orbiter RCS Thrust Level Vs Attitude Deadband $\pm\theta_o$

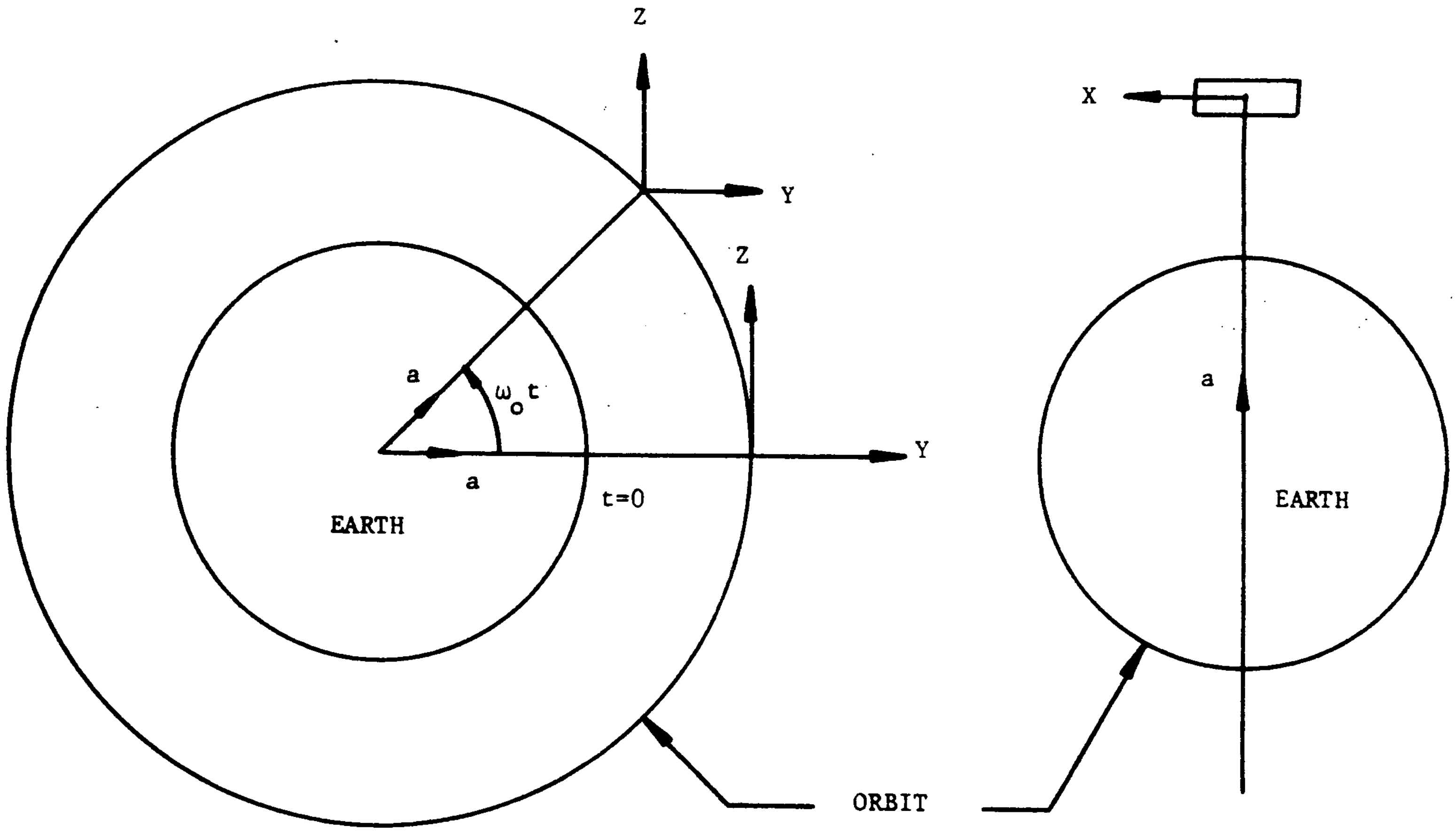

Figure A1-7. Sketch of Shuttle Orbiter X-POP Attitude

$$T_{gx}=3\omega_o^2\ a_y a_z\ (I_{zz}-I_{yy}) \tag{50}$$

$$T_{gy}=3\omega_o^2\ a_x a_z\ (I_{xx}-I_{zz}) \tag{51}$$

$$T_{gz}=3\omega_o^2\ a_x a_y\ (I_{yy}-I_{xx}) \tag{52}$$

where a_x, a_y, and a_z are the components of the local vertical unit vector $\hat{a}$ shown in figure A1-7. The components of $\hat{a}$ are

$$a_x=0 \tag{53}$$

$$a_y=\cos\ \omega_o t \tag{54}$$

$$a_z=\sin\ \omega_o t \tag{55}$$

Assume the shuttle orbiter is misaligned from the true X-POP attitude by two small rotational angles ε_y and ε_z about the Y and Z axes, respectively. The resulting local vertical vector $\hat{a}'$ equals

$$\hat{a}' = \begin{vmatrix} a_x' \\ a_y' \\ a_z' \end{vmatrix} = \begin{vmatrix} 1 & \varepsilon_z & -\varepsilon_y \\ -\varepsilon_z & 1 & 0 \\ \varepsilon_y & 0 & 1 \end{vmatrix} \begin{vmatrix} a_x \\ a_y \\ a_z \end{vmatrix}$$

$$\hat{a}' = \begin{vmatrix} \varepsilon_z \cos\ \omega_o t - \varepsilon_y \sin\ \omega_o t \\ \cos\ \omega_o t \\ \sin\ \omega_o t \end{vmatrix} \tag{56}$$

Assume that ε_y and ε_z are equal ($\varepsilon_y=\varepsilon_z=\varepsilon$). The resultant gravity gradient torques are

$$T_{gx}'=3\omega_o^2\, a_y'\, a_z'\, (I_{zz}-I_{yy})$$

$$=\frac{3\omega_o^2}{2}(I_{zz}-I_{yy})\sin 2\omega_o t \tag{57}$$

$$T_{gy}'=3\omega_o^2\, a_x'\, a_z'\, (I_{xx}-I_{zz})$$

$$=\frac{3\omega_o^2}{2}(I_{zz}-I_{xx})\,\varepsilon\,[1-\cos 2\omega_o t-\sin 2\omega_o t] \tag{58}$$

$$T_{gz}'=3\omega_o^2\, a_x'\, a_y'\, (I_{yy}-I_{xx})$$

$$=\frac{3\omega_o^2}{2}(I_{yy}-I_{xx})\,\varepsilon\,[1+\cos 2\omega_o t-\sin 2\omega_o t] \tag{59}$$

The total required impulse $\Sigma F\Delta t$ that the RCS must supply is directly proportional to the accumulated rectified angular momentum acting on the three vehicle axes. The rectified angular momentum $H_{gi}|_{X\text{-POP}}$ accumulated during one orbit due to the above gravity gradient torques are

$$H_{gx}|_{X\text{-POP}}=\int_0^{\frac{2\pi}{\omega_o}}|T_{gx}'|dt=6\omega_o(I_{zz}-I_{yy}) \tag{60}$$

$$H_{gy}|_{X\text{-POP}}=\int_0^{\frac{2\pi}{\omega_o}}|T_{gy}'|dt=\frac{3(4+\pi)\omega_o\varepsilon}{2}(I_{zz}-I_{xx}) \tag{61}$$

$$H_{gz}|_{X\text{-POP}}=\int_0^{\frac{2\pi}{\omega_o}}|T_{gz}'|dt=\frac{3(4+\pi)\omega_o\varepsilon}{2}(I_{yy}-I_{xx}) \tag{62}$$

Assume that ε equals $1.745\text{x}10^{-3}$ radian (1 degree). The accumulated momentums that the RCS system must counteract each orbit are

$$H_{gx}|_{X\text{-}POP} = 2\ 245 \text{ N-m-sec/orbit } (1\ 650 \text{ ft-lb-sec/orbit}) \tag{63}$$

$$H_{gy}|_{X\text{-}POP} = 1\ 470 \text{ N-m-sec/orbit } (1\ 080 \text{ ft-lb-sec/orbit}) \tag{64}$$

$$H_{gz}|_{X\text{-}POP} = 1\ 400 \text{ N-m-sec/orbit } (1\ 030 \text{ ft-lb-sec/orbit}) \tag{65}$$

The total rectified gravity gradient momentum that the RCS system must absorb equals

$$H_g|_{X\text{-}POP} = H_{gx}|_{X\text{-}POP} + H_{gy}|_{X\text{-}POP} + H_{gz}|_{X\text{-}POP}$$

$$= 5\ 115 \text{ N-m-sec/orbit } (3\ 760 \text{ ft-lb-sec/orbit}) \tag{66}$$

The total impulse $\Sigma F\Delta t|_{gg}$ per orbit needed to counteract $H_g|_{X\text{-}POP}$ equals

$$\Sigma F\Delta t|_{gg}/\text{orbit} = \frac{2\ H_g|_{X\text{-}POP}}{\ell}$$

$$= 560 \text{ N-sec/orbit } (126 \text{ lb-sec/orbit}) \tag{67}$$

The total mission impulse $\Sigma F\Delta t|_{gg}$ equals

$$\Sigma F\Delta t|_{gg}/\text{mission} = 59\ 400 \text{ N-sec/mission } (13\ 400 \text{ lb-sec/mission}) \tag{68}$$

The RCS system besides absorbing the rectified angular momentum $H_g|_{X\text{-}POP}$ must counteract the rectified momentum due to aerodynamic torques, $H_{aero}|_{ra}$. Assume that $H_{aero}|_{ra}$ equals

$$H_{aero}|_{ra} = 0.05\ H_g|_{X\text{-}POP}$$

$$= 256 \text{ N-m-sec/orbit } (188 \text{ ft-lb-sec/orbit}) \tag{69}$$

The impulse $\Sigma F\Delta t|_{aero}$ per orbit needed to absorb $H_{aero}|_{ra}$ equals

$$\Sigma F\Delta t|_{aero}/\text{orbit} = \frac{2\ H_{aero}|_{ra}}{\ell}$$

$$= 28 \text{ N-sec/orbit (6.3 lb-sec/orbit)} \tag{70}$$

The total mission impulse $\Sigma F\Delta t|_{aero}$ equals

$$\Sigma F\Delta t|_{aero}/\text{mission} = 2\ 970 \text{ N-sec/mission (669 lb-sec/mission)} \tag{71}$$

$\Sigma F\Delta t|_{gg}$ and $\Sigma F\Delta t|_{aero}$ are the minimum total impulses that are necessary to perfectly absorb the gravity gradient and aerodynamic rectified angular momentum. During portions of the orbit, the magnitude of the gravity gradient and aerodynamic torques are too small to prevent the vehicle control axes from limit cycling back and forth through the deadband. Assume that the additional impulse expended due to this limit cycling $\Sigma F\Delta T|_{LC}$ per orbit equals

$$\Sigma F\Delta t|_{LC}/\text{orbit} = 0.25(\Sigma F\Delta t|_{gg}/\text{orbit} + \Sigma F\Delta t|_{aero}/\text{orbit})$$

$$= 147 \text{ N-sec/orbit(33.1 lb-sec/orbit)} \tag{72}$$

The total mission $\Sigma F\Delta t|_{LC}$ equals

$$\Sigma F\Delta t|_{LC}/\text{mission} = 15\ 600 \text{ N-sec/mission (3 520 lb-sec/mission)} \tag{73}$$

The average time per axis between each RCS pulse t_f required to stabilize the shuttle orbiter equals

$$t_f = \frac{1.71\text{x}10^4\ F}{(\Sigma F\Delta t)'} \tag{74}$$

where

$$(\Sigma F\Delta t)' = \Sigma F\Delta t|_{gg}/\text{orbit} + \Sigma F\Delta t|_{aero}/\text{orbit}$$

$$+ \Sigma F\Delta t|_{LC}/\text{orbit}$$

$$= 735 \text{ N-m/orbit (542 ft-lb/orbit)}$$

In figure A1-8, t_f versus θ_o is plotted for the nominal thrust level F_{nom} shown in figure A1-6. For an attitude deadband θ_o ranging from 0.291 mrad (1 $\widehat{\text{min}}$) to 8.75 mrad (0.5 degree), the average time per axis between RCS pulses t_f varies from 103 to 605 seconds.

During the ASM mission, the shuttle orbiter is assumed to be maneuvered on the average of four times a day or 28 times a mission. A maneuver rate capability ω_{man} of 2.91×10^{-4} radian per second (1 degree per minute) is assumed about the shuttle orbiter axis corresponding to its maximum moment of inertia (i.e., Z axis). To perform this maneuver, the RCS system must impart the following impulse to the shuttle orbiter

$$\Sigma F\Delta t|_{man}/\text{maneuver} = \frac{4(I_{zz}\omega_{man})}{\ell}$$

$$= 3\ 260 \text{ N-sec/maneuver (734 lb-sec/maneuver)} \tag{75}$$

The total mission impulse $\Sigma F\Delta t|_{man}$ alloted for maneuvering is

$$\Sigma F\Delta t|_{man}/\text{mission} = 28\ (\Sigma F\Delta t|_{man}/\text{maneuver})$$

$$= 91\ 200 \text{ N-sec/mission (20 500 lb-sec/mission)} \tag{76}$$

After the shuttle orbiter is placed in its X-POP attitude by its baseline ACPS, the low thrust RCS system takes over control by absorbing the remaining residual momentum left by the baseline system. Assume that the shuttle orbiter is in a torque-free environment. For the shuttle orbiter baseline ACPS, this assumption was shown to be valid in section A1.1. Each vehicle axis will limit cycle between the limits of the ACPS attitude deadband $\pm\theta_o$. Figure A1-2 is a sketch of this ACPS attitude deadband. The lower limit, $-\theta_o$, is designated state a, and the upper limit is designated state b. Assume the i^{th} vehicle axis is at state a.

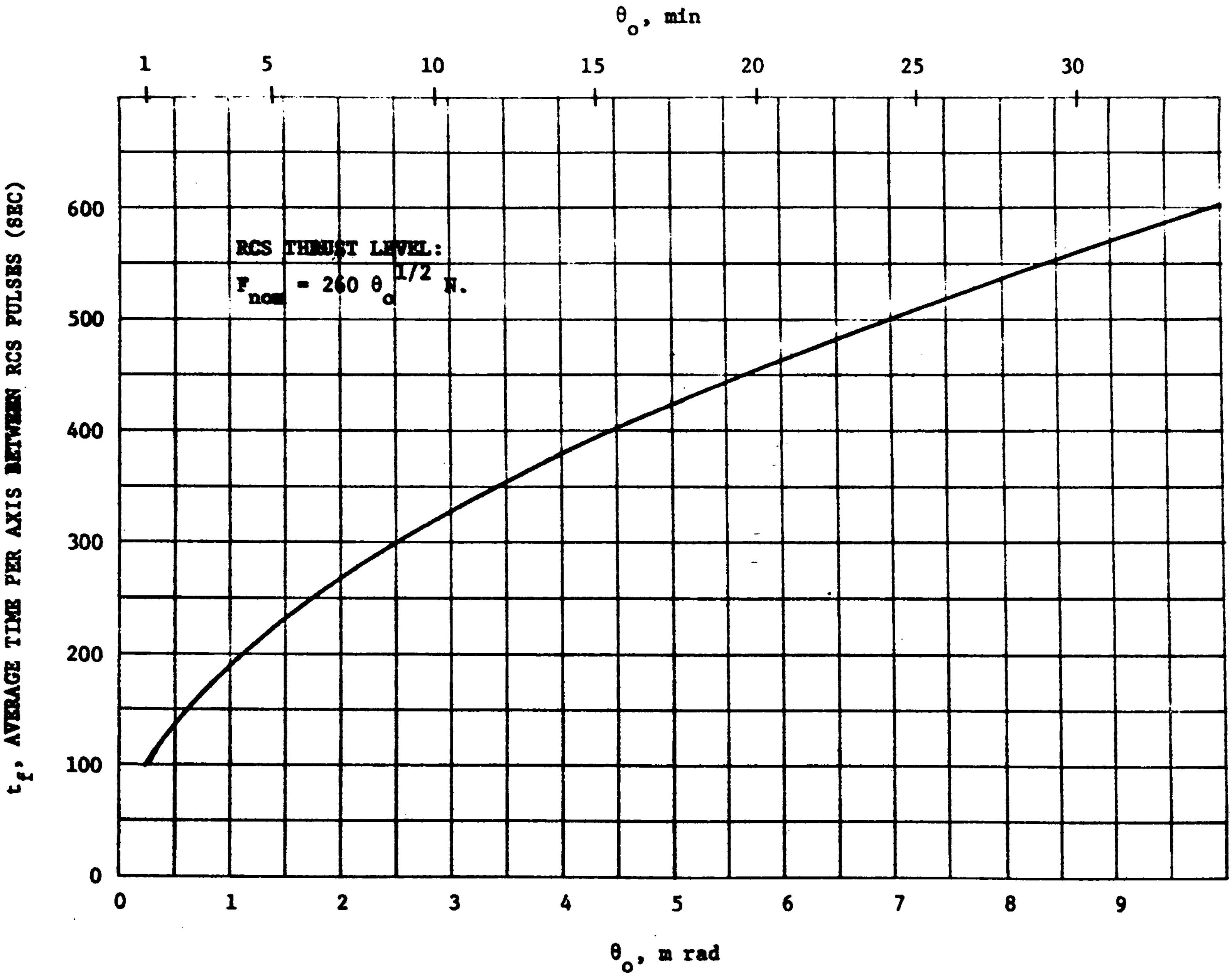

Figure A1-8. Average Time Per Axis Between RCS Pulses Vs Attitude Deadband $\pm\theta_o$

At this point, the RCS thrusters will fire sending the i^{th} axis towards state b. As the i^{th} axis traverses the deadband from a to b, the axial angular velocity ω_{ab} equals

$$\omega_{ab}=\omega_i+\omega_{ab}(0) \tag{77}$$

where ω_i is the change in angular rate about the i^{th} axis due to a single ACPS firing. The position of the axis θ_{ab} equals

$$\theta_{ab}=[\omega_i+\omega_{ab}(0)]t-\theta_o \tag{78}$$

When the axis reaches state b, the thrusters fire once more sending the vehicle back towards a. The angular velocity ω_{ba} and position θ_{ba} as the axis travels back towards a equal

$$\omega_{ba}=-\omega_i+\omega_{ba}(0) \tag{79}$$

$$\theta_{ba}=[-\omega_i+\omega_{ba}(0)]t+\theta_o \tag{80}$$

From equation 78, the time t_{ab} for the axis to traverse the deadband from state a to state b equals

$$\theta_{ab}=\theta_o=[\omega_i+\omega_{ab}(0)]t_{ab}-\theta_o$$

$$t_{ab}=\frac{2\theta_o}{\omega_i+\omega_{ab}(0)} \tag{81}$$

From equation 80, the time t_{ba} to return to state a equals

$$\theta_{ba}=-\theta_o=[-\omega_i+\omega_{ba}(0)]t_{ba}+\theta_o$$

$$t_{ba}=\frac{2\theta_o}{\omega_i-\omega_{ba}(0)} \tag{82}$$

Under steady state conditions

$$t_{ab}=t_{ba} \tag{83}$$

Therefore, using equations 81, 82, and 83,

$$\omega_{ab}(0)=-\omega_{ba}(0) \tag{84}$$

Since the angular velocity of the i^{th} axis cannot change instantaneously at either boundary of the deadband, the following expressions can be written using equations 77 and 79.

$$\omega_{ba}(0)=\omega_i+\omega_{ab}(0) \tag{85}$$

$$\omega_{ab}(0)=-\omega_i+\omega_{ba}(0) \tag{86}$$

Using equations 84, 85, and 86, the following expressions for $\omega_{ab}(0)$ and $\omega_{ba}(0)$ can be written

$$\omega_{ab}(0)=-\frac{\omega_i}{2} \tag{87}$$

$$\omega_{ba}(0)=\frac{\omega_i}{2} \tag{88}$$

The residual momentum that can be absorbed thus equals

$$H_{tran}=\sum_i I_i\omega_{ba}(0)=0.5\sum_i I_{ii}\omega_i \qquad (i = x,y,z) \tag{89}$$

From section A1.1, ω_i equals

ω_x=2.81 mrad/sec (0.161 deg/sec)

ω_y=0.482 mrad/sec ($27.6\text{x}10^{-3}$ deg/sec)

ω_z=0.463 mrad/sec ($21.6\text{x}10^{-3}$ deg/sec)

Substituting the above values of ω_i into equation 89, H_{tran} equals

H_{tran}=5 865 N-m-sec (4 320 ft-lb-sec)

The transitional impulse $\Sigma F\Delta t|_{tran}$ that the low thrust RCS must expend to absorb this residual momentum equals

$$\Sigma F\Delta t|_{tran} = \frac{2H_{tran}}{\ell} = 642 \text{ N-sec (144 lb-sec)}$$

When an RCS system is pulsed, part of its fuel is lost at the beginning and end of each pulse. This lost fuel is ejected from the RCS as raw fuel. Figure A1-9 is presented to explain the source of this loss. The pulse illustrated in this figure is typical of an RCS system. The long rise and tail-off times shown are important when an RCS thruster is being pulsed at a high rate. The sources of the rise time are (1) valve opening times, (2) ignition delays, and (3) incomplete mixing. Short ignition delays tend to promote incomplete mixing by setting up a high energy gaseous interface at the impingement point; the propellants are blown apart. This lost fuel is very important in regard to experiment contamination if the effluents are increased significantly or new chemical compounds different from the normal combustion products are introduced into the experimental environment. The curve shown in figure A1-9 is presented to show approximately how the fuel loss varies with pulse widths. To minimize fuel loss the pulse width should be as long as is consistent with the shuttle orbiter stability requirements.

For an effective pulse duration Δt of 80 msec, it is estimated that 5 percent of the fuel will be lost in the above way. This lost fuel can be measured in lost system impulse capability $\Sigma F\Delta t|_{lost}$. For the 7-day ASM mission, the lost system impulse capability equals

$$\Sigma F\Delta t|_{lost}/\text{mission}=0.05(\Sigma F\Delta t|_{gg}/\text{mission}+\Sigma F\Delta t|_{aero}/\text{mission}$$
$$+\Sigma F\Delta t|_{LC}/\text{mission} + \Sigma F\Delta T|_{man}/\text{mission}$$
$$+\Sigma F\Delta t|_{tran})=8\ 450\ \text{N-sec/mission}\ (1\ 900\ \text{lb-sec/mission}) \qquad (90)$$

The low thrust RCS system impulse $\Sigma F\Delta t$ required for the X-POP stabilized shuttle orbiter is sized in table A1-3. The contingency factor of 2 is added to provide a safety factor, an additional maneuver capability, and to account for other sources of disturbances such as crew motion not contained in this fuel budget. Much of this contingency fuel budget could be used if the average number of maneuvers per day is increased above the allotted four maneuvers a day, approximately one maneuver every fourth orbit. Note that the largest single fuel budget item is for maneuvering $\Sigma F\Delta t|_{MAN}$.

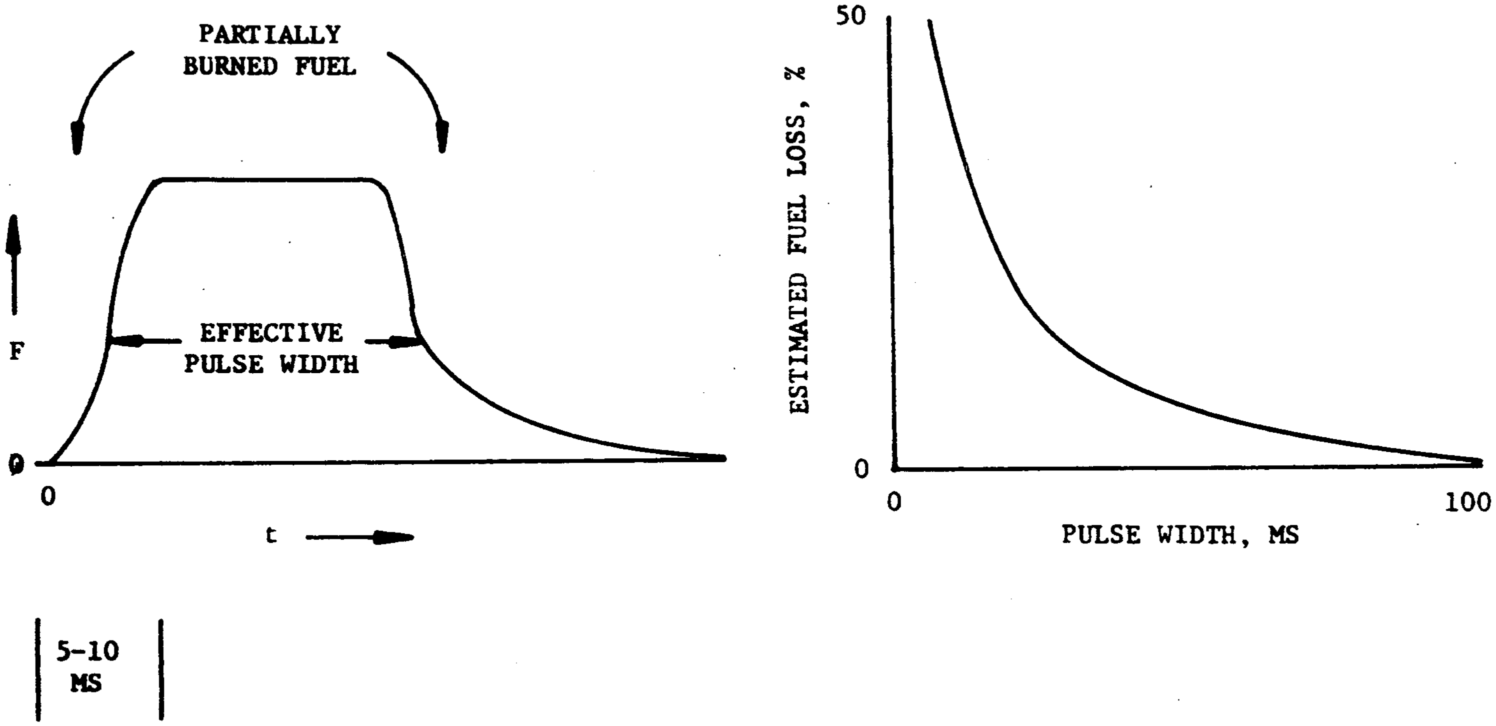

Figure A1-9. RCS Pulse Shape and Fuel Loss

Table A1-3. Sizing of the Low Thrust RCS Impulse for a X-POP Stabilized Shuttle Orbiter for a 7-Day ASM Mission

$\Sigma F\Delta t\|_{gg}$	59 400 N-sec	(13 400 lb-sec)
$\Sigma F\Delta t\|_{aero}$	2 970 N-sec	(669 lb-sec)
$\Sigma F\Delta t\|_{lc}$	15 600 N-sec	(3 520 lb-sec)
$\Sigma F\Delta t\|_{man}$	91 200 N-sec	(20 500 lb-sec)
$\Sigma F\Delta t\|_{tran}$	642 N-sec	(144 lb-sec)
$\Sigma F\Delta t\|_{loss}$	8 450 N-sec	(1 900 lb-sec)
Sub Total	178 262 N-sec	(40 133 lb-sec)
Contingency Factor	X 2	
Total $\Sigma F\Delta t\|$	356 524 N-sec	(80 266 lb-sec)

A1.4. REACTION CONTROL SYSTEM CONTAMINATION

A1.4.1. Effluents - For an RCS system using high performance bipropellants (e.g., N_2H_4/N_2O_4), the total weight of propellants used in a nominal 7-day mission (W_p) may be about 200 kg (440 lb). If we assume that it takes 30 minutes to sweep the resultant cloud away from the spacecraft, and that it is being continuously replaced, there will be an average of 145/(7)(48), or 0.43 kg of combustion products in the cloud throughout the mission. The total mass of combustion products in the cloud (M) then is

$$M=0.43 \text{ kg}$$

a. Local Density in the Cloud of Combustion Products - To determine local density, assume

1) Spherical symmetry (simpler)

2) A fixed mass exists in the cloud = M
(rate of clearing = rate of addition from thrusters)

3) A radial distribution varying like $1/r^4$ (typical of a process of this kind)

4) A minimum spacecraft radius = R_o.

Based on these assumptions, $p(r,\theta,\phi) = pcr$, and the total integral of ρ over all space must equal the cloud's total mass M:

$$M = \int_v \rho(r)dv = \int_{R_o}^{\infty} \rho(r)4\pi r^2 dr = 4\pi k\int_{R_o}^{\infty} \frac{dr}{r^2} = 4\pi k/R_o$$

If $\rho(r)=kr^{-4}$, $\rho(r)= \frac{MR_o}{4\pi r^4}$; where $R \geq R_o$.

Take R_o as 2 meters, the local density of combustion products at radius r is then

$$\rho(r)= \frac{(.43)(2)}{4\pi r^4} = \frac{0.07}{r^4} \text{ kg/m}^3;$$

and the local density at the surface (R).

$$\rho_s=.004 \text{ kg/m}^3.$$

b. Total Mass in a Cylindrical Column - To determine the total mass in a cylindrical column, the integration of $\rho(r)$ is performed over the semi-infinite "tube" or prism of a sufficiently small cross-section, for instance (1 cm by 1 cm)

$$M_{pc} = \int_{R_o}^{\infty} \rho(r)dr = \int_{R_o}^{\infty} \frac{MR_o}{4\pi} \frac{dr}{r^4} = -\frac{MR_o}{4\pi} \frac{1}{3r^3}\Bigg|_{R_o}^{\infty} = \frac{M}{12\pi R_o^2}$$

$$M_{pc} = \frac{.43}{12\pi R_o^2} = .003 \text{ kg/m}^2$$

c. Total Mass of Combustion Products Per Steradian - To determine the total mass of combustion products per steradian out to radius r

$$M_{p\Omega} = \frac{M}{4\pi}\left(1-\frac{R_o}{r}\right) \frac{\text{kg}}{\text{steradian}}$$

$$= .034 - \frac{.069}{r} \text{ kg/steradian}$$

and the total mass (to ∞) in a 1 steradian cone = $M_{P\Omega}$ = .034 kg/steradian.

d. Exhaust Plume Impingement - References 1 and 2 indicate that about 2% of a rocket plume will impinge beyond 90° from the nozzle axis over a radius averaging 12 meters. In 7 days, one RCS nozzle may exhaust (assuming six nozzles) 145/6 kg of products. Therefore, the combustion products impinging on surfaces of the vehicle may be about

$$M_1 = \frac{145}{6\pi r^2} = \frac{145}{6\pi(12)^2}$$

$$= 0.053 \text{ kg/m}^2$$

e. Uncombined Propellants - From section A1.3.2, it appears that about 5% of the propellants will remain uncombined at 80 milliseconds pulse width. Most of these uncombined propellants will be expelled into the cloud as a gas or as droplets. A smaller part of it will be carried much more slowly in the boundary layer of the nozzle and may merely run back to nearby surfaces.

The part that is carried in the boundary layer could create a serious contamination problem if the source were near a critical surface, as the material is cold and hence a large fraction of it might be deposited. This is probably not the case with the shuttle orbiter, as one would expect the RCS nozzles to be located at the extremities of the orbiter vehicle, and not near any critical optical surfaces.

f. Constituents of the RCS induced Atmosphere - Based on references 3 and 4, table A1-4 contains a list of potential products that appear to be typical for high performance propellants.

Most of these constiuents will be in the form of gases at temperatures near the exhaust temperature of 1200° to 1800° K. Much of the carbon, however, is likely to be in solid form, made up of small particles. The uncombined propellants, as previously mentioned, will be gaseous or droplets. The sodium potassium, and rare earths, which are potential fuel impurities, would appear mainly as gases. Nitric acid, a product of incomplete burning of MMH or UDMH, would appear as a gas. Ablative materials, complex hydrocarbons perhaps from nozzle liners if used, might appear largely in solid form.

Table A1-4. RCS Contamination Constituents

CONSTITUENT	% BY VOL IN CLOUD	ESTIMATED STICKING COEFFICIENTS @ LIQUID N_2 TEMPERATURES	IN SHADE	IN SUN
H_2O	7.1	1.0	.1	.01
H_2	46.2	0	0	0
N_2	24.0	0	0	0
CO	15.1	1.0	.1	.01
CO_2	1.5	1.0	.1	.01
C	1.1	1.0	.1	.01
UNCOMBINED PROPELLANTS	5.0	1.0	.1	.01
Na	0.003	0.5	.05	.005
K	0.003	0.5	.05	.005
HNO_3	UNK	1.0	.1	.01
ABLATIVE MATERIAL	UNK	0.5	.05	.005
RARE EARTHS	TRACE	0.5	.05	.005

The sticking coefficients were estimated in order to obtain a rough idea of the quantities that might accumulate on critical surfaces, either from the cloud or from direct impingement of the RCS exhaust. It was not possible for this study to attempt calculation of the accumulation of material on the critical surfaces, but only to make some comments about potential effects.

A1.4.2. Shuttle Contamination Model - The total contamination potential may be estimated by consideration of the data presented in table A1-5. The shuttle contamination model contains basic orbiter contamination sources (taken for the most part from the General Dynamics RAM reports) plus the estimated effluents expected from a small (4 lb) RCS stabilization system. The key issue is that portion of the potential contaminants that cannot be programmed for ejection when astronomy experiments are protected.

Fortunately, most of the potential contaminants will be used, or can be ejected at a time before or after the observation period. However, cabin leakage, outgassing, and that part of the RCS effluents needed to stabilize the orbiter during observation cannot be programmed. These effluents will be sources of continuous contamination throughout the mission and, except for outgassing, will be relatively constant.

It is seen that the addition of an RCS stabilization system would double the amount of unprogrammable contaminants, and would probably add significant quantities of some new elements to the induced atmosphere surrounding the spacecraft.

A1.4.3. Potential Effects of RCS Effluents

a. Introduction - The majority of the combustion by-products resulting from the firing of RCS engines are ejected at high velocities. These will leave the spacecraft area rapidly, and produce no interfering effects on the scientific instruments or subsystems. A portion of the exhaust material, however, leaves the engines at low velocities, and therefore remains close to the spacecraft, basically in orbits similar to that of the spacecraft. Eventually this material is accelerated away from the spacecraft by atmospheric drag and by radiation pressure, but while it is close to the spacecraft, scattering and absorption of electromagnetic energy may be expected.

Absorption by the contamination cloud, whether preferential (from atomic lines) or spectrally broad (attenuation by deposition material and/or by molecular bands) is a potential hazard when either absolute or relative intensity measurements are being made

Table A1-5. Contamination Model

SOURCE	MATERIAL	RATE OF DISCHARGE	PROGRAM DISCHARGE	ACPS	LOW THRUST RCS	CMG
FUEL CELL DUMP	H_2O	190 LB/DAY (1)	YES	✓	✓	✓
WASTE	H_2O	3.3 LB/MAN-DAY (1)	YES	✓	✓	✓
SHUTTLE CABIN LEAKAGE	$N_2 + O_2 + H_2O$	9.3 LB/DAY (1)	NO	✓	✓	✓
RESEARCH MODULE LEAKAGE	$N_2 + O_2 + H_2O$	10 LB/DAY (2)	NO	✓	✓	✓
OUTGASSING	ORGANIC GASES & PARTICLES	1 LB/DAY (3)	NO	✓	✓	✓
ACPS ($\pm$0.5 DEG)	H_2O, CO, ETC	815 LB/DAY (4)	NO	✓		
MAN & TRANS RCS	H_2O, CO, ETC	21 LB/DAY (4)	YES		✓	
RCS STABILIZATION	H_2O, CO, ETC	20 LB/DAY (4)	NO		✓	

NOTES:
(1) DATA EXTRACTED FROM RAM TASK 4.2/4.3 REVIEW DATED 10 DEC 1971
(2) DATA BASED ON SORTIE CAN CONCEPTUAL DESIGN, ASR-PD-DO-72-2, MARCH 1, 1972
(3) ESTIMATED BASED ON SKYLAB MODEL
(4) BASED ON PROPELLANT REQUIREMENTS

on the source, such as with a photometer, where the band pass may be wide enough to include an unexpected absorption line due to the cloud and thereby perturb the instrument intensity calibration.

For high resolution spectroscopy, in addition to degradation of absolute and relative intensity calibration of the instrument, the acquisition of data for spectral line profiles could be foiled by the unexpected influence of nearby or overlapping absorption lines and bands due to the contaminant cloud, particularly in the case of a complex profile such as the solar hydrogen Lyman α line at 121.6 nm and the resonance lines of Mg II (magnesium atoms with one electron removed, which have a single valence electron configuration like sodium) at λ 279.6 and 280.3 nm in the ultraviolet range. The Lyman α line already has a sharp absorption core due to atomic hydrogen between the earth and the sun with a column density of approximately 2×10^{12} cm^{-2} above 200 km altitudes, and is useful in determining that quantity. The spacecraft cloud could influence this measurement if atomic hydrogen was present in high concentrations.

Scattering effects must be considered if a large number of particles drifts within the field of view of an observing instrument. The most important source of energy for scattering is the sun, but earthshine and moonshine cannot be ignored. Noncoherent (or Mie) scattering could be a severe problem in the presence of sunlight (reference 5). Even for the worst case model, Rayleigh (or molecular or coherent) scattering due to interactions of photons with free molecules, does not appear to be a problem that requires reckoning (reference 6).

The contamination effects on the scientific instruments considered here are based on particular models that were assumed for the chemistry of combustion and for the exhaust ejection and dispersal processes. No detailed experimental verifications are available that lend support or discredit the models. The contamination effects discussed here should be considered as tentative estimates; supporting tests and detailed analyses will be necessary to develop better estimates.

The column densities assumed for the various chemical species, based on the models described above, are listed in table A1-6 and a summary of potential effects is given in table A1-7. Some of these contamination effects are discussed in the following paragraphs.

Table A1-6. Estimated Column Densities of Individual Chemical Species in the Contaminant Cloud

SPECIES	COLUMN DENSITY cm^{-2}	COLUMN THICKNESS atmo-cm
Water, total molecules	$8x10^{17}$	.03
vapor phase	$2x10^{17}$	.008
ice particles (D=1-100 μm)	($n=4x10^{4}$)	-
Hydrogen, molecular (H_2)	$5.2x10^{18}$	.19
atomic (H)	$1x10^{17}$	.004
Nitrogen (N_2)	$2.7x10^{18}$	.10
Carbon Monoxide (CO)	$1.7x10^{18}$	.06
Carbon Dioxide (CO_2)	$1.7x10^{17}$	.006
Carbon Granules (D≟0.1 μm)	($n≟2x10^{11}$)	-
Sodium (Na)	$2.4x10^{14}$	10^{-5}
Potassium (K)	$2.4x10^{14}$	10^{-5}
*Unburned propellants, N_2O_4	($1.4x10^{17}$)	-
$CH_3 \cdot NH:NH_2$	($4.2x10^{17}$)	-

*(Most likely in droplet form, no size estimate available).

Table A1-7. Potential RCS Contamination Effects

CONSTITUENT	POTENTIAL CLOUD EFFECTS	POTENTIAL DEPOSITION EFFECTS
H_2O	STRONG ABSORBTION BANDS IN IR & FOR $\lambda < 2000$ Å; SEVERE SUNLIGHT SCATTERING IF ICE IN CLOUD	SEVERE ABSORBTION ON IR INST; SEVERE SUNLIGHT SCATTERING IF ICE DEPOSITED ON SOLAR INST
H_2	ABSORBTION BANDS IN UV	NONE
N_2	OPAQUE FOR $\lambda < 1000$ Å	NONE
CO, CO_2	STRONG ABSORBTION BANDS IN IR	SEVERE ABSORBTION ON IR INST
C	POSSIBLE SUNLIGHT SCATTERING	POSSIBLE SUNLIGHT SCATTERING
Na, K	SEVERE ABSORBTION AT RESONANCE LINES	COULD BE SEVERE WITH WATER
HNO_3	POSSIBLE ABSORBTION BANDS	IF DILUTE, MAY ATTACK OPTICAL COATINGS
UNCOMBINED PROPELLANTS	ABSORBTION BANDS IN IR SCATTERING OF SUNLIGHT	UNKNOWN
ABLATIVE MATERIALS	POSSIBLE SCATTERING	POSSIBLE SCATTERING

b. Water - In its various forms, water is singled out as the most critical combustion byproduct, as far as contamination effects are concerned. It will be encountered mostly in the vapor and ice crystal phases, and occasionally condensed onto cool surfaces in the liquid phase.

In the vapor phase, the major effect anticipated is the absorption at selected wavelengths, which is important in the infrared and ultraviolet ranges. In the infrared range, for the assumed column density of 2×10^{17} cm^{-2}, attenuation will be observed at the 2.7, 6.3 and 60 µm bands, reaching depths of attenuation of between 2 and 20 percent (references 6, 7, 8). Infrared spectroscopy studies of celestial sources will therefore be partially masked by this selective absorption. If adequate measurements are made of the water vapor column density, it may be possible to partially compensate for this masking by subjecting the data to post-mission processing.

In the ultraviolet range, water vapor exhibits substantial absorption for wavelengths shorter than 180 nm (references 6, 9). The anticipated column density will result in absorption ranging from 4 to 30 percent between 110 and 180 nm, increasing to approximately 90 percent absorption at 100 nm and shorter wavelengths.

The nucleation of water into the form of ice crystals, or snow, is also anticipated. These crystals may be of comparatively large dimensions, with diameters ranging from 1 to 100 µm (reference 5). The larger particles will remain close to the spacecraft for extended periods. The primary effect of these ice particles will be scattering. The column densities of ice crystals predicted by the assumed model indicate that the scattered sunlight will be as much as four orders of magnitude brighter than the radiance of the night sky away from the galactic equator (reference 5). This may preclude observations of faint stellar sources during the sunlit portion of the orbit, and of the outer solar corona, if RCS is used for attitude control.

Deposition and condensation of water vapor on the optical surfaces within the instruments may also occur. A preliminary analysis suggests that this problem will be most pronounced with the cryogenically-cooled infrared telescope. Broadband absorption and scattering are anticipated from this type of condensate.

c. Hydrogen and Nitrogen - The most abundant species in the RCS exhaust is hydrogen. It is expected to be present mainly

in the molecular form, H_2, but may also appear in appreciable proportions as atomic hydrogen (due to the ineffectiveness of the radiative association mechanism for formation of molecular hydrogen (reference 10).

Molecular hydrogen in its ground state has no permanent dipole moment, and therefore shows only weak absorption in the infrared range (reference 11). Significant absorption is observed when the molecule is excited to electronic states, i.e., the Lyman and Werner progressions or bands, which start at 110.8 and 100.9 nm respectively (references 9, 10). In this range, absorption due to the anticipated column density will be as high as 85 percent (reference 2).

The excited levels of the hydrogen molecule have long lifetimes (reference 10). For these excited states, the dipole moment is not zero, which will result in absorption lines in the infrared range. The proportion of molecules in the excited states that should be expected is not known, and should be investigated carefully if RCS attitude control techniques are selected.

The atomic hydrogen component is a different problem. A small proportion of the hydrogen in the monoatomic form, say one percent of the anticipated hydrogen in the cloud, will result in an optical depth of 0.6 (45 percent absorption) at several of the wavelengths of the Lyman series. This will contribute to the far ultraviolet absorption due to the molecular bands, which was described above.

The condensation of hydrogen onto critical optical surfaces is not anticipated, even on cryogenically-cooled surfaces, due to its very low boiling temperature, 20.3 K.

Molecular nitrogen is not as abundant in the RCS exhaust as is hydrogen. It should be present mainly in the gaseous molecular form, N_2. The most prominent effect of the nitrogen "atmosphere" around the spacecraft will be observed in the far ultraviolet, beyond the line limit for atomic hydrogen at 91 nm. In this range, the absorption produced by the anticipated N_2 concentration could be as high as 99 percent (reference 6).

The gaseous nitrogen is not expected to condense onto critical optical surfaces, due to its low boiling temperature of 77 K. The single possible exception is the cryogenically-cooled infrared telescope, for which surface temperatures could be 27 K or lower.

d. Carbon Monoxide and Carbon Dioxide - These two stable oxides of carbon will appear in the RCS exhaust. The carbon monoxide (CO) concentration in the exhaust is expected to be approximately ten times higher than the carbon dioxide (CO_2) level, apparently due to an oxygen-poor combustion mixture.

Both of the carbon oxides show strong absorption in the ultraviolet range (references 9,13). The absorption spectrum of CO shows peaks at several discrete wavelengths within each band, reaching maximum values of nearly 10 percent. The anticipated column density would be opaque in the 20 to 70 nm extreme ultraviolet range. The absorption spectrum of CO_2 is generally smoother than part of CO. The anticipated concentration should result in moderate absorption (7-40 percent) at all wavelengths shorter than 160 nm, except at the 112 and 114 nm absorption peaks, for which it could be virtually opaque.

In the infrared range, CO will not cause any noticeable absorption problems. Carbon dioxide shows strong absorption peaks at 2.8, 4.3, and 15 μm, which will reach values of 35 percent absorption for the anticipated column density.

Condensation of the carbon oxides on critical optical surfaces is not possible except on the cryogenically-cooled infrared telescope.

e. Sodium and Potassium - The fuel used in the RCS engines may include sodium and potassium in "trace" concentrations, approximately 100 parts per million.

The effect of absorption at the sodium and potassium resonance wavelengths is virtually complete (total absorption) in a continuum if the supposed concentrations are correct. The supposed cloud concentration of sodium would hinder meaningful observations of the solar sodium D-lines, as well as observations of the sodium airglow emission layer, if Doppler line shifts are neglected. The Doppler shift ($\Delta\lambda/\lambda=v/c$) for a relative velocity equal to the orbital velocity ($\doteq 7.5 \times 10^5$ cm/sec) is about 0.15 Å. The full-width half-maximum of the Naλ5890 Å line is about 0.03 Å at 1200° K, and, so, one would assume that the shift is sufficient to prevent attenuation of the emission line of a source such as the airglow layer, but that the removal of radiation from a continuum would still occur at the shifted wavelength. However, for this relative motion with respect to the sun, the shifted absorption line would

still fall well within the Fraunhofer D_2 line (FWHM≐1Å). There could also be the situation where the relative velocity of the cloud and the source is small, causing serious absorption to occur at line center.

It is realized that the potential targets of Astronomy Sortie Missions include sources other than the sun or the earth's airglow. The problems that could be caused by absorption in the spacecraft cloud apply to those sources as well as the sun and the airglow. The spectral characteristics of the source being investigated should be considered, with respect to each experiment objective, for cloud perturbations of that spectrum.

Because of the sharpness of the spacecraft cloud absorption lines, the possibility of the use of certain strong absorption lines (such as the Na D-lines) as a wavelength calibration when viewing a source having emission (either line or continuum) in the region of the cloud line might be considered.

f. Droplets and Granules - Some of the material emitted with the RCS exhaust is expected to be in droplet or granule form. The free carbon resulting from incomplete propellant combustion has a tendancy to cluster or aggregate into granules. The interior surfaces of the RCS thruster nozzles will show a tendency to ablate, releasing small particles of solid material (mostly ceramics), and the fraction of the liquid propellants that does not burn at all at thruster startup and shutoff will come out of the nozzle mostly in droplet form.

These nongaseous forms will produce scattering of sunlight and scattering from other bright sources. Adhesion onto critical surfaces may also take place. We do not have enough detailed data concerning the RCS combustion process in small thrusters to allow a meaningful estimate of the importance of these residues as contaminants.

Since RCS thrusters may continue to be candidate devices for attitude control, it will be necessary to analyze and evaluate these possible effects to determine if and/or how they interfere with the Astronomy Sortie Missions scientific observations.

A1.5. OTHER CONSIDERATIONS FOR RCS SYSTEMS

A1.5.1. Temperature Range - A propellant for use in a reaction control system must possess a high degree of thermal stability.

This is required to resist heat soak-back from the combustion chamber which can be especially acute due to the interrupted flow demand required in this type of application. During periods of no flow, inlet plumbing can become sufficiently hot to allow the propellants to be heated to relatively high temperatures. Care must be taken to insure that the propellant temperatures do not exceed the safe level. Vapor phase decomposition of hydrazine in particular may be hazardous.

A1.5.2. Hazards - Most high performance propellants are toxic. Pure hydrazine forms detonatable vapors, which are high pressure gases that may also rupture bladders. In the Apollo 15 flight, 6 pounds of hydrazine were dumped through a hot nozzle and caused a fire that burned parachute shrouds.

A1.5.3. Materials Compatibility - Nitrogen tetroxide, especially, is rather incompatible with most elastomers; although recent bladder design has to a large degree circumvented this problem.

A1.5.4. Handling and Maintainability - Most of the above considerations suggest a handling and maintenance problem. This is little different than that already existing for the ACPS, but will add some to the magnitude and complexity.

A1.5.5. Reliability - Generally, hot gas bipropellant systems will be less reliable than monopropellant or cold gas systems. Hot gas control valves tend to be less reliable than cold gas valves, accumulators are required to stabilize the system, and of course, the bipropellant system has about twice as many components.

A1.5.6. Hardware Interfaces - All reaction control systems will have direct interfaces with the orbital vehicle, which will affect the orbiter design and development. These will be mainly electrical and structural; although the inclusion of any stability augmentation system will create some operational interfaces. An RCS system mounted externally on the orbiter will require inclusion of devices in the orbiter design for ejection of the RCS pods prior to reentry.

A1.6. REFERENCES

1. Etheridge, F. G. and Boudreaux, R. A., Attitude Control Rocket Exhaust Plume Effects on Spacecraft Functional Surfaces, Journal of Spacecraft and Rockets, January 1970, AIAA.

2. Boudreaux, R. A. and Etheridge, F. G., Attitude Control Rocket Exhaust Plume Impingement, AFRPL-TR-67-3, February 1967.

3. Elverum, G. W. Jr. and Stoudhammer, P., The Effect of Rapid Liquid-Phase Reactions on Injector Design and Combustion in Rocket Motors, Progress Report 30-4, JPC, Caltech, August 1959.

4. Sutton, G. P., Rocket Propulsion Elements, John Wiley and Sons, 1956.

5. Newkirk, G., Jr. (1967) The Optical Environment of Manned Spacecraft; Planetary and Space Science, 15, 1967.

6. Allen, C. W. (1963) Astrophysical Quantities; London, Athalone Press.

7. Fridovich, G., and J. R. Kinard (1972) Intensity-Half Width Products for Seven Lines in the 6.3 μm Water Vapor Band; Jour. Opt. Soc. Am. 62, 542.

8. Lawson, K. E. (1961) Infrared Absorption of Inorganic Substances; New York, Reinhold.

9. Hudson, R. D. (1971) Critical Review of Ultraviolet Photoabsorption Cross Sections for Molecules of Astrophysical and Aeronomic Interest; Reviews of Geophysics and Space Physics, 9, 305. Also reprinted by the National Bureau of Standards as National Standard Reference Data System publication NSRDS-NBS-38.

10. Green, A. E. S. (Ed.) (1966) The Middle Ultraviolet: Its Science and Technology; New York, Wiley.

11. Dalgarno, A., and E. L. Wright (1972) Infrared Emissivities of H_2 and HD Astrophysical Journal Letters, 174, L49.

12. Haddad, G. N., K. H. Loran, A. J. D. Farmer, and J. H. Carver (1968) An Experimental Determination of the Oscillator Strengths for some Transitions in the Lyman Bands of Molecular Hydrogen; Jour. Quant. Spectrosc. Radiat. Transfer, 8, 1193.

13. Thomson, B. A., P. Harteck, R. R. Reeves Jr. (1963) Ultraviolet Absorption Coefficients of CO_2, CO, O_2, H_2O, N_2O, NH_3, NO, SO_2 and CH_4 between 1850 and 4000 Å; Jour. Geophys. Res., 68, 6431.

14. Ratliff, Audeh, and Thornbill, Analysis of Exhaust Plumes From Skylab - Configuration R-4D Attitude Control Motors, MSFC Report CR-61332, March 1970.

15. Moore, W. W., Environmental Simulation Testing of Solar Cell Contamination By Hydrazine, MSFC Report.

APPENDIX A2

INTERFACES AND SUPPORT HARDWARE

INTRODUCTION

This appendix includes:

ABBREVIATIONS AND ACRONYMS

ITEM	ABBREVIATION OR ACRONYM
Cargo Lift Trailer (Used with Guppy)	CL Trailer
Environmental Cover and Control Unit (Covers and Protects SL and Pallet)	ECCU
Guppy Payload Pallet (Supports payload in Guppy)	--
Payload Carrier Processing Facility (Orbiter and payload processing area at Launch or Landing Site)	PCPF-LS
Payload Environmental Supply Unit (Provides atmosphere to payload in orbiter cargo bay)	PESU
Payload Integration Center - MSFC	PIC-MSFC
Payload Processing Facility (Receiving, assembly and inspection building at Launch or Landing Site)	PPF-LS
Payload Processing Facility - MSFC (Multi room building housing cleanrooms)	PPF-MSFC
Payload Transfer Dolly	PT Dolly
Payload Transportation Fixture	PT Fixture
Principal Investigator	PI
Product Integrity Engineer	PIE
Shuttle Maintenance and Checkout Facility (Launch Site cleanroom with airlock for maintaining the Shuttle orbiter)	MCF-LS
Sortie Lab	SL
Space Astronomy Control Facility	SACF

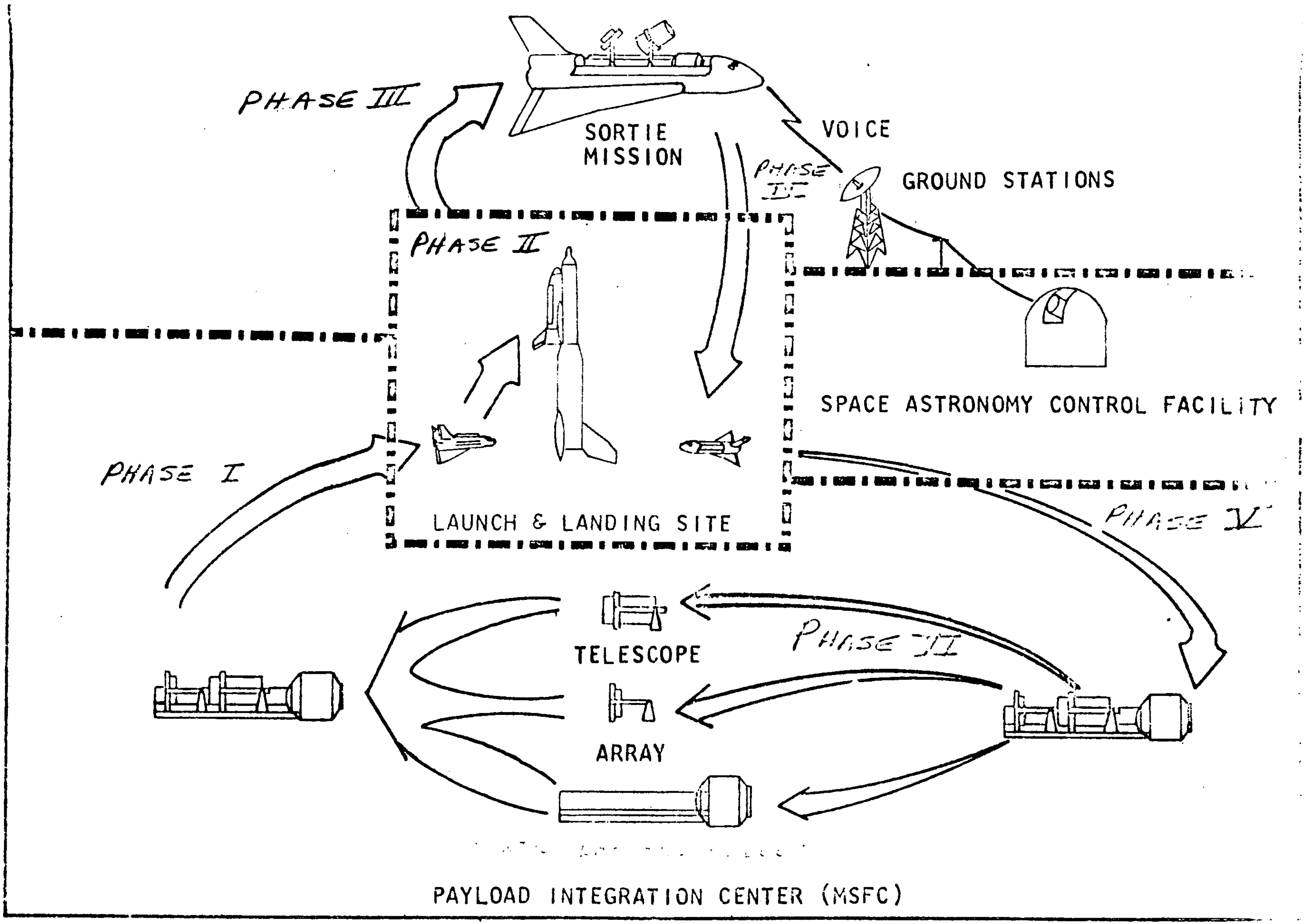

FIGURE 2.2-1 PRELIMINARY OPERATIONAL CONCEPT

PIC-MSFC TRANSIENT CREW

The Payload Integration Center - MSFC transient crew includes the following personnel:

1 Product Integrity Engineer (PIE)

2 Quality control engineers

1 ECCU Specialist

2 SL Pallet Engineers

2 SL Pallet Technicians

3 Scientists

3 Experiment Technicians

PIC-MSFC TRANSIENT GUPPY SUPPORT CREW

The PIC-MSFC crew to support the payload during loading in the Super Guppy aircraft, flight, and offloading includes the following personnel:

1 PIC

1 QC Engineer

1 ECCU Specialist

PHASE I - Pack, Ship, Deliver to Launch Site

Scope:

Pack refurbished and serviced payload at the PIC (MSFC), transfer to the Shuttle Launch Site, and deliver to the Launch Site payload processing facility.

Duration:

42 hours

Facilities:

Payload Processing Facility - MSFC

Airlock

Payload Assembly Area

MSFC Airport

Launch Site Airport

Payload Processing Facility - Launch Site

Airlock

Clean Area

Manpower:

14 PIC (MSFC) Transient Crew

3 PIC (MSFC) Transient Guppy Support Crew

2 Crane Operators

6 Handling Crew

2 PPF-MSFC Facility Crew

2 PPF-LS Facility Crew

2 Tractor Operator (PT Dolly)

2 Escort Vehicle drivers

1 State Patrolman

1 Tractor Operator (CL Trailer)

1 Guppy Cargomaster

3 Guppy Crew

2 General Mechanics

Support Equipment:

1 PT Fixture	1 State Patrol Escort Car
1 ECCU	2 13-Ton Portable Cranes
1 PT Dolly	1 CL Trailer
1 Tractor (PT Dolly)	1 Tractor (CL Trailer)
1 Payload Lifting Sling Set	1 Super Guppy Aircraft
1 Lo-Boy and Tractor, With Tiedowns	2 Ladders
2 Escort Vehicles	1 Cleaning Supplies Set
	4 Work Stands

EVENTS SEQUENCE AND RESOURCE REQUIREMENTS

PHASE I

FUNCTION	DURATION	FACILITIES	MANPOWER		SUPPORT EQUIPMENT	
			NO.	SKILL	NO.	DESCRIPTION
A. Install ECCU, purge and stabilize, using facility supplies	8 hours	Payload assembly area of PPF-MSFC	14 2 6 2	PIC-MSFC transient crew Crane operators Handling crew PPF-MSFC facility crew	1 1	PT Fixture ECCU
B. Place payload on PT Dolly, move into airlock and activate ECCU	2 hours	Payload assembly area of PPF-MSFC and airlock of PPF-MSFC	14 2 6 2 2	PIC-MSFC transient crew Crane operators Handling crew Tractor operator (PT Dolly) PPF-MSFC facility crew	1 1 1 1 1	PT Fixture ECCU PT Dolly Tractor (PT Dolly) Payload lifting sling set
C. Lift payload from PT Dolly, place on Lo-Boy and tie down	3 hours	Airlock of PPF-MSFC	14 2 6 2 2 2	PIC-MSFC transient crew Crane operators Handling crew Tractor operator (Lo-Boy) Tractor operator (PT Dolly) PPF-MSFC facility crew	1 1 1 1 1 1	PT Fixture PT Dolly ECCU 25 ton Lo-Boy and tractor, with tiedowns Tractor (PT Dolly) Payload lifting sling set
D. Transport payload to Super Guppy aircraft at MSFC airport	4 hours	None	2 3 6 2 1	Tractor operator (Lo-Boy) PIC-MSFC transient Guppy Support crew Handling crew Escort vehicle drivers State patrolman	1 2 1 1 1	25 ton Lo-Boy and tractor, with tiedowns Escort vehicles State patrol escort car PT Fixture ECCU
E. Place Guppy Payload Pallet on CL Trailer; lift payload from Lo-Boy and place on Pallet	3 hours	MSFC airport	1 2 3 2 6 1 2	Guppy Cargomaster Tractor operator (Lo-Boy) PIC-MSFC transient Guppy Support crew Crane operators Handling crew Tractor operator (CL Trailer) General mechanics	1 1 1 2 1 1 1 1	25 ton Lo-Boy and tractor, with tiedowns PT Fixture ECCU 13 ton portable crane CL Trailer Tractor (CL Trailer) Super Guppy aircraft Payload lifting sling set
F. Load payload into Super Guppy aircraft and secure, and connect payload to Guppy support	3 hours	MSFC airport	1 6 1 2	Guppy Cargomaster Handling crew Tractor operator (CL Trailer) General mechanics	1 1 1 1 1	PT Fixture ECCU CL Trailer Tractor (CL Trailer) Super Guppy aircraft
G. Fly payload from MSFC airport to launch site airport	4 hours	None	3 3	PIC-MSFC transient Guppy Support crew Guppy Crew	1 1 1	PT Fixture ECCU Super Guppy aircraft
H. Prepare to unload payload (includes visual check, review of ECCU recorded data and disconnect of payload from Guppy support)	3 hours	LS airport	3 1 2	PIC-MSFC transient Guppy Support crew Guppy Cargomaster General mechanics	1 1 2 1	PT Fixture ECCU Ladders Super Guppy aircraft

EVENTS SEQUENCE AND RESOURCE REQUIREMENTS

PHASE I (continued)

FUNCTION	DURATION	FACILITIES	MANPOWER NO.	MANPOWER SKILL	SUPPORT EQUIPMENT NO.	SUPPORT EQUIPMENT DESCRIPTION
I. Unload payload from Super Guppy onto CL Trailer and activate ECCU	2 hours	Launch Site airport	1	Guppy Cargomaster	1	PT Fixture
			6	Handling crew	1	ECCU
			1	Tractor operator (CL Trailer)	1	CL Trailer
			3	PIC-MSFC transient Guppy Support crew	1	Tractor (CL Trailer)
					1	Super Guppy aircraft
			2	General mechanics		
J. Transfer payload to Lo-Boy and return Guppy Payload Pallet to aircraft	2 hours	Launch Site airport	1	Guppy Cargomaster	1	PT Fixture
			6	Handling crew	1	ECCU
			3	PIC-MSFC transient Guppy Support crew	1	CL Trailer
					1	Tractor (CL Trailer)
			2	Crane operators	1	Super Guppy aircraft
			1	Tractor operator (CL Trailer)	2	13 ton portable cranes
			2	Tractor operators (Lo-Boy)	1	25 ton Lo-Boy and tractor, with tiedowns
			2	General mechanics	1	Payload lifting sling set
K. Transfer payload on Lo-Boy into PPF-LS airlock, connect ECCU to facilities support	4 hours	Airlock of PPF-LS	2	Tractor operators (Lo-Boy)	1	PT Fixture
			6	Handling crew	1	ECCU
			2	Escort vehicle drivers	1	25 ton Lo-Boy and tractor, with tiedowns
			14	PIC-MSFC transient crew	2	Escort vehicles
			2	Facility crew		
L. Transfer payload from Lo-Boy to PT Dolly, wipe down all exposed surfaces, and move into clean area of PPF-LS	4 hours	Airlock and clean area of PPF-LS	2	Crane Operators	1	PT Fixture
			6	Handling crew	1	ECCU
			2	Tractor operators	1	25 ton Lo-Boy and tractor, with tiedowns
			14	PIC-MSFC transient crew	1	PT Dolly
			2	Facility crew	1	Tractor (PT Dolly)
			2	Tractor operator (PT Dolly)	4	Work stands
					1	Cleaning supplies set
					1	Payload lifting sling set

PHASE II - Receipt-to-Launch at Launch Site

Scope:

Perform receiving inspection of payload at the Launch Site payload processing facility, verifying environments encountered, status of operating systems, and installing (and verifying) items that were not integrated at the PIC (MSFC). The flight-ready payload is installed in the orbiter, installation is verified, and monitored during orbiter prelaunch operations. Final servicing is performed on-pad during the pre-countdown period. The last operation is launch.

Duration:

190 hours

Facilities:

Payload Processing Facility - Launch Site

Airlock

Clean Area

Payload Carrier Processing Facility - Launch Site

Airlock

Clean area

Shuttle Launch Pad

Manpower:

14 PIC-MSFC Transient Crew

2 PPF-LS Facility Crew

2 Crane Operators

6 Handling Crew

2 PI

2 Cryogenics servicemen

Manpower: (Continued)

2 Tractor Operators (PT Dolly)

2 Escort Vehicle Drivers

2 PCPF-LS Facility Crew

6 Payload Installation Technicians

4 Orbiter Electrical Technicians

4 Orbiter Mechanical Technicians

1 PESU Specialist

Support Equipment:

1 PT Fixture

1 PT Dolly

6 Work Stands and Platform

1 ECCU

1 ECCU Lifting Sling Set

1 Cryogenics Servicing Unit

1 Battery Handling Equipment

1 Checkout Console

1 Tractor (PT Dolly)

2 Escort Vehicles

1 Cleaning Supplies

1 Payload Lifting Slings

1 PESU

EVENTS SEQUENCE AND RESOURCE REQUIREMENTS

PHASE II

FUNCTION	DURATION	FACILITIES	MANPOWER NO.	MANPOWER SKILL	SUPPORT EQUIPMENT NO.	SUPPORT EQUIPMENT DESCRIPTION
A. Review and interpretation of ECCU recorded data	4 hours	Clean area of PPF-LS	14 2	PIC-MSFC transient crew PPF-LS Facility crew	1 1 1 1	PT Fixture PT Dolly Work stand ECCU
B. Stabilize PPF-LS as 100,000 clean room	8 hours (Starts at beginning) of A	Clean area of PPF-LS	14 2	PIC-MSFC transient crew PPF-LS Facility crew	1 1 1	PT Fixture PT Dolly ECCU
C. Remove ECCU; perform receiving inspection	16 hours	Clean area of PPF-LS	14 2 6 2 1	PIC-MSFC transient crew Crane operators Handling crew PPF-LS Facility crew PI	1 1 1 6 1	PT Fixture PT Dolly ECCU Work stands and platform ECCU lifting sling set
D. Service Gamma-Ray detector Cryogenic cooling unit (on ECCU)	4 hours	Clean area of PPF-LS	14 2	PIC-MSFC transient crew Cryogenics servicemen	1 1 1 1	PT Fixture PT Dolly ECCU Cryogenics Servicing Unit
E. Install and secure ECCU and connect to facilities support	2 hours	Clean area of PPF-LS	14 2 6	PIC-MSFC transient crew Crane operators Handling crew	1 1 1 1	PT Fixture PT Dolly ECCU ECCU lifting sling set
F. Install flight batteries in SL	4 hours	Clean area of PPF-LS	14	PIC-MSFC transient crew	1 1 1 1	PT Fixture PT Dolly ECCU Battery handling equipment
G. Verify flight battery installation, verify readiness to mate payload with orbiter	3 hours	Clean area of PPF-LS	14	PIC-MSFC transient crew	1 1 1 1	PT Fixture PT Dolly ECCU Checkout console
H. Move payload on PT Dolly into PPF-LS airlock, disconnect ECCU facilities support, move to PCPF-LS airlock, connect ECCU to facilities support, wipe down all exposed surfaces, and move into clean area	5 hours	Airlock and clean area of PPF-LS, and airlock and clean area of PCPF-LS	14 2 2 6 2 2	PIC-MSFC transient crew Tractor operator (PT Dolly) Escort vehicle drivers Handling crew PPF-LS Facility crew PCPF-LS Facility crew	1 1 1 1 2 4 1	PT Fixture PT Dolly ECCU Tractor (PT Dolly) Escort vehicles Work stands Cleaning supplies

EVENTS SEQUENCE AND RESOURCE REQUIREMENTS

PHASE II (continued)

FUNCTION	DURATION	FACILITIES	MANPOWER NO.	MANPOWER SKILL	SUPPORT EQUIPMENT NO.	SUPPORT EQUIPMENT DESCRIPTION
I. Stabilize PCPF-LS as 100,000 clean room	8 hours	Clean area of PCPF-LS	14 2	PIC-MSFC transient crew Facility crew	1 1 1	PT Fixture PT Dolly ECCU
J. Remove ECCU, attach crane to payload, release payload from PT Fixture	5 hours	Clean area of PCPF-LS	14 2 6	PIC-MSFC transient crew Crane operators Handling crew	1 1 1 4 1 1	PT Fixture PT Dolly ECCU Work stands ECCU lifting sling set Payload lifting sling set
K. Install Payload in Orbiter - Structural mate and secure; Connect electrical and mechanical service lines to orbiter; Connect access tunnel to orbiter; Connect controls and displays in orbiter; Connect electrical and mechanical umbilicals; and Connect PESU	6 hours	Clean area of PCPF-LS	14 2 6 6 4 1 4	PIC-MSFC transient crew Crane operators Handling crew Payload installation technicians Orbiter electrical technicians PESU specialist Orbiter mechanical technicians	1 4 1	Payload lifting slings Work stands PESU
L. Verify payload to orbiter interfaces - Hazard warning Data management and voice Control and Display Ground power Tunnel leak check Fluid systems leak check	6 hours	Clean area of PCPF-LS	14 2 6 6 4 4 1	PIC-MSFC transient crew Crane operators Handling crew Payload installation technicians Orbiter electrical technicians Orbiter mechanical technicians PESU specialist	1 1	Checkout console PESU
M. Close orbiter payload bay doors, begin purge of bay, orbiter preparation, mate to booster, transfer to launch pad, mate to pad, preliminary checks	95 hours	Airlock and clean area of PCPF-LS and Shuttle launch pad	14 4 4 1 2	PIC-MSFC transient crew Orbiter electrical technicians Orbiter mechanical technicians PESU specialist PI	1	PESU
N. Service Payload - High pressure gas systems Cryogenics systems Fuel cell service and activation Verify cryogenics refrigeration operation	4 hours	Shuttle launch pad	14 4 4 1 2	PIC-MSFC transient crew Orbiter electrical technicians Orbiter mechanical technicians PESU specialist PI	1	PESU
O. Orbiter cabin closeout, countdown preparation, countdown	24 hours	Shuttle launch pad	14 4 4 1 2	PIC-MSFC transient crew Orbiter electrical technicians Orbiter mechanical technicians PESU specialist PI	1	PESU
P. Launch						

PHASE III - Ascent and orbital flight

Scope:

Begins with liftoff and includes all flight operations through preparation for deorbit.

Duration:

168 hours

Facilities:

Space Astronomy Control Facility

Offices

Observatory

Shuttle Mission Control (Payload Monitor Only)

Landing Site (Mission Monitor)

Manpower:

Portion of Space Astronomy Control Facility personnel, scheduled in 2 twelve hour shifts to provide continuous coverage of mission.

1 Telescope PI

1 Wide Coverage X-Ray Array PI

1 Array PI

9 Experiment specialists

14 PIC-MSFC Transient Crew

Support Equipment:

Telephone voice and facsimile link between SACF and Shuttle Mission Control

C.2

EVENTS SEQUENCE AND RESOURCE REQUIREMENTS

PHASE III

FUNCTION	DURATION			FACILITIES	MANPOWER		SUPPORT EQUIPMENT
	SOLAR	SIII	IR		NO.	SKILL	
A. Boost, insert, transfer, attitude stabilization	2:30	2:30	2:30	Shuttle Mission Control (Payload Monitor Only) LS Monitor			
B. SL checkout and crew ingress	1:00	1:14	1:00	Shuttle Mission Control (Payload Monitor Only) LS Monitor			
C. Payload inspection, deployment and checkout	3:51	2:14	6:30	Shuttle Mission Control Space Astronomy Control Facility LS Monitor	1 1 1 9	Telescope PI Wide coverage X-Ray array PI Array PI Equipment specialists	Telephone voice and facsimile link between SACF and Shuttle Mission Control
D. Experimentation	154:29	155:27	151:35	Shuttle Mission Control Space Astronomy Control Facility LS Monitor	2	Twelve hour shift support by 9 Experiment specialists and 3 PIs	Telephone voice and facsimile link between SACF and Shuttle Mission Control
E. Payload shutdown and retract	2:47	3:14	2:50	Shuttle Mission Control Space Astronomy Control Facility	2	Twelve hour shift support by 9 Experiment specialists and 3 PIs	Telephone voice and facsimile link between SACF and Shuttle Mission Control
F. Secure SL and Pallet	:32	:32	:32	Shuttle Mission Control Landing Site	2	Twelve hour shift support by 9 Experiment specialists and 3 PIs	Telephone voice and facsimile link between SACF and Shuttle Mission Control
G. Checkout Orbiter	1:00	1:00	1:00	------	--	--------	--------

PHASE IV - Deorbit, safe, and remove payload, inspect and service payload

Scope:

Begins after the payload is secured and the orbiter is checked out with initiation of deorbit. Includes descent flight, landing of the orbiter, and safing and inspecting of the orbiter at the landing site. Transfer from the landing site to the payload carrier processing facility and processing through the airlock into the clean area is performed with the payload in the orbiter.

In the cleanroom, the orbiter cargo bay doors are opened, the payload is removed and placed on the PT Fixture which is located on the PT Dolly, and the ECCU is installed. The payload is then transferred to the landing site payload processing facility for inspection, data tape and film removal, and battery removal.

Duration:

42 hours

Facilities:

Shuttle Mission Control (Payload Monitor Only)

Landing Site

Payload Carrier Processing Facility-Landing Site

Airlock

Clean area

Payload Processing Facility-Landing Site

Airlock

Clean Area

Manpower:

14 PIC-MSFC Transient Crew

2 PCPF-LS Facility Crew

2 Crane Operators

6 Handling Crew

- Orbiter Ground Crew

2 Tractor Operator (PT Dolly)

2 Escort Vehicle Drivers

2 PPF-LS Facility Crew

Support Equipment:

1 PESU

1 PT Fixture

1 PT Dolly

1 ECCU

1 ECCU Lifting Sling Set

4 Work Stands

1 Tractor (PT Dolly)

2 Escort Vehicles

1 Cleaning Supplies

1 Guide Rail Set (for payload removal)

1 Battery Handling Equipment

EVENTS SEQUENCE AND RESOURCE REQUIREMENTS

PHASE IV

FUNCTION	DURATION	FACILITIES	MANPOWER NO.	MANPOWER SKILL	SUPPORT EQUIPMENT NO.	SUPPORT EQUIPMENT DESCRIPTION
A. Initiate deorbit, descend, and land orbiter	1 hour	Shuttle Mission Control Landing Site				
B. Safe, inspect, service, connect PESU, and transfer orbiter to PCPF-LS, process orbiter through airlock and move into clean area	13 hours	Landing Site Airlock of PCPF-LS and clean area of PCPF-LS	- - 14	Orbiter ground crew Facility crew PIC-MSFC transient crew	1	PESU
C. Service ECCU	3 hours (Simultaneous with B)	Airlock of PCPF-LS	14 2 2 6	PIC-MSFC transient crew Facility crew Crane operators Handling crew	1 1 1 1	ECCU PT Fixture PT Dolly ECCU lifting sling set
D. Disconnect payload from orbiter and switch to facility supplies, open and secure payload bay doors	2 hours	Clean area of PCPF-LS	14 2 -	PIC-MSFC transient crew Facility crew Orbiter ground crew	4	Work stands
E. Visual inspection of payload	1 hour	Clean area of PCPF-LS	14 -	PIC-MSFC transient crew Orbiter ground crew	4	Work stands
F. Remove payload from orbiter bay and place on PT Fixture located on PT Dolly	2 hours	Clean area of PCPF-LS	14 2 - 6 2 2	PIC-MSFC transient crew Facility crew Orbiter ground crew Handling crew Crane operators Tractor operators (PT Dolly)	1 1 1 4 1	PT Fixture PT Dolly Tractor (PT Dolly) Work stands Guide rail set (for payload removal)
G. Install and secure ECCU	2 hours	Clean area of PCPF-LS	14 2 6 2 2	PIC-MSFC transient crew Facility crew Handling crew Crane operators Tractor operators (PT Dolly)	1 1 1 1 1	PT Fixture PT Dolly Tractor (PT Dolly) ECCU ECCU lifting sling set
H. Move payload or PT Dolly into PCPF-LS airlock, move to PPF-LS airlock, wipe down all exposed surfaces, and move into clean area of PPF-LS	5 hours	Clean area of PCPF-LS Airlock of PCPF-LS Airlock of PPF-LS Clean area of PPF-LS	14 2 2 2 2 6	PIC-MSFC transient crew Tractor operator (PT Dolly) Escort vehicle drivers PCPF-LS Facility crew PPF-LS Facility crew Handling crew	1 1 1 1 2 4 1	PT Fixture PT Dolly ECCU Tractor (PT Dolly) Escort vehicles Work stands Cleaning supplies
I. Remove ECCU, remove payload film and tape, remove flight batteries, inspect SRM, pallet, and experiments	16 hours	Clean area of PPF-LS	14 2 2 6 2	PIC-MSFC transient crew Tractor operator (PT Dolly) PPF-LS Facility crew Handling crew PI	1 1 1 1 4 1 1	PT Fixture PT Dolly ECCU Tractor (PT Dolly) Work stands ECCU lifting sling set Battery handling equipment

PHASE V - Pack, ship, deliver to PIC (MSFC)

Scope:

Pack returned payload at the PPF-LS, transfer to MSFC, and deliver to the MSFC payload processing facility.

Duration:

34 hours

Facilities:

Payload Processing Facility-Landing Site

Airlock

Clean area

Landing Site Airport

MSFC Airport

Payload Processing Facility - MSFC

Airlock

Assembly Bay

Manpower:

14 PIC-MSFC Transient Crew

3 PIC-MSFC Transient Guppy Support Crew

2 Crane Operators

6 Handling Crew

2 PPF-MSFC Facility Crew

2 PPF-LS Facility Crew

2 Tractor Operator (PT Dolly)

2 Tractor Operator (Lo-Boy)

2 Escort Vehicle Drivers

1 State Patrolman

1 Tractor Operator (CL Trailer)

Manpower: (continued)

1 Guppy Cargomaster

3 Guppy Crew

2 General Mechanics

Support Equipment:

1 PT Fixture

1 ECCU

1 PT Dolly

1 Tractor (PT Dolly)

1 Payload lifting sling set

1 Lo-Boy and tractor, with tiedowns

2 Escort vehicles

1 State Patrol Escort

2 13-Ton Portable Cranes

1 CL Trailer

1 Tractor (CL Trailer)

1 Super Guppy aircraft

2 Ladders

1 Cleaning Supplies Set

4 Work Stands

EVENTS SEQUENCE AND RESOURCE REQUIREMENTS

PHASE V

FUNCTION	DURATION	FACILITIES	MANPOWER NO.	MANPOWER SKILL	SUPPORT EQUIPMENT NO.	SUPPORT EQUIPMENT DESCRIPTION
A. Service ECCU	3 hours (simultaneous operation - complete at start of B)	Airlock of PPF-LS	14	PIC-MSFC transient crew	1	PT Dolly
			2	Crane operators	1	Tractor (PT Dolly)
			6	Handling crew	1	ECCU
			2	Tractor Operators (PT Dolly)		
			2	Facility crew		
B. Install and secure ECCU	2 hours	Clean area of PPF-LS	14	PIC-MSFC transient crew	1	ECCU lifting sling set
			2	Crane operators	1	PT Fixture
			6	Handling crew	1	PT Dolly
			2	Tractor operators (PT Dolly)	1	ECCU
					4	Work stands
					1	Tractor (PT Dolly)
C. Move payload into airlock activate ECCU, and load onto Lo-Boy	3 hours	Airlock of PPF-LS	14	PIC-MSFC transient crew	1	PT Fixture
			2	Crane operators	1	PT Dolly
			6	Handling crew	1	Tractor (PT Dolly)
			2	Tractor operators (PT Dolly)	1	ECCU
			2	Facility crew	1	25 ton Lo-Boy and tractor, with tiedowns
			2	Tractor crew (Lo-Boy)	1	Payload lifting sling set
D. Transport payload to Super Guppy aircraft at airport	4 hours	Landing Site airport	3	PIC-MSFC transient Guppy Support crew	1	PT Fixture
					1	ECCU
			2	Tractor crew (Lo-Boy)	1	25 ton Lo-Boy and tractor, with tiedowns
			2	Escort vehicle drivers	2	Escort vehicles
E. Place Guppy Payload Pallet on CL Trailer, place payload on pallet and secure	3 hours	Landing Site airport	3	PIC-MSFC transient Guppy Support crew	1	PT Fixture
					1	ECCU
			2	Tractor crew (Lo-Boy)	1	25 ton Lo-Boy and tractor, with tiedowns
			6	Handling crew	2	13 ton portable cranes
			1	Tractor operator (CL Trailer)	1	Payload lifting sling set
			1	Guppy Cargomaster	1	CL Trailer
			2	Crane operators	1	Tractor (CL Trailer)
					1	Super Guppy aircraft
F. Load payload into Super Guppy and secure, attach ECCU to Guppy services	3 hours	Landing Site airport	3	PIC-MSFC transient Guppy Support crew	1	PT Fixture
					1	ECCU
			6	Handling crew	1	CL Trailer
			1	Tractor operator (CL Trailer)	1	Tractor (CL Trailer)
			1	Guppy Cargomaster	1	Super Guppy aircraft
G. Fly payload from Landing Site to PIC-MSFC	4 hours	Landing Site airport MSFC airport	3	PIC-MSFC transient Guppy Support crew	1	PT Fixture
					1	ECCU
			3	Guppy crew	1	Super Guppy aircraft

EVENTS SEQUENCE AND RESOURCE REQUIREMENTS

PHASE V (continued)

FUNCTION	DURATION	FACILITIES	MANPOWER NO.	MANPOWER SKILL	SUPPORT EQUIPMENT NO.	SUPPORT EQUIPMENT DESCRIPTION
H. Prep. to unload payload (visual check, review of ECCU recorded data, and disconnect ECCU from Guppy services)	3 hours	MSFC airport	3	PIC-MSFC transient Guppy Support crew	1	PT Fixture
					1	ECCU
			1	Guppy Cargomaster	1	Super Guppy aircraft
			2	General mechanics	2	Ladders
I. Unload payload from Super Guppy onto CL Trailer and activate ECCU	2 hours	MSFC airport	3	PIC-MSFC transient Guppy Support crew	1	PT Fixture
					1	ECCU
			1	Guppy Cargomaster	1	Super Guppy aircraft
			6	Handling crew	1	CL Trailer
			1	Tractor operator (CL Trailer)	1	Tractor (CL Trailer)
J. Transfer payload to Lo-Boy, and return Guppy Payload Pallet to aircraft	2 hours	MSFC airport	1	Guppy Cargomaster	1	PT Fixture
			6	Handling crew	1	ECCU
			3	PIC-MSFC transient Guppy Support crew	1	Super Guppy aircraft
					1	CL Trailer
			2	Crane operators	1	Tractor (CL Trailer)
			1	Tractor operator (CL Trailer)	1	25 ton Lo-Boy and tractor, with tiedowns
			2	Tractor operators (Lo-Boy)	2	13 ton portable cranes
					1	Payload lifting sling set
K. Transfer payload, on Lo-Boy into PPF-MSFC airlock, connect ECCU to facilities support	4 hours	Airlock of PPF-MSFC	2	Tractor operator (Lo-Boy)	1	PT Fixture
			3	PIC-MSFC transient Guppy Support crew	1	ECCU
					1	25 ton Lo-Boy
			2	Escort vehicle drivers	2	Escort vehicles
			2	Facility crew	1	State Patrol escort car
			1	State patrolman		
L. Transfer payload from Lo-Boy to PT Dolly, wipe down all exposed surfaces, move into clean area of PPF-MSFC, and place payload on floor pads	4 hours	Airlock of PPF-MSFC and Assembly Bay of PPF-MSFC	2	Crane operators	1	PT Fixture
			6	Handling crew	1	ECCU
			2	Tractor operators (Lo-Boy)	1	25 ton Lo-Boy and tractor, with tiedowns
			14	PIC-MSFC transient crew	1	PT Dolly
			2	Facility crew	1	Tractor (PT Dolly)
			2	Tractor operators (PT Dolly)	4	Work stands
					1	Cleaning supplies set
					1	Payload lifting sling set

Phase VI - Refurbish, integrate, and service payload at the Payload Integration Center (MSFC)

Scope:

With the payload on the payload transportation fixture protected by the ECCU and located in the assembly bay of the Payload Processing Facility at MSFC, the assembly bay is stabilized as a class 100,000 cleanroom. The ECCU is removed and the telescopes and arrays are removed and taken to individual refurbishment rooms. Subsystem components of the SL and Pallet are removed, serviced, modified and replaced.

When the SL and Pallet are ready to receive new telescopes and arrays, the flight units are installed and verified. Finally, the integrated payload is exercised in a combined systems test, completion of which constitutes readiness for flight.

Throughout Phase VI, responsible engineers and scientists at the MSFC Payload Integration Center prepare and revise mission program and individual experiment flight plans. Further, flight crews are trained (using simulators, spares, and training aid devices) throughout this phase.

Duration:

135 hours

Facilities:

Payload Processing Facility - MSFC

Assembly Bay

Individual Refurbishment and Rooms

Simulator and Crew Training Facility

Space Astronomy Control Facility (Planning)

Launch Site (Planning)

Mission Control Center (Planning)

Manpower:

14 PIC-MSFC Transient Crew

1 Telescope Team, having:

- 1 Telescope Engineer
- 5 Telescope Technicians

1 Array Team, having:

- 1 Array Engineer
- 5 Array Technicians

1 SL Pallet Team, having:

- 1 SL Pallet Engineer
- 4 SL Technicians

PIC Ground Support Personnel: (Portion)

- 2 Crane Operators
- 6 Handling Crew
- 2 Facility Crew
- 2 Tractor Operators (PT Dolly)
- \- Tractor Operator (Lo-Boy)
- \- Electric Tractor Operator

Instruction and Planning Personnel:

- 2 Telescope Operation Instructors
- 2 Array Operation Instructors
- 2 Simulator Instructors
- 3 Mission Planning Specialists
- 1 Planning Supervisor

1 Telescope PI

1 Array PI

2 Flight Experiment Trainees

Support Equipment:

1 PT Fixture

1 PT Dolly

1 ECCU

1 ECCU Lifting Sling Set

6 Work Stands

10 Work Tables

2 Polaroid Cameras

1 Ground Cooling Set

4 Payload Mounting Locks

4 Cable Slings

1 Telescope Handling Dolly

1 Array Handling Dolly

1 Electric Tractor

2 Video Tape Recorders

2 Instrumentation Tape Recorders

2 Digital Processing Consoles

2 Electronic Test Sets

2 Optical Alginment Test Sets

1 Pallet Payload Simulator

1 Computer and Peripheral Equipment

1 Reproduction Equipment

4 Portable Hoists

4 Push-Cart Dollies

EVENTS SEQUENCE AND RESOURCE REQUIREMENTS
PHASE VI

FUNCTION	DURATION	FACILITIES	MANPOWER NO.	MANPOWER SKILL	SUPPORT EQUIPMENT NO.	SUPPORT EQUIPMENT DESCRIPTION
A. Stabilize PPF-MSFC as 100,000 clean room	8 hours	PPF-MSFC Assembly Bay	14 2	PIC-MSFC Transient crew Facility crew	1 1 1	PT Fixture PT Dolly ECCU
B. Remove ECCU	2 hours	PPF-MSFC Assembly Bay	14 2 6	PIC-MSFC Transient crew Crane operators Handling crew	1 1 1 1	PT Fixture PT Dolly ECCU ECCU lifting sling set
C. Physically inspect entire payload and document inspection on film and paper. Check recorder strip charts from ECCU	8 hours	PPF-MSFC Assembly Bay	14 1 1 1 1 	PIC Transient crew Telescope PI Array PI Telescope Team Having: 1 Telescope engineer 5 Telescope technicians Array Team Having: 1 Array engineer 5 Array technicians	1 1 2 6 10	Detailed telescope check list Detailed array check list Polaroid cameras Work stands Work tables
D. Activate payload mounts and lock in vertical positions for disassembly	2 hours	PPF-MSFC Assembly Bay	14 1 1	PIC Transient crew Telescope team Array team	6 1 4	Work stands Ground cooling set Payload mounting locks
E. Remove telescope payload from mount	6 hours	PPF-MSFC Assembly Bay	14 1 1	PIC Transient crew Telescope PI Telescope team	4 2 1	Cable slings Work stands Telescope handling dolly
F. Remove array payload from mount	4 hours	PPF-MSFC Assembly Bay	14 1 2 1	PIC Transient crew Array team Crane operators Array PI	4 2 1	Cable slings Work stands Array handling dolly
G. Move telescope and array to individual refurbishment rooms	1 hour	PPF-MSFC Assembly Bay Payload refurbishment rooms in PPF-MSFC	1 1 1	Array team Telescope team Electric tractor operator	1 1 1	Array handling dolly Telescope handling dolly Electric tractor
H. Refurbishment of individual telescope and array payloads VI-H-T1 VI-H-T2 VI-H-T3 VI-H-T4 VI-H-A1 VI-H-A2 VI-H-A3 VI-H-A4 VI-H-A5		PPF-MSFC Assembly Bay Payload refurbishment rooms in PPF-MSFC				

SEE FUNCTIONS FOR EACH PAYLOAD

EVENTS SEQUENCE AND RESOURCE REQUIREMENTS

PHASE VI (continued)

FUNCTION	DURATION	FACILITIES	MANPOWER NO.	MANPOWER SKILL	SUPPORT EQUIPMENT NO.	SUPPORT EQUIPMENT DESCRIPTION
I. Remove subsystem payload peculiar components from pallet and SL (failed; life-limited; to be updated)	20 hours	PPF-MSFC Assembly Bay	14 1 1 1 1 4	PIC Transient crew Telescope team Array team SL team SL engineer SL technicians	4 4 4	Portable hoists Push cart dollys Cable slings
J. Replacement of subsystem payload peculiar components for new payload on pallet and SL	30 hours	PPF-MSFC Assembly Bay	14 1 1 1	PIC Transient crew Telescope team Array team SL team	4 4 4	Portable hand operated hoists Push cart dollys Cable slings
K. Move new telescope and array payloads from individual refurbishment rooms to assembly bay	2 hours	Payload refurbishment rooms in PPF-MSFC PPF-MSFC Assembly Bay	1 1 1	Telescope team Array team Electric tractor operator	1 1 1	Telescope handling dolly Array handling dolly Electric tractor
L. Install telescope payload in mount	16 hours	PPF-MSFC Assembly Bay	14 1 1	PIC Transient crew Telescope PI Telescope team	4 2 1	Cable slings Work stands Telescope handling dolly
M. Install array payload in mount	10 hours	PPF-MSFC Assembly Bay	14 1 1	PIC Transient crew Array PI Array team	4 2 1	Cable slings Work stands Array handling dolly
N. Perform CST after removal of payload mounting physical locks	22 hours	PPF-MSFC Assembly Bay	14 1 1 1 1	PIC Transient crew Telescope PI Telescope team Array PI Array team	2 2 2 2 2	Video tape recorders Instrumentation tape recorder Digital processing consoles Electronic test sets Optical alignment test sets
O. Train flight experiment crewmen	Continuous during refurbishment phase	Simulator facility PPF-MSFC	1 1 2 2 2	Telescope PI Array PI Telescope operation instructors Array operation instructors Simulator operators	1 10	Pallet payload simulator Training and devices
P. Prepare integrated mission program plan	Continuous during refurbishment phase	PIC-MSFC; Space Astronomy control facility; Launch Site; Mission Control Center	3 1	Mission planning specialists Planning supervisor	1 1	Computer and peripheral equipment Reproduction equipment
Q. Prepare integrated experiment flight plan	Continuous during refurbishment phase	PIC-MSFC; Space Astronomy control facility; Launch Site; Mission Control Center	3 1	Mission planning specialists Planning supervisor	1 1	Computer and peripheral equipment Reproduction equipment
R. Final inspection of integrated payload	4 hours	PPF-MSFC Assembly Bay	14 1 1 1 1 2	PIC Transient crew Telescope team Array team Telescope PI Array PI Flight experiment crew	1 1 6 10 2	Detailed telescope check list Detailed array check list Work stands Work tables Polaroid cameras

EVENTS SEQUENCE AND RESOURCE REQUIREMENTS

PHASE VI - H-T1 (PHOTOHELIOGRAPH)

FUNCTION	DURATION	FACILITIES	MANPOWER NO.	MANPOWER SKILL	SUPPORT EQUIPMENT NO.	SUPPORT EQUIPMENT DESCRIPTION
A. Inspection of Payload	4 hours	PPF-MSFC individual refurbishment room	1 1	Telescope Team, Having: 1 Telescope engineer 5 Telescope technicians Telescope PI	2 1 1 1	Work stands Telescope handling dolly Detailed telescope inspection check list Polaroid camera
B. Removal of particular (failed; life limited; updated) components	12 hours	PPF-MSFC individual refurbishment room	1 1	Telescope team Telescope PI	2 2 4	Portable hand operated hoists Push cart dollys Cable slings
OPTIONAL ITEMS IF REQUIRED						
B-1 Removal of mirrors for recoating	20 hours	PPF-MSFC individual refurbishment room	1 1 1	Telescope team Telescope PI Crane operator	2 1 4	Mirror handling dolly 5 ton overhead crane Cable slings
B-2 Move mirrors to vacuum support facility	4 hours	PPF-MSFC individual refurbishment room and vacuum deposit room	1 2	Electric tractor operator Facility technicians	2 1	Mirror handling dolly Electric tractor
B-3 Recoating of mirrors	24 hours	Vacuum deposit room	3	Vacuum deposit equipment operator	2	Mirror holding fixture
B-4 Move mirrors to refurbishment room	8 hours	PPF-MSFC individual refurbishment room	1 2	Electric tractor operator Facility technicians	2 1	Mirror handling dolly Electric tractor
B-5 Reinstall mirrors in instrument	32 hours	PPF-MSFC individual refurbishment room	1 1 1	Telescope team Telescope PI Crane operator	2 1 4	Mirror handling dolly 5 ton overhead crane Cable slings
C. Replacement of particular components	15 hours	PPF-MSFC individual refurbishment room	1 1	Telescope team Telescope PI	2 2 4	Portable hand operated hoists Push cart dollys Cable slings
D. Perform CST and return to refurbishment room	30 hours	PPF-MSFC vacuum chamber facility; simulator facility; optical support lab	1 1 1 1 2 2 2	Telescope team Telescope PI Electric tractor operator Crane operator Vacuum chamber operators Optical lab technicians Simulator operators	1 1 4 1 1 1 1 1 1 1 1 1	Telescope handling dolly 5 ton overhead crane Cable slings Laser interferometer in special case Video tape recorder Instrumentation recorder Monitoring and control console Optical test set Electronic test set Digital processing equipment Digital tape recorders Electrical tractor
E. Inspection of payload	8 hours	PPF-MSFC individual refurbishment room	1 1	Telescope team Telescope PI	2 1 1 1	Work stands Detailed telescope inspection check list Polaroid camera Telescope handling dolly
F. Prep. for return to pallet mounting	4 hours	PPF-MSFC individual refurbishment room	1 1 2	Telescope team Telescope PI Facility technicians	1 1 1	Telescope handling dolly Protective cover Flight log and flight ready documents

EVENTS SEQUENCE AND RESOURCE REQUIREMENTS

PHASE VI - H-T2 (XUV SHG; X-RAY TELESCOPE AND ICOC)

FUNCTION	DURATION			FACILITIES	MANPOWER		SUPPORT EQUIPMENT	
	XUV	X-RAY	ICOC		NO.	SKILL	NO.	DESCRIPTION
A. Inspection of payload		4 hours		PPF-MSFC individual refurbishment room	1 3 3	Telescope team chief Telescope Teams, Each Having: 1 Telescope engineer 5 Telescope technicians Telescope PI	4 1 1 1	Work stands Solar telescope package handling dolly Detailed telescope package inspection check list Polaroid camera
B. Dismantle package into 3 major instruments		8 hours		PPF-MSFC individual refurbishment room	3 1 3 1	Telescope teams Telescope team chief Telescope PI Crane operator	3 1 4 4 1	Telescope handling dollys 5 ton overhead crane Cable slings Work stands Solar telescope package handling dolly
C. Removal of particular* (failed; life limited; to be updated) components	8.0	12.0	8.0	PPF-MSFC individual refurbishment room	3 1 3	Telescope teams Telescope team chief Telescope PI	6 6 6	Portable hand operated hoists Push cart dollys Cable slings
OPTIONAL ITEMS IF REQUIRED								
C-1 Remove mirror for recoating	4.0	20.0	4.0	PPF-MSFC individual refurbishment room	1 1	Telescope PI Telescope team	1	Mirror handling dolly
C-2 Move mirror to vacuum deposit support facility	4.0	4.0	4.0	PPF-MSFC individual refurbishment room and deposit room	2	Facility technicians	1	Mirror handling dolly
C-3 Recoating of mirror	24.0	48.0	12.0	Vacuum deposit room	3	Vacuum deposit equipment operator	1	Mirror holding fixture
C-4 Move mirror to refurbishment room	4.0	8.0	2.0	PPF-MSFC individual refurbishment room	2	Facility technicians	1	Mirror handling dolly
C-5 Reinstall mirror in instrument	24.0	48.0	12.0	PPF-MSFC individual refurbishment room	1 1	Telescope team Telescope PI	1	Mirror handling dolly
D. Replacement of particular components	12.0	18.0	12.0	PPF-MSFC individual refurbishment room	3 1 3	Telescope teams Telescope team chief Telescope PI	6 6 6	Portable hand operated hoists Push cart dollys Cable slings
E. Reassemble 3 major instruments into solar telescope package		12 hours		PPF-MSFC individual refurbishment room	3 1 3 1	Telescope teams Telescope team chief Telescope PI Crane operator	4 1 3 1 4	Work stands 5 ton overhead crane Special telescope handling dolly Solar telescope package handling dolly Cable slings

EVENTS SEQUENCE AND RESOURCE REQUIREMENTS
PHASE VI - H-T2 (cont)

FUNCTION	DURATION	FACILITIES	MANPOWER NO.	MANPOWER SKILL	SUPPORT EQUIPMENT NO.	SUPPORT EQUIPMENT DESCRIPTION
F. Perform CST and return to refurbishment room	30 hours	PPF-MSFC simulator facility; optical support lab	3	Telescope teams	1	Electric tractor
			1	Telescope team chief	1	Solar telescope package handling dolly
			3	Telescope PI	1	5 ton overhead crane
			1	Electric tractor operator	4	Cable slings
			1	Crane operator	3	Video tape recorded
			2	Simulator operators	3	Instrumentation tape recorder
			2	Optical lab technicians	3	Monitoring and control console
					3	Optical test set
					3	Electronic test set
					3	Digital processing equipment
					3	Digital tape recorder
G. Inspection of payload	8 hours	PPF-MSFC individual refurbishment room	3	Telescope teams	4	Work stands
			1	Telescope team chief	1	Solar telescope package handling dolly
			3	Telescope PI	1	Detailed telescope package inspection check list
					1	Polaroid camera
H. Prep. for return to pallet mounting	4 hours	PPF-MSFC individual refurbishment room	3	Telescope team	1	Solar telescope package handling dolly
			1	Telescope team chief	1	Protective cover
			3	Telescope PI	1	Flight log and flight ready documents
			2	Facility technicians		

EVENTS SEQUENCE AND RESOURCE REQUIREMENTS
PHASE VI - H-T3 (STRATOSCOPE III)

FUNCTION	DURATION	FACILITIES	MANPOWER NO.	MANPOWER SKILL	SUPPORT EQUIPMENT NO.	SUPPORT EQUIPMENT DESCRIPTION
A. Inspection of payload	4 hours	PPF-MSFC individual refurbishment room	1 1	Telescope Team Having: 1 Telescope engineer 5 Telescope technicians Telescope PI	2 1 1 1	Work stands Telescope handling dolly Detailed telescope inspection check list Polaroid camera
B. Removal of particular (failed; life limited; to be updated) components	12 hours	PPF-MSFC individual refurbishment room	1 1	Telescope team Telescope PI	2 2 4	Portable hand operated hoists Push cart dollys Cable slings
OPTIONAL ITEMS IF REQUIRED						
B-1 Removal of mirrors for recoating	40 hours	PPF-MSFC individual refurbishment room	1 1 1	Telescope team Telescope PI Crane operator	2 1 4	Mirror handling dolly 5 ton overhead crane Cable slings
B-2 Move mirrors to vacuum deposit support facility	4 hours	PPF-MSFC individual refurbishment room and vacuum deposit room	1 2	Electric tractor operator Facility technicians	2 1	Mirror handling dolly Electric tractor
B-3 Recoating of mirrors	32 hours	Vacuum deposit room	3	Vacuum deposit equipment operator	2	Mirror holding fixtures
B-4 Move mirrors to refurbishment room	8 hours	PPF-MSFC individual refurbishment room	1 2	Electric tractor operator Facility technicians	2 1	Mirror handling dolly Electric tractor
B-5 Reinstall mirrors in instrument	60 hours	PPF-MSFC individual refurbishment room	1 1 1	Telescope team Telescope PI Crane operator	2 1 4	Mirror handling dolly 5 ton overhead crane Cable slings
C. Replacement of particular components	15 hours	PPF-MSFC individual refurbishment room	1 1	Telescope team Telescope PI	2 2 4	Portable hand operated hoists Push cart dollys Cable slings
D. Perform CST and return to refurbishment room	40 hours	PPF-MSFC simulator facility; optical support lab	1 1 1 1 2 2	Telescope team Telescope PI Electric tractor operator Crane operator Optical lab technicians Simulator operators	1 1 1 4 1 1 1 1 1 1	Electric tractor Telescope handling dolly 5 ton overhead crane Cable slings Video tape recorder Instrumentation tape recorder Monitoring and control console Optical test set Electronic test set Digital tape recorder
E. Inspection of payload	8 hours	PPF-MSFC individual refurbishment room	1 1	Telescope team Telescope PI	2 1 1 1	Work stands Detailed telescope inspection check list Polaroid camera Telescope handling dolly
F. Prep. for return to pallet mounting	4 hours	PPF-MSFC individual refurbishment room	1 1 2	Telescope team Telescope PI Facility technicians	1 1 1	Telescope handling dolly Protective cover Flight log and flight ready documents

EVENTS SEQUENCE AND RESOURCE REQUIREMENTS

PHASE VI - H-T4 (IR TELESCOPE)

FUNCTION	DURATION	FACILITIES	MANPOWER NO.	MANPOWER SKILL	SUPPORT EQUIPMENT NO.	SUPPORT EQUIPMENT DESCRIPTION
A. Inspection of Payload	4 hours	PPF-MSFC individual refurbishment room	1 1	Telescope Team Having: 1 Telescope engineer 5 Telescope technicians Telescope PI	2 1 1 1	Work stands Special telescope handling dolly Detailed telescope inspection check list Polaroid camera
B. Purging of cryogenic cooling shroud	4 hours	PPF-MSFC individual refurbishment room	1 2	Telescope team Facility technicians	1 1 1	Facility gas supply source Gas supply line with valve Gas exhaust line with valve
C. Removal of particular (failed; life limited; to be updated) components	15 hours	PPF-MSFC individual refurbishment room	1 1	Telescope team Telescope PI	2 2 4	Portable hand operated hoists Push cart dollys Cable slings
OPTIONAL ITEMS IF REQUIRED						
C-1 Removal of mirrors for recoating	40 hours	PPF-MSFC individual refurbishment room	1 1 1	Telescope team Telescope PI Crane operator	2 1 4	Special mirror handling dolly 5 ton overhead crane Cable slings
C-2 Move mirrors to vacuum deposit facility	4 hours	PPF-MSFC individual refurbishment room and vacuum deposit room	1 2	Electric tractor operator Facility technicians	2 1	Special mirror handling dolly Electric tractor
C-3 Recoating of mirrors	32 hours	Vacuum deposit room	3	Vacuum deposit equipment operator	2 1	Special mirror handling dolly Electric tractor
C-4 Move mirrors to refurbishment room	8 hours	PPF-MSFC individual refurbishment room	1 2	Electric tractor operator Facility technicians	2 1	Special mirror handling dolly Electric tractor
C-5 Reinstall mirrors in instrument	60 hours	PPF-MSFC individual refurbishment room	1 1 1	Telescope team Telescope PI Crane operator	1 2 4	5 ton overhead crane Special mirror handling dolly Cable slings
D. Replacement of particular components	20 hours	PPF-MSFC individual refurbishment room	1 1	Telescope team Telescope PI	2 2 4	Portable hand operated hoists Push cart dollys Cable slings
E. Perform CST and return to refurbishment room	40 hours	PPF-MSFC simulator facility; optical support lab	1 1 1 1 2 2	Telescope team Telescope PI Electric tractor operator Crane operator Optical lab technicians Simulator operators	1 1 1 4 1 1 1 1 1 1 1 1 1	Electric tractor Special telescope handling dolly 5 ton overhead crane Cable slings Facility cryogenic gas supply source Cryogenic gas supply line with valve Cryogenic gas exhaust line with valve Video tape recorder Instrumentation tape recorder Monitoring and control console Optical test set Electronic test set Digital tape recorder

EVENTS SEQUENCE AND RESOURCE REQUIREMENTS

PHASE VI - H-T4 (cont)

FUNCTION	DURATION	FACILITIES	MANPOWER NO.	MANPOWER SKILL	SUPPORT EQUIPMENT NO.	SUPPORT EQUIPMENT DESCRIPTION
F. Inspection of Payload	8 hours	PPF-MSFC simulator facility; optical support lab	1	Telescope team	2	Work stands
			1	Telescope PI	1	Special telescope handling dolly
					1	Detailed telescope inspection check list
					1	Polaroid camera
G. Prep. for return to Pallet Mounting	4 hours	PPF-MSFC simulator facility; optical support lab	1	Telescope team	1	Special telescope handling dolly
					1	Protective cover
					1	Flight log and flight ready documents

EVENTS SEQUENCE AND RESOURCE REQUIREMENTS
PHASE VI - H-A1 (WIDE COVERAGE X-RAY DETECTOR)

FUNCTION	DURATION	FACILITIES	MANPOWER NO.	MANPOWER SKILL	SUPPORT EQUIPMENT NO.	SUPPORT EQUIPMENT DESCRIPTION
A. Inspection of Payload	4 hours	PPF-MSFC individual refurbishment room	1	Array Team Having:	1	Special array handling dolly
				1 Array engineer	4	Work stands
				5 Array technicians	1	Detailed array inspection check list
			1	Array PI	1	Polaroid camera
B. Removal of particular (failed; life limited; to be updated) components	12 hours	PPF-MSFC individual refurbishment room	1	Array team	1	Special array handling dolly
			1	Array PI	4	Work stands
					2	Portable hand operated hoists
					2	Push cart dollys
					4	Cable slings
C. Replacement of particular components	15 hours	PPF-MSFC individual refurbishment room	1	Array team	1	Special array handling dolly
			1	Array PI	4	Work stands
					2	Portable hand operated hoists
					2	Push cart dollys
					4	Cable slings
D. Perform CST and return to refurbishment room	24 hours	PPF-MSFC simulator facility; X-ray source calibration facility	1	Array team	1	Special array handling dolly
			1	Array PI	1	Electric tractor
			1	Electric tractor operator	1	Instrumentation tape recorder
			2	X-ray room technicians	1	Monitoring and control console
			2	Simulator operators	1	Electronic test set
					1	Digital processing unit
					1	Digital tape recorder
E. Inspection of payload	4 hours	PPF-MSFC individual refurbishment room	1	Array team	4	Work stands
			1	Array PI	1	Special array handling dolly
					1	Detailed array inspection check list
					1	Polaroid camera
F. Prep. for return to pallet mounting	4 hours	PPF-MSFC individual refurbishment room	1	Array team	1	Special array handling dolly
			1	Array PI	1	Protective cover
			2	Facility technicians	1	Flight log and flight ready documents

EVENTS SEQUENCE AND RESOURCE REQUIREMENTS

PHASE VI - H-A2 (NARROW BAND SPECTROMETER/POLARIMETER)

FUNCTION	DURATION	FACILITIES	MANPOWER NO.	MANPOWER SKILL	SUPPORT EQUIPMENT NO.	SUPPORT EQUIPMENT DESCRIPTION
A. Inspection of payload	4 hours	PPF-MSFC individual refurbishment room	1	Array Team Having: 1 Array engineer 5 Array technicians	1	Array handling dolly
					4	Work stands
					1	Detailed array inspection check list
			1	Array PI	1	Polaroid camera
B. Gas purging and replenishment in sectored proportional counters	3 hours	PPF-MSFC individual refurbishment room	1	Array team	1	Array handling dolly
			1	Array PI	4	Work stands
					1	Facility gas storage area
					1	Gas supply line
					1	Gas exhaust line
C. Removal of particular (failed; life limited; to be updated) components	12 hours	PPF-MSFC individual refurbishment room	1	Array team	1	Array handling dolly
			1	Array PI	4	Work stands
					2	Portable hand operated hoists
					4	Cable slings
					2	Push cart dollys
D. Replacement of particular components	15 hours	PPF-MSFC individual refurbishment room	1	Array team	1	Array handling dolly
			1	Array PI	4	Work stands
					2	Portable hand operated hoists
					4	Cable slings
					2	Push cart dollys
E. Perform CST and return to refurbishment room	24 hours	PPF-MSFC simulator facility; X-ray source calibration facility	1	Array team	1	Array handling dolly
			1	Array PI	1	Electric tractor
			1	Electric tractor operator	1	Instrumentation tape recorder
			2	X-Ray room technician	1	Monitoring and control console
			2	Simulator operator	1	Electronic test set
					1	Digital processing unit
					1	Digital tape recorder
F. Inspection of payload	4 hours	PPF-MSFC individual refurbishment room	1	Array team	4	Work stands
			1	Array PI	1	Array handling dolly
					1	Detailed array inspection check list
					1	Polaroid camera
G. Prep. for return to pallet mounting	4 hours	PPF-MSFC individual refurbishment room	1	Array team	1	Array handling dolly
			1	Array PI	1	Protective cover
			2	Facility technician	1	Flight log and flight ready documents

[illegible] SEQUENCE AND RESOURCE REQUIREMENTS
[illegible]SE VI - H-A3 (γ-RAY SPECTROMETER AND LOW BACKGROUND γ-RAY DETECTOR)

FUNCTION	DURATION	FACILITIES	MANPOWER NO.	MANPOWER SKILL	SUPPORT EQUIPMENT NO.	SUPPORT EQUIPMENT DESCRIPTION
A. Inspection of Payload	4 hours	PPF-MSFC individual refurbishment room and controlled low humidity atmosphere	1 1	Array Team Having: 1 Array engineer 5 Array technicians Array PI	1 4 1 1	Array handling dolly Work stands Detailed array inspection check list Polaroid camera
B. Removal of continuously cryo cooled spectrometer detector unit and movement to cryogenic work room	4 hours	PPF-MSFC individual refurbishment room, controlled low humidity atmosphere, and cryogenic work room	1 1 1	Array team Array PI Facility technician	1 4 1 1	Array handling dolly Work stands Portable hand operated hoist Cryogenic handling and movement cart
C. Inspection, adjustment, calibration of detector unit	24 hours	Cryogenic work room	2 1	Facility technician Array PI	1 1 1 1	Cryogenic handling and movement cart Facility gas storage area Cryogenic gas supply line Cryogenic gas exhaust line
D. Removal of particular (failed; life limited; to be updated) components	12 hours	PPF-MSFC individual refurbishment room	1 1	Array team Array PI	1 4 2 4 2	Array handling dolly Work stands Portable hand operated hoist Cable sling Push cart dolly
E. Replacement of particular components	15 hours	PPF-MSFC individual refurbishment room	1 1	Array team Array PI	1 4 2 4 2	Array handling dolly Work stands Portable hand operated hoists Cable slings Push cart dollys
F. Installation of continuously cryo cooled spectrometer detector unit	4 hours	PPF-MSFC individual refurbishment room	1 1 *1	Array team Array PI Facility technician	1 4 1 1	Array handling dolly Work stands Portable hand operated hoist Cryogenic handling and movement cart
G. Perform CST and return to refurbishment room	24 hours	PPF-MSFC simulator facility; γ-Ray source calibration facility	1 1 1 2 2 *1	Array team Array PI Electric tractor operator γ-Ray room technicians Simulator operators Facility technician	1 1 1 1 1 1 1	Array handling dolly Electric tractor Instrumentation tape recorder Monitoring and control console Electronic test set Digital processing unit Digital tape recorder
H. Inspection of payload	4 hours	PPF-MSFC individual refurbishment room	1 1	Array team Array PI	1 4 1 1	Array handling dolly Work stands Detailed array inspection check list Polaroid camera
I. Prep. for return to pallet mounting	4 hours	PPF-MSFC individual refurbishment room	1 1 *2	Array team Array PI Facility technician	1 1 1 1 **1	Array handling dolly Protective cover Flight log and flight ready documents Cryogenic gas supply line Cryogenic gas exhaust line

* [illegible] and cryogenic flow and supply to detector must be monitored periodically by technician
** [illegible] ...nifolded to facility cryo supply for long term storage

EVENTS SEQUENCE AND RESOURCE REQUIREMENTS

PHASE VI - H-A4 (LARGE MODULATION COLLIMATOR)

FUNCTION	DURATION	FACILITIES	MANPOWER NO.	MANPOWER SKILL	SUPPORT EQUIPMENT NO.	SUPPORT EQUIPMENT DESCRIPTION
A. Inspection of payload	4 hours	PPF-MSFC individual refurbishment room	1	Array Team Having: 1 Array engineer 5 Array technicians	1 4 1	Array handling dolly Work stands Detailed array inspection check list
			1	Array PI	1	Polaroid camera
B. Dry gas purge of instrument	3 hours	PPF-MSFC individual refurbishment room	1 1 2	Array team Array PI Facility technician	1 4 1 1	Array handling dolly Work stands Facility gas storage supply Gas purge and blanket unit
C. Removal of particular (failed; life limited; to be updated) components	12 hours	PPF-MSFC individual refurbishment room	1 1	Array team Array PI	1 4 2 4 2	Array handling dolly Work stands Portable hand operated hoists Cable slings Push cart dollys
D. Replacement of particular components	15 hours	PPF-MSFC individual refurbishment room	1 1	Array team Array PI	1 4 2 4 2	Array handling dolly Work stands Portable hand operated hoists Cable slings Push cart dollys
E. Gas purge and replenishment of gas in proportional counters	3 hours	PPF-MSFC individual refurbishment room	1 1 2	Array team Array PI Facility technician	1 4 1 1 1	Array handling dolly Work stands Facility gas storage supply Gas supply line Gas exhaust line
F. Perform CST and return to refurbishment room	24 hours	PPF-MSFC simulator facility; X-ray source calibration facility	1 1 1 2 2	Array team Array PI Electric tractor operator X-Ray room technician Simulator operator	1 1 1 1 1 1 1	Array handling dolly Electric tractor Instrumentation tape recorder Monitoring and control console Electronic test set Digital processing unit Digital tape recorder
G. Inspection of payload	4 hours	PPF-MSFC individual refurbishment room	1 1	Array team Array PI	1 4 1 1	Array handling dolly Work stands Detailed array inspection check list Polaroid camera
H. Prep. for return to pallet mounting	4 hours	PPF-MSFC individual refurbishment room	1 1 2	Array team Array PI Facility technicians	1 1 1	Array handling dolly Protective cover Flight log and flight ready documents

ANALYSIS SEQUENCE AND RESOURCE REQUIREMENTS

PHASE VI - H-A5 (LARGE AREA X-RAY DETECTOR AND COLLIMATED PLANE CRYSTAL SPECTROMETER)

FUNCTION	DURATION	FACILITIES	MANPOWER NO.	MANPOWER SKILL	SUPPORT EQUIPMENT NO.	SUPPORT EQUIPMENT DESCRIPTION
A. Inspection of payload	4 hours	PPF-MSFC individual refurbishment room	2 2	Array Teams, Each Having: 1 Array engineer 5 Array technicians Array PI	1 4 1 1	Array handling dolly Work stands Detailed array inspection check list Polaroid camera
B. Disassembly into 2 separate instruments	4 hours	PPF-MSFC individual refurbishment room	2 2 1	Array teams Array PIs Crane operator	1 2 4 1 4	Array handling dolly Instrument handling dolly Work stands 5 ton overhead crane Cable slings
C. Dry gas purge of large area X-ray detector	3 hours	PPF-MSFC individual refurbishment area	1 1 1	Array team Array PI Facility technician	1 1 1 1	Instrument handling dolly Work stand Facility gas storage area Gas purge and blanket unit
D. Removal of particular (failed; life limited; to be updated) components (Both instruments)	24 hours	PPF-MSFC individual refurbishment room	2 2	Array teams Array PI	2 4 2 4 2	Instrument handling dolly Work stands Portable hand operated hoist Cable slings Push cart dollys
E. Replacement of particular (Both instruments)	30 hours	PPF-MSFC individual refurbishment room	2 2	Array teams Array PI	2 4 2 4 2	Instrument handling dolly Work stands Portable hand operated hoist Cable slings Push cart dollys
F. Gas purging and replenishment in sectored proportional counters of large area X-ray detector	3 hours	PPF-MSFC individual refurbishment room	1 1 1	Array teams Array PI Facility technician	1 1 1 1 1	Instrument handling dolly Work stand Facility gas storage area Gas supply line Gas exhaust line
G. Reassemble instruments into array package	5 hours	PPF-MSFC individual refurbishment room	2 2 1	Array teams Array PI Crane operator	2 1 4 1 4	Instrument handling dollys Array handling dolly Work stands 5 ton overhead crane Cable slings
H. Perform CST and return to refurbishment room	24 hours	PPF-MSFC simulator facility; X-ray source calibration facility	2 2 1 2 2	Array teams Array PI Electric tractor operator X-ray room technician Simulator operator	1 1 2 2 2 2 2	Array handling dolly Electric tractor Instrumentation tape recorder Monitoring and control console Electronic test set Digital processing unit Digital tape recorder

EVENTS SEQUENCE AND RESOURCE REQUIREMENTS

PHASE VI - H-5A (continued)

FUNCTION	DURATION	FACILITIES	MANPOWER		SUPPORT EQUIPMENT	
			NO.	SKILL	NO.	DESCRIPTION
I. Inspection of payload	4 hours	PPF-MSFC individual refurbishment room	2	Array teams	1	Array handling dolly
			2	Array PI	4	Work stands
					1	Detailed array inspection check list
					1	Polaroid camera
J. Prep. for return to pallet mounting	4 hours	PPF-MSFC individual refurbishment room	2	Array teams	1	Array handling dolly
			2	Array PI	1	Protective cover
			2	Facility technician	1	Flight log and flight ready documents

SPACE ASTRONOMY CONTROL FACILITY FUNCTIONS AND RESOURCES

FUNCTION	DURATION	FACILITIES	MANPOWER NO.	MANPOWER SKILL	SUPPORT EQUIPMENT DESCRIPTION
PHASE I					
PI consultation support to Payload Integration Center Transient Crew	42 hours		1 1 1	Telescope PI Wide coverage X-ray array PI Array PI	Telephone voice and facsimile link between SACF and PIC (MSFC) and Shuttle Launch Site
PHASE II					
PI representative support at Shuttle Launch Site	190 hours	Office at Shuttle Launch Site	1 1	Telescope PI Wide coverage X-ray array PI	Telephone voice link between Shuttle Launch Site and SACF
PHASE III					
Experiment Operations Support and Control Support realtime experiment operation Consult with experiment designers for problem solving Coordinate operations for targets of opportunity Liaison with PIC (MSFC) Liaison with Launch and Landing Site	168 hours	Office at SACF Observatory Facility	1 1 1 9	Telescope PI Wide coverage X-ray array PI Array PI Experiment specialists	Telephone voice and facsimile link between SACF and Shuttle Mission Control, the PIC (MSFC) and Shuttle Launch Site
Coordinate World Wide Observatories Consult with astronomers Evaluate targets suggested by other observatories Arrange for observation by other observatories to support and complement these missions		Office at SACF Observation Facility	1 1 1 9	Telescope PI Wide coverage X-ray array PI Array PI Experiment specialists	Telephone voice between SACF and cooperating world-wide observatories
PHASE IV					
PI representative support at Shuttle Landing Site	42 hours	Office at Shuttle Landing Site	1 1 1	Telescope PI Wide coverage X-ray array PI Array PI	Telephone voice link between Orbiter Landing Site and SACF
PHASE V					
PI consultation support to Payload Integration Center Transient Crew	34 hours		1 1 1	Telescope PI Wide coverage X-ray array PI Array PI	Telephone voice link between Orbiter Landing Site and SACF
Remove scientific film and tape data packages; package for shipment to SACF deliver to SACF by courier		Experiment/carrier processing facility Pack and ship facility	4 1	Experiment technician Courier	Commercial air Landing Site to SACF

SPACE ASTRONOMY CONTROL FACILITY FUNCTIONS AND RESOURCES

FUNCTION	DURATION	FACILITIES	MANPOWER NO.	MANPOWER SKILL	SUPPORT EQUIPMENT DESCRIPTION
PHASE VI					
Process Photographic Film Reduce Electronic Data	135 hours	Film Processing Lab Computer Facility	2 2	Film processing technicians Computer programmer/operator	Processing equipment and chemicals to process: 95,000 frames per mission for Solar Payloads 8,000 frames per mission for S III Payloads 3AB, 3AC, 3AD, and 3AE Tape readers, computers, and printers to process: 4.1 X 10^9 bits per mission for Solar Payload 1-2 1.9 X 10^9 bits per mission for 3AB 4.6 X 10^9 bits per mission for 3AC 3.6 X 10^9 bits per mission for 3AD 3.8 X 10^9 bits per mission for 3AE 1.3 X 10^9 bits per mission for 4AB 4.0 X 10^9 bits per mission for 4AC 3.0 X 10^9 bits per mission for 4AD 3.5 X 10^9 bits per mission for 4AE
File and disseminate data		Pack and Ship Facility Library Facility	1 1 1	Telescope PI Wide coverage X-ray array PI Array PI	Tables, chairs, viewers, projectors for 3 scientists
Prepare and maintain experiment mission program plans		Office at SACF	1 1 1 3	Telescope PI Wide coverage X-ray array PI Array PI Experiment specialists	Desks, chairs, typewriters, reproduction equipment
Prepare detailed experiment flight plans		Office at SACF	1 1 1 3	Telescope PI Wide coverage X-ray array PI Array PI Experiment specialists	Desks, chairs, typewriters, reproduction equipment
Support training of flight crew		Payload Integration Center	3	Experiment specialists	

APPENDIX A3

MISSION PROFILE

<u>INTRODUCTION</u> <u>PAGE</u>

This appendix includes:

STRATOSCOPE III PAYLOAD 3AC
MISSION ASSUMPTIONS

1. Sortie Lab is pressurized on ground and isolated from shuttle by crew access hatch.
2. Inclination 0.497 radian (28.5 degrees)
3. Operations altitude 463 km (250 n. mi.)
4. Fly mission anytime of year; launch anytime of day.
5. Initiate deorbit 45 minutes prior to revolution 107 which passes within orbiter crossrange capability at 166 hrs. 42 min. elapsed time. Total mission duration launch to initiate deorbit is 165 hr. 57 min.

STRATOSCOPE III PAYLOAD 3AC
MISSION SEQUENCE AND FLIGHT PROFILE

ELAPSED TIME (HR:MIN)	EVENT
00:00	LIFTOFF
00:06.5	INSERT INTO 93 X 185 KM (50 X 100 NMI) ORBIT
00:50.1	TRANSFER TO 185 X 463 KM (100 X 250 NMI) ORBIT AT FIRST APOGEE
01:36.1	CIRCULARIZE AT 463 KM (250 NMI) ORBIT AT FIRST APOGEE. STABILIZE, CHECKOUT ORBITER SYSTEMS, UPDATE EPHEMERIS, OPEN ORBITER CARGO BAY DOORS, VERIFY READINESS TO PROCEED WITH EXPERIMENT OPERATIONS
02:00	ORBITER COARSE-ATTITUDE ACQUISITION
02:30	REMOTE CHECKOUT OF SORTIE LAB SUBSYSTEMS VERIFICATION: ELECTRICAL POWER; ENVIRONMENTAL CONTROL/LIFE SUPPORT; CONTROL & DISPLAY; THERMAL CONTROL; COMMUNICATIONS/DATA MANAGEMENT; GUIDANCE, NAVIGATION AND CONTROL
02:45	VERIFY SORTIE LAB HABITABILITY AND OPEN CREW ACCESS HATCH
03:00	SORTIE LAB CHECKOUT BY SCIENTIFIC CREW VERIFY EC/LS CAUTION AND WARNING SUBSYSTEM; VERIFY COMMUNICATIONS/DATA MANAGEMENT SUBSYSTEM; VERIFY SUBSYSTEMS CONTROL AND DISPLAY PANELS; VERIFY ELECTRICAL POWER DISTRIBUTION TO PALLET; VERIFY PALLET THERMAL CONTROL SUBSYSTEM; TURN ON GUIDANCE, NAVIGATION AND CONTROL SUBSYSTEM
03:30	PERFORM VISUAL INSPECTION OF TELESCOPE AND ARRAYS
	<u>TELESCOPE DEPLOYMENT</u>
03:40	RELEASE TELESCOPE GIMBAL MOUNT LAUNCH LOCKS
03:42	ROTATE DEPLOYMENT YOKE TO 90 DEGREE POSITION AND LOCK
03:57	PITCH TELESCOPE COARSE GIMBAL INTO INITIAL OPERATIONS POSITION
04:12	RELEASE AZIMUTH TABLE LOCKS
04:14	RELEASE LAUNCH LOCKS TO PROTECT PRIMARY AND SECONDARY MIRRORS ASSEMBLIES
	<u>TELESCOPE POST-DEPLOYMENT CHECKOUT</u>
04:16	OPEN COVERS ON OPTICS, EXTEND SHIELD
04:28	FUNCTIONAL CHECK CONSOLE SYSTEMS
04:40	ACTIVATE AND CHECKOUT DRIVES
04:46	TURN ON MAIN POWER TO INSTRUMENT DETECTORS
04:48	MONITOR TEMPERATURE CONTROL SYSTEM UNTIL STABILIZATION (24 MINUTES REQUIRED)

ELAPSED TIME (HR:MIN)	EVENT
	GAMMA-RAY SPECTROMETER AND LOW BACKGROUND GAMMA-RAY DETECTOR DEPLOYMENT
04:50	RELEASE ARRAY GIMBAL MOUNT LAUNCH LOCKS
04:52	ROTATE ARRAY DEPLOYMENT YOKE TO 90-DEGREE POSITION AND LOCK
04:07	PITCH ARRAY COARSE GIMBAL INTO INITIAL OPERATIONS POSITION
04:22	RELEASE AZIMUTH TABLE LOCKS
	WIDE COVERAGE X-RAY DEPLOYMENT
04:24	RELEASE ARRAY MOUNT LAUNCH LOCKS
04:26	DEPLOY WIDE COVERAGE X-RAY ARRAYS
04:41	ROTATE WIDE COVERAGE X-RAY ARRAY HALVES INTO OPERATIONS POSITION
	WIDE COVERAGE X-RAY ARRAY CHECKOUT
04:51	PERFORM SAFETY CHECK
04:53	TURN ON ELECTRICAL POWER
04:54	PERFORM ELECTRICAL CHECK
04:55	PERFORM BUILT-IN CALIBRATION
	GAMMA-RAY SPECTROMETER AND LOW BACKGROUND GAMMA-RAY DETECTOR CHECKOUT
05:05	PERFORM VISUAL SAFETY CHECK
05:15	TURN ON ELECTRICAL POWER
05:17	RELEASE LAUNCH RESTRAINTS AND DEPLOY DETECTOR PACKAGE
05:19	PERFORM FUNCTIONAL CHECK
05:29	PERFORM ELECTRONICS CALIBRATION
05:39	ESTABLISH ORIENTATION REFERENCES
05:44	INITIATE REPEATABLE ON-ORBIT OPERATIONS SEQUENCE FOR TELESCOPE AND ARRAYS

...THE WIDE COVERAGE X-RAY ARRAY AND THE GAMMA RAY SPECTROMETER AND LOW BACKGROUND GAMMA RAY DETECTOR ARE OPERATED CONTINUOUSLY (EXCEPT FOR PERIODS OF AUTOMATIC SHUTDOWN DURING PASSAGE THRU THE SOUTH ATLANTIC ANOMALY) UNTIL TERMINATION OF EXPERIMENT OPERATIONS AT 161 HRS 11 MINUTES.

TYPICAL REPEATABLE ON-ORBIT OPERATIONS SEQUENCE FOR STRATOSCOPE III, REQUIRING 91 MINUTES PER CYCLE (70 MINUTES PER CYCLE OBERVATION TIME) IS PERFORMED 102 TIMES (PLUS ONE PARTIAL CYCLE ENDING AT...

161:11	RETRACT SHIELD, CLOSE COVERS ON TELESCOPE OPTICS
161:31	SECURE LAUNCH LOCKS TO PROTECT PRIMARY AND SECONDARY MIRRORS ASSEMBLIES OF TELESCOPE
161:37	SECURE TELESCOPE AZIMUTH TABLE LOCKS
161:39	TURN OFF ELECTRICAL POWER TO WIDE COVERAGE X-RAY ARRAY
161:41	ROTATE WIDE COVERAGE X-RAY ARRAY HALVES INTO STOWING POSITION
161:47	RETRACT WIDE COVERAGE X-RAY ARRAYS INTO STOWED POSITION

162:02	SECURE ARRAY MOUNT LOCKS
162:04	TURN OFF ARRAY CONTROLS AND DISPLAYS
162:06	RETRACT GAMMA-RAY ARRAY DETECTOR PACKAGE AND SECURE LAUNCH RESTRAINTS
162:11	SWITCH GAMMA-RAY ARRAYS ELECTRICAL POWER TO STANDBY
162:13	SECURE GAMMA-RAY ARRAYS AZIMUTH TABLE LOCKS
162:15	PITCH ARRAY COARSE GIMBAL INTO STOWING POSITION
162:45	RELEASE ARRAY DEPLOYMENT YOKE, ROTATE INTO STOWED POSITION AND LOCK
163:15	SWITCH GAMMA-RAY ARRAYS CONTROLS AND DISPLAY PANELS TO MONITOR CRYO SYSTEM ONLY
163:17	PITCH TELESCOPE COARSE GIMBAL INTO STOWED POSITION
163:47	RELEASE DEPLOYMENT YOKE LOCK AND ROTATE INTO STOWED POSITION
164:17	SECURE TELESCOPE GIMBAL MOUNT LAUNCH LOCKS
164:19	TURN OFF TELESCOPE THERMAL CONTROL SYSTEM
164:21	TURN OFF MAIN POWER TO INSTRUMENT DETECTORS
164:23	TURN OFF CONTROLS AND DISPLAYS PANELS
	SECURE SORTIE LAB AND PALLET
164:24	TURN OFF SORTIE LAB GUIDANCE, NAVIGATION AND CONTROLS SUBSYSTEM; SWITCH PALLET THERMAL CONTROL SYSTEM TO STANDBY; SWITCH PALLET ELECTRICAL POWER DISTRIBUTION TO STANDBY
164:31	SCIENTIFIC CREW TRANSFER TO ORBITER STATIONS
164:41	CLOSE ACCESS HATCH TO SORTIE LAB
164:51	SWITCH SORTIE LAB SUBSYSTEMS TO STANDBY
164:57	CHECKOUT ORBITER, PREPARE FOR RETURN TO EARTH
165:57	INITIATE DEORBIT

TYPICAL REPEATABLE ON-ORBIT OPERATIONS SEQUENCE

STRATOSCOPE III

The Stratoscope III telescope is limited to viewing no closer than 45 degrees to the Sun and 15 degrees to the Earth and Moon. This constraint permits targets within the 15% of the celestial sphere more than 83.4 degrees from the orbit plane (in either direction) to be continuously viewable. Targets not within the cones of continuous visibility are viewable from at least 50 minutes per orbit to 93.7 minutes per orbit, depending on their angle from the orbit plane, except for about 15% of the celestial sphere which is continuously occulted by the Sun.

Based on these constraints, a desired observation duration of 70 minutes was selected for developing the following typical repeatable on-orbit operations sequence:

MINUTES	FUNCTION
12	A. Point Telescope to Acquire Target
1	B. Select Filter or Grating
7	C. Calibrate
70	D. Observe
1	E. Rotate Mirror
TOTAL 91	

IR TELESCOPE PAYLOAD 4AC
MISSION ASSUMPTIONS

1. Sortie Lab is pressurized on ground and isolated from shuttle by crew access hatch.
2. Inclination 0.497 radian (28.5 degrees)
3. Operations altitude 463 km (250 n. mi.)
4. Fly missions during new moon periods; launch anytime of day
5. Initiate deorbit 45 minutes prior to revolution 107 which passes within orbiter crossrange capability at 166 hrs. 42 min. elapsed time. Total mission duration launch to initiate deorbit is 165 hrs. 57 min.

IR TELESCOPE PAYLOAD 4AC
MISSION SEQUENCE AND FLIGHT PROFILE

ELAPSED TIME (HR:MIN)	EVENT
00:00	LIFTOFF
00:06.5	INSERT INTO 93 X 185 KM (50 X 100 NMI) ORBIT
00:50.1	TRANSFER TO 185 X 463 KM (100 X 250 NMI) ORBIT AT FIRST APOGEE
01:36.1	CIRCULARIZE AT 463 KM (250 NMI) ORBIT AT FIRST APOGEE. STABILIZE, CHECKOUT ORBITER SYSTEMS, UPDATE EPHEMERIS, OPEN ORBITER CARGO BAY DOORS, VERIFY READINESS TO PROCEED WITH EXPERIMENT OPERATIONS
02:00	ORBITER COARSE-ATTITUDE ACQUISITION
02:30	REMOTE CHECKOUT OF SORTIE LAB SUBSYSTEMS VERIFICATION; ELECTRICAL POWER; ENVIRONMENTAL CONTROL/LIFE SUPPORT; CONTROL AND DISPLAY; THERMAL CONTROL; COMMUNICATIONS/DATA MANAGEMENT; GUIDANCE, NAVIGATION AND CONTROL
02:45	VERIFY SORTIE LAB HABITABILITY AND OPEN CREW ACCESS HATCH
03:00	SORTIE LAB CHECKOUT BY SCIENTIFIC CREW VERIFY EC/LS CAUTION AND WARNING SUBSYSTEM; VERIFY COMMUNICATIONS/DATA MANAGEMENT SUBSYSTEM; VERIFY SUBSYSTEMS CONTROL AND DISPLAY PANELS; VERIFY ELECTRICAL POWER DISTRIBUTION TO PALLET; VERIFY PALLET THERMAL CONTROL SUBSYSTEM; TURN ON GUIDANCE, NAVIGATION AND CONTROL SUBSYSTEM
03:30	PERFORM VISUAL INSPECTION OF TELESCOPE AND ARRAYS
	<u>TELESCOPE DEPLOYMENT</u>
03:40	RELEASE TELESCOPE GIMBAL MOUNT LAUNCH LOCKS
03:42	ROTATE DEPLOYMENT YOKE TO 90 DEGREE POSITION AND LOCK
03:57	PITCH TELESCOPE COARSE GIMBAL INTO INITIAL OPERATIONS POSITION
04:12	RELEASE AZIMUTH TABLE LOCKS
04:14	OPEN TELESCOPE COVER
04:16	SETUP TELESCOPE AND INSTRUMENTS MONITOR TEMPERATURE CONTROL SYSTEM UNTIL STABILIZATION (APPROXIMATELY 3 ORBITS)
	<u>GAMMA-RAY SPECTROMETER AND LOW BACKGROUND GAMMA-RAY DETECTOR DEPLOYMENT</u>
04:50	RELEASE ARRAY GIMBAL MOUNT LAUNCH LOCKS
04:52	ROTATE ARRAY DEPLOYMENT YOKE TO 90-DEGREE POSITION AND LOCK
05:07	PITCH ARRAY COARSE GIMBAL INTO INITIAL OPERATIONS POSITION
05:22	RELEASE AZIMUTH TABLE LOCKS

ELAPSED TIME (HR:MIN)	EVENT
	WIDE COVERAGE X-RAY DEPLOYMENT
05:24	RELEASE ARRAY MOUNT LAUNCH LOCKS
05:26	DEPLOY WIDE COVERAGE X-RAY ARRAYS
05:41	ROTATE WIDE COVERAGE X-RAY ARRAYS HALVES INTO OPERATIONS POSITION
	WIDE COVERAGE X-RAY ARRAY CHECKOUT
05:51	PERFORM SAFETY CHECK
05:53	TURN ON ELECTRICAL POWER
05:54	PERFORM ELECTRICAL CHECK
05:55	PERFORM BUILT-IN CALIBRATION
	GAMMA-RAY SPECTROMETER AND LOW BACKGROUND GAMMA-RAY DETECTOR CHECKOUT
06:05	PERFORM VISUAL SAFETY CHECK
06:15	TURN ON ELECTRICAL POWER
06:17	RELEASE LAUNCH RESTRAINTS AND DEPLOY DETECTOR PACKAGE
06:19	PERFORM FUNCTIONAL CHECK
06:29	PERFORM ELECTRONICS CALIBRATION
06:39	ESTABLISH ORIENTATION REFERENCES
06:44	INITIATE REPEATABLE ON-ORBIT OPERATIONS SEQUENCE FOR ARRAYS

...THE WIDE COVERAGE X-RAY ARRAY AND THE GAMMA RAY SPECTROMETER AND LOW BACKGROUND GAMMA RAY DETECTOR ARE OPERATED CONTINUOUSLY (EXCEPT FOR PERIODS OF AUTOMATIC SHUTDOWN DURING PASSAGE THRU THE SOUTH ATLANTIC ANOMALY) UNTIL TERMINATION OF EXPERIMENT OPERATIONS AT 161 HRS. 35 MIN...

ELAPSED TIME (HR:MIN)	EVENT
	IR TELESCOPE POST-TEMPERATURE STABILIZATION CHECKOUT
09:00	ALIGN TELESCOPE AND INSTRUMENT AXES WITH SORTIE CAN AND PALLET GUIDANCE, NAVIGATION AND CONTROL SYSTEM REFERENCES
09:30	CALIBRATE INSTRUMENT DETECTORS OF IR TELESCOPE
10:00	INITIATE REPEATABLE ON-ORBIT OPERATIONS SEQUENCE FOR IR TELESCOPE

...TYPICAL REPEATABLE ON-ORBIT OPERATIONS SEQUENCE FOR IR TELESCOPE REQUIRING 93.7 MINUTES PER CYCLE (54.7 MINUTES PER CYCLE OBSERVATION TIME) PERFORM 97 TIMES, COMPLETING OPERATIONS AT 161 HRS. 35 MINUTES...

ELAPSED TIME (HR:MIN)	EVENT
161:35	CLOSE COVERS ON TELESCOPE
161:37	SECURE TELESCOPE AZIMUTH TABLE LOCKS
161:39	TURN OFF ELECTRICAL POWER TO WIDE COVERAGE X-RAY ARRAY
161:41	ROTATE WIDE COVERAGE X-RAY ARRAY HALVES INTO STOWING POSITION
162:02	SECURE ARRAY MOUNT LOCKS
162:04	TURN OFF ARRAY CONTROLS AND DISPLAYS
162:06	RETRACT GAMMA-RAY ARRAY DETECTOR PACKAGE AND SECURE LAUNCH RESTRAINTS
162:11	SWITCH ELECTRICAL POWER TO GAMMA-RAY ARRAY TO STANDBY

ELAPSED TIME (HR: MIN)	EVENT
162:13	SECURE GAMMA-RAY ARRAYS AZIMUTH TABLE LOCKS
162:15	PITCH ARRAY COARSE GIMBAL INTO STOWING POSITION
162:45	RELEASE ARRAY DEPLOYMENT YOKE, ROTATE INTO STOWED POSITION AND LOCK
163:15	SWITCH GAMMA-RAY ARRAYS CONTROLS AND DISPLAY PANELS TO MONITOR CRYO SYSTEM ONLY
163:17	PITCH TELESCOPE COARSE GIMBAL INTO STOWED POSITION
163:47	RELEASE DEPLOYMENT YOKE LOCK AND ROTATE INTO STOWED POSITION
164:17	SECURE TELESCOPE GIMBAL MOUNT LAUNCH LOCKS
164:19	SWITCH TELESCOPE THERMAL CONTROL SYSTEM TO STANDBY
164:21	TURN OFF MAIN POWER TO INSTRUMENT DETECTORS
164:23	TURN OFF CONTROLS AND DISPLAYS PANELS
	<u>SECURE SORTIE LAB AND PALLET</u>
164:25	TURN OFF SORTIE LAB GUIDANCE, NAVIGATION AND CONTROLS SUBSYSTEM; SWITCH PALLET TO STANDBY; THERMAL CONTROL SUBSYSTEM; SWITCH ELECTRICAL POWER DISTRIBUTION TO PALLET TO STANDBY
164:31	SCIENTIFIC CREW TRANSFER TO ORBITER STATIONS
164:41	CLOSE ACCESS HATCH TO SORTIE LAB
164:51	SWITCH SORTIE LAB SUBSYSTEMS TO STANDBY
164:57	CHECKOUT ORBITER, PREPARE FOR RETURN TO EARTH
165:57	INITIATE DEORBIT

TYPICAL REPEATABLE ON-ORBIT OPERATIONS SEQUENCE
ONE-METER IR TELESCOPE

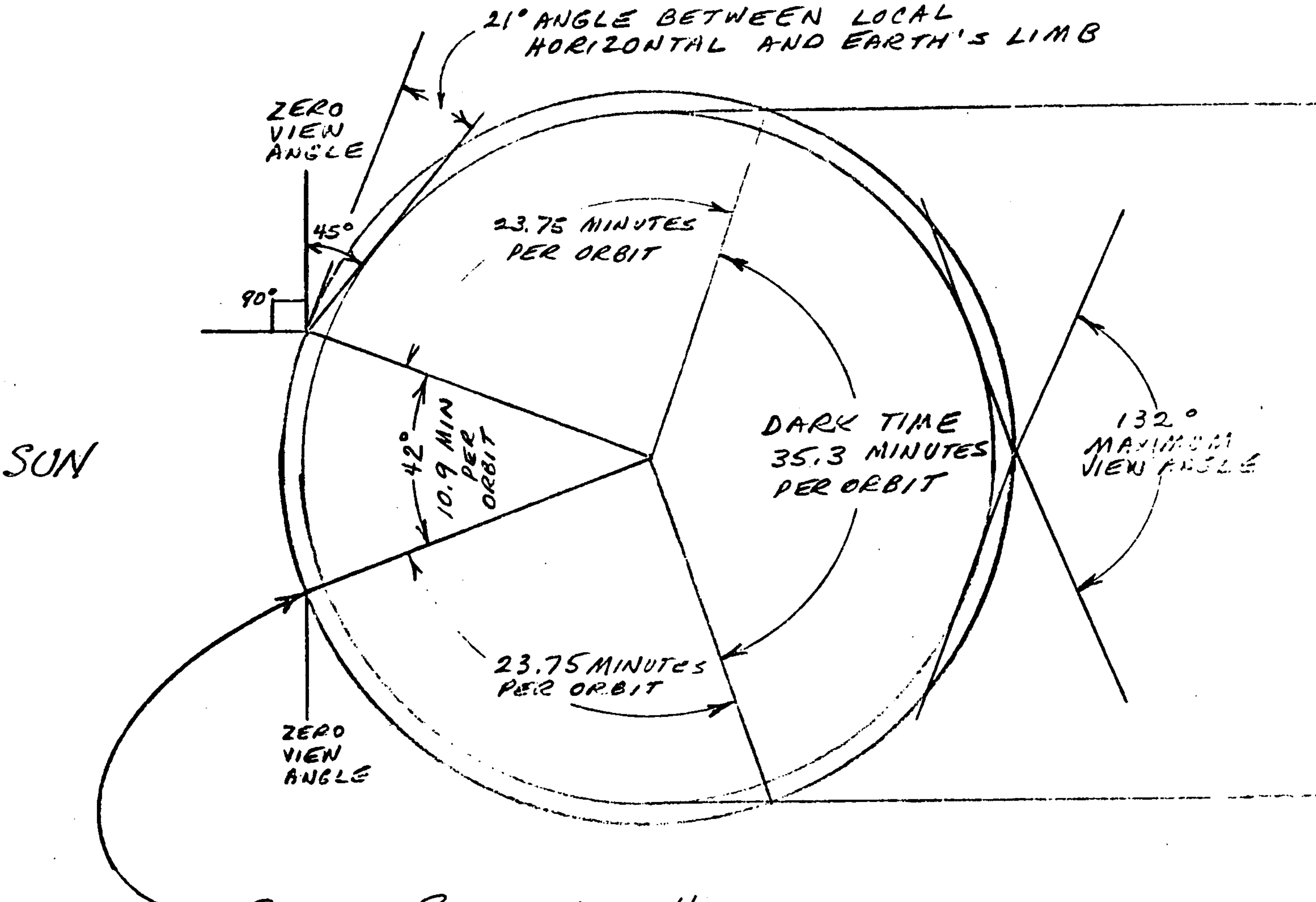

START SEQUENCE HERE

MINUTES	FUNCTION
12.0	PERIODIC CHECKOUT
6.0	PERIODIC CALIBRATION
3.0	GUIDE STAR ACQUISITION
3.0	OBJECT LOCATION
7.65	OBJECT OBSERVATION
3.0	GUIDE STAR ACQUISITION
3.0	OBJECT LOCATION
32.3	OBJECT OBSERVATION
3.0	GUIDE STAR ACQUISITION
3.0	OBJECT LOCATION
14.75	OBJECT OBSERVATION
3.0	ROTATE BEAM-DIRECTING MIRROR
TOTAL 93.70	

SOLAR PAYLOAD 1-2
FINAL MISSION ASSUMPTIONS

1. Sortie Lab is pressurized on ground and isolated from Shuttle by crew access hatch.
2. Inclination 1.16 to 1.57 radians (66.5 to 90 degrees) depending on time of year of mission.
3. Operations altitude variable with inclination from 592 km (320 n.mi.) at 1.16 radians to 463 km (250 n. mi.) at 1.57 radians.
4. Orbital passes within the crossrange capability of the orbiter vary with altitude and inclination. At 463 km altitude and an inclination of 1.57 radians, orbit 107 passes within the crossrange capability at 167 hr. 15 min. Deorbit is initiated 45 minutes prior to this pass at 166 hr. 30 min. elapsed time.
5. Typical repeatable Photoheliograph cycle is based upon manual control of experiment equipment and sortie lab pallet subsystems to perform pointing, alignment, and focusing functions. The times required and shown assume improvement in these functions after the first time. Target selection (shown as zero after the first time) is performed during previous observation period.
6. Typical repeatable X-Ray Focusing Telescope cycle is based upon manual control of experiment equipment and sortie lab pallet subsystems to perform pointing, alignment, and focusing functions. The times required and shown assume improvement in these functions after the first time. Target selection (shown as zero after the first time) is performed during previous observation period.

SOLAR PAYLOAD 1-2
FINAL MISSION SEQUENCE AND FLIGHT PROFILE

ELAPSED TIME (HR:MIN)	EVENT
00:00	LIFTOFF
00:06.5	INSERT INTO 93 X 185 (50 X 100 NMI) ORBIT
00:50.1	TRANSFER TO 185 KM X FINAL ORBIT ALTITUDE OF 463 KM TO 592 KM (250 TO 320 NMI) AT FIRST APOGEE
01:35.1	CIRCULARIZE AT FINAL ORBIT ALTITUDE AT FIRST APOGEE. STABILIZE, CHECKOUT ORBITER SYSTEMS, UPDATE EPHEMERIS, OPEN ORBITER CARGO BAY DOORS, VERIFY READINESS TO PROCEED WITH EXPERIMENT OPERATIONS
02:00	ORBITER COARSE-ATTITUDE ACQUISITION
02:30	REMOTE CHECKOUT OF SORTIE LAB SUBSYSTEMS VERIFICATION: ELECTRICAL POWER; ENVIRONMENTAL CONTROL/LIFE SUPPORT; CONTROL AND DISPLAY; THERMAL CONTROL; COMMUNICATIONS/DATA MANAGEMENT; GUIDANCE, NAVIGATION AND CONTROL
02:45	VERIFY SORTIE LAB HABITABILITY AND OPEN CREW ACCESS HATCH
03:00	SORTIE LAB CHECKOUT BY SCIENTIFIC CREW VERIFY EC/LS CAUTION AND WARNING SUBSYSTEM; VERIFY COMMUNICATIONS/DATA MANAGEMENT SUBSYSTEM; TURN ON SUBSYSTEMS CONTROL AND DISPLAY PANELS; TURN ON ELECTRICAL POWER DISTRIBUTION TO PALLET TURN ON PALLET THERMAL CONTROL SUBSYSTEM; TURN ON GUIDANCE, NAVIGATION AND CONTROL SUBSYSTEM
03:30	PERFORM VISUAL INSPECTION OF TELESCOPES
	<u>PHOTOHELIOGRAPH CHECKOUT</u>
03:40	TURN ON CONTROL AND DISPLAY PANEL, IMAGE CONTROL SUBSYSTEM SERVOS, CAMERA AND FILTER CONTROL AND THERMAL CONTROL ELECTRONICS
03:48	RELEASE LAUNCH LOCKS TO PROTECT PRIMARY AND SECONDARY MIRROR ASSEMBLIES
03:50	TURN ON AND STABILIZATION OF TELESCOPE THERMAL CONTROL FLUID SYSTEMS AND SPECTRAL FILTER THERMAL CONTROL
	<u>PHOTOHELIOGRAPH</u>
04:20	RELEASE TELESCOPE GIMBAL MOUNT LAUNCH LOCKS
04:22	ROTATE DEPLOYMENT YOKE TO 90 DEGREE POSITION AND LOCK
04:37	PITCH TELESCOPE COARSE GIMBAL INTO INITIAL OPERATIONS POSITION
04:52	RELEASE AZIMUTH TABLE LOCKS

ELAPSED TIME (HR:MIN)	EVENT
	PHOTOHELIOGRAPH POST-DEPLOYMENT CHECKOUT
04:54	OPEN APERTURE DOOR
04:56	ENABLE ALIGNMENT AND FOCUS SERVOS AND ACHIEVE THERMAL EQUILIBRIUM
	XUV SPECTROHELIOGRAPH CHECKOUT
05:06	TURN ON CONTROL AND DISPLAY PANEL, IMAGE CONTROL SUBSYSTEM SERVOS, AND CAMERA CONTROL
05:16	ADJUST BAND SELECTION GRATING
	X-RAY FOCUSING TELESCOPE CHECKOUT
05:31	TURN ON CONTROL AND DISPLAY PANELS, IMAGE ELECTRONICS, CAMERA PROGRAMMING ELECTRONICS, FILTER WHEEL CONTROL, THERMAL CONTROL ELECTRONICS, PHOTOMULTIPLIER DETECTOR ELECTRONICS
05:41	TELESCOPE MAIN POWER SWITCHING, THERMAL CONTROL STATUS, APERTURE DOOR POSITION CONTROL, FILTER WHEEL POSITION SELECTION, DETECTOR SELECTION
05:59	IMAGING SYSTEM CAMERA FRAME RATE SELECTION, IMAGE INTENSIFIER HIGH VOLTAGE CONTROL, GRATING POSITION, INITIATE AND STOP MODE OPERATION
06:02	CRYSTAL SPECTROMETER SYSTEM SLIT SIZE CONTROL, SCAN RANGE CONTROL, SCAN SEQUENCE CONTROL, CRYSTAL POSITION CONTROL, CALIBRATE, INITIATE AND STOP MODE OPERATION
06:10	PROPORTIONAL COUNTER HIGH VOLTAGE CONTROL, CALIBRATE, PULSE HEIGHT ANALYZER RESOLUTION WIDTH, INITIATE AND STOP MODE OPERATION
06:14	H-ALPHA SLIT CAMERA POWER ON, FILTER HEATER ON AND STATUS, HIGH VOLTAGE CONTROL
06:17	PHOTOMULTIPLIER DETECTOR SYSTEM HIGH VOLTAGE POWER CONTROL, DISCRIMINATOR LEVEL CONTROL, FLARE ALERT DISPLAY
06:22	SOLAR X-RAY MONITOR TELESCOPE MAIN POWER CONTROL HIGH VOLTAGE CONTROL, BRIGHTNESS CONTROL
06:24	H-ALPHA MONITOR TELESCOPE MAIN POWER CONTROL, HIGH VOLTAGE CONTROL, FILTER HEATER CONTROL, THERMAL STATUS
	CORONAGRAPHS
06:27	TURN ON CONTROL AND DISPLAY PANEL, OCCULTING DISCS CONTROL SUBSYSTEMS, CAMERA AND FILTER CONTROL, AND THERMAL CONTROL ELECTRONICS
06:37	TURN ON AND STABILIZATION OF TELESCOPE THERMAL CONTROL SYSTEMS

ELAPSED TIME (HR:MIN)	EVENT
	TELESCOPE DEPLOYMENT
07:07	RELEASE TELESCOPE GIMBAL MOUNT LAUNCH LOCKS
07:09	ROTATE DEPLOYMENT YOKE TO 90 DEGREE POSITION AND LOCK
07:24	PITCH TELESCOPE COARSE GIMBAL INTO INITIAL OPERATIONS POSITION
07:39	RELEASE AZIMUTH TABLE LOCKS
	XUV SPECTROHELIOGRAPH POST-DEPLOYMENT CHECKOUT
07:41	UNCOVER SUN SENSOR AND SPECTROHELIOGRAPH OPTICS
08:11	INITIAL CALIBRATION QUIET SUN PLAGES PHOTOS
08:26	INITIAL CALIBRATION QUIET SUN (INNER) CORONA
08:41	INITIAL CALIBRATION STANDARD LAMPS (INTERNAL)
	CORONAGRAPHS POST-DEPLOYMENT CHECKOUT
09:11	OPEN COVERS AND LENS CAPS ON BOTH 1-6 SOLAR RADII AND 5-30 SOLAR RADII CORONAGRAPHS, ERECT SUN SENSOR
09:22	ACQUIRE SUN IN TELESCOPE FOV
09:28	ENABLE ALIGNMENT SERVOS AND ACHIEVE THERMAL EQUILIBRIUM
09:40	ADJUST POSITIONS OF EXTERNAL OCCULTING DISCS TO OBTAIN MAXIMUM SUPPRESSION OF DIFFRACTION EFFECTS FOR 1-6 SOLAR RADII
09:55	ADJUST POSITIONS OF EXTERNAL OCCULTING DISCS TO OBTAIN MAXIMUM SUPPRESSION OF DIFFRACTION EFFECTS FOR 5-30 SOLAR RADII CORONAGRAPH
10:10	ADJUST INTENSITY CALIBRATION WEDGES FOR 1-6 SOLAR RADII CORONAGRAPH
10:22	ADJUST INTENSITY CALIBRATION WEDGES FOR 5-30 SOLAR RADII CORONAGRAPH
10:32	INITIATE OBSERVATION PROGRAMS

...PHOTOHELIOGRAPH

PERFORM TYPICAL REPEATABLE ON-ORBIT OPERATIONS SEQUENCE, 24 TIMES, PLUS 96 ADDITIONAL MINUTES, ACHIEVING 24X282=6768 PLUS 56=6824 MINUTES (113 HR 44 MIN) TOTAL OPERATIONS TIME.

...X-RAY FOCUSING TELESCOPE

PERFORM TYPICAL REPEATABLE ON-ORBIT OPERATIONS SEQUENCE 40 TIMES, PLUS 200 ADDITIONAL MINUTES, ACHIEVING 40X162=6480 PLUS 142=6622 MINUTES (110 HR. 22 MIN) TOTAL OPERATIONS TIME.

...XUV SPECTROHELIOGRAPH AND CORONAGRAPHS

OBTAIN/EXPOSURE EVERY 3 MINUTES DURING QUIET SUN AND ACTIVE SUN MODES. OBTAIN 2 EXPOSURES PER MINUTE DURING A FLARE. OPERATE CONTINUOUSLY UNTIL...

	X-RAY FOCUSING TELESCOPE SHUTDOWN
161:32	TURN OFF IMAGE ELECTRONICS, CAMERA PROGRAMMING ELECTRONICS, FILTER WHEEL CONTROL, THERMAL CONTROL ELECTRONICS, PHOTOMULTIPLIER, DETECTOR ELECTRONICS

ELAPSED TIME (HR:MIN)	EVENT
	XUV SPECTROHELIOGRAPH SHUTDOWN
161:42	COVER SUN SENSOR AND OPTICS
162:05	TURN OFF IMAGE CONTROL SUBSYSTEM SERVOS, AND CAMERA CONTROL
	CORONAGRAPHS SHUTDOWN
162:11	RETRACT SUN SENOR, CLOSE COVERS AND LENS CAPS
162:21	TURN OFF OCCULTING DISCS CONTROL SUBSYSTEM, CAMERA AND FILTER CONTROL AND THERMAL CONTROL ELECTRONICS
	TELESCOPE RETRACT
162:27	SECURE AZIMUTH TABLE LOCKS
162:33	PITCH TELESCOPE COARSE GIMBAL INTO STOWED POSITION
163:03	RELEASE DEPLOYMENT YOKE LOCK AND ROTATE INTO STOWED POSITION
163:33	SECURE TELESCOPE GIMBAL MOUNT LAUNCH LOCKS
163:37	TURN OFF CONTROL AND DISPLAY PANEL
	PHOTOHELIOGRAPH SHUTDOWN AND RETRACT
163:43	CLOSE PHOTOHELIOGRAPH APERTURE DOOR
163:45	SECURE LAUNCH LOCKS TO PROTECT PHOTOGELIOGRAPH PRIMARY AND SECONDARY MIRRORS ASSEMBLIES
163:47	SECURE TELESCOPE AZIMUTH TABLE LOCKS
163:49	PITCH TELESCOPE COARSE GIMBAL INTO STOWED POSITION
164:19	RELEASE DEPLOYMENT YOKE LOCK AND ROTATE INTO STOWED POSITION
164:49	SECURE TELESCOPE GIMBAL MOUNT LAUNCH LOCKS
164:52	TURN OFF PHOTOHELIOGRAPH THERMAL CONTROL FLUID SYSTEMS, SPECTRAL FILTER THERMAL CONTROL, AND CONTROLS AND DISPLAYS PANELS
	SECURE SORTIE LAB AND PALLET
164:58	TURN OFF SORTIE LAB GUIDANCE, NAVIGATION AND CONTROL SUBSYSTEM; TURN OFF PALLET THERMAL CONTROL SUBSYSTEM; TURN OFF ELECTRICAL POWER DISTRIBUTION TO PALLET
165:04	SCIENTIFIC CREW TRANSFER TO ORBITER STATIONS
165:14	CLOSE ACCESS HATCH TO SORTIE LAB
165:24	SWITCH SORTIE LAB SUBSYSTEMS TO STANDBY
165:30	CHECKOUT ORBITER, PREPARE FOR RETURN TO EARTH
166:30	INITIATE DEORBIT

TYPICAL REPEATABLE ON-ORBIT OPERATIONS SEQUENCE
PHOTOHELIOGRAPH

MODE	FUNCTION	TIME IN MINUTES							
		OP. 1	OP. 2	OP. 3	OP. 4	OP. 5	OP. 6	OP. 7	TOTAL
QUIET SUN	A. SELECT TARGET	3			0	0	0		3
	B. POINT TELESCOPE TO ACQUIRE TARGET	3			3	3	3		12
	C. ALIGN SECONDARY MIRROR RELATIVE TO PRIMARY MIRROR TRANSVERSELY AND IN TILT	6			1	1	1		9
	D. ADJUST FOCUS, MOVING SECONDARY MIRROR AND CELL ASSEMBLY AXIALLY ALONG OPTICAL AXIS OF MIRROR	12			3	3	3		21
	E. OBSERVE TARGET	18			18	18	18		72
ACTIVE SUN	F. SELECT TARGET	0	0	0			0	0	0
	G. POINT TELESCOPE TO ACQUIRE TARGET	3	3	3			3	3	15
	H. ALIGN (SAME AS C. ABOVE)	3	1	1			1	1	7
	I. ADJUST FOCUS (SAME AS D. ABOVE)	3	3	3			3	3	15
	J. OBSERVE TARGET	30	30	30			30	30	150
FLARE	K. SELECT TARGET							0	0
	L. POINT TELESCOPE TO ACQUIRE TARGET							3	3
	M. ALIGN (SAME AS C. ABOVE)							1	1
	N. ADJUST FOCUS (SAME AS D. ABOVE)							3	3
	O. OBSERVE TARGET							60	60

TOTAL TIME FOR REPEATABLE SEQUENCE, MINUTES 371

REPEATABLE OPERATIONS TIME, MINUTES 282

TYPICAL REPEATABLE ON-ORBIT OPERATIONS SEQUENCE
X-RAY FOCUSING TELESCOPE

MODE	FUNCTION	TIME IN MINUTES							
		OP 1	OP 2	OP 3	OP 4	OP 5	OP 6	OP 7	TOTAL
QUIET SUN	A. Select Target	3			0	0	0		3
	B. Point Telescope to Acquire Target	3			3	3	3		12
	C. Operate Imaging System	5			5	5	5		20
	D. Index to Crystal Spectrometer	1			1	1	1		4
	E. Operate Crystal Spectrometer	3			3	3	3		12
ACTIVE SUN	F. Select Target	0	0	0			0	0	0
	G. Point Telescope to Acquire Target	3	3	3			3	3	15
	H. Operate Crystal Spectrometer	3	3	3			3	3	15
	I. Index to Imaging System	1	1	1			1	1	5
	J. Operate Imaging System	5	5	5			5	5	25
	K. Index Grating In	1	1	1			1	1	5
	L. Operate Imaging System Plus Grating	5	5	5			5	5	25
	M. Index to Proportional Counter	1	1	1			1	1	5
	N. Operate Proportional Counter	1	1	1			1	1	5
	O. Index to Crystal Spectrometer	1	1	1			1	1	5
FLARE	P. Identify Target							0	0
	Q. Point Telescope to Acquire Target							3	3
	R. Index to Imaging System and Grating							1	1
	S. Operate Imaging System and Grating							60	60

TOTAL TIME FOR REPEATABLE SEQUENCE, MINUTES	220
REPEATABLE OPERATIONS TIME	162
QUIET SUN IMAGING SYSTEM OPERATIONS	20
ACTIVE AND FLARE IMAGING SYSTEM OPERATIONS	110

TYPICAL REPEATABLE ON-ORBIT
OPERATIONS SEQUENCE
XUV SPECTROHELIOGRAPH AND
INNER AND OUTER CORONAGRAPHS

1 exposure every 3 minutes during quiet sun and active sun modes;

2 exposures per minute during a flare

TRADEOFF STUDY REPORT

PROGRAM: ASTRONOMY SORTIE MISSIONS DEFINITION STUDY

TITLE: PERFORMING CRITICAL ROLES AND FUNCTIONS

DATE: MAY 31, 1972

PREPARED BY:

R. Shedko

R. Shedko

L. Fredrickson

L. Fredrickson

APPROVED BY:

W. P. Pratt
Study Manager

I. SUMMARY

The problem addressed in this tradeoff study was the selection of preliminary designs for telescope functions that are performed repetitively during on-orbit operations. These functions were identified as "critical" in analyses of operations to determine methods of utilizing men effectively in astronomy sortie missions.

Three methods of performing each critical function were compared with respect to effect on mission success, cost, complexity, and flexibility. The three methods are: manned, automatic, and fixed.

The design choice for all of these critical functions was determined to be "manned" except for the observing operations of the XUV Spectroheliograph and the Coronagraphs. These were determined to be "automatic" design choice. A "fixed" design was not selected for any operation, and for many was considered "not applicable" (N/A).

The results of this study depend heavily on the approach used in considering cost. The program guideline of manning the telescopes by two observers who are not part of the Shuttle flight crew, with a duty cycle such that operations 24 hours per day are supported, provides the manned method without a cost penalty that must be charged to the experiment function. For the automatic method, the cost of providing the flight equipment penalizes this alternative.

II. CONTENTS

III. STATEMENT OF PROBLEM

Effective utilization of man requires his application (1) to tasks requiring the unique capabilities of human judgment and manual skills, (2) to non-repetitive functions, and (3) to repeatable functions that are best performed by the crew. The preliminary mission profiles showed that the telescope operations (but not the SL Pallet activation, experiment deployment, retraction, and deactivation operations) were repeatable and of such a nature as to present a choice of method in accomplishing them.

The problem then, was to determine which of these repetitive operating functions should be performed by the flight crew, which should be automated, and which could be eliminated by fixing the hardware and making no adjustment possible. Those repetitive operations that must be automated for technical reasons, such as the stabilizing of telescope on targets, were not analyzed in this problem.

IV. DESCRIPTION OF THE SELECTION SCHEME AND CRITERIA USED

The scheme to select one of the three operations methods (manned, automated or fixed) involved estimating the effect of performing the functions by each of the methods on mission success, cost, complexity, and flexibility. The criteria were compared by estimating the best method for each function and assigning a value of 10 to that parameter. The other methods were then estimated at values from one to nine. Adding the scores

for each of the four comparison criteria resulted in a total score. The highest total score was selected as the preliminary design choice. The considerations made for each criterion were as follows:

1. Mission Success - Which method gives the greatest assurance of acquiring the most scientific data? Will one method give more time to observe and collect data? Does the method permit recovery from malfunction? If the method precludes satisfying mission objectives of a telescope, it was determined to be "not applicable" and the choice was narrowed to the remaining two methods.
2. Cost - Which is the lowest cost method? Since experiment crewmen are provided, no cost penalty was assessed for the manned method. The factors estimated here were cost of the flight hardware required for each method.
3. Complexity - Which method requires the most elaborate equipment and operations? Must operations be performed only when in contact with a ground station? The least complex, that is, the simplest method was selected as best.
4. Flexibility - Which method can best respond to real-time (or near-real-time) changes that become desirable? Which method can best recover from malfunction or operate in an alternate mode?

V. DESCRIPTION OF THE CANDIDATE SOLUTIONS

Three methods of performing the critical functions of experiment operations were apparent candidates. They were manned, automatic, and fixed.

1. Manned - This method uses the experiment flight crew to initiate, control, adjust, stop, and monitor a function. A variety of

controls and displays may be required, but the essential ingredient is that the flight crewman manually performs the function and assesses its completion.

2. Automatic - This method used flight equipment to initiate, control, adjust, stop, and monitor a function. A crewman may be present to observe and assess the performance of the function, but normally he takes no action.

3. Fixed - This method (which is not applicable to all functions) eliminates the function by fixing the hardware making no control or adjustment possible.

VI. EVALUATION OF THE CANDIDATES

The candidates were evaluated using a subjective scoring technique, the best rated 10, the others proportionately less than 10, for each of the four comparison criteria: Mission Success, Cost, Complexity, and Flexibility. In performing the scoring, consideration was given to the presently known hardware concepts for each telescope and for the operations to be accomplished. The scoring included subjective engineering judgment of the overall difficulty of the function and the sophistication of the equipment as well as differences between the methods.

VII. SELECTION OF PREFERRED APPROACH

Tables 1 through 5 present the data that were generated in comparing the candidate solutions for each of the functions of the Astronomy Sortie Missions telescopes. Based on the total scores shown in these tables, a preliminary design choice was selected for each function.

The comparisons were made by estimating the method that is best for each of the four criteria (Mission Success, Cost, Complexity, and Flexibility) and assigning a value of 10 to that method. The less desirable methods were

then assessed values lower than 10, the scores were added for each method, and the highest total score chosen for preliminary design.

VIII. RECOMMENDATION

The "manned" method was chosen for each function of all of the telescopes except "observing" for the XUV Spectroheliograph and the Coronagraphs. These two functions were chosen to be "automatic".

IX. SUBSEQUENT EVALUATION

The technique used in selecting these choices was subjective and was based on a concept of the hardware involved in performing the functions. Some of the total scores were very nearly ties and the resulting design choices should be reviewed as system analyses and definitions are developed.

TABLE 1

CRITICAL ROLES AND FUNCTIONS

PHOTOHELIOGRAPH

FUNCTION	METHOD	COMPARISON CRITERIA				TOTAL SCORE	PRELIMINARY RESULT
		MISSION SUCCESS	COST	COMPLEXITY	FLEXIBILITY		
SELECT	Manned	10	10	10	10	40	Design Choice
	Automatic	8	1	1	8	18	
	Fixed	N/A	N/A	N/A	N/A	N/A	
POINT	Manned	10	10	10	10	40	Design Choice
	Automatic	8	1	4	9	22	
	Fixed	N/A	N/A	N/A	N/A	N/A	
ALIGN	Manned	8	10	10	10	38	Design Choice
	Automatic	10	6	3	4	23	
	Fixed	3	3	6	1	13	
FOCUS	Manned	8	10	10	10	38	Design Choice
	Automatic	10	6	3	4	23	
	Fixed	3	3	6	1	13	
OBSERVE	Manned	10	10	10	10	40	Design Choice
	Automatic	8	3	4	8	23	
	Fixed	N/A	N/A	N/A	N/A	N/A	

TABLE 2

CRITICAL ROLES AND FUNCTIONS

X-RAY TELESCOPE

FUNCTION	METHOD	COMPARISON CRITERIA				TOTAL SCORE	PRELIMINARY RESULT
		MISSION SUCCESS	COST	COMPLEXITY	FLEXIBILITY		
SELECT	Manned	10	10	10	10	40	Design Choice
	Automatic	8	1	1	8	18	
	Fixed	N/A	N/A	N/A	N/A	N/A	
POINT	Manned	10	10	10	10	40	Design Choice
	Automatic	8	1	4	9	22	
	Fixed	N/A	N/A	N/A	N/A	N/A	
INDEX	Manned	10	10	10	10	40	Design Choice
	Automatic	9	7	7	9	32	
	Fixed	N/A	N/A	N/A	N/A	N/A	
OBSERVE	Manned	10	10	10	10	40	Design Choice
	Automatic	9	9	9	9	36	
	Fixed	N/A	N/A	N/A	N/A	N/A	

TABLE 3

CRITICAL ROLES AND FUNCTIONS

XUV SPECTROHELIOGRAPH AND CORONAGRAPHS

FUNCTION	METHOD	COMPARISON CRITERIA: MISSION SUCCESS	COST	COMPLEXITY	FLEXIBILITY	TOTAL SCORE	PRELIMINARY RESULT
SELECT MODE	Manned	9	10	10	10	39	Design Choice
	Automatic	10	7	7	9	33	
	Fixed	N/A	N/A	N/A	N/A	N/A	
OBSERVE	Manned	5	10	10	10	35	
	Automatic	10	9	9	9	37	Design Choice
	Fixed	N/A	N/A	N/A	N/A	N/A	

TABLE 4

CRITICAL ROLES AND FUNCTIONS

STRATOSCOPE III

FUNCTION	METHOD	COMPARISON CRITERIA				TOTAL SCORE	PRELIMINARY RESULT
		MISSION SUCCESS	COST	COMPLEXITY	FLEXIBILITY		
POINT	Manned	9	10	10	10	39	Design Choice
	Automatic	10	6	6	6	28	
	Fixed	N/A	N/A	N/A	N/A	N/A	
SELECT FILTER OR GRATING	Manned	10	10	10	10	40	Design Choice
	Automatic	8	9	9	8	34	
	Fixed	N/A	N/A	N/A	N/A	N/A	
CALIBRATE	Manned	9	8	8	10	35	Design Choice
	Automatic	10	4	4	8	26	
	Fixed	6	10	10	4	30	
OBSERVE	Manned	10	10	10	10	40	Design Choice
	Automatic	7	8	8	6	29	
	Fixed	N/A	N/A	N/A	N/A	N/A	
ROTATE MIRROR	Manned	9	10	10	10	39	Design Choice
	Automatic	10	9	9	9	37	
	Fixed	N/A	N/A	N/A	N/A	N/A	

TABLE 5

CRITICAL ROLES AND FUNCTIONS

IR TELESCOPE

FUNCTION	METHOD	COMPARISON CRITERIA				TOTAL SCORE	PRELIMINARY RESULT
		MISSION SUCCESS	COST	COMPLEXITY	FLEXIBILITY		
PERIODIC CHECKOUT	Manned	8	10	10	10	38	Design Choice
	Automatic	10	9	9	9	37	
	Fixed	N/A	N/A	N/A	N/A	N/A	
PERIODIC CALIBRATE	Manned	8	9	9	10	36	Design Choice
	Automatic	10	8	8	9	35	
	Fixed	4	10	10	4	28	
ACQUIRE GUIDE STAR	Manned	9	10	10	10	39	Design Choice
	Automatic	10	8	8	9	35	
	Fixed	N/A	N/A	N/A	N/A	N/A	
LOCATE OBJECTIVE	Manned	10	10	10	10	40	Design Choice
	Automatic	8	7	7	7	29	
	Fixed	N/A	N/A	N/A	N/A	N/A	
OBSERVE	Manned	9	10	10	10	39	Design Choice
	Automatic	10	9	9	8	36	
	Fixed	N/A	N/A	N/A	N/A	N/A	
ROTATE MIRROR	Manned	9	10	10	10	39	Design Choice
	Automatic	10	9	9	9	37	
	Fixed	N/A	N/A	N/A	N/A	N/A	

APPENDIX A4

ASTRONOMY SORTIE MISSION

FAILURE MODE AND EFFECTS ANALYSIS

MAY 1972

INTRODUCTION

Preliminary Failure Mode and Effects Analyses (FMEA) were performed on the Astronomy Sortie Mission support subsystems, astronomy experiment instruments, and arrays to identify the mission critical single failure points and provide a basis for the determination of redundancy and inflight maintenance requirements.

The FMEA's included in this appendix were performed to the component/assembly level based on the available conceptual designs for the baseline ASM subsystems and experiments. Each failure mode identified was classified with respect to safety/mission criticality using the following categories;

Category I - Failure which results in a potential crew safety hazard.

Category II - Failure which results in total loss of experiment capability or inability to meet primary mission objectives

Category III - Failure which results in partial loss of primary objectives or loss of all secondary objectives.

Category IV - Failure which results in only partial secondary data loss or has no significant effect.

Where possible, the required inflight and post mission corrective actions were identified.

ASTRONOMY SORTIE MISSION
FAILURE MODE AND EFFECTS ANALYSIS

INSTRUMENT OR SUBSYSTEM	FAILURE MODE	CAUSE OF FAILURE	EFFECT OF FAILURE: CREW	EFFECT OF FAILURE: EXPERIMENT/ MISSION	FAILURE CRITICALITY CATEGORY	CORRECTIVE ACTION: DURING MISSION	CORRECTIVE ACTION: POST MISSION	RECOMMENDATIONS/ REMARKS
Low Background Gamma-Ray Detector								
Detector Modules (4)	Loss of any one detector module	Failure of the module or any of its parts	None	<u>Experiment</u>: Loss of part of experiment data <u>Mission</u>: Degraded mission	III	None	Repair or Replace	Since there are four identical detector modules loss of any one will cause loss of all data
Electronics Package	Loss of electronics for any one detector	Failure of a portion of elec. package associated with one detector module	None	<u>Experiment</u>: Loss of part of experiment package <u>Mission</u>: Degraded mission	III	None	Repair or Replace	Loss of one portion does not cause loss of all data

ASTRONOMY SORTIE MISSION
FAILURE MODE AND EFFECTS ANALYSIS

INSTRUMENT OR SUBSYSTEM	FAILURE MODE	CAUSE OF FAILURE	EFFECT OF FAILURE: CREW	EFFECT OF FAILURE: EXPERIMENT/ MISSION	FAILURE CRITICALITY CATEGORY	CORRECTIVE ACTION: DURING MISSION	CORRECTIVE ACTION: POST MISSION	RECOMMENDATIONS/ REMARKS
Narrow-Band Spectrometer/ Polarimeter								
Narrow-Band Detectors (Nine)	Loss of one of two continuum radiation modules	Sectored proportional counter failure or loss of associated electronics	No effect	Experiment: Loss of temperature determination for the X-ray source at one energy level. Mission: Minor mission degradation.	III	None	Repair or replace defective energy level module	Loss of one energy level X-ray source temperature determining module
	Loss of one of seven line intensity module	Sectored proportional counter failure or loss of associated electronics	No effect	Experiment: Loss of polarization measurement of X-ray flux generation for one element Mission: Minor mission degradation	III	None	Repair or replace defective line intensity module	Loss of polarization measurement for one element of X-ray flux generation
	Structural mounting frame failure	Jammed launch restraints or failure to elevate supporting gimbals	None	Experiment: Loss of ability to decouple drift between experiment axis and shuttle orientation Mission: Degraded mission	III	Viewing of specific X-ray sources will require re-orientation of the Shuttle	Repair or replace defective structural mounting component	SFP Loss of all data pertaining to measurement of X-ray intensity and polarization of a selected source
	Central Data Processor failure	Loss of memory units, pulse height analyzers, readout or control circuits	Loss of real time monitoring of the experiments operation	Experiment: Loss of objective of this experiment. Loss of stored data results in experiment degradation Mission: Degraded mission	III	None	Repair or replace defective data processor unit	

ASTRONOMY SORTIE MISSION
FAILURE MODE AND EFFECTS ANALYSIS

INSTRUMENT OR SUBSYSTEM	FAILURE MODE	CAUSE OF FAILURE	EFFECT OF FAILURE		FAILURE CRITICALITY CATEGORY	CORRECTIVE ACTION		RECOMMENDATIONS/ REMARKS
			CREW	EXPERIMENT/ MISSION		DURING MISSION	POST MISSION	
Gamma-Ray Spectrometer								
Crystal Detectors (One of Four)	Loss of gamma ray photon detection for the 0.06 to 10 MeV energy range	Deployment mechanism failure	No effect	**Experiment:** Loss of extended range of measurements into the higher energy level **Mission:** Minor mission degradation	III	None	Repair or replace defective components	Loss of X-ray and Gamma-ray line emissions in the 0.06 to 10 MeV energy level
Scintillation Guard Shield	Fails to limit field of review of instrument	Sodium-doped iodide flakes off crystals	No effect	**Experiment:** Loss of collimation and rejection through the defined aperture **Mission:** Minor degradation	III	None	Repair or replace sodium-doped iodide coatings	
Cryogenic Refrigerator	Loss of crystal detector temperature control	Mechanical valve failure	None	**Experiment:** Temperature rise above 200K deteriorates detector characteristics **Mission:** Minor degradation	III	None	Repair or replace defective components	Loss of X-ray and Gamma-ray line emissions in the 0.06 to 10 MeV energy level
Electronics Package	Loss of output data	Electrical circuit failure	None	**Experiment:** Loss of basic information relative to scientific objective of this experiment **Mission:** Minor degradation	III	None	Repair or replace defective electronics	

ASTRONOMY SORTIE MISSION
FAILURE MODE AND EFFECTS ANALYSIS

INSTRUMENT OR SUBSYSTEM	FAILURE MODE	CAUSE OF FAILURE	EFFECT OF FAILURE: CREW	EFFECT OF FAILURE: EXPERIMENT/MISSION	FAILURE CRITICALITY CATEGORY	CORRECTIVE ACTION: DURING MISSION	CORRECTIVE ACTION: POST MISSION	RECOMMENDATIONS/ REMARKS
WIDE COVERAGE X-RAY DETECTOR								
X-Ray Detector Units and Dome Structure	Loss of one or more Detector Units	Failure of one (or more) of the detector modules	None	Experiment: Degradation of ability to detect and locate transient X-ray emissions. Mission: Degradation of mission.	III	None	Repair or Replace	There are "many" detector modules on the dome. Loss of one (or more) detectors degrades data but does not cause loss of all data.
Central Data Processor	Loss of all data output of the experiment.	Failure of circuits or any of their parts.	None	Experiment: Loss of random transient emission detection. Mission: Degradation of mission.	III	None	Repair or Replace	SFP Loss of all data causes loss of experiment.
LARGE MODULATION COLLIMATOR								
Modulation Collimator Modules	Loss of any one module.	Failure of any part of detector.	None	Experiment: Partial loss of ability to measure properties of X-Ray sources. Mission: Degradation of mission.	III	None	Replace or repair	Since there are multiple modules loss of any one will not cause loss of all data.
Central Data Processor	Loss of processing of data signals.	Failure of circuits or any of their parts.	None	Experiment: Loss of experiment output data. Mission: Degradation of mission.	III	None	Replace or repair	SFP Loss of signal processing causes loss of all data.

ASTRONOMY SORTIE MISSION
FAILURE MODE AND EFFECTS ANALYSIS

INSTRUMENT OR SUBSYSTEM	FAILURE MODE	CAUSE OF FAILURE	EFFECT OF FAILURE		FAILURE CRITICALITY CATEGORY	CORRECTIVE ACTION		RECOMMENDATIONS/ REMARKS
			CREW	EXPERIMENT/ MISSION		DURING MISSION	POST MISSION	
COLLIMATED PLANE CRYSTAL SPECTROMETER								
Collimator (one of three)	Fails to limit field of view.	Improper alignment.	None	Experiment: Spectral information of x-ray sources will not be limited to the specified bands. Mission: Minor mission degradation.	III	None	Repair or replace defective components	Partial loss of high resolution data for both point and extended sources.
Crystal Assembly (one of three)	Fails to diffract x-rays to proportional counter and pulse height analyzer	Cracked crystals	None	Experiment: Loss of one-third of the energy range coverage and spectral resolution. Mission: Minor mission degradation.	III	None	Repair or replace defective components	Partial loss of high resolution data for both point and extended sources.
Proportional Counter (one of three)	Fails to detect intensity of diffracted x-rays.	Loss of inert gas.	None		III	None	Repair or replace defective components.	
Pulse Height Analyzer (one of three)	Loss of output	Failure of electrical parts.	None	Experiment: Loss of one-third of the energy range coverage and spectral resolution. Mission: Minor degradation.	III	None	Repair or replace defective components.	Partial loss of high resolution data for both point and extended sources.

ASTRONOMY SORTIE MISSION
FAILURE MODE AND EFFECTS ANALYSIS

INSTRUMENT OR SUBSYSTEM	FAILURE MODE	CAUSE OF FAILURE	EFFECT OF FAILURE: CREW	EFFECT OF FAILURE: EXPERIMENT/ MISSION	FAILURE CRITICALITY CATEGORY	CORRECTIVE ACTION: DURING MISSION	CORRECTIVE ACTION: POST MISSION	RECOMMENDATIONS/ REMARKS
COLLIMATED PLANE CRYSTAL SPECTRO-METER (Continued)								
Detector Drive Mechanism	Loss of associated drive mechanism to fine point the instrument.	Failure of mechanical or electrical parts.	None		III	None	Repair or replace defective components.	
Central Data Processor and Control Electronics	No output to real time data management or tape recorders.	Failure of any associated electrical or mechanical parts.	None	<u>Experiment</u>: Loss of all data for energy range and spectral resolution. <u>Mission</u>: Degraded mission.	III	None	Repair or replace defective components.	<u>SFP</u> Loss of all experiment data related to x-ray sources in the 0.5 to 10 KeV energy range.
LARGE AREA X-RAY DETECTOR								
Detector Modules (6)	Loss of any one detector causes partial loss of ability to detect incident x-ray energy.	Failure of any part of detector.	None	<u>Experiment</u>: Loss of expected output of experiment. <u>Mission</u>: Degraded mission.	III	None	Replace or repair	Since there are six detector modules loss any one will not cause loss of all data.
Central Data Processor	Loss of pulse height analysis.	Failure of circuits or any of their parts.	None	<u>Experiment</u>: Loss of or inaccurate experiment output.	III	None	Replace or repair	<u>SFP</u> Loss of pulse height analysis causes loss of output of all detectors.

ASTRONOMY SORTIE MISSION
FAILURE MODE AND EFFECTS ANALYSIS

INSTRUMENT OR SUBSYSTEM	FAILURE MODE	CAUSE OF FAILURE	EFFECT OF FAILURE: CREW	EFFECT OF FAILURE: EXPERIMENT/ MISSION	FAILURE CRITICALITY CATEGORY	CORRECTIVE ACTION: DURING MISSION	CORRECTIVE ACTION: POST MISSION	RECOMMENDATIONS/ REMARKS
PHOTOHELIOGRAPH	a) Failure of H- Camera	1. Failure of shutter 2. Failure of torque motors or drive 3. Failure of controls 4. Failure of filter	None	Partial Data Loss	III	None	Repair or replace as required.	Replace camera after 4 flights.
	b) Failure of Broad Band Camera	1. Failure of shutter 2. Failure of torque motors or drive 3. Failure of controls 4. Failure of filter	None	Partial Data Loss	III	None	Repair or replace as required.	Replace camera after 4 flights.
	c) Failure of Spectrograph	1. Camera failure 2. Misalignment	None	Partial Data Loss	III	None	Repair or replace as required.	Replace camera after 4 flights.
	d) Primary Mirror Failure	1. Warped or distorted 2. Deterioration of coating.	None	Loss of part of Astronomy Data	III	None	Repair or replace as required.	
	e) Secondary Mirror Failure	1. Deterioration of coating.	None	Loss of part of Astronomy Data	III	None	Repair or replace as required.	
	f) Loss of Internal Alignment of Man Optics	1. Failure of motor, align, electr., detector, or laser 2. Fail of IDT or filter	None	Loss of part of Astronomy Data	III	None	Repair or replace as required.	

ASTRONOMY SORTIE MISSION
FAILURE MODE AND EFFECTS ANALYSIS

INSTRUMENT OR SUBSYSTEM	FAILURE MODE	CAUSE OF FAILURE	EFFECT OF FAILURE: CREW	EFFECT OF FAILURE: EXPERIMENT/ MISSION	FAILURE CRITICALITY CATEGORY	CORRECTIVE ACTION: DURING MISSION	CORRECTIVE ACTION: POST MISSION	RECOMMENDATIONS/ REMARKS
PHOTOHELIOGRAPH (Continued)	g) Loss of Focus	1. Failure of motor, align, control, electronics. 2. Failure of IDT or filter.	None	Loss of Part of Astronomy Data	III	None	Repair or replace as required.	
	h) Failure of the folding mirror.	1. Failure of motor, control, fine pointing electronics. 2. Failure of IDT or filter.	None	Loss of Astronomy Data	III	None	Repair or replace as required.	
	i) Failure of aperture door to open.	1. Structural failure. 2. Failure of motor, control, or mechanism.	None	Loss of All Astronomy Data.	III	None	Repair or replace as required.	
	j) Loss of Display	1. Failure of Vidicon.	None	Degraded Operation	III	None	Repair or replace as required.	
	k) Failure of Wave Length Control	1. Part Failure	None	Partial Data Loss	III	None	Repair or replace as required.	
XUV SPECTRO-HELIOGRAPH	a) Failure of Aperture Door to open.	1. Failure of Actuator, Motor or Control 2. Structural Failure	None	Loss of XUV Data	III	None	Repair or replace as required.	
	b) Failure of Aperture Door to Close	1. Failure of Actuator, Motor, or Control 2. Structural Failure	None	Degraded Operation due to Thermal Unbalance.	III		Repair or replace as required.	

ASTRONOMY SORTIE MISSION
FAILURE MODE AND EFFECTS ANALYSIS

INSTRUMENT OR SUBSYSTEM	FAILURE MODE	CAUSE OF FAILURE	EFFECT OF FAILURE		FAILURE CRITICALITY CATEGORY	CORRECTIVE ACTION		RECOMMENDATIONS/ REMARKS
			CREW	EXPERIMENT/ MISSION		DURING MISSION	POST MISSION	
XUV SPECTRO-HELIOGRAPH (Continued)	**c) Failure of Concave Grating**	**1. Failure of motor, drive mechanism, or control 2. Structural Failure.**	**None**	Loss of XUV Data	III	None	Repair or re-place as re-quired.	
	d) Failure of Film Camera	**1. Failure of shutter, shutter control, drive mechanism or motor. 2. Failure of film transport mechanism or drive motor.**	**None**	Loss of XUV Data	III	None	Repair or re-place as re-quired.	Replace camera after 4 flights.
	e) Failure of Filter	1. Structural Failure	None	Degraded Operation due to loss of Thermal Protection.	III	None	Repair or re-place as re-quired.	
	f) Failure of Rejection Mirrors	1. Structural Failure or Misalignment	None	Degraded Operation due to Loss of Thermal Pro-tection	III	None	Repair or re-place as re-quired.	
	g) Failure of Aspect Sensor	1. Vidicon Failure 2. Electronic Part Failure 3. Mechanical Failure	None	Degraded Operation	III	None	Repair or re-place as re-quired.	
X-RAY FOCUSING TELESCOPE								
Large Aperture Grazing In-cidence Tele-scope	No anticipated failure modes.	N/A	N/A	N/A	III	N/A	N/A	

ASTRONOMY SORTIE MISSION
FAILURE MODE AND EFFECTS ANALYSIS

INSTRUMENT OR SUBSYSTEM	FAILURE MODE	CAUSE OF FAILURE	EFFECT OF FAILURE: CREW	EFFECT OF FAILURE: EXPERIMENT/MISSION	FAILURE CRITICALITY CATEGORY	CORRECTIVE ACTION: DURING MISSION	CORRECTIVE ACTION: POST MISSION	RECOMMENDATIONS/REMARKS
X-RAY FOCUSING TELESCOPE (Continued)								
X-Ray Transmission Grating	Binds or freezes in either of two possible positions.	Mechanical Malfunction	None	Experiment: Loss of part of the function of the experiment. Mission: Degraded Mission	III	None	Repair	Only a portion of the data that might be desired could be obtained.
Filter Wheel	Binds or freezes in one of six possible positions.	Mechanical Malfunction	None	Experiment: Loss of selection of data to be observed. Mission: Degraded Mission	III	None	Repair	Only a portion of the data that might be desired could be obtained.
Turret	Binds or freezes in one of three possible positions.	Mechanical Malfunction	None	Experiment: Loss of selection of data to be observed. Mission: Degraded Mission	III	None	Repair	Only a portion of the data that might be desired could be obtained.
Image Intensifier Converter	Fails to convert X-Ray image to optical image.	Failure of any part of converter.	None	Experiment: Loss of ability to convert X-Ray images. Mission: Degraded Mission	III	None	Replace or repair	Partial loss of experiment data.

ASTRONOMY SORTIE MISSION:
FAILURE MODE AND EFFECTS ANALYSIS

INSTRUMENT OR SUBSYSTEM	FAILURE MODE	CAUSE OF FAILURE	EFFECT OF FAILURE		FAILURE CRITICALITY CATEGORY	CORRECTIVE ACTION		RECOMMENDATIONS/ REMARKS
			CREW	EXPERIMENT/ MISSION		DURING MISSION	POST MISSION	
Film Camera	Fails to record optical images.	Failure of camera or any of its parts.	None	Experiment: Loss of one portion of experiment data and loss of one means of identifying data. Mission: Degraded Mission	III	None	Repair or replace	Partial loss of experiment data. • Replace camera after 4 flights.
Camera Programming Electronics	Loss of camera control. (Loss of output)	Failure of the camera programming electronics unit or any of its parts.	None	Experiment: Loss of one portion of experimental data and loss of one means of identifying data. Mission: Degraded Mission	III	None	Repair or replace	Partial loss of experiment data.
Crystal Spectrometer	Loss of output.	Failure of the unit or any of its parts.	None	Experiment: Loss of one portion of the experiment. Mission: Degraded Mission	III	None	Repair or replace	Partial loss of experiment data.
Crystal Spectrometer Electronics	Loss of output.	Failure of the unit or any of its parts.	None	Experiment: Loss of one portion of the experiment. Mission: Degraded Mission	III	None	Repair or replace	Partial loss of experiment data.

ASTRONOMY SORTIE MISSION
FAILURE MODE AND EFFECTS ANALYSIS

INSTRUMENT OR SUBSYSTEM	FAILURE MODE	CAUSE OF FAILURE	EFFECT OF FAILURE		FAILURE CRITICALITY CATEGORY	CORRECTIVE ACTION		RECOMMENDATIONS/ REMAKRS
			CREW	EXPERIMENT/ MISSION		DURING MISSION	POST MISSION	
X-RAY FOCUSING TELESCOPE (Continued)								
Proportional Counter	Loss of output	Failure of the unit or any of its parts.	None	Experiment: Loss of one portion of the experiment. Mission: Degraded Mission	III	None	Replace or repair	Loss of a portion of experiment data.
Proportional Counter Electronics	Loss of output	Failure of the unit or any of its parts.	None	Experiment: Loss of one portion of the experiment. Mission: Degraded Mission	III	None	Replace or repair	Loss of a portion of experiment data.
H-α Slit Camera	Loss of output	Failure of the unit or any of its part.	None	Experiment: Loss of telescope pointing capability. Mission: Degraded Mission	III	None	Replace or repair	Loss of quality of experiment data. o Replace camera after 4 flights.
Photomultiplier Detector Solar Activity Monitor	Loss of output	Failure of the unit or any of its parts.	None	Experiment: Loss of camera exposure times and frame rates Mission: Degraded Mission	III	None	Repair or replace	Loss of quality of experiment data.
Photomultiplier Detector Electronics	Loss of output	Failure of the unit or any of its parts.	None	Experiment: Loss of camera exposure times and frame rates Mission: Degraded Mission	III	None	Repair or replace	Loss of quality of experiment data

ASTRONOMY SORTIE MISSION

FAILURE MODE AND EFFECTS ANALYSIS

INSTRUMENT OR SUBSYSTEM	FAILURE MODE	CAUSE OF FAILURE	EFFECT OF FAILURE		FAILURE CRITICALITY CATEGORY	CORRECTIVE ACTION		RECOMMENDATIONS/ REMARKS
			CREW	EXPERIMENT/ MISSION		DURING MISSION	POST MISSION	
IR TELESCOPE	a) Failure of primary mirror	1. Mirror warped or misaligned 2. Deteriora- tion of coating	None	Loss of astronomy data	II	None	Repair or replace as required	Critical SFP
	b) Failure of secondary mirror	1. Misaligned 2. Deteriora- tion of coating	None	Loss of astronomy data	II	None	Repair or replace as required	Critical SFP
	c) Failure of liquid neon cooling system	1. Loss of coolant	None	Partial loss of data	III	None	Repair or replace as required	
	d) Failure of aperture door to open	1. Failure of actuator, motor, control 2. Structural failure	None	Loss of all astronomy data	II	None	Repair or replace as required	Critical SFP
	e) Failure of the interfero- meter	1. Part failure 2. Mechanical failure	None		III	None	Repair or replace as required	
	f) Failure of the detector array	1. Mechanical failure			III	None	Repair or replace as required	
	g) Failure of liquid helium cooling system	1. Loss of coolant	None	Partial loss of data	III	None	Repair or replace as required	
	h) Failure of the optical telescope	1. Misalign- ment	None	Loss of pointing and stabilization	II	None	Repair and replace as required	Critical SFP
	i) Failure of imaging system	1. Failure of imaging tube 2. Failure of electronics	None	Loss of visible light data	III	None	Repair or replace as required	
	j) Failure of optical reference	1. Star tracker failure		Loss of pointing and stabilization	II	None	Repair or replace as required	Critical SFP

ASTRONOMY SORTIE MISSION

FAILURE MODE AND EFFECTS ANALYSIS

INSTRUMENT OR SUBSYSTEM	FAILURE MODE	CAUSE OF FAILURE	EFFECT OF FAILURE		FAILURE CRITICALITY CATEGORY	CORRECTIVE ACTION		RECOMMENDATIONS/ REMARKS
			CREW	EXPERIMENT/ MISSION		DURING MISSION	POST MISSION	
CORONAGRAPH (IC)	a) Failure of occulting disk assembly	1. Mechanical failure resulting in misalignment. 2. Failure of drive mechanism or motor.	None	Loss of IC Data	III	None	Repair or replace as required.	
	b) Failure of Optical Assy.	1. Misalignment	None	Loss or degradation of IC Data	III	None	Repair or replace as required.	
	c) Failure of Film Camera	1. Failure of Shutter, control, drive mechanism or motor. 2. Failure of film transport mechanism or drive motor.	None	Loss of IC Data	III	None	Repair or replace as required.	Camera life limitation 50,000 cycles - Replace every 4 flights.
	d) Failure of Aspect Sensor	1. Vidicon failure 2. Elect. part failure 3. Mechanical failure	None	Degraded operation	III	None	Repair or replace as required.	
	e) Failure of Thermal Mirrors	1. Misalignment	None	Degraded operation	III	None	Repair or replace as required.	
CORONAGRAPH (OC)	(Same as a) thru e) above)	Same as above for Fail Modes a) thru e)	None	Same as above for Failure Modes a) thru e)	III	None	Repair or replace as required.	
OPTICAL BENCH	a) Misalignment	Structural Failure	None	Loss of IC or OC data or both	III	None	Repair or replace as required.	
STRATOSCOPE III	a) Failure of F-12 Camera	1. Launch & Ascent Environment 2. Wearout	None	Partial loss of Exp. Data	III	None	Replace failed item.	

INSTRUMENT OR SUBSYSTEM	FAILURE MODE	CAUSE OF FAILURE	EFFECT OF FAILURE: CREW	EFFECT OF FAILURE: EXPERIMENT/ MISSION	FAILURE CRITICALITY CATEGORY	CORRECTIVE ACTION: DURING MISSION	CORRECTIVE ACTION: POST MISSION	REMARKS
STRATOSCOPE III (CONT'D)	b) Failure of F-96 Camera	1. Launch & Ascent Environment 2. Wearout	None	Partial loss of Exp. Data	III	None	Replace Failed item	
	c) Failure of Low Speed, Hi Resol Spectrograph	1. Camera Failure due to Launch Env or Wearout 2. Misalignment of Mirrors, Collimater, grating, or Camera due to Launch Env or Space Thermal Env.	None	Partial loss of Exp Data	III	None	Replace failed item	
	d) Failure of High Speed, Low Resol Spectrograph	1. Camera failure due to Launch Env or Wearout. 2. Misalignment of mirrors, Collimater, grating, or Camera due to Launch Env. or Space Thermal Env.	None	Partial loss of Exp Data	III	None	Replace failed item	
	e) Primary Mirror Distorted or Misaligned	1. Warping due to thermal environment 2. Support structure misalignment	None	Possible loss of all Astronomy Data	II	Adjust force actuators on mirror, adjust temperature, or adjust tilt, focus, or decenter to compensate	Repair as Required	Critical SPF
	f) Primary Mirror Contaminated	1. Materials Outgassing 2. Spacecraft Propulsion	None	Possible loss of all Astronomy Data	II	None	Clean Mirror	Critical SPF
	g) Secondary Mirror distorted or misaligned	1. Warping due to Thermal env. 2. Support structure misalignment	None	Possible loss of all Astronomy data	II	Adjust Tilt, focus, decentering to compensate	Repair as required	Critical SPF

INSTRUMENT OR SUBSYSTEM	FAILURE MODE	CAUSE OF FAILURE	EFFECT OF FAILURE: CREW	EFFECT OF FAILURE: EXPERIMENT/MISSION	FAILURE CRITICALITY CATEGORY	CORRECTIVE ACTION: DURING MISSION	CORRECTIVE ACTION: POST MISSION	REMARKS
STRATOSCOPE III (CONT'D)	h) Secondary mirror contaminated	1. Materials outgassing 2. Spacecraft propulsion	None	Possible loss of all astronomy data	II	None	Clean mirror	Critical SFP
	i) Failure of beam directing mechanism	1. Launch and ascent environment or space thermal env.	None	Possible loss of all astronomy data	II	None	Repair as required	Critical SFP
	j) Failure of aperture door to open	1. Misalignment or binding 2. Failure of drive motor or actuator	None	Loss of all astronomy data	II	None	Repair as required	Critical SFP
	k) Failure of aperture door to close	1. Misalignment or binding 2. Failure of drive motor or actuator	None	None	III	Program operation to prevent pointing at bright lights	Repair as required	
	l) Failure of light shade to extend	1. Misalignment or binding 2. Drive motor or mechanism failure	None	Loss of or degradation of astronomy data	II	None	Repair as required	Critical SFP
	m) Failure of light shade to close	1. Misalignment or binding 2. Drive motor or mechanism failure	None	Inability to return telescope into bay for return to earth	II	Jettison light shade or total telescope	Repair as required	Critical SFP

ASTRONOMY SORTIE MISSION

FAILURE MODE AND EFFECTS ANALYSIS

ASM GN&C SUBSYSTEM

INSTRUMENT OR SUBSYSTEM	FAILURE MODE	CAUSE OF FAILURE	EFFECT OF FAILURE: CREW	EFFECT OF FAILURE: EXPERIMENT/MISSION	FAILURE CRITICALITY CATEGORY	CORRECTIVE ACTION: DURING MISSION	CORRECTIVE ACTION: POST MISSION	RECOMMENDATIONS/REMARKS
ATM DGCMGs - functions are to stabilize the Shuttle Orbiter in an X-POP (X-axis perpendicular to the orbital plane) attitude, and to provide ability to maneuver the Shuttle Orbiter	Loss of ability to stabilize the SO in X-POP attitude. Loss of ability to maneuver the SO	Failure of the circuitry or its associated parts	None	Failure would result in loss of mission	III	None - No EVA during mission	Inspect and repair as necessary	NOTE: Two of the three ATM DGCMGs will perform the required functions
ASM PALLET RATE GYRO PACKAGE - functions are to measure SO body rates, imputted to CMG system to stabilize SO, imputted to a set of strapdown equation for computing SO attitude.	Loss of SO body rates input to CMG system Loss of rate input for computation of SO attitude	Failure of the circuitry or its associated parts	None	Failure would result in loss of mission	II	None - No EVA during mission	Inspect and repair as necessary	Critical SFP
ASM TELESCOPE RATE GYRO PACKAGE - functions are to measure ASM telescope rotational rates for input to telescope fine stabilization system for stability requirements, and for input to a set of strapdown equations of computation of telescope attitude	Loss of telescope stability Loss of telescope pointing capability	Failure of circuitry or its associated parts	None	Failure would result in loss of telescope experiment	II	None - No EVA during mission	Inspect and repair as necessary	Critical SFP

ASTRONOMY SORTIE MISSION

FAILURE MODE AND EFFECTS ANALYSIS

INSTRUMENT OR SUBSYSTEM	FAILURE MODE	CAUSE OF FAILURE	EFFECT OF FAILURE		FAILURE CRITICALITY CATEGORY	CORRECTIVE ACTION		RECOMMENDATIONS/ REMARKS
			CREW	EXPERIMENT/ MISSION		DURING MISSION	POST MISSION	
THREE STRAPDOWN STAR TRACKERS - functions are to measure telescope attitude, to update both the SO and telescope strapdown equations. For the SO strapdown equations, the measured telescope attitude must be reflected through the telescopes wide angle gimbals.	Loss of telescope attitude data to update the telescope and SO strapdown equations	Failure of circuitry or its associated parts	None	Failure would result in loss of experiment pointing and possible loss of mission	III	None - No EVA during mission	Inspect and repair as necessary	NOTE: It is conceivable that two of the three STs could supply adequate data for updating strapdown equations
TWO WIDE ANGLE GIMBAL EXPERIMENT POINTING ASSEMBLIES The telescopes and High Energy Arrays are mounted on two separate wide angle gimbals, one gimbal points the Telescope and the other points the High Energy Arrays with respect to the SO.	Loss of wide angle gimbal for pointing of Telescope	Circuitry, mechanical or wheel jamming	None	Failure would result in loss of Telescope experiment	II	None - No EVA during mission	Inspect and repair as necessary	Critical SFP
	Loss of Telescope Wide Angle gimbal readout	Failure of circuitry or associated parts	None	Failure would result in loss of mission	II			Critical SFP
	Loss of High Energy Array Gimbal for Pointing	Circuitry on mechanical failure	None	Failure would result in loss of High Energy Array experiment	III			
TELESCOPE FINE STABILIZATION ASSEMBLY - function is to stabilize the Telescope with respect to the SO. Three (3) rotational degrees of freedom to completely isolate the telescope from SO perturbations	Loss of Telescope fine stabilization	Failure of the circuitry or its associated parts	None	Failure would result in loss of telescope experiment	II	None - No EVA during mission	Inspect and repair as necessary	Critical SFP

ASTRONOMY SORTIE MISSION

FAILURE MODE AND EFFECTS ANALYSIS

Payload Control and Display Console Subsystem

INSTRUMENT OR SUBSYSTEM	FAILURE MODE	CAUSE OF FAILURE	EFFECT OF FAILURE: CREW	EFFECT OF FAILURE: EXPERIMENT/ MISSION	FAILURE CRITICALITY CATEGORY	CORRECTIVE ACTION: DURING MISSION	CORRECTIVE ACTION: POST MISSION	RECOMMENDATIONS/ REMARKS
1. Display, CRT	Display loss or degradation	Electrical failure or phosphor degradation	None	Degraded experiment and support S/S monitoring capability	III	None - experiment operation may continue using one CRT	Replace failed unit	Two CRT displays are provided each having the identical capability to display experiment video and/or computer data
2. Generator, Multifunction Symbol	Loss of CRT displays	Sync, timing, memory, sweep or refresh failure	None	Loss of experiment and support S/S monitoring capability	III	None	Replace failed unit	Note: Unit provides two channels of data handling, one for each CRT. Adequate redundancy to eliminate SFPs effecting both CRTs or backup required
3. Keyboard Subsystem	Loss of experiment command capability	Incorrect or no output	None	Probable termination of experiment operation	II	Replace - See Remarks	Replace	Provide redundant subsystem or on-board spare. Critical SFP
4. Viewer, Microfilm	Loss of display	Projection system and/ or film transport	None	Loss of procedures display	III	Use hard copy procedures	Replace	
5. Controller, Hand	Loss of manual pointing control	Electrical or mechanical failure	None	Operational degradation due to loss of manual control of target acquisition	III	Replace with on-board spare	Replace	Provide on-board spare and provide redundant cabling in console
6. Mission Time Display	Loss of Readout	Electrical failure or burn-out of display elements	None	Possible degradation of experiment data if sequence start time critical	III	May be possible to display time on CRT	Replace	
7. Timer, Event	Readout or command (Start/Stop) Loss	Clock, display element, or electrical failure	None	Unable to time sequences or provide auto start/stop of timed sequences	III	Use mission time display as backup	Replace	

ASTRONOMY SORTIE MISSION

FAILURE MODE AND EFFECTS ANALYSIS

Payload Control and Display Console Subsystem

INSTRUMENT OR SUBSYSTEM	FAILURE MODE	CAUSE OF FAILURE	EFFECT OF FAILURE: CREW	EFFECT OF FAILURE: EXPERIMENT/ MISSION	FAILURE CRITICALITY CATEGORY	CORRECTIVE ACTION: DURING MISSION	CORRECTIVE ACTION: POST MISSION	RECOMMENDATIONS/ REMARKS
8. Indicator, Advisory	Loss of display	Loss of bus voltage, lamp burnout, or loss of signal	None	Loss of an individual Alert Status Indicator	III	Status may be displayed on CRT	Replace	NOTE: Bus voltage and lamp elements have design redundancy. Functions monitored are non-time crew action
9. Recorder Strip Chart	No or Eratic output	Element, amplifier, or power supply failure	None	Loss of an individual channel of data recording. Loss of all channels for power supply failure.	III	Use alternate channel, if possible	Remove and repair	Provide redundant power supplies

APPENDIX B1-1

PAYLOAD DATA ANALYSIS

INTRODUCTION

This appendix defines the data requirements for the Baseline Payload Combinations. Data rates and formats are derived from the instrument Baseline Experiment Definition Documents (BEDD's) of Volume II, Book 2. Operating times are derived from the on-orbit operational sequences. Total data to be stored on board is calculated for the proposed mission and requirements for immediate display of data are indicated in percentages of the incoming data. Data to be telemetered during the 7-day mission consists mainly of engineering and status data to inform the Principal Investigator at the Space Astronomy Control Facility of experiment operation. A sampling of scientific digital data from the Infrared Telescope and the arrays is included.

DATA ANALYSIS FOR PAYLOAD: SOLAR 1-2

SOURCE/CLASS	FORMAT	DATA RATE	OPERATING MODE & TIME	DISPOSITION OF DATA: STORAGE FILM/TAPE	REALTIME DISPLAY	CALL-UP DISPLAY	TELEMETER TO GRD (%) TOTAL	COMMENTS/NOTES
PAYLOAD #1 –								
PHOTOHELIOGRAPH – (PHG)								
SCIENTIFIC: BROADBAND CAMERA	FILM	1FR/10SEC	(FUNCTION	15,000 FRAMES	—	—	—	
H-ALPHA CAMERA	FILM	1FR/3-10SEC	OF SOLAR	24,000 FRAMES	—	—	—	
SPECTROGRAPH	FILM	1FR/30-60-100SEC	ACTIVITY)	3600 FRAMES	—	—	—	
ENGINEERING (STATUS/OPERATION)	DIGITAL	1500BPS	(CONTIN.) 151 H	814.5 MB	20%	—	(20%) 162.9MB	($151H = 543 \times 10^3$ SEC)
H-ALPHA MONITOR	ANALOG	4MHZ	CONTINUOUS	2%-VIDEO	100%	—	—	
SUBSYSTEM, SUPPORT: P&CS	DIGITAL	32BPS	(CONTIN.) 158 H	35.22MB	1%	5%	(5%) 1.96MB	($158H = 568 \times 10^3$ SEC)
POWER	DIGITAL	20BPS						
THERMAL	DIGITAL	10BPS						
PAYLOAD #2 –								
XUV SPECTROHELIOGRAPH – (SHG)								
SCIENTIFIC	FILM	1FR/3MIN	(CONTIN.) 151 H	3020 FRAMES	—	—	—	
ENGINEERING	DIGITAL	60BPS	(CONTIN.) 151 H	32.58MB	10%	20%	(20%) 6.52MB	
INNER & OUTER CORONAGRAPHS (IC & OC)								
SCIENTIFIC: IC	FILM	1FR/3MIN	(CONTIN.) 151 H	3020 FRAMES	—	—	—	
OC	FILM	1FR/3MIN	(CONTIN.) 151 H	3020 FRAMES	—	—	—	
ENGINEERING	DIGITAL	100BPS	(CONTIN.) 151 H	54.3 MB	10%	20%	(20%) 1.09MB	
X-RAY TELESCOPE (XRT)								
SCIENTIFIC: IMAGING SYSTEM	FILM	1FR/12 SEC	86% (OF 151 H)	5000 FRAMES	—	—	—	(MAX DATA RATE – 1 FR/SEC)
SPECTROGRAPH	DIGITAL	2,000BPS	12% (OF 151 H)	130.3 MB	1%	—	(1%) 1.31 MB	
COUNTER	DIGITAL	2,000BPS	2% (OF 151 H)	21.7MB	1%	—	(1%) 0.22MB	
ENGINEERING	DIGITAL	8 BPS	(CONTIN.) 151 H	4.3MB	10%	20%	(20%) 0.86MB	
SUBSYSTEM, SUPPORT: P&CS	DIGITAL	40 BPS	(CONTIN.) 158H	51.2MB	1%	5%	(5%) 2.56MB	
POWER	DIGITAL	30BPS						
THERMAL	DIGITAL	20BPS						
CREW ANNOTATION	ANALOG	3KHZ	AS REQUIRED	100%	—	—	20%	
MONITORS								
H-ALPHA (PAYLOAD #2)	ANALOG	4MHZ	CONTINUOUS	2%-VIDEO	100%	—	—	
H-ALPHA SLIT (XRT)	ANALOG	4MHZ	14% (OF 151 H)	—	100%	—	—	
SOLAR ACTIVITY (XRT)	DIGITAL	120BPS	(CONTIN.) 151 H	65.2 MB	100%	—	(20%) 13.04MB	SCINTILLATION DETECTOR
X-RAY (FULL SUN)	ANALOG (DIGITAL)	4MHZ (HOLD-1FRAME)	CONTINUOUS (1FRAME/ORBIT)	2% VIDEO (2.59MB)	100% —	— —	— (2.59MB/ORBIT)	(525 TV LINES, Q=8)
XUV (FULL SUN)	ANALOG (DIGITAL)	4MHZ (HOLD-1FRAME)	CONTINUOUS (1FRAME/ORBIT)	2% VIDEO (2.59MB)	100% —	— —	— (2.59MB/ORBIT)	(525 TV LINES, Q=8)
(MAXIMUM)	DIGITAL	3940 BPS (4KBPS)		1209.3 MB (1.21GB) (PLUS 476.6MB FOR XRAY & XUV MONITORS)			190.26MB (PLUS 5.18MB PER ORBIT FOR X-RAY & XUV MON.)	
	FILM			56,660 FRAMES				
	ANALOG	4MHZ						

DATA ANALYSIS FOR PAYLOAD: STELLAR 3AB

SOURCE/CLASS	FORMAT	DATA RATE	OPERATING MODE & TIME	DISPOSITION OF DATA: STORAGE FILM/TAPE	REALTIME DISPLAY	CALL-UP DISPLAY	TELEMETER TO GRD (%) TOTAL	COMMENTS/NOTES
TELESCOPE-STRATOSCOPE III								
SCIENTIFIC: SPECTROGRAPH/POLARIMETER	FILM (70MM)	1 FR/MIN	70/91 MIN	7140 FRAMES	—	—	—	
FIELD CAMERA	FILM (70MM)	1 FR/10MIN	70/91 MIN	714 FRAMES	—	—	—	
ENGINEERING (STATUS/OPERATION)	DIGITAL	2200 BPS	(CONT) 119H30M	946 MB	20%	—	(20%) 189MB	($119H30M = 430 \times 10^3$ SEC)
FIELD MONITOR	ANALOG	4 MHZ	CONTINUOUS	2%-VIDEO	100%	—	—	
SUBSYSTEMS, SUPPORT	—							
PC & S (32), POWER (20), THERMAL (10)	DIGITAL	62 BPS	(CONT) 155H27M	34.7 MB	1%	5%	(5%) 1.74MB	($155H27M = 560 \times 10^3$ SEC)
ARRAY-NARROW BAND SPECTROM/POLAR.								
SCIENTIFIC: SIGNAL PULSES	DIGITAL	1000 BPS	(CONT) 152H27M	603.0 MB	0.1%	—	(1%) 6.03MB	($152H27M = 548 \times 10^3$ SEC)
COUNT RATES	DIGITAL	100 BPS						
ENGINEERING	DIGITAL	8 BPS	(CONT) 155H27M	4.5MB	1%	5%	(20%) 0.9 MB	
SUBSYSTEMS, SUPPORT								
P&C (12), TIMING (20), POWER (4)	DIGITAL	36 BPS	(CONT) 155H27M	20.1 MB	1%	5%	(5%) 1.0MB	
EQUIPMENT SUPPORT-ARRAY								WIDE COVERAGE X-RAY DETECTOR
SCIENTIFIC	DIGITAL	640 BPS	(CONT) 152H27M	351.0 MB	0.1%	—	(1%) 3.50MB	
ENGINEERING	DIGITAL	16 BPS	(CONT) 155H27M	8.9MB	1%	5%	(5%) 0.45MB	
REFERENCE DATA	DIGITAL	4 BPS	(CONT) 156H30M	2.3 MB	10%	10%	(10%) 0.23MB	
SCIENTIFIC-SUPPORT	DIGITAL	120 BPS	(CONT) 156H30M	67.7 MB	10%	10%	(10%) 6.77MB	FLUX DETECTOR-SAA
CREW ANNOTATION	ANALOG	3 KHZ	AS REQUIRED	100%			20%	
(MAXIMUM)	DIGITAL	4186 BPS (4.2KBPS)		2038.2MB (2.04GB)			209.6 MB	
	FILM			7854 FRAMES				
	ANALOG	4 MHZ						

DATA ANALYSIS FOR PAYLOAD: STELLAR 3AC

SOURCE/CLASS	FORMAT	DATA RATE	OPERATING MODE & TIME	DISPOSITION OF DATA: STORAGE FILM/TAPE	REALTIME DISPLAY	CALL-UP DISPLAY	TELEMETER TO GRD (%) TOTAL	COMMENTS/NOTES
TELESCOPE - STRATOSCOPE III								
SCIENTIFIC: SPECTROGRAPH/POLARIMETER	FILM 70MM	1FR/MIN	70/91 MIN	7140 FRAMES	—	—	—	
FIELD CAMERA	FILM 70MM	1FR/10MIN	70/91 MIN	714 FRAMES	—	—	—	
ENGINEERING STATUS OPERATION	DIGITAL	2200 BPS	(CONT) 119H 30M	946 MB	20%	—	(20%) 189 MB	(119H30M=430X10^3 SEC)
FIELD MONITOR	ANALOG	4 MHZ	CONTINUOUS	2%-VIDEO	100%	—	—	
SUBSYSTEMS SUPPORT	—							
PC&S, POWER, THERMAL (32) (20) (10)	DIGITAL —	62 BPS	(CONT) 155H27M	34.7 MB	1%	5%	(5%) 1.74MB	(155H27M=560X10^3 SEC)
ARRAYS (GROUP C)								
#1. SCIENTIFIC: DETECTOR	DIGITAL	1920 BPS	(CONT) 152H27M	1079.3 MB	0.1%	1%	(1%) 10.76MB	GAMMA-RAY SPECTROMETER
SHIELD	DIGITAL	48 BPS						
ENGINEERING	DIGITAL	8 BPS	(CONT) 155H27M	4.5MB	1%	5%	(20%) 0.89MB	
S/S, SUPT. (P&C, TIMING, POWER)	DIGITAL	32 BPS	(CONT) 155H27M	17.9MB	1%	5%	(5%) 0.89MB	
#2 SCIENTIFIC: DETECTOR	DIGITAL	3200 BPS	(CONT) 152H27M	1780.3 MB	0.1%	1%	(1%) 17.80MB	LOW BACKGROUND GAMMA-RAY DETECTOR (152H27M=548X10^3 SEC)
SHIELD	DIGITAL	32 BPS						
COLLIMATOR VETO	DIGITAL	16 BPS						
ENGINEERING	DIGITAL	8 BPS	(CONT) 155H27M	4.5MB	1%	5%	(20%) 0.90MB	
S/S, SUPT. (P&C, TIMING, POWER)	—	—	—	—	—	—	—	(INCLUDED WITH ARRAY #1)
EQUIPMENT, SUPPORT - (ARRAY)								WIDE COVERAGE X-RAY DETECTOR
SCIENTIFIC	DIGITAL	640 BPS	(CONT) 152H27M	351.0 MB	0.1%	—	(1%) 3.50MB	
ENGINEERING	DIGITAL	16 BPS	(CONT) 155H27M	8.9 MB	1%	5%	(5%) 0.45MB	
REFERENCE DATA	DIGITAL	4 BPS	(CONT) 156H30M	23 MB	10%	10%	(10%) 0.23MB	(156H30M=564X10^3 SEC)
SCIENTIFIC SUPPORT	DIGITAL	120 BPS	(CONT) 156H30M	67.7 MB	10%	10%	(10%) 6.77MB	FLUX DETECTOR - SAA
CREW ANNOTATION	ANALOG	3KHZ	AS REQUIRED	100%	—	—	20%	
(MAXIMUM)	DIGITAL	8302 BPS (8.3 KBPS)		4297 MB (4.3 GB)			234.1 MB	
	FILM			7854 FRAMES				
	ANALOG	4 MHZ						

DATA ANALYSIS FOR PAYLOAD: STELLAR 3AD

SOURCE/CLASS	FORMAT	DATA RATE	OPERATING MODE & TIME	DISPOSITION OF DATA: STORAGE FILM/TAPE	REALTIME DISPLAY	CALL-UP DISPLAY	TELEMETER TO GRD (%) TOTAL	COMMENTS/NOTES
TELESCOPE - STRATOSCOPE III								
SCIENTIFIC: SPECTROGRAPH/POLARIMETER	FILM (70MM)	1 FR/MIN	70/91 MIN.	7140 FRAMES	—	—	—	
FIELD CAMERA	FILM (70MM)	1 FR/10 MIN	70/91 MIN.	714 FRAMES	—	—	—	
ENGINEERING (STATUS/OPERATION)	DIGITAL	2200 BPS	(CONT) 119H 30M	946 MB	20%	—	(20%) 189 MB	(119H30M=430X10³ SEC)
FIELD MONITOR	ANALOG	4 MHZ	CONTINUOUS	2%-VIDEO	100%	—	—	
SUBSYSTEMS, SUPPORT	—							
PC & S	DIGITAL	32 BPS						
POWER	DIGITAL	20 BPS						
THERMAL	DIGITAL	10 BPS	(CONT) 155H 27M	34.7 MB	1%	5%	(5%) 1.74MB	(155H27M=560X10³ SEC)
ARRAY - LARGE MOD. COLLIMATOR								
SCIENTIFIC: SIGNAL PULSES	DIGITAL	1000 BPS						
MONITOR PULSES	DIGITAL	90 BPS	(CONT) 152H 27M	592.0MB	0.1%	—	(1%) 5.92MB	(152H27M=548X10³ SEC)
ENGINEERING	DIGITAL	90 BPS	(CONT) 155H27M	50.4MB	1%	5%	(20%) 10.1MB	
SUBSYSTEMS, SUPPORT	—							
P & C	DIGITAL	224 BPS						
TIMING	DIGITAL	24 BPS	(CONT) 155H27M	141.1 MB	1%	5%	(5%) 7.05MB	
POWER	DIGITAL	4 BPS						
EQUIPMENT, SUPPORT - (ARRAY)								
SCIENTIFIC	DIGITAL	640 BPS	(CONT) 152H27M	351.0MB	0.1%	-	(1%) 3.50MB	WIDE COVERAGE X-RAY DETECTOR
ENGINEERING	DIGITAL	16 BPS	(CONT) 155H 27M	8.9 MB	1%	5%	(5%) 0.45 MB	
REFERENCE DATA	DIGITAL	4 BPS	(CONT) 156H 30M	2.3 MB	10%	10%	(10%) 0.23MB	(156H30M=564X10³ SEC)
SCIENTIFIC-SUPPORT	DIGITAL	120 BPS	(CONT) 156H 30M	67.7 MB	10%	10%	(10%) 6.77MB	FLUX DETECTOR-SAA
CREW ANNOTATION	ANALOG	3 KHZ	AS REQUIRED	100%	—	—	20%	
(MAXIMUM)	DIGITAL	4374 BPS (4.4 KBPS)		2194.1MB (2.2GB)			224.76MB	
	FILM			7854 FRAMES				
	ANALOG	4 MHZ						

DATA ANALYSIS FOR PAYLOAD: STELLAR 3AE

SHEET 1 OF ____
PAYLOAD 3AE

SOURCE/CLASS	FORMAT	DATA RATE	OPERATING MODE & TIME	DISPOSITION OF DATA: STORAGE FILM/TAPE	REALTIME DISPLAY	CALL-UP DISPLAY	TELEMETER TO GRD (%) TOTAL	COMMENTS/NOTES
TELESCOPE-STRATOSCOPE III								
SCIENTIFIC: SPECTROGRAPH/POLARIMETER	FILM (70MM)	1FR/MIN	70/91 MIN	7140 FRAMES	—	—	—	
FIELD CAMERA	FILM (70MM)	1FR/10MIN	70/91 MIN	714 FRAMES	—	—	—	
ENGINEERING (STATUS/OPERATION)	DIGITAL	2200 BPS	CONT 119H 30M	946MB	20%	—	(20%) 189MB	(119H30M = 430X10^3 SEC)
FIELD MONITOR	ANALOG	4MHZ	CONTINUOUS	2% VIDEO	100%	—	—	
SUBSYSTEMS, SUPPORT	—							
PC & S	DIGITAL	32BPS	(CONT) 155H27M	34.7 MB	1%	5%	(5%) 1.74MB	(155H27M = 560X10^3 SEC)
POWER	DIGITAL	20BPS						
THERMAL	DIGITAL	10BPS						
ARRAYS (GROUP E)								
#1 SCIENTIFIC	DIGITAL	4000 BPS	(CONT) 152H27M	2192.0 MB	0.1%	1%	(1%) 21.92MB	LARGE AREA X-RAY DETECTOR
ENGINEERING	DIGITAL	160BPS	(CONT) 155H27M	89.6MB	1%	5%	(20%) 17.92MB	
S/S, SUPT. (P&C 13, TIMING 20, POWER 7)	DIGITAL	40BPS	(CONT) 155H27M	22.4MB	1%	5%	(5%) 1.12MB	
#2 SCIENTIFIC	DIGITAL	1280BPS	(CONT) 152H27M	702.0MB	0.1%	1%	(1%) 7.02MB	COLLIMATED PLANE CRYSTAL SPECTROMETER
ENGINEERING	DIGITAL	8BPS	(CONT) 155H27M	4.5MB	1%	5%	(20%) 0.90MB	
S/S, SUPT. (P&C, TIMING, POWER)	—	—	—	—	—	—	—	(INCLUDED WITH ARRAY #1)
EQUIPMENT SUPPORT - (ARRAY)								WIDE COVERAGE X-RAY DETECTOR
SCIENTIFIC	DIGITAL	640 BPS	(CONT) 152H27M	351.0 MB	0.1%	—	(1%) 3.50MB	
ENGINEERING	DIGITAL	16 BPS	(CONT) 155H27M	8.9 MB	1%	5%	(5%) 0.45MB	
REFERENCE DATA	DIGITAL	4 BPS	(CONT) 156H30M	2.3 MB	10%	10%	(10%) 0.23MB	(156H30M = 564X10^3 SEC)
SCIENTIFIC-SUPPORT	DIGITAL	120 BPS	(CONT) 156H30M	67.7 MB	10%	10%	(10%) 6.77MB	FLUX DETECTOR - SAA
CREW ANNOTATION	[illegible]	3KHZ	AS REQUIRED	100%	—	—	20%	
(MAXIMUM)	DIGITAL	8530 BPS (8.6KBPS)		4421.1 MB (4.43 GB)			250.57MB	
	FILM			7854 FRAMES				
	ANALOG	4MHZ						

DATA ANALYSIS FOR PAYLOAD: STELLAR 4AB

SHEET 1 OF ___
PAYLOAD 4AB

SOURCE/CLASS	FORMAT	DATA RATE	OPERATING MODE & TIME	DISPOSITION OF DATA: STORAGE FILM/TAPE	REALTIME DISPLAY	CALL-UP DISPLAY	TELEMETER TO GRD (%) TOTAL	COMMENTS/NOTES
TELESCOPE-INFRARED								
SCIENTIFIC: DETECTOR ARRAY	DIGITAL	200BPS	33% (OF 88.5 HR)	21.2 MB	1%	—	(1%) 0.21MB	
INTERFEROMETER	DIGITAL	1200BPS	33% (OF 88.5HR)	127.3 MB	1%	—	(1%) 1.27MB	
ENGINEERING (STATUS/OPERATION)	DIGITAL	1160BPS	(CONT) 155H 54M	653.0MB	20%	—	(20%) 130.60MB	(155H54M=562X10^3 SEC)
FIELD MONITOR	ANALOG	11MHZ	CONTINUOUS	2%-VIDEO	100%	—	—	
SUBSYSTEMS, SUPPORT	DIGITAL	200BPS	(CONT) 155H 54M	112.3MB	1%	5%	(5%) 5.61MB	
ARRAY - NARROW BAND SPECTROM/POLARIM.								
SCIENTIFIC: SIGNAL PULSES	DIGITAL	1000 BPS	(CONT) 154H 51M	614.0MB	0.1%	—	(1%) 6.14MB	(154H51M=558X10^3 SEC)
COUNT RATES	DIGITAL	100BPS						
ENGINEERING	DIGITAL	8 BPS	(CONT) 155H20M	4.5MB	1%	5%	(20%) 0.9 MB	(155H20M=560X10^3 SEC)
SUBSYSTEMS, SUPPORT P&C, TIMING, POWER (12) (20) (4)	DIGITAL	36 BPS	(CONT) 156H45M	20.4MB	1%	5%	(5%) 1.02MB	(156H45M=565X10^3 SEC)
EQUIPMENT SUPPORT-ARRAY								WIDE COVERAGE X-RAY DETECTOR
SCIENTIFIC	DIGITAL	640 BPS	(CONT) 154H51M	359.6 MB	0.1%	—	(1%) 3.60MB	
ENGINEERING	DIGITAL	16 BPS	(CONT) 155H20M	9.0 MB	1%	5%	(5%) 0.45MB	
REFERENCE DATA	DIGITAL	4 BPS	(CONT) 156H45M	2.3 MB	10%	10%	(10%) 0.23MB	
SCIENTIFIC-SUPPORT	DIGITAL	120 BPS	(CONT) 156H45M	67.8 MB	10%	10%	(10%) 6.78MB	FLUX DETECTOR-SAA
CREW ANNOTATION	ANALOG	3 KHZ	AS REQUIRED	100%			20%	
(MAXIMUM)	DIGITAL	4484 BPS (4.5 KBPS)		1991.4MB (2.0GB)			156.8MB	
	ANALOG	11MHZ						

DATA ANALYSIS FOR PAYLOAD: STELLAR 4AC

SHEET 1 OF ____
PAYLOAD 4AC

SOURCE/CLASS	FORMAT	DATA RATE	OPERATING MODE & TIME	DISPOSITION OF DATA: STORAGE FILM/TAPE	REALTIME DISPLAY	CALL-UP DISPLAY	TELEMETRY TO GRD (%) TOTAL	COMMENTS/NOTES
TELESCOPE-INFRARED								
SCIENTIFIC: DETECTOR ARRAY	DIGITAL	200 BPS	33% (OF 88.5 HR)	21.2 MB	1%	—	(1%) 0.21MB	
INTERFEROMETER	DIGITAL	1200 BPS	33% (OF 88.5 HR)	127.3 MB	1%	—	(1%) 1.27MB	
ENGINEERING (STATUS/OPERATION)	DIGITAL	1160 BPS	(CONT) 155H 54M	653.0MB	20%	—	(20%) 130.60MB	(155H54M=562X10^3 SEC)
FIELD MONITOR	ANALOG	11MHZ	CONTINUOUS	2%-VIDEO	100%	—	—	
SUBSYSTEMS, SUPPORT	DIGITAL	200BPS	(CONT) 155H 54M	112.3MB	1%	5%	(5%) 5.61MB	
ARRAYS (GROUP C)								
#1 SCIENTIFIC: DETECTOR	DIGITAL	1920 BPS	(CONT) 154H51M	1098.8 MB	0.1%	1%	(1%) 10.99MB	GAMMA-RAY SPECTROMETER
SHIELD	DIGITAL	48 BPS						
ENGINEERING	DIGITAL	8BPS	(CONT) 155H20M	4.5MB	1%	5%	(20%) 0.90MB	(155H20M=560X10^3 SEC)
S/S, SUPT (P&C, TIMING, POWER)	DIGITAL	36BPS	(CONT) 156H45M	20.4MB	1%	5%	(5%) 1.01MB	(156H45M=565X10^3 SEC)
#2 SCIENTIFIC: DETECTOR	DIGITAL	3200 BPS						LOW BACKGROUND GAMMA-RAY DETECTOR
SHIELD	DIGITAL	32 BPS	(CONT) 154H51M	1814.8MB	0.1%	1%	(1%) 18.15MB	(154H51M=558X10^3 SEC)
COLLIMATOR VETO	DIGITAL	16 BPS						
ENGINEERING	DIGITAL	8BPS	(CONT) 155H20M	4.5MB	1%	5%	(20%) 0.90MB	
S/S, SUPT. (P&C, TIMING, POWER)	—	—	—	—	—	—	—	INCLUDED WITH ARRAY #1
EQUIPMENT, SUPPORT - (ARRAY)								WIDE COVERAGE X-RAY DETECTOR
SCIENTIFIC	DIGITAL	640BPS	(CONT) 154H51M	359.6MB	0.1%	—	(1%) 3.60MB	
ENGINEERING	DIGITAL	16BPS	(CONT) 155H20M	9.0MB	1%	5%	(5%) 0.45MB	
REFERENCE DATA	DIGITAL	4BPS	(CONT) 156H45M	2.3MB	10%	10%	(10%) 0.23MB	
SCIENTIFIC-SUPPORT	DIGITAL	120BPS	(CONT) 156H45M	67.8MB	10%	10%	(10%) 6.78MB	FLUX DETECTOR- SAA
CREW ANNOTATION	ANALOG	3KHZ	AS REQUIRED	100%	—	—	20%	
(MAXIMUM)	DIGITAL	8608 BPS (8.6KBPS)		4295.5MB (4.3GB)			180.7 MB	
	ANALOG	11 MHZ						

DATA ANALYSIS FOR PAYLOAD: STELLAR 4AD

SHEET 1 OF ___

PAYLOAD 4AD

SOURCE/CLASS	FORMAT	DATA RATE	OPERATING MODE & TIME	DISPOSITION OF DATA				COMMENTS/NOTES
				STORAGE FILM/TAPE	REALTIME DISPLAY	CALL-UP DISPLAY	TELEMETER TO GRD (%) TOTAL	
TELESCOPE-INFRARED								
SCIENTIFIC: DETECTOR ARRAY	DIGITAL	200BPS	33%(OF 88.5HR)	21.2 MB	1%	—	(1%) 0.2MB	
INTERFEROMETER	DIGITAL	1200BPS	33%(OF 88.5HR)	127.3MB	1%	—	(1%) 1.27MB	
~~ENGINEERING (STATUS/OPERATION)~~	DIGITAL	~~1160 BPS~~	~~(CONT)155H54M~~	~~653.0MB~~	20%	—	(20%) 130.60MB	(155H54M=562X10^{3}SEC)
FIELD MONITOR	ANALOG	~~11MHZ~~	~~CONTINUOUS~~	2%-VIDEO	100%	—		
SUBSYSTEMS, SUPPORT	DIGITAL	200BPS	(CONT)155H54M	112.3MB	1%	5%	(5%) 5.61MB	
ARRAY-LARGE MOD. COLLIMATOR								
SCIENTIFIC: SIGNAL PULSES	DIGITAL	1000BPS	(CONT)154H51M	603.0MB	0.1%	—	(1%) 6.03MB	(154H51M=558X10^3 SEC)
MONITOR PULSES	DIGITAL	80BPS						
ENGINEERING	DIGITAL	90BPS	(CONT)155H20M	50.4MB	1%	5%	(20%) 10.1 MB	(155H20M=560X10^3 SEC)
SUBSYSTEMS, SUPPORT	—							
PEC	DIGITAL	224 BPS	(CONT)156H45M	142.4MB	1%	5%	(5%) 7.12 MB	(156H45M=565X10^3 SEC)
TIMING	DIGITAL	24BPS						
POWER	DIGITAL	4BPS						
EQUIPMENT, SUPPORT - (ARRAY)								
SCIENTIFIC	DIGITAL	640BPS	(CONT)154H51M	359.6MB	0.1%	—	(1%) 3.60MB	WIDE COVERAGE X-RAY DETECTOR
ENGINEERING	DIGITAL	16BPS	(CONT)155H20M	9.0MB	1%	5%	(5%) 0.45MB	
REFERENCE DATA	DIGITAL	4BPS	(CONT)156H45M	2.3MB	10%	10%	(10%) 0.23MB	
SCIENTIFIC-SUPPORT	DIGITAL	120BPS	(CONT)156H45M	67.8MB	10%	10%	(10%) 6.78MB	FLUX DETECTOR- SAA
CREW ANNOTATION	ANALOG	3KHZ	AS REQUIRED	100%	—	—	20%	
(**MAXIMUM**)	DIGITAL	4762 BPS (4.8KBPS)		2148.1 MB (2.15 GB)			172.0 MB	
	ANALOG	11 MHZ						

DATA ANALYSIS FOR PAYLOAD: STELLAR 4AE

SHEET 1 OF ___

PAYLOAD 4AE

SOURCE/CLASS	FORMAT	DATA RATE	OPERATING MODE & TIME	DISPOSITION OF DATA: STORAGE FILM/TAPE	REALTIME DISPLAY	CALL-UP DISPLAY	TELEMETER TO GRD (%) TOTAL	COMMENTS/NOTES
TELESCOPE-INFRARED								
SCIENTIFIC: DETECTOR ARRAY	DIGITAL	200 BPS	33% (OF 88.5 HR)	21.2 MB	1%	—	(1%) 0.21 MB	
INTERFEROMETER	DIGITAL	1200 BPS	33% (OF 88.5 HR)	127.3 MB	1%	—	(1%) 1.27 MB	
ENGINEERING (STATUS/OPERATION)	DIGITAL	1160 BPS	(CONT) 155H 54M	653.0 MB	20%	—	(20%) 130.60 MB	(155H54M = 562 $\times 10^3$ SEC)
FIELD MONITOR	ANALOG	11 MHZ	CONTINUOUS	2%-VIDEO	100%	—	—	
SUBSYSTEMS, SUPPORT	DIGITAL	200 BPS	(CONT) 155H 54M	112.3 MB	1%	5%	(5%) 5.61 MB	
ARRAYS (GROUP E)								
#1 SCIENTIFIC:	DIGITAL	4000 BPS	(CONT) 154H 51M	2232.0 MB	0.1%	1%	(1%) 22.32 MB	LARGE AREA X-RAY
ENGINEERING	DIGITAL	160 BPS	(CONT) 155 H20M	90.0 MB	1%	5%	(20%) 18.0 MB	DETECTOR
S/S, SUPT. (P&C 13, TIMING 20, POWER 7)	DIGITAL	40 BPS	(CONT) 156 H45M	23.0 MB	1%	5%	(5%) 1.15 MB	(156H45M = 565 $\times 10^3$ SEC)
#2 SCIENTIFIC	DIGITAL	1280 BPS	(CONT) 154 H51M	719.2 MB	0.1%	1%	(1%) 7.19 MB	COLLIMATED PLANE
ENGINEERING	DIGITAL	8 BPS	(CONT) 155 H20M	4.5 MB	1%	5%	(20%) 0.9 MB	CRYSTAL SPECTROMETER
S/S, SUPT. (P&C, TIMING, POWER)	—	—	—	—	—	—	—	(INCLUDED WITH ARRAY #1)
EQUIPMENT, SUPPORT- (ARRAY)								WIDE COVERAGE X-RAY
SCIENTIFIC	DIGITAL	640 BPS	(CONT) 154H51M	359.6 MB	0.1%	—	(1%) 3.60 MB	DETECTOR
ENGINEERING	DIGITAL	16 BPS	(CONT) 155H20M	9.0 MB	1%	5%	(5%) 0.45 MB	(155H20M = 560 $\times 10^3$ SEC)
REFERENCE DATA	DIGITAL	4 BPS	(CONT) 156H45M	2.3 MB	10%	10%	(10%) 0.23 MB	(154H51M = 558 $\times 10^3$ SEC)
SCIENTIFIC-SUPPORT	DIGITAL	120 BPS	(CONT) 156H45M	67.8 MB	10%	10%	(10%) 6.78 MB	FLUX DETECTOR- SAA
CREW ANNOTATION	ANALOG	3 KHZ	AS REQUIRED	100%	—	—	20%	
[illegible])	DIGITAL	8839 BPS (8.9 KBPS)		4421.2 MB (4.43 GB)			198.31 MB	
	ANALOG	11 MHZ						

APPENDIX B1-2

PAYLOAD ELECTRICAL POWER ANALYSIS

INTRODUCTION

This appendix outlines and summarizes the electrical power requirements for the baseline mission payloads. The power requirements for the scientific instruments and for supporting equipment were derived from the Baseline Experiment Definition Documents of Volume II, Book 2. Subsystem power requirements were derived for the stabilization systems and for the supporting electronic assemblies defined in Volume III, Section 3.

ELECTRICAL POWER ANALYSIS FOR PAYLOAD: SOLAR 1-2

Instrument/Equipment Description-(Power)	PC&S Power	Support Electronics - Power			Totals	
		Data	Electrical	C&D		
Photoheliograph - Instruments 50 W - Subsystem 30 W #1 Mount	250 W	25 W	4 W		359 W	906 W
SHG - Instruments 50 W - Monitor 12 W IC/OC Assembly 40 W - Sun Sensor 11 W XRT - Instruments 110 W - Monitor 10 W - H-Alpha 10 W #2 Mount Correlation Tracker 25 W	250 W	25 W	4 W		547 W	
CMG Assembly - Pallet	150 W	5 W	4 W			159 W
Controls & Displays				415 W		
		(55 W)	(12 W)	(415 W)		
TOTALS 348 W	650 W	482 W				1480 Watts

ELECTRICAL POWER ANALYSIS FOR PAYLOAD: S'.RATOSCOPE III

Instrument/Equipment Description- (Power)	PC&S Power	Support Electronics - Power			Totals	
		Data	Electrical	C&D		
Stratoscope III - Telescope 140 W Mount	250 W	25 W	4 W		419 W	519 W
Array Group A - Wide Coverage Detector 70 W - Flux Detector 30 W					100 W	
Controls and Displays				400 W	400 W	663 W
CMG Assy - Pallet	150 W	5 W	4 W		159 W	
Array Mount (Groups B,C,D,E)	75 W	25 W	4 W		104 W	
		55 W	12 W	400 W		
Common Subtotals (240 W)	(475 W)	(467 W)				
3AB 410 W (NB Spect/Polarim 170 W)	475 W	467 W			3AB- $\boxed{\text{1352 WATTS}}$	
3AC 338 W (Gamma Ray Spect 34 W) (Lo-Bkgnd Det 64 W)	475 W	467 W			3AC- $\boxed{\text{1280 WATTS}}$	
3AD 441 W (Lg Mod Collim 201 W)	475 W	467 W			3AD- $\boxed{\text{1383 WATTS}}$	
3AE 502 W (Lg Area X-Ray 200 W) (Coll. Xtal. Spect 62 W)	475 W	467 W			3AE- $\boxed{\text{1444 WATTS}}$	

ELECTRICAL POWER ANALYSIS FOR PAYLOAD: INFRARED TELESCOPE

Instrument/Equipment Description- (Power)	PC&S Power	Support Electronics - Power			Totals	
		Data	Electrical	C&D		
Infrared Telescope - Instruments 40 W - Support 40 W Mount	250 W	25 W	4 W		359 W	459 W
Array Group A - Wide Coverage Detector 70 W - Flux Detector 30 W					100 W	
Controls and Displays				325 W	325 W	588 W
CMG Assembly-Pallet	150 W	5 W	4 W		159 W	
Array Mount (Groups B,C,D,E)	75 W	25 W	4 W		104 W	
		55 W	12 W	325 W		
Common Subtotals (180 W)	(475 W)	(392 W)				
4AB 350 W (NB Spect/Polarim 170 W)	475 W	392 W			4AB-	1217 WATTS
4AC 278 W (Gamma Ray Spect 34 W) (Lo-Bkgnd Det 64 W)	475 W	392 W			4AC -	1145 WATTS
4AD 381 W (Lg Mod Collim 201 W)	475 W	392 W			4AD -	1248 WATTS
4AE 442 W (Lg Area X-Ray 200 W) (Coll Xtal Spect 62 W)	475 W	392 W			4AE -	1309 WATTS

APPENDIX B2-1

I.R. TELESCOPE STRESS ANALYSIS

(A)

ANALYSIS OF

26 July 1972

ANALYSIS OF LIQUID NEON I.R. TELESCOPE ANNULAR, CONCENTRIC CYL. TANK.

BUCKLING OF CYLINDER SUBJECTED TO EXT. PRESS.

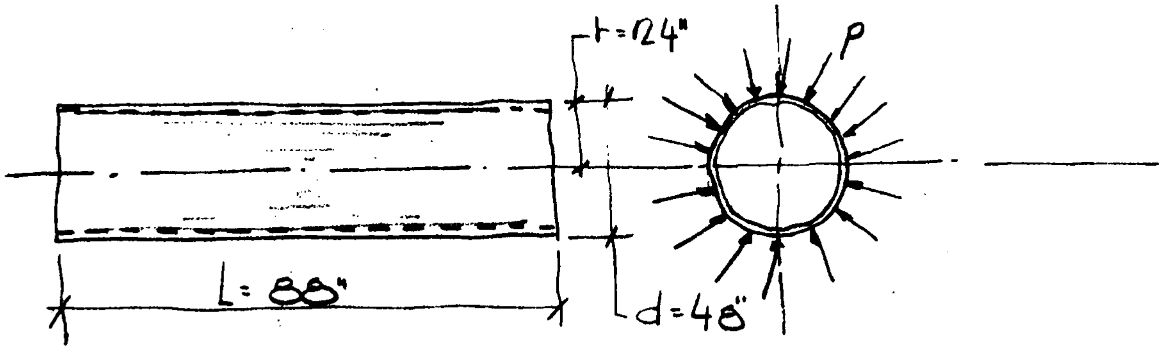

$t_{(est)} = 0.20"$

$L = 88"$

$r = 24"$

$\frac{L^2}{rt} = \frac{(.88)^2(10^4)}{24(0.2)} = \frac{.775(10^4)}{4.8} = 1.6(10^3) = 1600 > 100$ ∴ NOT A SHORT CYL.

FOR LONG CYL. $\left[100\frac{t}{r} < \left(\frac{L}{r}\right)^2 < 5\frac{r}{t}\right]$

$100\frac{t}{r} = 100\frac{0.2}{24} = \frac{20}{24} = 0.834, \left(\frac{L}{r}\right)^2 = \left(\frac{88}{24}\right)^2 = 13.4, \frac{5r}{t} = \frac{5(24)}{.2} = 600$

So $[.834 < 13.4 < 600]$ OK WE HAVE LONG CYL. CASE

DEN 065098 (3-56)

PREPARED BY T. J. D. CHECKED BY ______ REVISED BY ______

OK USE EQ. #15 SECT. C3.1.6 PG #10

$$F_{CR.} = 0.93E\left(\frac{t}{r}\right)^{3/2}\left(\frac{t}{L}\right) = 0.93(22)(10^6)\left(\frac{.2}{24}\right)^{3/2}\left(\frac{24}{88}\right) \text{psi}$$
$$= 0.93(22)(10^6)(7.56)(10^{-4})(.273) = .93(2200)(7.56)(2.73)$$
$$= 4{,}210 \text{ psi}$$

FOR SHELL LONGITUDINAL & AXIAL STRESS DUE TO 30 psi EXTERNAL CRUSHING PRESSURE.

FOR UNIT WIDTH SECTION OF SKIN

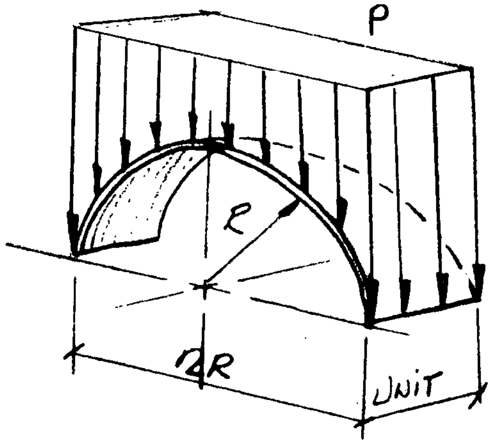

$p = 30$ psi
$R = 24$ in.
$t = 0.20$ in

$$f_L(1)t = pR(1)$$
$$f_L = \frac{PR}{t} = \frac{30 \text{ psi } (24) \text{ in}}{0.2 \text{ in}} = \frac{720}{.2} \text{ psi} = 3{,}600 \text{ psi}$$
$$\hat{f}_{ULT} = 2f_L = 2(3{,}600) \text{ psi} = 7{,}200 \text{ psi}$$

$\hat{f}_{ULT}$ MUST BE AT OR BELOW F_{CR} FOR BUCKLING.

PREPARED BY T. J. D. CHECKED BY ____ REVISED BY ____

TRY $t_i = 0.25$ in.

THEN

$$f_{(ULT)} = \frac{60\ psi\ (24)\ in}{0.25\ in.} = 5{,}750\ psi$$

AND

$$F_{CR.} = 0.93(22)(10^6)\left(\frac{.25}{24}\right)^{3/2}\left(\frac{24}{88}\right) psi$$
$$= 20.4(10^6)(1.04)(10^{-3})(.273)$$
$$= 5{,}800\ psi$$

CRIPPLING CONTROLS INNER CYL. SHELL THICKNESS "t"
@ 0.25 in.

FOR OUTER CYLINDER $F_{ULT} = 104{,}000$ psi
(SHELL IN TENSION)

$$t_o = \frac{PR}{F_{ULT.}} = \frac{60\ psi\ (26\ in)}{104(10^3)\ psi} = 15(10^{-3})\ in. = 0.015\ in$$

SUMMARY

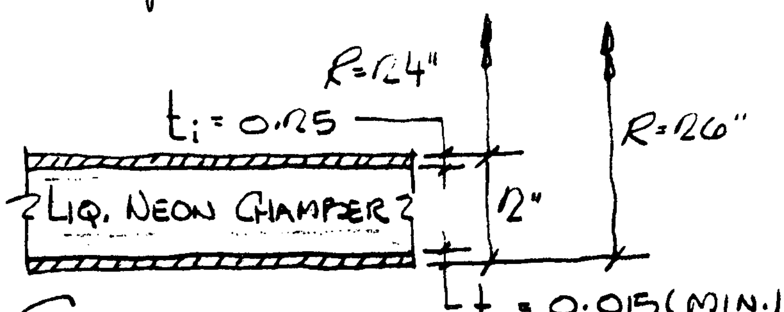

SECTION THRU
CONCENTRIC TANK WALL

DEN 065098 (3-56)

PREPARED BY T.J.D. CHECKED BY ______ REVISED BY ______

FOR LONGITUDINAL STRESS

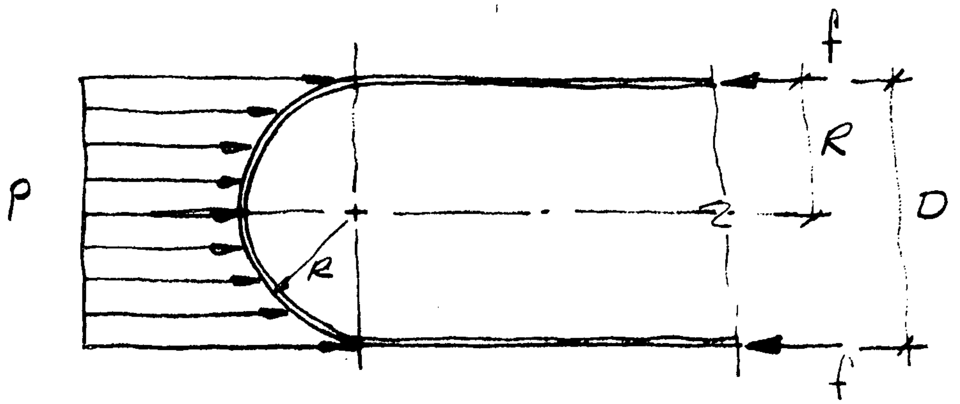

$C = \pi D = 2\pi R$

$p \pi R^2 = f(2)\pi R t$

$pR = f(2t)$

$f_{i\,(ULT)} = \frac{pR}{2t} = \frac{60\text{ psi }(24)\text{in.}}{2(0.25)\text{in.}} = \frac{720}{1/4} = 2,880\text{ psi}$

OK USE AS INNER SHELL CONTROLLED BY BUCKLING.

$f_{o\,ULT} = \frac{60\text{ psi }(26\text{in})}{2(0.015)} = \frac{60(26)}{30(10^{-3})}\text{ psi} = 52(10^3)\text{ psi}$

$f_{o\,ULT} = 52,000\text{ psi}$

INNER SHELL $t_i = 0.25$ in. @ $R = 24$ in.

OUTER SHELL $t_o = 0.015$ in. @ $R = 26$ in (MIN.)

DEN 06508 (3-56)

PREPARED BY T. J. D. CHECKED BY ____ REVISED BY ____

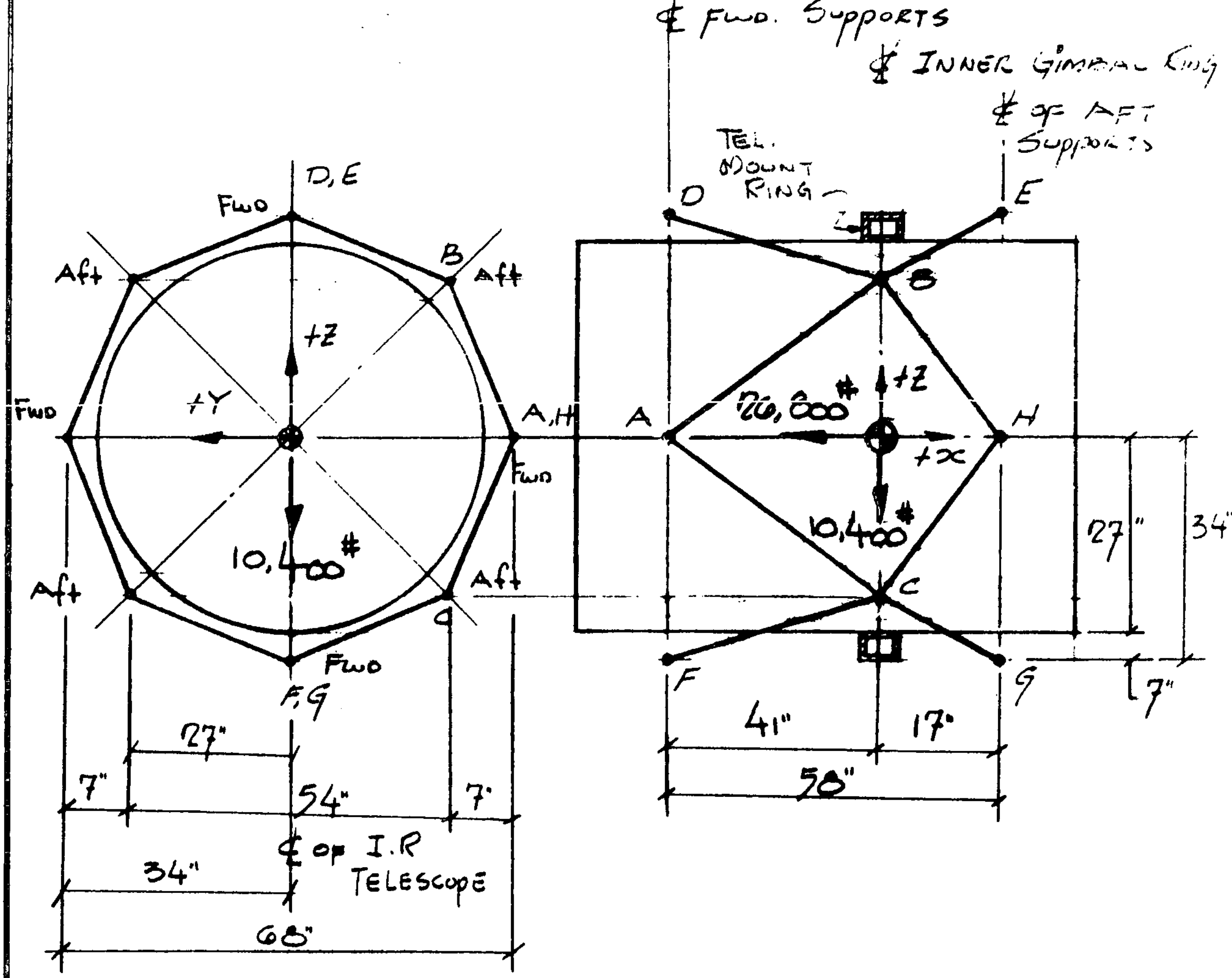

FRONT VIEW OUTBOARD PROFILE

LOAD FACTORS

$W = 4{,}550^{\#}$

$W_{DES} = 1.5W = 6{,}800^{\#}$

* $N_x = -3.96g$ $F_x = 6800^{\#}(-3.96) = -26{,}800^{\#}$

$N_Y = -0.90g$ $F_Y = 6800^{\#}(0.90) = -6{,}100^{\#}$

$N_Z = -1.53g$ $F_Z = 6800^{\#}(-1.53) = -10{,}400^{\#}$

* REF. IDC# 0433172-100

DEN 065098 (3-56)

PREPARED BY T.J.D. CHECKED BY____ REVISED BY____

3 AUG. 1972

LOADS ON TRUSS STRUCTURE:

LATERAL

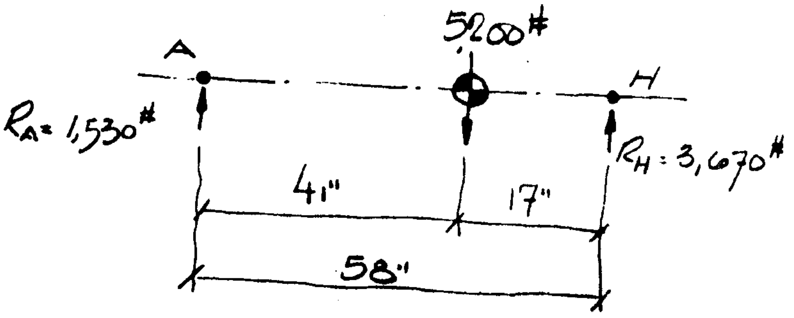

$R_A = 5200^{\#}\left(\frac{17}{58}\right) = 1530^{\#}$

$R_H = 5200^{\#}\left(\frac{41}{58}\right) = 3{,}670^{\#}$

TRUSS GEOMETRY

FWD. STRUTS

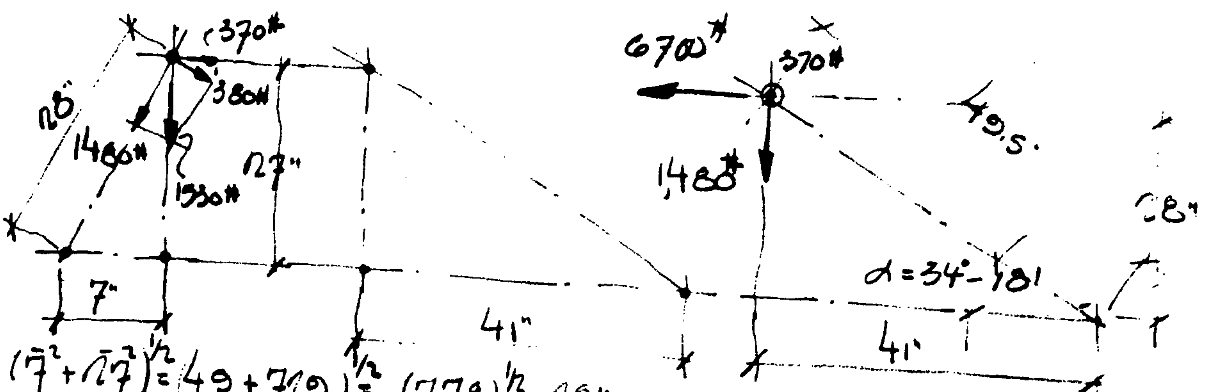

$(7^2 + 27^2)^{1/2} = (49 + 729)^{1/2} = (778)^{1/2} = 28"$

TRUE VIEW

$(28^2 + 41^2)^{1/2} = (778 + 1675)^{1/2} = (2435)^{1/2} = 49.5"$

PREPARED BY T. J.D. CHECKED BY REVISED BY

DEN 065098 (9-58)

$\alpha = \tan^{-1}\frac{28}{41} = \tan^{-1} 0.682 = 34°\text{-}18'$

AFT STRUTS

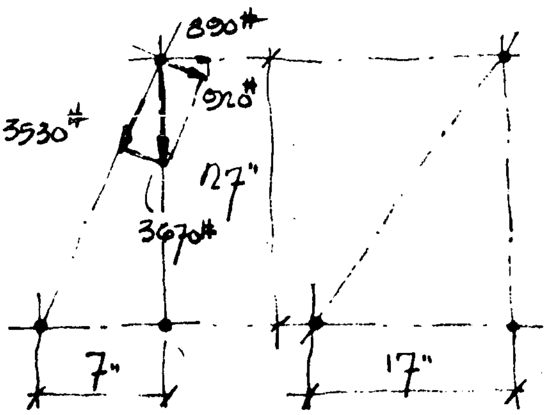

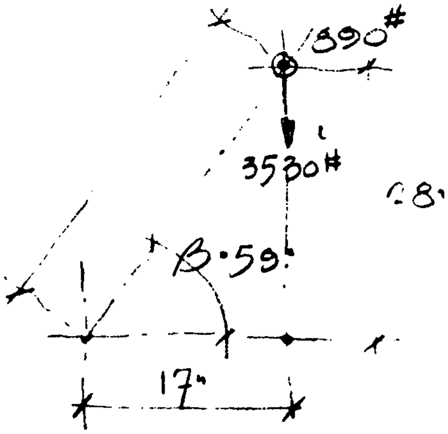

$(28^2+17^2)^{1/2} = (784+289)^{1/2} = (1073)^{1/2} = 32.9"$

$\beta = \tan^{-1}\frac{28}{17} = \tan^{-1} 1.65 = 59°$

LOAD COMPONENTS

FWD

$1{,}530\#\left(\frac{27}{28}\right) = 1{,}480\#$

$1530\#\left(\frac{7}{28}\right) = 380\#$

AFT

$3{,}670\#\left(\frac{27}{28}\right) = 3{,}530\#$

$3{,}670\#\left(\frac{7}{28}\right) = 920\#$

LONGITUDINAL (FWD)

$\frac{26{,}800\#}{4} = \underline{6{,}700\#}$

FWD. ATTACHMENT JOINT

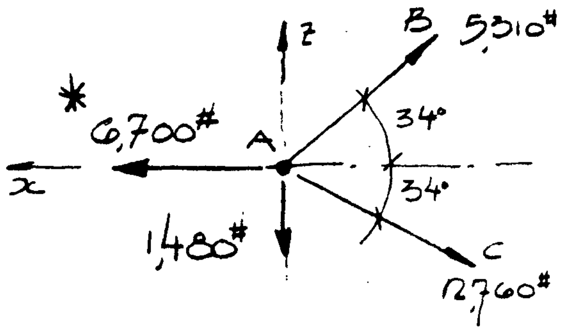

$(+\uparrow)\ \Sigma F_z = -1480^{\#} + AB\sin 34° - AC\sin 34° = 0$

$$\boxed{-1480^{\#} + .56AB - .56AC = 0} \qquad Eq.\ \#1$$

$(\overset{+}{\rightarrow})\ \Sigma F_x = -6700^{\#} + AB\cos 34° + AC\cos 34° = 0$

$$\boxed{-6700^{\#} + .83AB + .83AC = 0} \qquad Eq\ \#2$$

$(.83)(Eq\ \#1) \qquad -1230^{\#} + .47AB - .47AC = 0$

$(.56)(Eq\ \#2) \qquad \underline{-3750^{\#} + .47AB + .47AC = 0}$

$-4{,}980^{\#} + .94AB = 0$

$AB = \dfrac{4{,}980^{\#}}{.94} = 5{,}310^{\#}$ (TENSION)

$-6{,}700^{\#} + .83AB + .83AC = 0$

$-6700^{\#} + .83(5310)^{\#} + .83AC = 0$

$AC = \dfrac{6700^{\#} - 4410^{\#}}{.83} = \dfrac{2290^{\#}}{.83} = 2{,}760^{\#}$ (TENSION)

* THE TOTAL AXIAL LOAD IS ASSUMED TO BE CARRIED IN THE FWD. ATT. JOINTS.

DEN 065098 (3-58)

PREPARED BY T. J. D. CHECKED BY ____ REVISED BY ____

FOR COMPRESSIVE BUCKLING LOAD IN STRUTS

$P_{CR} = 5310^{\#}$

$E = 22(10^6)$ psi (INVAR)
$L = 50$ in.
$L^2 = 2500$ in^2

$$P_{CR} = \frac{\pi^2 E I}{L^2}$$

$$I = \frac{P_{CR} L^2}{\pi^2 E} = \frac{(5.3)(\cancel{10^3})^{\#}(2.5)(\cancel{10^3})\,in^2}{\pi^2\, 22(\cancel{10^6})\,^{\#}/_{\square''}} = \frac{13.25}{217} = 0.061\, in^4$$

USING MIN. OF $1.5''\phi \times .002$ WALL TUBE
$I = 0.078\, in.^4$ OK.

$A = \pi(.75)^2 - \pi(.69)^2 = \pi(.56 - .14) = .15\pi\,\square'' = 0.47\,\square''$

$f(des) = \frac{P}{A} = \frac{5310^{\#}}{.47\,\square''} = 11{,}300$ psi (P_{CR} CONTROLS)

CHECK AFT STRUT JOINT

PREPARED BY T. J. D. CHECKED BY REVISED BY

DEN 06098 (3-58)

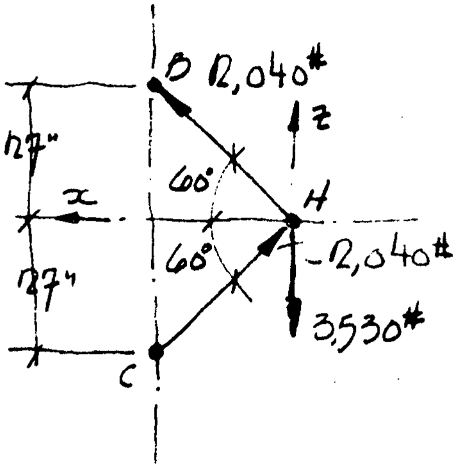

$$-3{,}530^{\#} + \overline{BH}\,\sin 60^\circ + \overline{CH}\,\sin 60^\circ = 0$$

$$-3{,}530^{\#} + 2(.867)\,\overline{BH}$$

$$(\overline{BH} = \overline{CH} \text{ AS } \Sigma F_x = 0)$$

$$BH = \frac{3530^{\#}}{1.73} = 2{,}040^{\#}$$

CHECK LOADS ON TEL. TO INNER GIMBAL RING MOUNTING INTERFACE

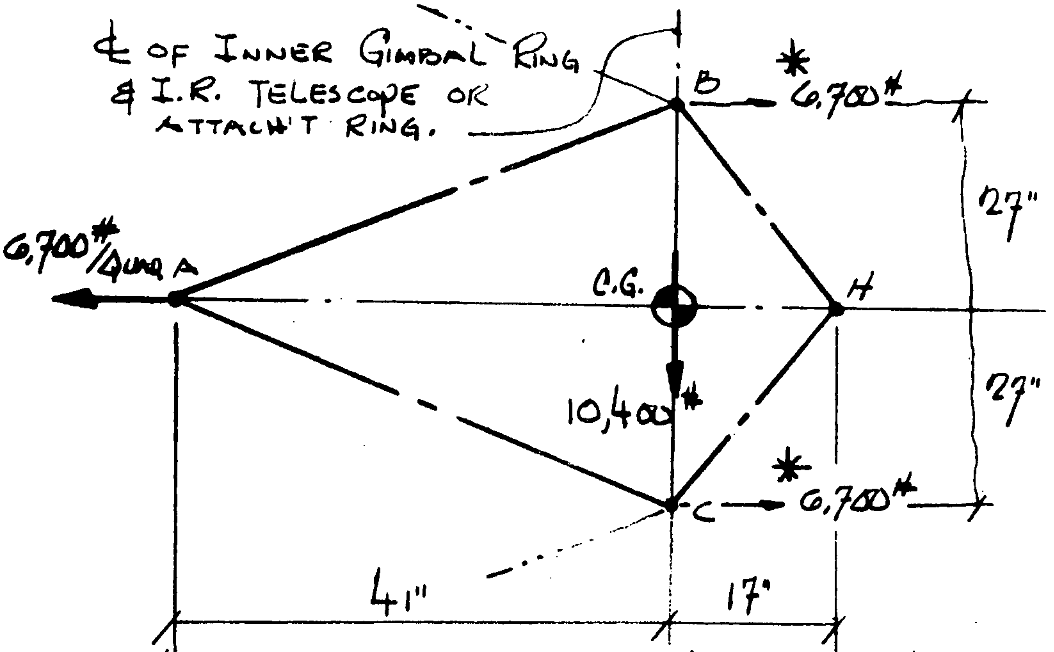

* 3,350# ALSO COMES INTO JOINTS B & C FROM ADJACENT PANELS.

DEN 06508 (3-58)

PREPARED BY T.J.D. CHECKED BY ________ REVISED BY ________

C.G. OF TELESCOPE PAYLOAD IS ON ℄ OF GIMBAL RING THEREFORE LINE OF REACTION IS THRU GIMBAL RING ℄ PAYLOAD TRUSS TO TELESCOPE SUPPORT RING ATTACHMENTS ARE COMMON TO TELESCOPE SUPPORT RING / GIMBAL RING ATTACHMENTS THEREFORE THERE ARE NO TORSIONAL LOADS IN THE TELESCOPE SUPPORT RING - POSSIBLY ONLY BENDING DUE TO INNER GIMBAL RING BENDING

CONSIDER WORST LOAD CASE AS RING IN COMPRESSION FROM 2-POINT REACTION FOR BASIC SIZING

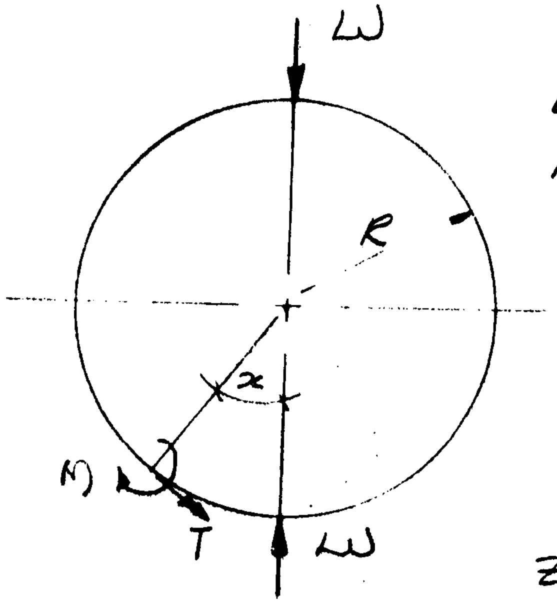

$W = 10{,}400\#/2 = 5{,}200\#$

$R = \frac{82''}{2} = 41''$

$M_{MAX} = .318WR = .318(5.2)(10^3)41''$
$= 68(10^3)\#\text{-in}$

$T = \frac{1}{2} W Z$

$Z = \sin X = \text{MAX} @ X = 90° = 1.0$

$T = .5W = .5(5200)\text{ in-}\# = 2.6(10^3)\text{ in-}\#$

DEN 065098 (3-56)

TRY $3\frac{1}{2} \times 3\frac{1}{2} \times \frac{1}{4}$ RING @ 84" O.D.

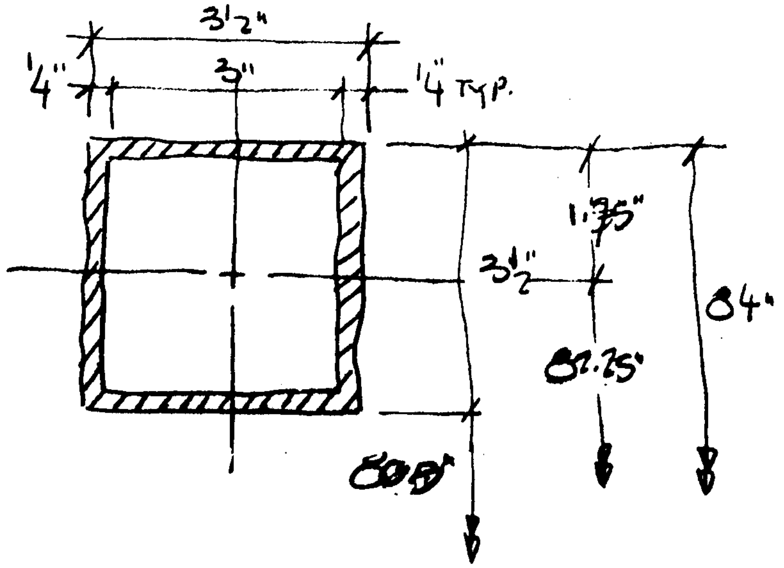

$$I = \frac{(3.5)(3.5)^3}{12} - \frac{(3)(3)^3}{12} = 12.5\,in^4 - 6.75\,in^4 = 5.75\,in^4$$

$$A = (3.5)(3.5)\,\square'' - (3)(3)\,\square'' = 12.25\,\square'' - 9\,\square'' = 3.25\,\square''$$

$$f = \frac{Mc}{I} + \frac{P}{A} = \frac{68(10^3)\#\text{-in}\,(1.75)}{5.75\,in^4} + \frac{5200\#}{3.25\,\square''} = 20{,}700\,psi + 1600\,psi$$

$= 22{,}300$ psi OK USE $3\frac{1}{2} \times 3\frac{1}{2} \times \frac{1}{4}$ WALL RING

APPENDIX B2-2

EXPERIMENT MOUNT STRESS ANALYSIS

ANALYSIS
OF

GIMBAL RING, LAUNCH LOCKS & ERECTION ARMS   10 AUG. 1972

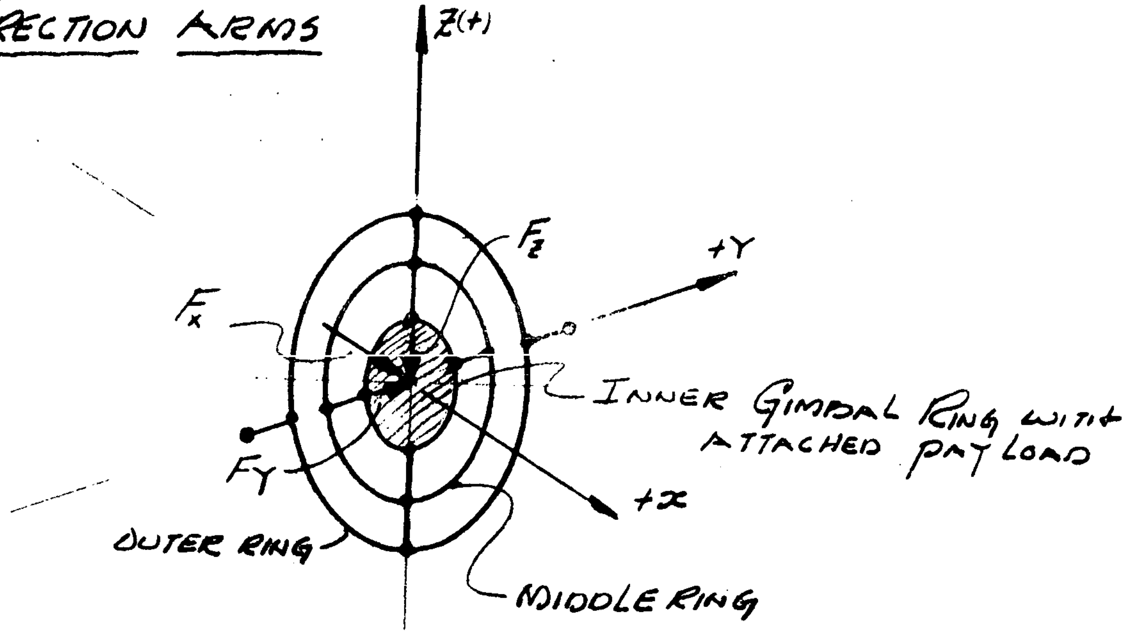

LOAD CONDITIONS ON SHUTTLE PAYLOADS AS DETERMINED FROM FLIGHT CONDITIONS
MAXIMUM ORBITER TO LH_2/LOX DROP TANK ATTACHMENT LOADS

ORBITER C.G. LOADS

$$F_Z = \begin{Bmatrix} +380K \\ -532K \end{Bmatrix}$$

$$F_Y = \begin{Bmatrix} +300K \\ -310K \end{Bmatrix}$$

$$F_X = \begin{Bmatrix} +14K \\ -1{,}377K \end{Bmatrix}$$

ORBITER C.G. LOAD FACTORS

$$N_Z = \frac{-532k}{347.5k} = -1.53 \text{ g's.}$$

$$N_Y = \frac{-310K}{347.5k} = -0.90 \text{ g's.}$$

$$N_X = \frac{-1{,}377k}{347.5k} = -3.96 \text{ g's.}$$

ORBITER WEIGHT @ +64 SEC WITH (2) ABORT MOTORS ATTACHED = 347.5 KIPS

PREPARED BY T. J. D.   CHECKED BY ____   REVISED BY ____

DEN 06508 (3-56)

PAYLOAD IS THE SOLAR PACKAGE

SOLAR PACKAGE TOTAL COMP. WT. = 3,531 #
SOLAR PACKAGE SHELL @W ATTACH.
AND STIFFNER RINGS = 1,005 #
TOTAL UNIT WT. = 4,536 #

LOAD FACTORS

$$\begin{bmatrix} N_Z = -1.53 \text{ go.} \\ N_Y = -0.90 \text{ go.} \\ N_X = -3.96 \text{ go.} \end{bmatrix}$$

LOADS AT PAYLOAD ATTACHMENT RING.

$$F_Z = -1.53(4,536)^{\#} = -6,940^{\#}$$
$$F_Y = -0.9(4,536)^{\#} = -4,083^{\#}$$
$$F_X = -3.96(4,536)^{\#} = -17,963^{\#}$$

COORDINATE SYSTEM

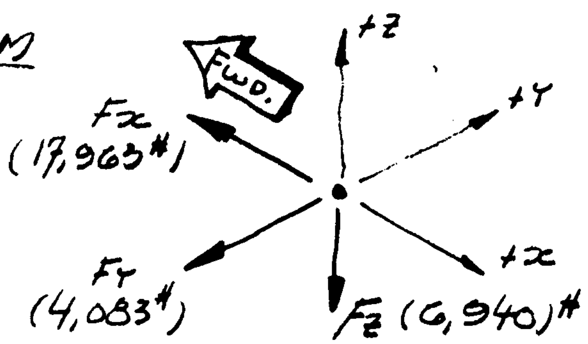

INTERNAL GIMBAL RING LOADS

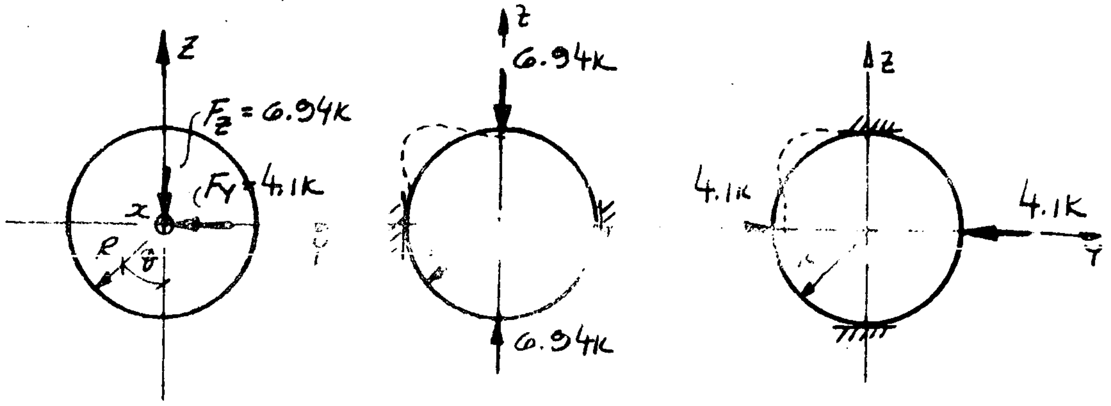

APPROXIMATE MOMENT & SHEAR

$$M_{(MAX)} = 0.5W_1R + 0.5W_2R = 0.5R(F_Z + F_Y) = 0.5(42")(7.1)K$$
$$= 149 \text{ in.-K} = 149,000 \text{ \#-in.}$$

$$V_{(MAX)} = 0.5W_1\cos\phi + 0.5W_2\cos\phi = 0.5\cos\phi(7.1)K$$
$$= 0.5(7.1)K \quad @ \phi = 0°$$
$$= 3.55K = 3,550 \text{ \#}$$

CONSIDERING ALUMINUM FOR INNER GIMBAL RING CONSTRUCTION

$F_{t(ULT)} = 57,000$ psi.

$F_{YIELD} = 40,000$ psi.

$F_{(CRIP.)} = 29,000$ psi

PREPARED BY T.J.D. CHECKED BY REVISED BY

DEN 06508 (3-56)

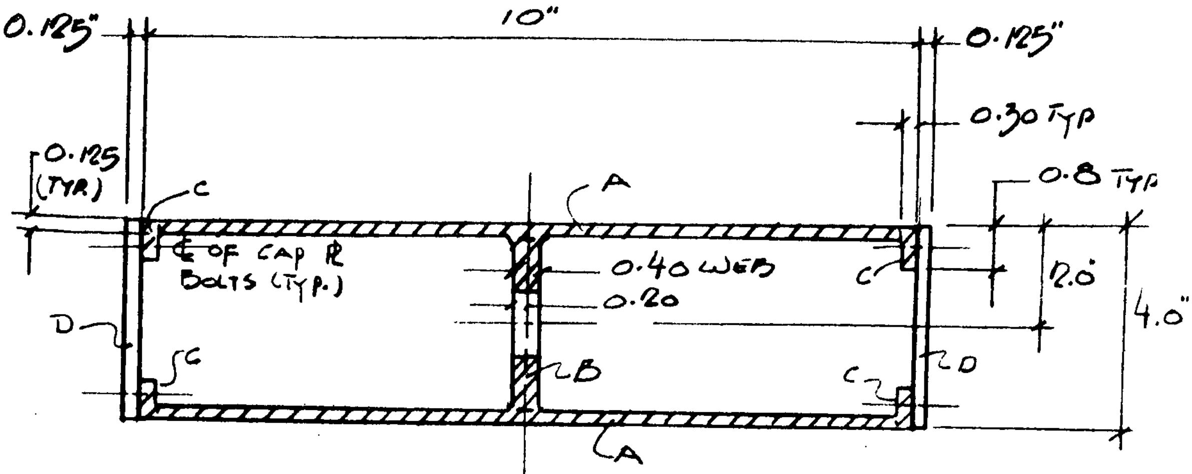

SECTION THRU INNER
GIMBAL RING

"t" (typ.) = 0.125"

Web "t" = 0.40"

Cap "t" = 0.125"

Tab "t" = 0.30"

$$A = 2(9.3)(.125)\phi'' + 4(.3)(.8)\phi' + 2(.125)(4) + 0.4(3.75)\phi''$$
$$= 2.32\phi'' + 0.96\phi'' + 1.0\phi'' + 1.50\phi''$$
$$= 5.78\phi''$$

$$\left.\begin{aligned} I_{oB} &= 0.4\,\frac{(3.75)^3}{12} = 1.76\ in^4 \\ 4 I_{oC} &= 4(.3)\frac{(.8)^3}{12} = .045\ in^4 \\ 2 I_{oD} &= 2(.125)\frac{(4)^3}{12} = 1.33\ in^4 \end{aligned}\right\} \Sigma I_o = 3.13\ in^4$$

DEN 06508 (3-56)

PREPARED BY T.J.D. CHECKED BY REVISED BY

$$I = \Sigma I_o + \Sigma A Y^2 = 3.13\,in^4 + 2(9.4)(\tfrac{1}{8})(1.94)^2 + 4(.3)(.8)(1.6)^2$$
$$= 3.13\,in^4 + 8.84\,in^4 + 2.45\,in^4$$
$$= 14.42\,in^4$$

$$M_{LIMIT} = 149{,}000\ \#\text{-in.}$$
$$M_{DESIGN} = 1.5\,(149{,}000\ \#\text{-in}) = 224{,}000\ \#\text{-in.}$$

$$f_{b\,des} = \frac{Mc}{I} + \frac{P}{A} = \frac{224(10^3)\#\text{-in}\,(2)\,in}{14.42\,in^4} + \frac{6{,}940^\#}{5.78\,\square''}$$
$$= 31.2(10^3)\,psi + 1{,}200\,psi = 32{,}400\,psi$$

$$V_{Limit} = 3{,}550^\#$$
$$V_{des.} = 1.5(3{,}550)^\# = 5{,}320^\#$$

$$f_{v\,des.} = \frac{5320^\#}{5.78\,\square''} = 920\,psi$$

CRIPPLING LOAD WILL NOT CONTROL AS FLANGE EDGES ARE CONTINUOUSLY SUPPORTED BY END CAPS.

RING LOOKS GOOD FOR LOAD CONDITION AND CANNOT BE REDUCED BELOW 4"×10" BASIC DIM'S. FOR HARDWARE CONSIDERATIONS.

DEN 06098 (3-56)

PREPARED BY T. J. D. CHECKED BY ______ REVISED BY ______

Longitudinal Loading

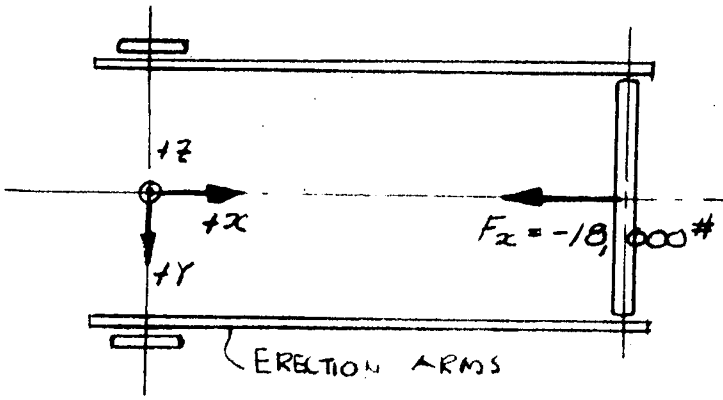

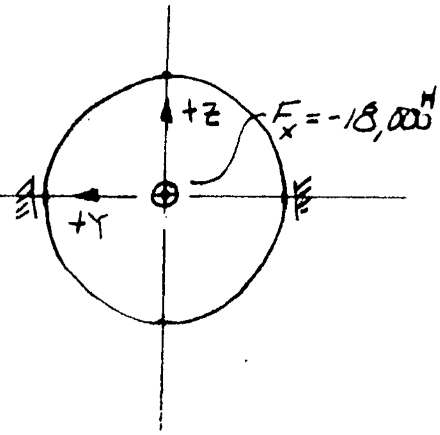

Plan View of Orbiter
Payload Bay

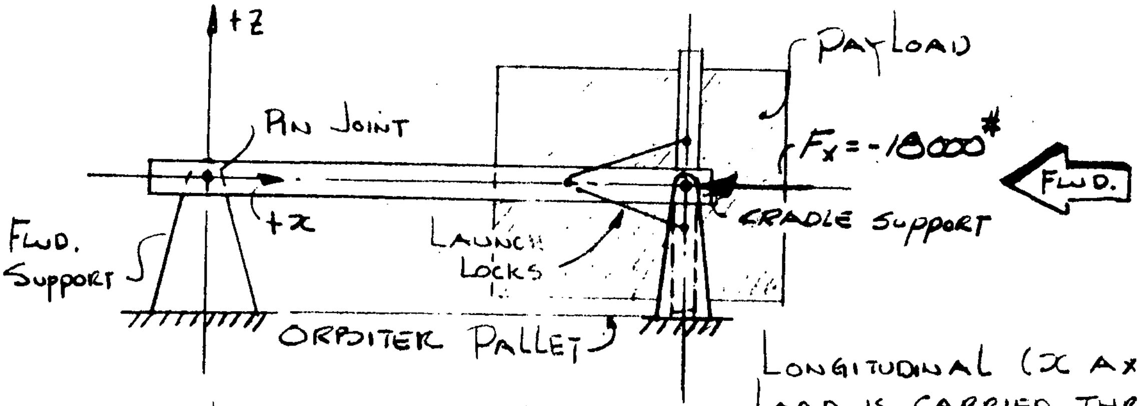

Elevation at Orbiter
Payload Bay

Longitudinal (x axis) Load is carried thru Inner Gimbal Ring to Launch Locks thru Erection Arms to Fwd. Support

$$F_x = -3.96(4,536)^{\#} \approx 18,000^{\#}$$

DEN 065098 (3-56)

PREPARED BY T. J. D CHECKED BY REVISED BY

Longitudinal Load Diagram.

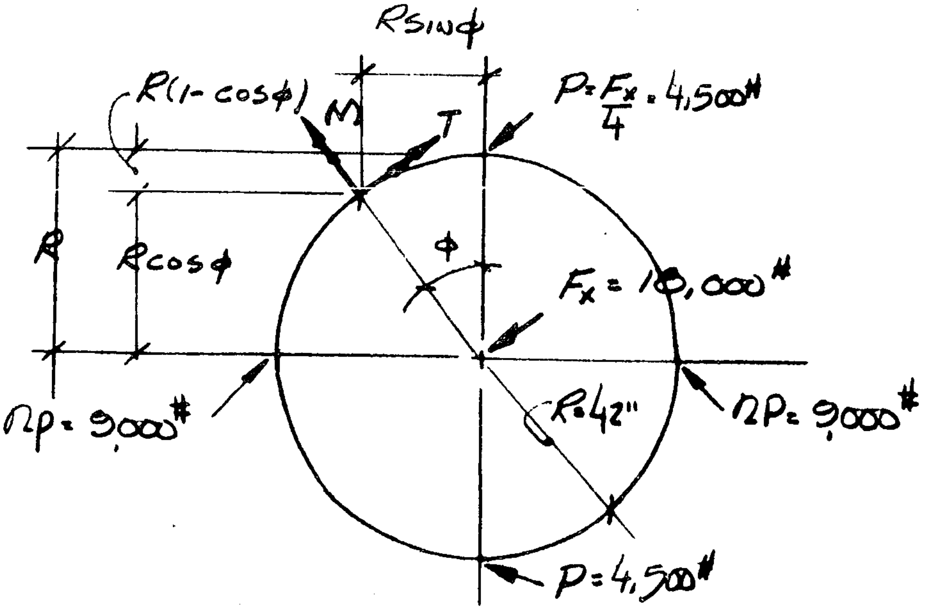

$T = PR(1-\cos\phi)$

$M = PR\sin\phi$

$V = nP$

$M_{max} = PR = 4{,}500\#(42") = 189(10^3)\#\text{-in.}$

$V = nP = 9000\#$

$T_{max} = PR = 189(10^3)\text{ in.-}\#$

Using Previously Determined Section Properties

$$f_{b_{des}} = \frac{1.5(189)(10^3)(2)}{14.42} = 39{,}400 \text{ psi}$$

DEN 04509B (3-56)

PREPARED BY T. J. D. CHECKED BY REVISED BY

CHECK LAUNCH LOCKS

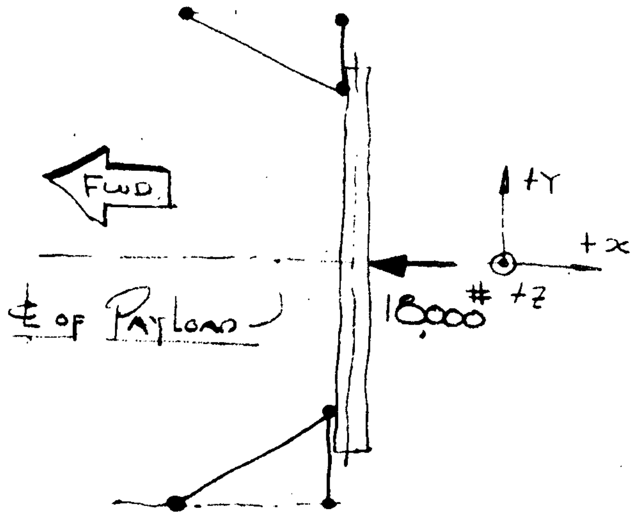

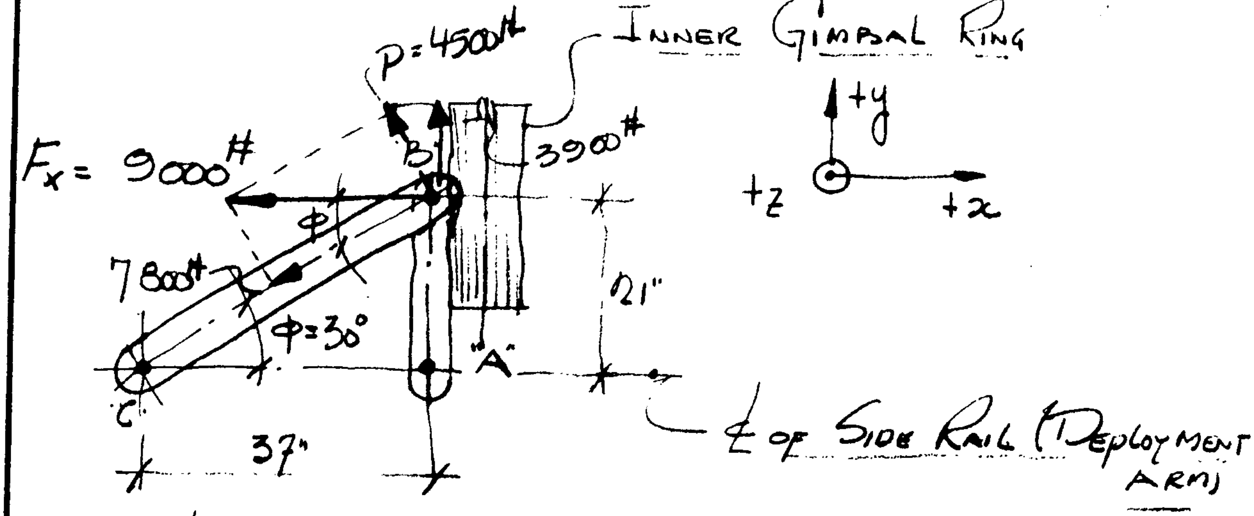

$\phi = \tan^{-1}\frac{21}{37} = \tan^{-1} .568 = 30°$

$\frac{\overline{CB}}{9000\#} = \cos 30°$

$\overline{CB} = 9000\#(.867) = 7,800\#$

$P = 9000 \sin 30° = 4500\#$

$\overline{AB} = 4500\# \cos 30° = 3,900\#$

PREPARED BY T. J. D. CHECKED BY REVISED BY

DESIGN LOADS

$\overline{CB}_{(DES)} = 1.5\,\overline{CB}_{LIMIT} = 1.5(7800^{\#}) = 11,700^{\#}$

$\overline{AB}_{(DES.)} = 1.5\,\overline{AB}_{LIMIT} = 1.5(3,900^{\#}) = 5,850^{\#}$

FOR LAUNCH LOCKS

USE STEEL TUBE

TRY 1.5" O.D x .063" WALL

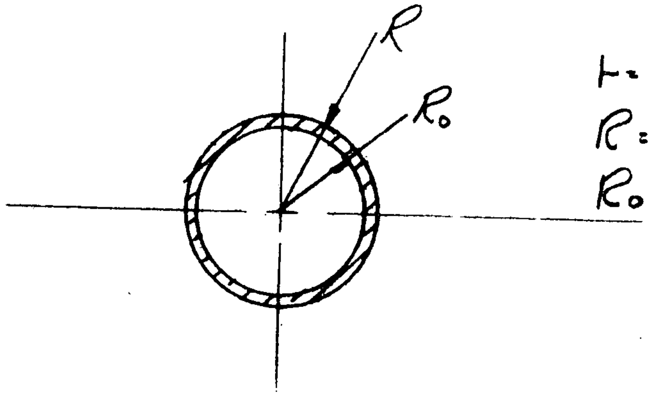

r = Radius of Gyration

$R = 0.75"$

$R_o = 0.69"$

$r = \sqrt{\frac{1}{4}(R^2 + R_o^2)} = \sqrt{\frac{1}{4}(.75^2 + .69^2)} = \sqrt{\frac{1}{4}(.56 + .47)} = \frac{1}{2}\sqrt{1.03}$

$r = 0.5(1.015) = 0.5\text{ in}$

$\frac{l}{r} = \frac{37"}{.5} = 74"$ (INTERMEDIATE Col.)

$I = \frac{\pi}{4}(R^4 - R_o^4) = \frac{\pi}{4}(.75^4 - .69^4) = \frac{\pi}{4}(10^{-4})(3140 - 2270)\text{ in}^4$

$I = \frac{\pi}{4}(870)(10^{-4}) = .069 \text{ in}^4$

$E = 29(10^6)$ psi

$L = L' = 37'$

CHECK CRIT. LOAD FOR COL BUCKLING

$P_c = \frac{\pi^2 E I}{L^2} = \frac{\pi^2 (29)(10^6)(.69)(10^{-1})}{(3.7)^2(10^2)} = \frac{\pi^2(29)(10^3)(.69)}{13.7}$ #

$P_c = \frac{198}{13.7}(10^3) = \underline{14,400\#}$, $\bar{C}B_{DES} = \underline{11,700\#}$

OK USE 1.5" O.D × .062 WALL TUBE

CHECK SHORT STRUT

TRY 1.0" ϕ × .050 WALL

$R = 0.50"$

$R_o = 0.45"$

$E = 29(10^6)$ psi

$L = 21"$

$I = \frac{\pi}{4}(R^4 - R_o^4) = \frac{\pi}{4}(5^4 - 4.5^4)(10^{-4}) \text{ in}^4 = \frac{\pi}{4}(625 - 410)(10^{-4})$

$I = \frac{\pi}{4}(215)(10^{-4}) = 168(10^{-4}) = .017 \text{ in}^4$

DEN 065098 (3-56)

PREPARED BY T. J. D CHECKED BY REVISED BY

$$P_c = \frac{\pi^2 E I}{L^2} = \frac{\pi^2 (29)(10^6)(.17)(10^3)}{(2.1)^2(10^3)}$$

(with "4" written above the 10^6)

$$= \frac{\pi^2(29)(.17)(10^3)}{4.4} = \frac{49}{4.4}(10^3)\# = 10.5(10^3)\#$$

$P_c = 10{,}500\#$, $\overline{AB}_{(DES.)} = 5{,}850\#$

ok use 1.0" ϕ x .062" WALL

Check Side Rails for Compressive Buckling Load (Deployment Arms

Set $P_c = 1.5(9000\#) = 15{,}000\#$ (CRIT. BUCKLING LOAD)
$L = 130"$
$K = 1.0$ (Pin Ended Col. Both Ends)
$E = 10(10^6)$ psi

$$I_{req} = \frac{P_c L^2}{\pi^2 E} = \frac{15(10^3)\#(1.3)^2(10^4)\,in^2}{\pi^2\, 10(10^6)\,\#/\square"} = \frac{25.3(10^7)\,in^4}{9.86(10^7)}$$

$= 2.57\ in^4$

DEN 065098 (3-56)

PREPARED BY T. J.D CHECKED BY REVISED BY

TRY SECTION

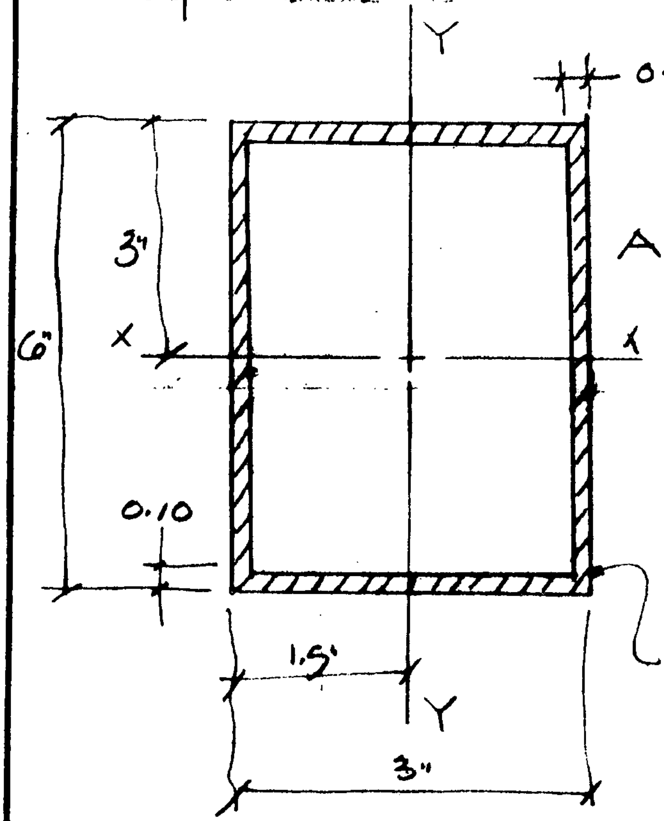

$A = [3(6) - 5.8(2.8)]\ in^2 = 1.75\square''$

$f_c = \frac{1500^{\#}}{1.75\square''} = 8{,}560\ ^{\#}/\square''$

OK

X-SECTION THRU SIDE RAIL

$I_{YY} = \frac{6(3)^3}{12} in^4 - \frac{5.8(2.8)^3}{12} = 13.5\ in^4 - 10.6\ in^4 = 2.9\ in^4$

OK $I_{YY} = 2.9 > I_{req}$ OF $2.57\ in^4$ (MOMENT OF INERTIA ABOUT LEAST AXIS)

SUMMARY

SIDE RAIL $A = 1.75\square''$ $I = 2.9\ in^4$

LAUNCH LOCKS 1.5"ϕ x .062 WALL (LONG STRUT)

1.0"ϕ x .062 WALL (SHORT STRUT)

CHECK SECTION OF OUTER GIMBAL RING SUPPORTING THE CENTER RING AT TOP CENTER THRU THE FLEX PIVOT.

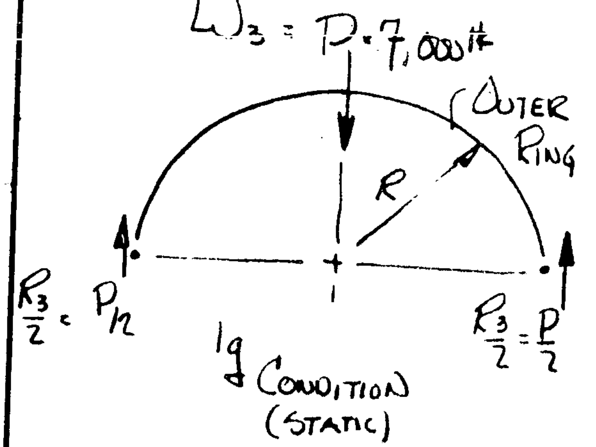

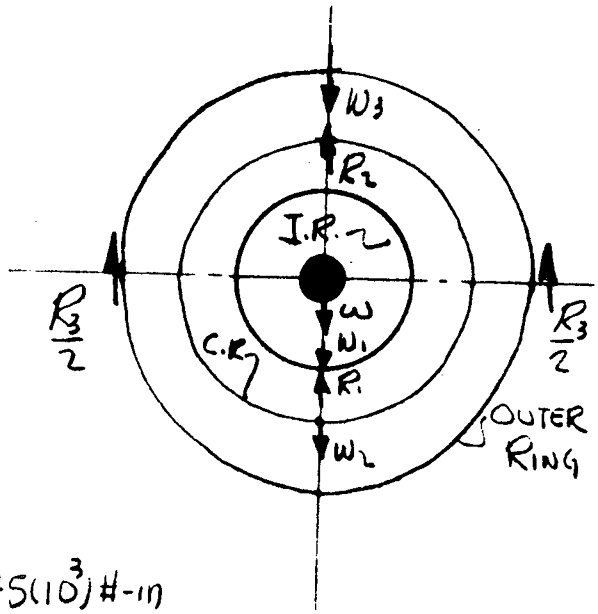

$$M_{MAX\,(LIMIT)} = \frac{PR}{2} = \frac{7{,}000^{\#}}{2}(50'') = 175(10^3)\#\text{-in}$$

USE SAME BASIC SECTION AS INNER RING FOR 149,000 #-in

$$f_{b\,LIMIT} = \frac{175}{149}(20{,}600) + 1200 = (24{,}200 + 1200)\,psi = 25{,}400\,psi$$

$$f_{b\,des} = 1.5(25{,}400)\,psi = 38{,}100\,psi \quad OK$$

USE SAME BASIC SECTION

PREPARED BY T. J. D CHECKED BY ______ REVISED BY ______

ANALYSIS
OF

(28 AUGUST 1972)

ARRAY SUPPORT FRAME STIFFNESS & DEFLECTION

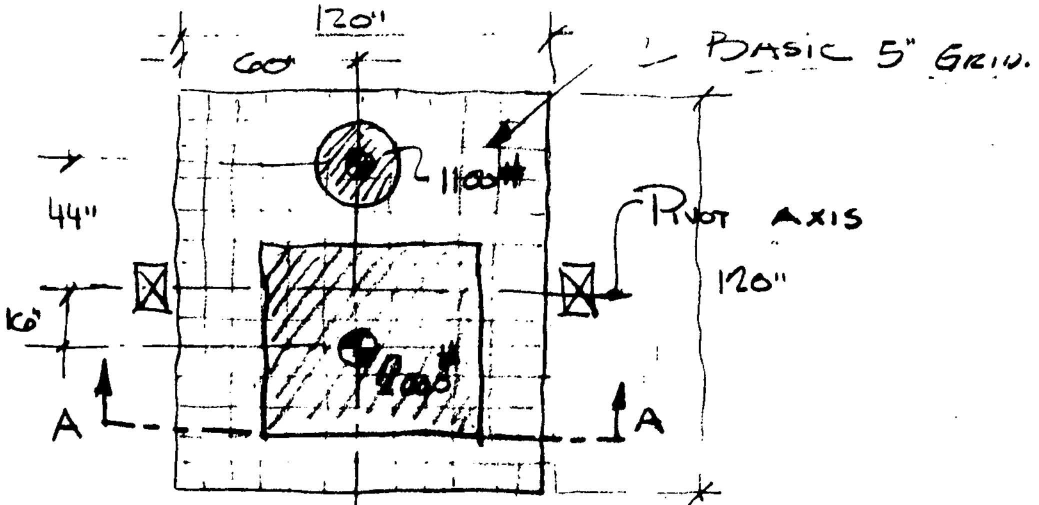

PLAN OF ARRAY

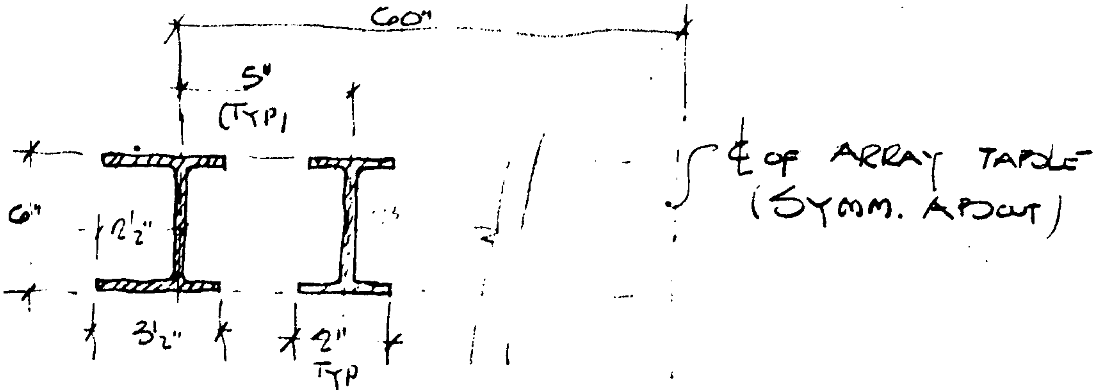

SECTION AA

TYPICAL CROSS SECTION HAS 23 "I" MEMBERS & 2 EDGE MEMBERS

$$A = 23[(.4)(2)+(5.6)(.125)] + 2[(.4)(3.5)+(5.6)(.125)]$$

$$= 23[.8+.7] + 2[1.4+.7] = 23(1.5) + 2(2.1) = 34.5 + 4.2$$

$$= 38.7 \,\square''$$

DEN 065098 (3-56)

PREPARED BY T. J. D. CHECKED BY REVISED BY

$$I = 23\left[\frac{(.125)(5.6)^3}{12} + (.4)(2)(2.9^2)\right] + 2\left[\frac{(.125)(5.6)^3}{12} + (.4)(3.5)(2.9^2)\right]$$

$$I = 23\left[1.84 + 6.7\right] + 2\left[1.84 + 11.7\right]$$

$$I = 23(8.54) + 2(13.54) = 197 + 27.1 = 224 \text{ in}^4$$

FOR SIMPLE BEAM CONFIGURATION
WITH $N_x = 3.96g$

$$F_x = N_x P = 3.96(3100^{\#}) = 12{,}300^{\#}$$

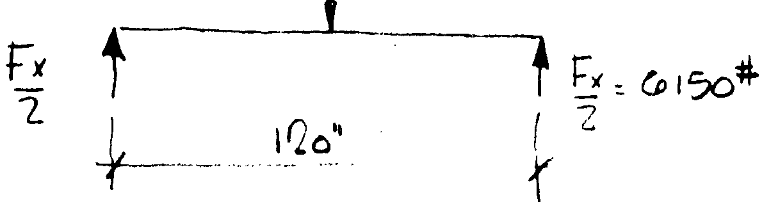

$$V = \frac{F_x}{2} = 6150^{\#}$$

$$M = \left(\frac{F_x}{2}\right)\left(\frac{l}{2}\right) = \frac{F_x l}{4} = \frac{12.3(10^3)^{\#}(120)\text{in}}{4} = 370(10^3)\ \#\text{-in.}$$

$$f_b = \frac{Mc}{I} = \frac{370(10^3)\ \#\text{-in}\ (3)''}{224 \text{ in}^4} = 4.94(10^3) \text{ psi} = 4{,}940 \text{ psi}$$

$$\Delta = \frac{F_x l^3}{48EI} = \frac{12.3(10^3)(1.2)^3(10^6)}{48(10^7)(224)} = \frac{21.4(10^9)}{107(10^9)} = \underline{0.2 \text{ in}}$$

DEN 065098 (3-58)

PREPARED BY T.J.D. CHECKED BY ______ REVISED BY ______

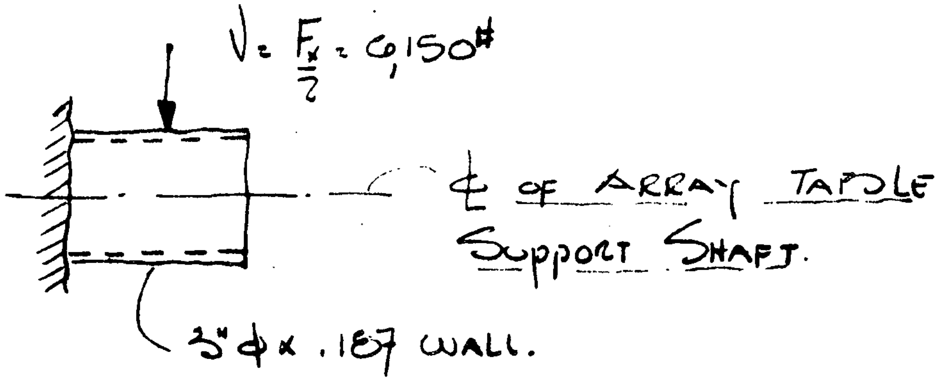

$$f_v = \frac{V}{A} = \frac{6150\#}{\pi(1.5^2 - 1.313^2)} = \frac{6150\#}{\pi(2.25-1.72)\,\text{in}^2} = \frac{6150\#}{.53\pi\,\text{in}^2} = 3{,}700\ \text{psi}$$

FOR LOADING IN CANTILEVER MODE

$$F_x = N_x P = 3.96(1100\#) = 4350\#$$

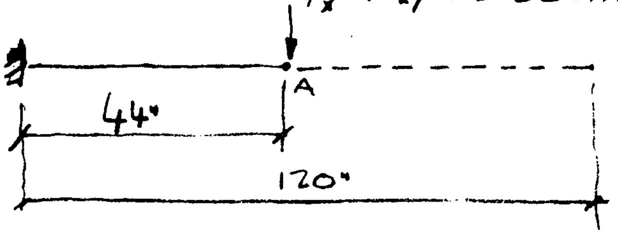

$$M = F_x l = 4.35(10^3)\#(44)" = 192(10^3)\#\text{-in}$$

$$f_b = \frac{Mc}{I} = \frac{192(10^3)\#\text{-in}\,(3)"}{224\,\text{in}^4} = 2.56(10^3)\#\text{-in}$$

$$\Delta_A = \frac{F_x l^3}{3EI} = \frac{4.35(10^3)\#(.44)^3(10^6)}{3(10^7)(224)} = \frac{.375(10^9)}{6.72(10^9)} = 0.05\ \text{in}$$

DEN 065098 (3-56)

PREPARED BY______ CHECKED BY______ REVISED BY______

Common Mount ~ Lower Yoke

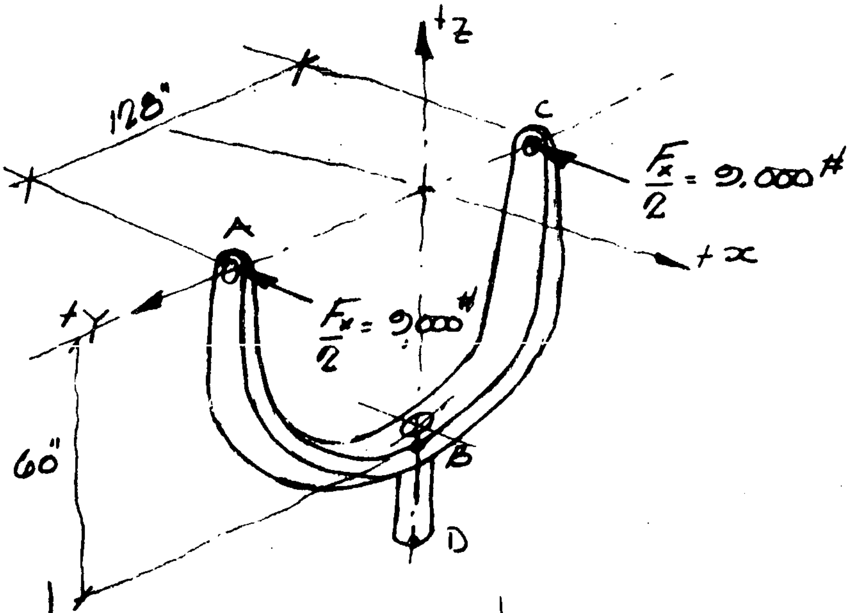

Lower Yoke and Load Diagram

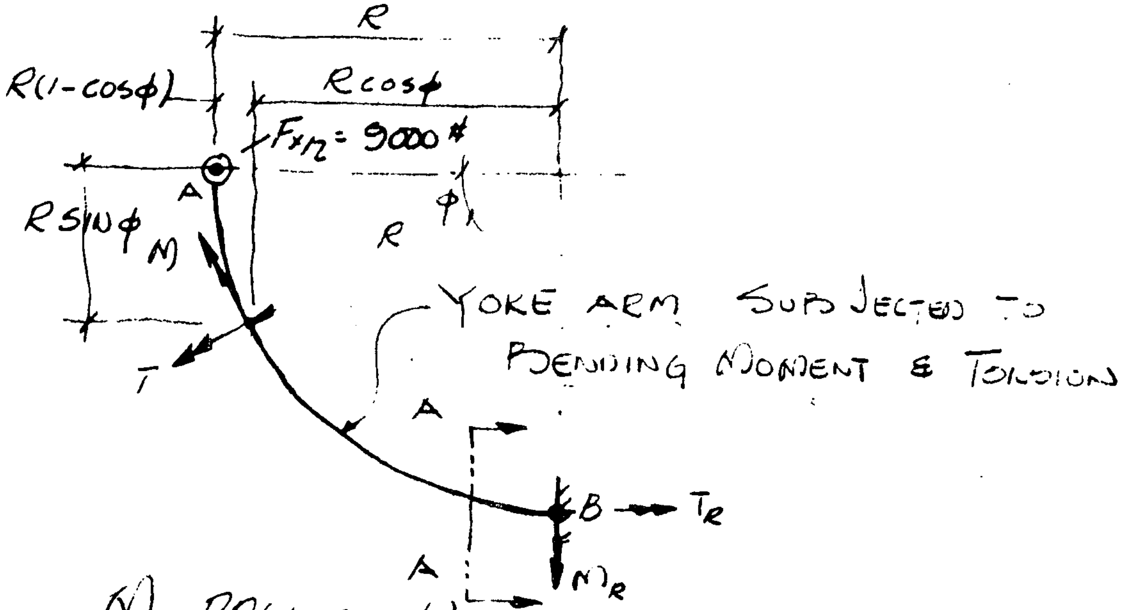

$M = PR(1-\cos\phi)\ \#\text{-in}$

$T = PR\sin\phi\ \text{in.-}\#$

DEN 065098 (3-56)

M_{MAX} OCCURS WHEN $\phi = 90°$ OR $\cos\phi = 0$

T_{MAX} ALSO OCCURS WHEN $\phi = 90°$ OR $\sin\phi = 1.0$ ASSUMING FIXITY CONDITION @ SHAFT MOUNTING POINT.

$$M_{MAX} = PR(1-\cos\phi) = PR = 9(10^3)\# (60")$$
$$= 540(10^3)\#\text{-in.}$$

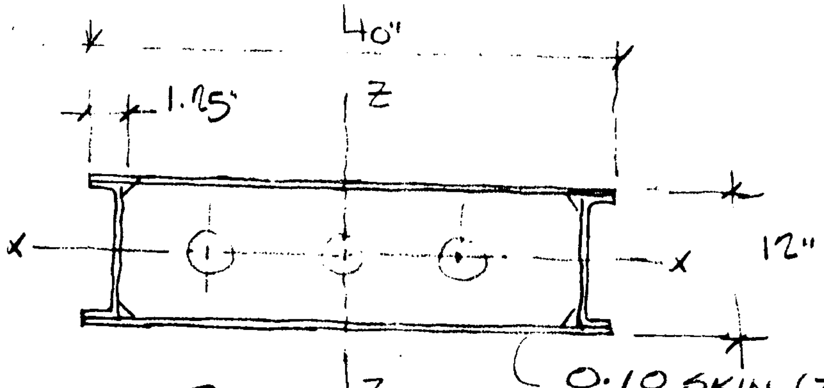

SECTION A-A
(@ YOKE BASE)

M_{MAX} IS ABOUT THE Z-Z AXIS

$$A = 2(40)(.1) + 2[(11.8)(.1) + 2(1.15)(.1)]$$
$$= 8\square" + 2[1.18 + .23]\square" = 8\square" + 2.82 = 10.82\square"$$

DEN 065098 (3-56)

PREPARED BY ______ CHECKED BY ______ REVISED BY ______

$$I = \frac{.2(40)^3}{12} + 2(1.41)(19.5)^2 = \frac{.2(64)(10^3)}{12}in^4 + 2.82(3.8)(10^2)$$

$$I = 1.07(10^3)in^4 + 10.7(10^2) = 1070 in^4 + 1070 in^4 = 2140 in^4$$

$$f_b = \frac{M c}{I} = \frac{540(10^3)\#\text{-}in\,(20)}{2.14(10^3)\,in^4} = 5{,}000\,psi \quad (\text{due to } M)$$

$$f_T = \frac{T}{2t_1(a-t)(b-t_1)}$$

FROM ROARK pg. 176

WHERE [t = thickness of short side "b" & t_1 = thickness of long side "a"]

$$f_T = \frac{540(10^3)in\text{-}\#}{2(.1)(40-.1)(12-.1)}$$

$t = t_1 = 0.10$
$a = 40"$
$b = 12"$

$$f_t = \frac{540(10^3)in\text{-}\#}{2(.1)(39.9)(11.9)} = \frac{540(10^3)in\text{-}\#}{95} = 5.7(10^3)\,psi$$

$$f_t = 5{,}700\,psi$$

$$f_{des_{(TOT)}} = 1.5 f_b + 1.5 f_t = 1.5(5000 + 5700) = 1.5(10{,}700)\,psi$$
$$= 16{,}000\,psi$$ (stress can be higher in corners of box due to torsion)

ANALYSIS OF

BRGS SELECTED FOR MAIN SHAFT ARE TIMKEN TAPERED ROLLER BRGS WITH 9"φ I.D & 14"φ O.D.

LOAD CAP. RADIAL = 155,000#

SHAFT STRENGTH, ANALYSIS

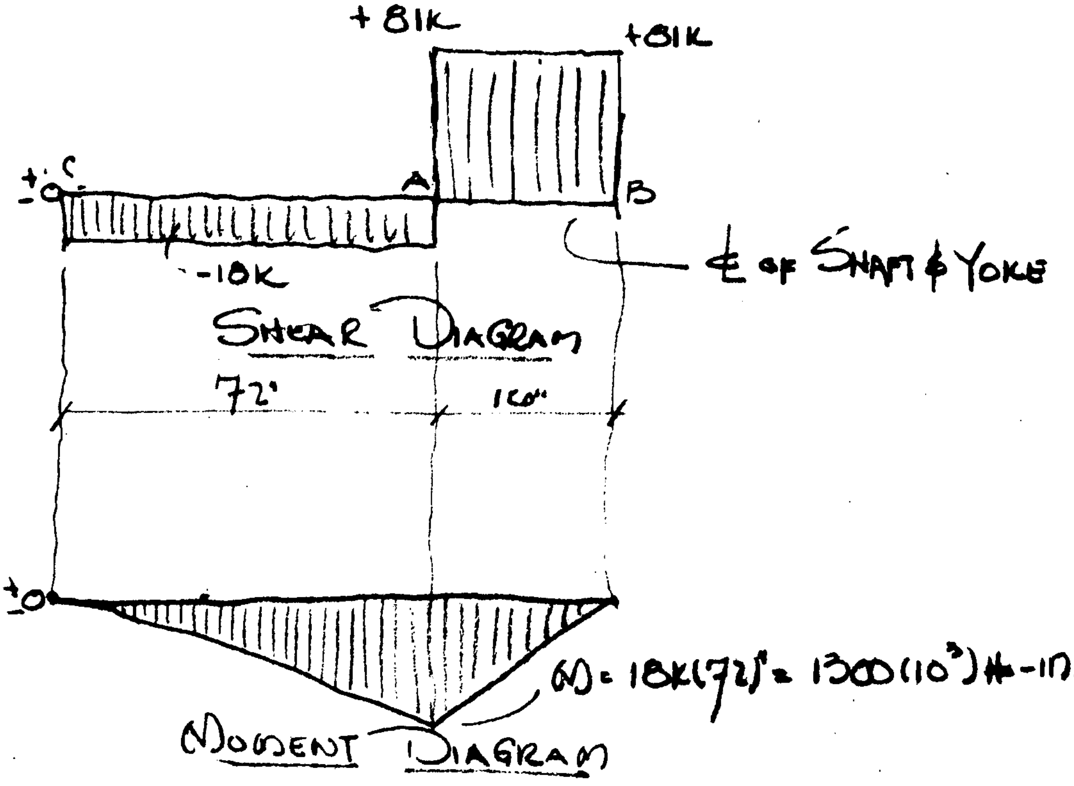

$V_{DES} = 1.5(81K) = 121,500\#$

$M_{DES} = 1.5(1300(10^3)\#\text{-in} = 1.95(10^6)\#\text{-in}$

SHAFT SIZE = 9" O.D × 0.82 WALL

MATERIAL STAINLESS STEEL TYPE 303

SHAFT X-SECT. AREA

$$A = \pi(R_o^2 - R_i^2) = \pi(4.5^2 - 3.68^2) = \pi(20.2 - 13.6)\,in^2$$

$$A = 6.6\pi\,in^2 = 20.7\,in^2$$

$$f_{v_{ult}} = \frac{V}{A} = \frac{121{,}500\#}{20.7\,in^2} = 5{,}850\ psi \quad OK$$

$$I = \frac{\pi}{4}(R_o^4 - R_i^4) = \frac{\pi}{4}(4.5^4 - 3.68^4) = \frac{\pi}{4}(411 - 184)\,in^4$$

$$= 227\frac{\pi}{4}\,in^4 = 179\,in^4$$

$$f_{b_{ult}} = \frac{Mc}{I} = \frac{1.95(10^6)\#\text{-}in\,(4.5)in}{179(10^0)\,in^4} = 4.9(10^4)\,psi = 49{,}000\ psi$$

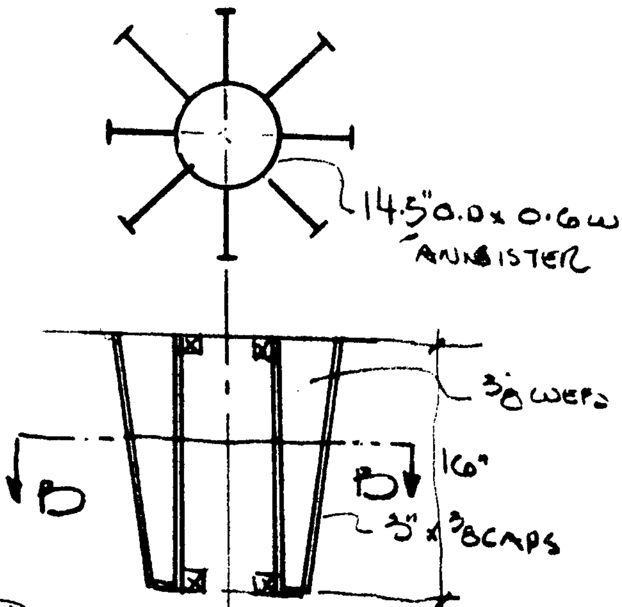

BASIC YOKE SHAFT CANNISTER ASSY.

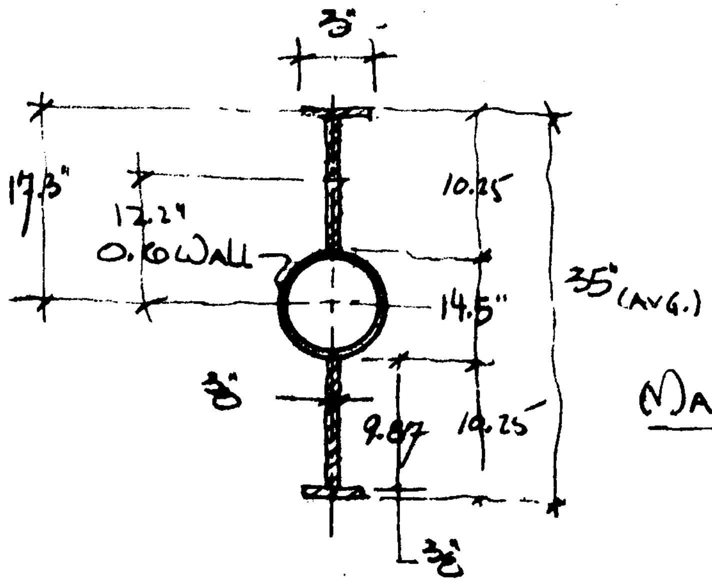

MAT'L. ALUMINUM

SECTION B-B

$$I_{TUBE} = \frac{\pi}{4}(R_o^4 - R_i^4) = \frac{\pi}{4}(7.25^4 - 6.65^4)\,in^4 = \frac{\pi}{4}(2760 - 1970)\,in^4$$
$$= 790\,\frac{\pi}{4}\,in^4 = \underline{620}\,in^4$$

$$I_{(TOTAL)} = I_{TUBE} + (9.87)(.375)(12.2^2)(2) + 2(3)(.375)(17.3)^2$$
$$= 620\,in^4 + 1100\,in^4 + 675\,in^4$$
$$= 2395\,in^4$$

$$f_{b\,des} = \frac{Mc}{I} = \frac{1.95(10^6)\,\#\text{-}in\,(17.5)\,in}{2.395(10^3)\,in^4} = 14.3(10^3)\,psi$$
$$= \underline{14,300}\,psi$$

DEN 06098 (3-56)

PREPARED BY T. J. D. CHECKED BY ______ REVISED BY ______

ANALYSIS
OF

Gamma Ray Spectrometer Mount I

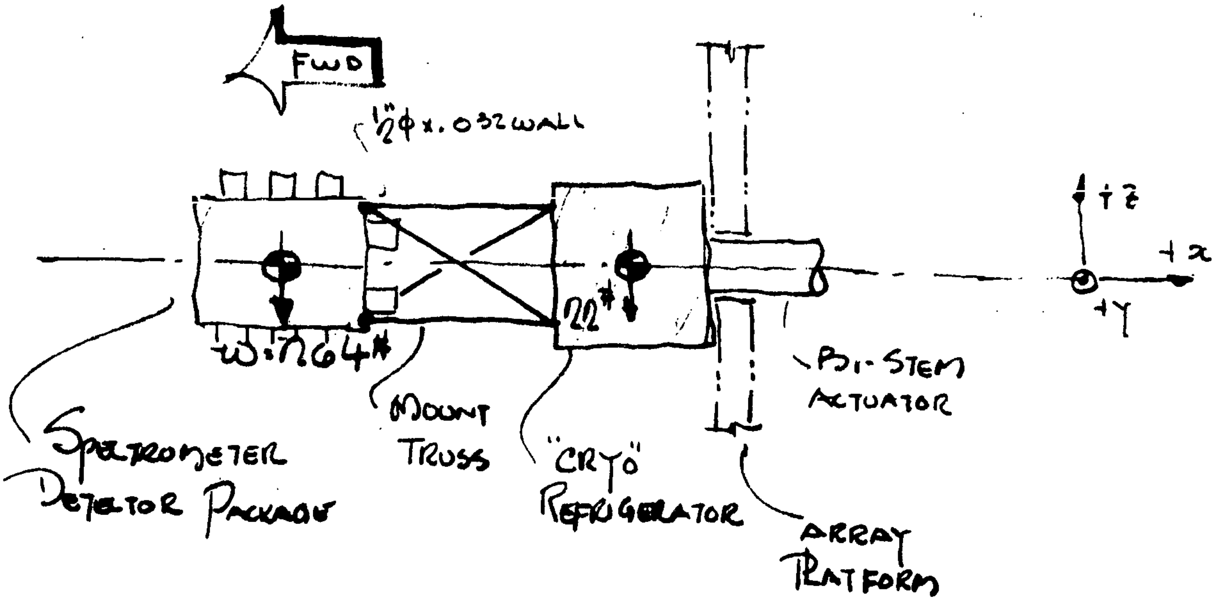

$N_x = +4\,g$

$N_z = -1.53\,g$

$F_{x_{LIMIT}} = 4(264)^{\#} = 1{,}030^{\#}$

$F_{z_{LIMIT}} = -1.53(264)^{\#} = 405^{\#}$

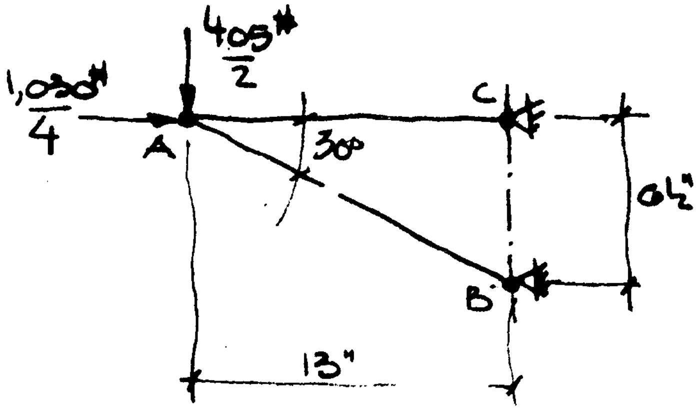

PREPARED BY T.J.D. CHECKED BY ____ REVISED BY ____

$$P_{x\,DES} = \frac{1030^{\#}}{4}(1.5) = 385^{\#}$$

$$P_{z\,DES} = \frac{405}{2}(1.5) = 303^{\#}$$

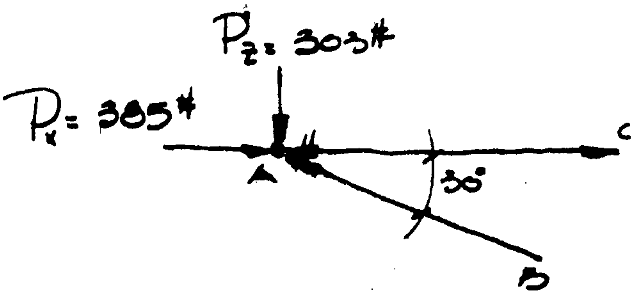

$$(+\uparrow)\ \Sigma F_z = -303^{\#} + .5\overline{AB} = 0$$

$$\overline{AB} = \frac{303^{\#}}{.5} = 606^{\#}$$

$$(+\rightarrow)\ \Sigma F_x = 385^{\#} - .867\overline{AB} - \overline{AC} = 0$$

$$385^{\#} - .867(606^{\#}) = \overline{AC}$$

$$385^{\#} - 525^{\#} = \overline{AC}$$

$$\overline{AC} = -140^{\#} = 140^{\#} \rightarrow$$

Check member $\overline{AB}$ for buckling load

$$L_{AC} = 13/.867 \text{ in.} = 15 \text{ in.}$$

$$P_{(CRIT)} = \frac{\pi^2 EI}{L^2}$$

USING 1/2"ϕ x .032 WALL TUBING
MATL. ALUM
$E = 10^7$ psi

$I = \frac{\pi}{4}(R_o^4 - R_i^4)$ $R_o = .25"$
$R_i = .218"$

$I = \frac{\pi}{4}(.25^4 - .218^4) = \frac{\pi}{4}(.0039 - .0023)\,in^4$

$I = \frac{\pi}{4}(.0016)\,in^4 = .00125\,in^4 = 13(10^{-4})\,in^4$

$A = \pi(R_o^2 - R_i^2) = \pi(.25^2 - .218^2) = \pi(.063 - .047)$
$= \pi(.016)\,\square" = .05\,\square"$

$P_c = \dfrac{\pi^2(10^7)\frac{\#}{\square"}(13)(10^{-4})\,in^4}{(15)^2\,in^2} = \dfrac{13\pi^2(10^3)}{225} = .5702(10^3)\#$

$= 5{,}702\#$ OK FOR 1/2"ϕ x .032 WALL

SHEAR STRESS $= f_{v_{ult}} = \dfrac{V_T}{4A} = \dfrac{405\#(1.5)}{4(.05\square")} = \dfrac{607\#}{.2\square"} = 3{,}040$ psi
OK

Appendix B3

STABILIZATION AND CONTROL

B3.1. QUATERNIONS: COMPUTING SPACECRAFT ATTITUDE

The attitude of a spacecraft with respect to some reference frame can be described by a set of four parameters called quaternions. These four parameters are based on Euler's theorem that states that the rotational displacement of a rigid body from some initial orientation can be described by a single rotation about a fixed axis. This axis is referred to as an eigenaxis since it is common to both the reference and vehicle coordinate frames. The quaternions describe the attitude of a spacecraft by defining the eigenaxis and the appropriate angular displacement about this axis necessary to transfer from the reference frame to vehicle space.

B3.1.1. <u>Definition</u> - Assume that the rigid body shown in figure B3-1 is rotated with respect to some reference frame XYZ about an eigenaxis $\vec{E}$ defined by the three directional angles α, β, and γ through an angular displacement θ. Assume that $\vec{E}$ is a unit vector.

$$\vec{E}=\cos\alpha\hat{i}+\cos\beta\hat{j}+\cos\gamma\hat{k} \tag{1}$$

where $\hat{i}$, $\hat{j}$, and $\hat{k}$ are unit vectors along the X, Y, and Z axes, respectively. Let the reference coordinates x,y,z define the location of a point P in the body prior to the rotation θ about $\vec{E}$.

Define a second coordinate system x'y'z' such that x' lies along the eigenaxis $\vec{E}$, y' lies in the YZ plane, and z' forms the remaining axis of the orthogonal coordinate triad x'y'z'. Let $\hat{i}'$, $\hat{j}'$, and $\hat{k}'$ be unit vectors along x', y', and z', respectively. $\hat{i}'$, $\hat{j}'$, and $\hat{k}'$ in terms of $\hat{i}$, $\hat{j}$, and $\hat{k}$ equal

$$\hat{i}'=\vec{E}=\cos\alpha\hat{i}+\cos\beta\hat{j}+\cos\alpha\hat{k} \tag{2}$$

$$\hat{j}'=\frac{\hat{i}x\hat{i}'}{\sin\alpha}=-\frac{\cos\alpha}{\sin\alpha}\hat{j}+\frac{\cos\beta}{\sin\alpha}\hat{k} \tag{3}$$

$$\hat{k}'=\hat{i}'x\hat{j}'=\frac{1}{\sin\alpha}[(\cos^2\beta+\cos^2\gamma)\hat{i}-\cos\alpha\cos\beta\hat{j}$$
$$-\cos\alpha\cos\gamma\hat{k}] \tag{4}$$

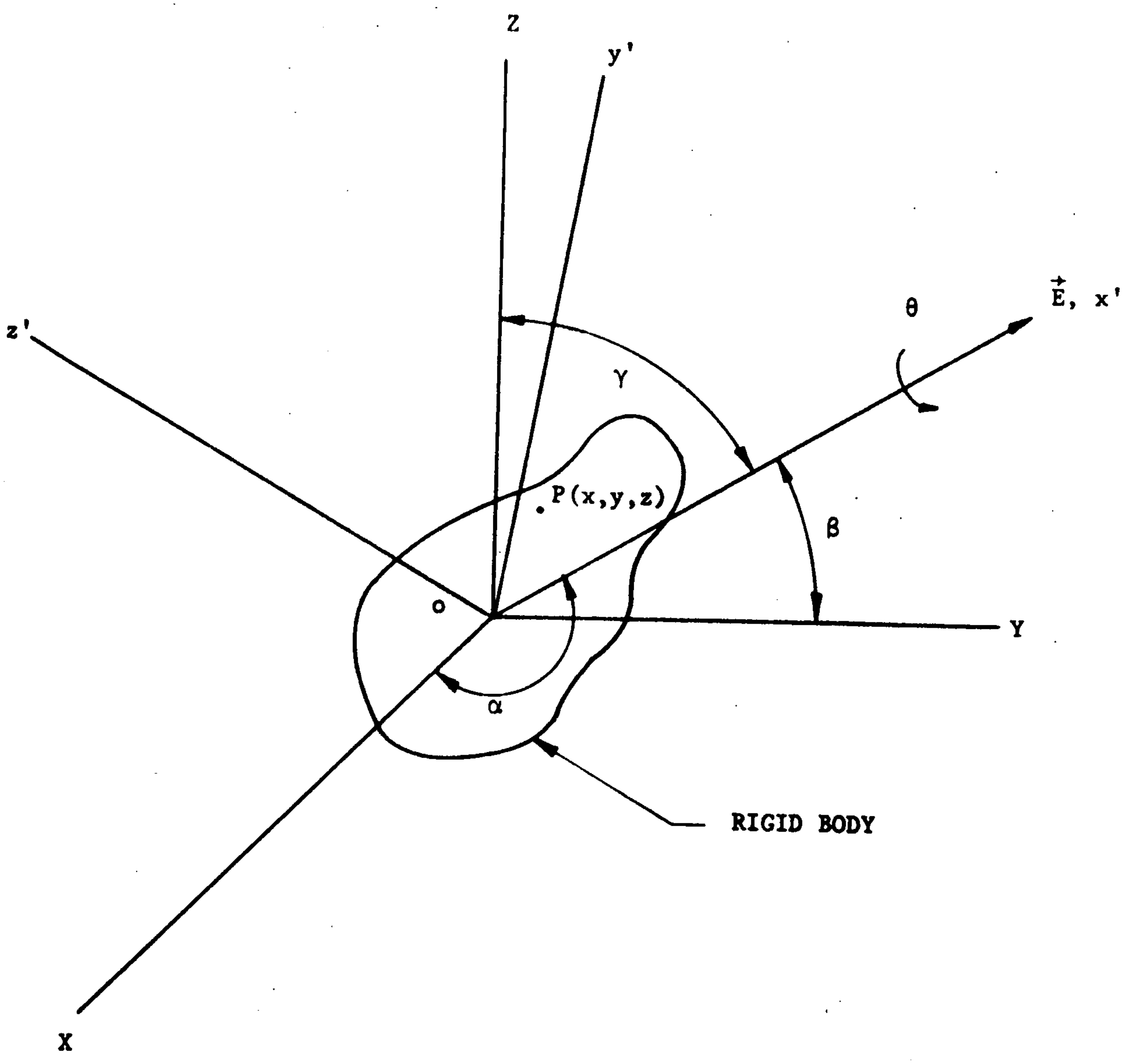

Figure B3-1. Rigid Body Coordinate Systems

The transformation from x'y'z' to XYZ space can be defined by the following transformation:

$$\begin{vmatrix} X \\ Y \\ Z \end{vmatrix} = [\Phi_{R\leftarrow R'}] \begin{vmatrix} x' \\ y' \\ z' \end{vmatrix} \tag{5}$$

where

$$[\Phi_{R\leftarrow R'}] = \begin{vmatrix} \cos\alpha & 0 & \dfrac{\cos^2\beta+\cos^2\gamma}{\sin\alpha} \\ \cos\beta & -\dfrac{\cos\gamma}{\sin\alpha} & -\dfrac{\cos\alpha\cos\beta}{\sin\alpha} \\ \cos\gamma & \dfrac{\cos\beta}{\sin\alpha} & -\dfrac{\cos\alpha\cos\gamma}{\sin\alpha} \end{vmatrix}$$

Define a third coordinate system $X_vY_vZ_v$ that is fixed to the rigid body. Assume that prior to the rotation θ about $\vec{E}$, that the two coordinate systems x'y'z' and $X_vY_vZ_v$ are aligned. The coordinates of point P in body space $X_vY_vZ_v$ are

$$\begin{vmatrix} X_v \\ Y_v \\ Z_v \end{vmatrix} = [\Phi_{R'\leftarrow R}] \begin{vmatrix} x \\ y \\ z \end{vmatrix} \tag{6}$$

where

$$[\Phi_{R'\leftarrow R}] = \begin{vmatrix} \cos\alpha & \cos\beta & \cos\gamma \\ 0 & -\dfrac{\cos\gamma}{\sin\alpha} & \dfrac{\cos\beta}{\sin\alpha} \\ \dfrac{\cos^2\beta+\cos^2\gamma}{\sin\alpha} & -\dfrac{\cos\alpha\cos\beta}{\sin\alpha} & -\dfrac{\cos\alpha\cos\gamma}{\sin\alpha} \end{vmatrix}$$

Now assume the rigid body is rotated about the eigenaxis $\vec{E}$ (X_v axis) through the angle θ. This rotation can be thought of as a transformation from the x'y'z' coordinate frame to the new location of the $X_vY_vZ_v$ coordinate system as shown in figure B3-2. The resulting transformation from $X_vY_vZ_v$ to x'y'z' is

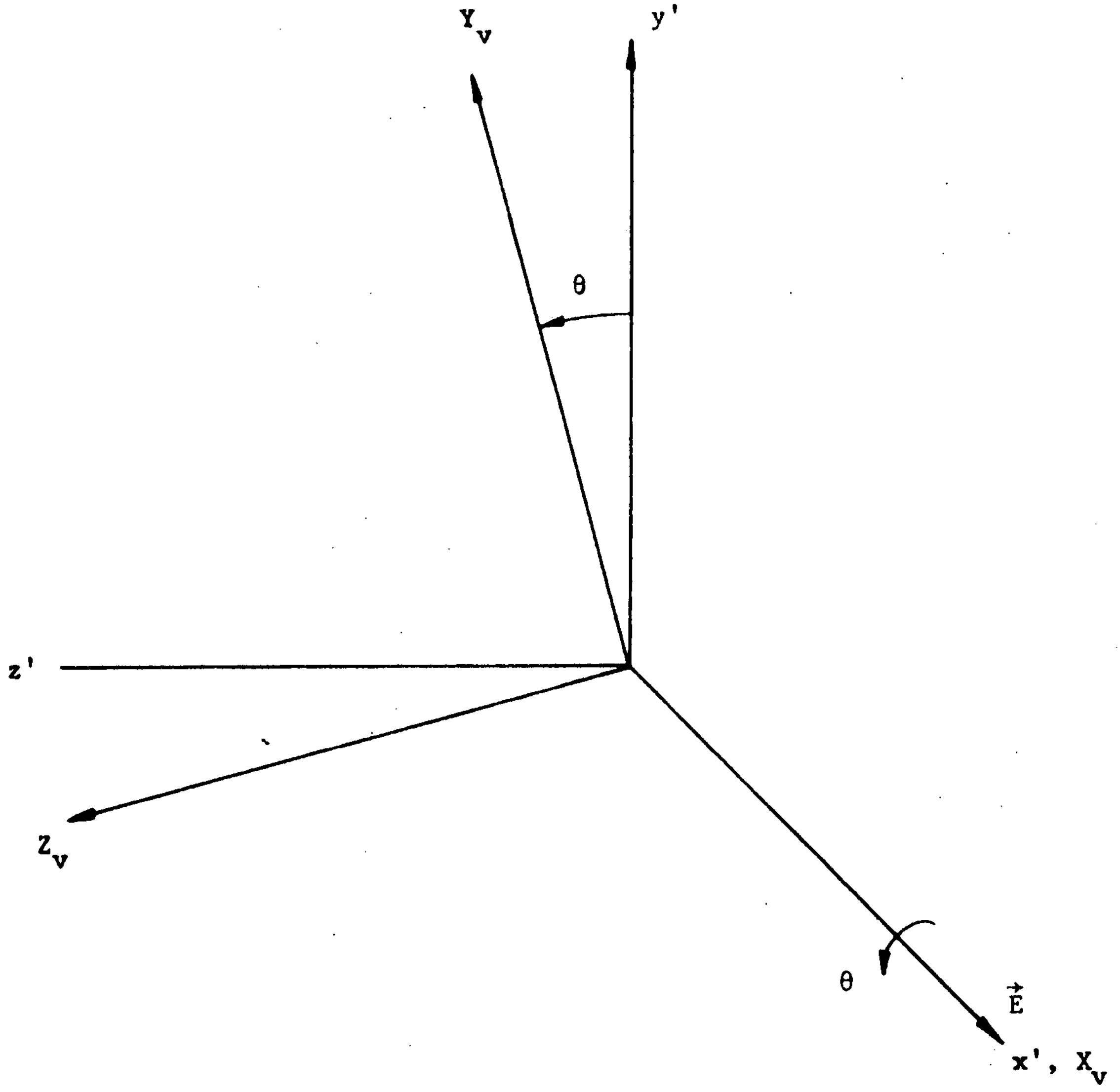

Figure B3-2. **Rotational Displacement θ of $X_vY_vZ_v$ From x'y'z'**

$$\begin{vmatrix} x' \\ y' \\ z' \end{vmatrix} = [\Phi_{R'\leftarrow v}] \begin{vmatrix} X_v \\ Y_v \\ Z_v \end{vmatrix} \tag{7}$$

where

$$[\Phi_{R'\leftarrow v}] = \begin{vmatrix} 1 & 0 & 0 \\ 0 & \cos\theta & -\sin\theta \\ 0 & \sin\theta & \cos\theta \end{vmatrix}$$

The new location of point P in the XYZ reference frame due to the rotational displacement θ about $\vec{E}$ is given by the following transformation.

$$\begin{vmatrix} X \\ Y \\ Z \end{vmatrix} = [\Phi_{R\leftarrow R'}][\Phi_{R'\leftarrow v}][\Phi_{R'\leftarrow R}] \begin{vmatrix} x \\ y \\ z \end{vmatrix} \tag{8}$$

Let

$$[\Phi] = [\Phi_{R\leftarrow R'}][\Phi_{R'\leftarrow v}][\Phi_{R'\leftarrow R}] \tag{9}$$

such that

$$\begin{vmatrix} X \\ Y \\ Z \end{vmatrix} = [\Phi] \begin{vmatrix} x \\ y \\ z \end{vmatrix} \tag{10}$$

The transformation $[\Phi]$ describes the new location of the rigid body with respect to the XYZ reference frame. $[\Phi]$ equals

$$[\Phi] = \begin{vmatrix} a_{11} & a_{12} & a_{13} \\ a_{21} & a_{22} & a_{23} \\ a_{31} & a_{32} & a_{33} \end{vmatrix} \tag{11}$$

where

$$a_{11}=1-2\sin^2(\tfrac{\theta}{2})\sin^2\alpha$$

$$a_{12}=2[\sin^2(\tfrac{\theta}{2})\cos\alpha\cos\beta-\sin(\tfrac{\theta}{2})\cos(\tfrac{\theta}{2})\cos\gamma]$$

$$a_{13}=2[\sin^2(\tfrac{\theta}{2})\cos\alpha\cos\gamma+\sin(\tfrac{\theta}{2})\cos(\tfrac{\theta}{2})\cos\beta]$$

$$a_{21}=2[\sin^2(\tfrac{\theta}{2})\cos\beta\cos\alpha+\sin(\tfrac{\theta}{2})\cos(\tfrac{\theta}{2})\cos\gamma]$$

$$a_{22}=1-2\sin^2(\tfrac{\theta}{2})\sin^2\beta$$

$$a_{23}=2[\sin^2(\tfrac{\theta}{2})\cos\beta\cos\gamma-\sin(\tfrac{\theta}{2})\cos(\tfrac{\theta}{2})\cos\alpha]$$

$$a_{31}=2[\sin^2(\tfrac{\theta}{2})\cos\gamma\cos\alpha-\sin(\tfrac{\theta}{2})\cos(\tfrac{\theta}{2})\cos\beta]$$

$$a_{32}=2[\sin^2(\tfrac{\theta}{2})\cos\gamma\cos\beta+\sin(\tfrac{\theta}{2})\cos(\tfrac{\theta}{2})\cos\alpha]$$

$$a_{33}=1-2\sin^2(\tfrac{\theta}{2})\sin^2\gamma$$

The relative orientation of the two coordinate systems, $X_vY_vZ_v$ with respect to XYZ, can be specified by either the transformation $[\Phi]$ or by the single axis rotation defined by $\vec{E}$ and θ that would align both coordinate frames. The following four parameters q_1, q_2, q_3, and q_4 can be used to specify $\vec{E}$ and θ.

$$q_1=\cos(\tfrac{\theta}{2}) \tag{12}$$

$$q_2=E_x\sin(\tfrac{\theta}{2}) \tag{13}$$

$$q_3=E_y\sin(\tfrac{\theta}{2}) \tag{14}$$

$$q_4=E_z\sin(\tfrac{\theta}{2}) \tag{15}$$

These four parameters are referred to as the four Euler rotational quaternions. E_x, E_y, and E_z are the directional cosines that define $\vec{E}$ ($E_x=\cos\alpha$, $E_y=\cos\beta$, $E_z=\cos\gamma$). These four quaternions q_1,

q_2, q_3, and q_4 are often written in the form of a complex number $\vec{q}$.

$$\vec{q}=q_1+q_2\hat{i}+q_3\hat{j}+q_4\hat{k} \tag{16}$$

where $\hat{i}$, $\hat{j}$, and $\hat{k}$ are the unit vectors along the X, Y, and Z reference axes, respectively.

These four quaternions q_1, q_2, q_3, and q_4 are sufficient to determine completely the transformation $[\Phi]$. It can be shown that the nine components of $[\Phi]$ a_{11}, a_{12}, ..., a_{33} can be written in terms of these four quaternions.

$$a_{11}=q_1^2+q_2^2-q_3^2-q_4^2 \tag{17}$$

$$a_{12}=2(q_2q_3-q_1q_4) \tag{18}$$

$$a_{13}=2(q_2q_4+q_1q_3) \tag{19}$$

$$a_{21}=2(q_2q_3+q_1q_4) \tag{20}$$

$$a_{22}=q_1^2-q_2^2+q_3^2-q_4^2 \tag{21}$$

$$a_{23}=2(q_3q_4-q_1q_2) \tag{22}$$

$$a_{31}=2(q_2q_4-q_1q_3) \tag{23}$$

$$a_{32}=2(q_1q_2+q_3q_4) \tag{24}$$

$$a_{33}=q_1^2-q_2^2-q_3^2+q_4^2 \tag{25}$$

Since the transformation $[\Phi]$ completely describes the location of the rigid body shown in figure B3-1 with respect to the XYZ reference frame and since $[\Phi]$ can also be written in terms of q_1, q_2, q_3, and q_4, these four quaternions like $[\Phi]$ also completely specify the orientation of the $X_vY_vZ_v$ coordinate frame.

The advantages of using quaternions instead of a transformation like $[\Phi]$ for determining the attitude of a spacecraft are (1) only four parameters instead of the nine components of $[\Phi]$, a_{11},

a_{12}, ..., a_{33}, must be determined, (2) the quaternions can be readily computed from sensed body rates as will be shown in the next section, and (3) the form of the quaternions can be readily used by the spacecraft's attitude control system.

B3.1.2. Strapdown Equations - The strapdown equations are a set of equations that are used to digitally compute the four quaternions by using sensed body rates. In the case of a spacecraft, these body rates ω_x, ω_y, and ω_z are normally sensed and measured by at least three rate gyros rigidly mounted to the vehicle.

Assume that the orientation of the rigid body shown in figure B3-3 is due to the Euler rotations ψ, η, and ϕ. The order of these rotations is (1) an angular rotation ψ about the Z axis, (2) a η rotation about the displaced X axis, and (3) a ϕ rotation about the displaced Z axis. The ψ, η, and ϕ Euler rotations correspond to the following transformations $[\Phi]_\psi$, $[\Phi]_\eta$, and $[\Phi]_\phi$, respectively.

$$[\Phi]_\psi = \begin{vmatrix} \cos\psi & \sin\psi & 0 \\ -\sin\psi & \cos\psi & 0 \\ 0 & 0 & 1 \end{vmatrix} \tag{26}$$

$$[\Phi]_\eta = \begin{vmatrix} 1 & 0 & 0 \\ 0 & \cos\eta & \sin\eta \\ 0 & -\sin\eta & \cos\eta \end{vmatrix} \tag{27}$$

$$[\Phi]_\phi = \begin{vmatrix} \cos\phi & \sin\phi & 0 \\ -\sin\phi & \cos\phi & 0 \\ 0 & 0 & 1 \end{vmatrix} \tag{28}$$

The transformation from the reference coordinate system XYZ to the rigid body coordinate frame $X_vY_vZ_v$ equals

$$\begin{vmatrix} X_v \\ Y_v \\ Z_v \end{vmatrix} = [\Phi]_\phi [\Phi]_\eta [\Phi]_\psi \begin{vmatrix} X \\ Y \\ Z \end{vmatrix} \tag{29}$$

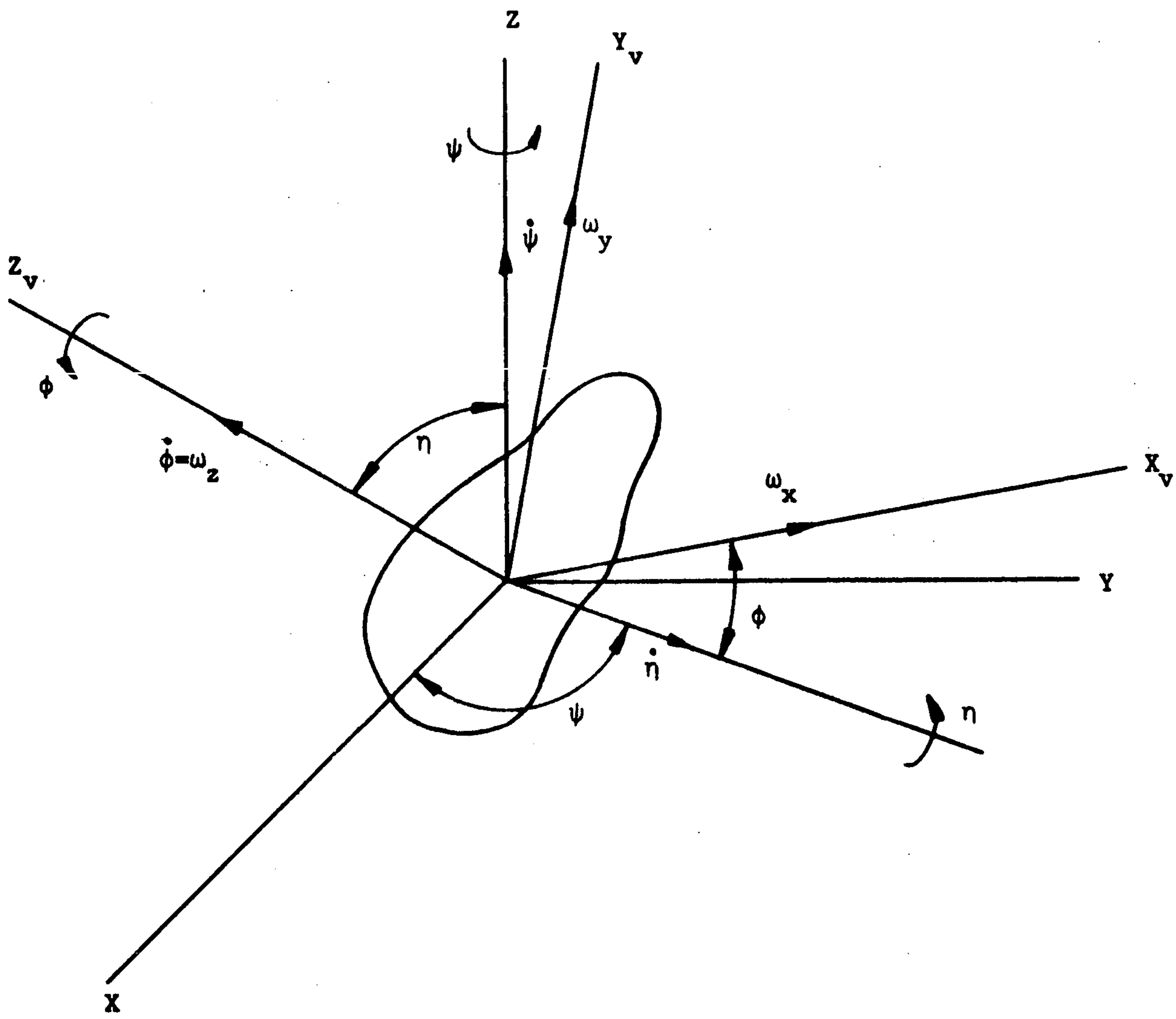

Figure B3-3. **Euler Rotations ψ, η, ϕ**

The rigid body rates ω_x, ω_y, and ω_z can be written in terms of the three Euler rates $\dot{\psi}$, $\dot{\eta}$, and $\dot{\phi}$ as follows

$$\begin{vmatrix} \omega_x \\ \omega_y \\ \omega_z \end{vmatrix} = [\Phi]_\phi [\Phi]_\eta [\Phi]_\psi \begin{vmatrix} 0 \\ 0 \\ \dot{\psi} \end{vmatrix} + [\Phi]_\phi [\Phi]_\eta \begin{vmatrix} \dot{\eta} \\ 0 \\ 0 \end{vmatrix} + [\Phi]_\phi \begin{vmatrix} 0 \\ 0 \\ \dot{\phi} \end{vmatrix} \tag{30}$$

Simplifing the above expression, ω_x, ω_y, and ω_z equal

$$\begin{vmatrix} \omega_x \\ \omega_y \\ \omega_z \end{vmatrix} = [\Phi]_{\dot{\psi}\dot{\eta}\dot{\phi}} \begin{vmatrix} \dot{\psi} \\ \dot{\eta} \\ \dot{\phi} \end{vmatrix} \tag{31}$$

where

$$[\Phi]_{\dot{\psi}\dot{\eta}\dot{\phi}} = \begin{vmatrix} \sin\eta\sin\phi & \cos\phi & 0 \\ \sin\eta\cos\phi & -\sin\phi & 0 \\ \cos\eta & 0 & 1 \end{vmatrix}$$

The Euler rates $\dot{\psi}$, $\dot{\eta}$, and $\dot{\phi}$ as a function of the body rates ω_x, ω_y, and ω_z equal

$$\begin{vmatrix} \dot{\psi} \\ \dot{\eta} \\ \dot{\phi} \end{vmatrix} = [\Phi]^{-1}_{\dot{\psi}\dot{\eta}\dot{\phi}} \begin{vmatrix} \omega_x \\ \omega_y \\ \omega_z \end{vmatrix} \tag{32}$$

where

$$[\Phi]^{-1}_{\dot\psi\dot\eta\dot\phi}=\begin{vmatrix} \frac{\sin\phi}{\sin\eta} & \frac{\cos\phi}{\sin\eta} & 0 \\ \cos\phi & -\sin\phi & 0 \\ -\frac{\sin\phi\cos\eta}{\sin\eta} & -\frac{\cos\phi\cos\eta}{\sin\eta} & 1 \end{vmatrix}$$

$[\Phi]^{-1}_{\dot\psi\dot\eta\dot\phi}$ is the inverse of $[\Phi]_{\dot\psi\dot\eta\dot\phi}$.

The three Euler rotations ψ, η, and ϕ can be represented by three complex quaternions. The following quaternions $\vec{q}_\psi$, $\vec{q}_\eta$, and $\vec{q}_\phi$ correspond to the ψ, η, and ϕ Euler rotations, respectively.

$$\vec{q}_\psi=\cos\frac{\psi}{2}+\sin\frac{\psi}{2}\hat{k} \tag{33}$$

$$\vec{q}_\eta=\cos\frac{\eta}{2}+\sin\frac{\eta}{2}\hat{i} \tag{34}$$

$$\vec{q}_\phi=\cos\frac{\phi}{2}+\sin\frac{\phi}{2}\hat{k} \tag{35}$$

The quaternion $\vec{q}$ that describes the final orientation of the rigid body as the results of the three Euler rotations ψ, η, and ϕ can be computed by performing the following quaternion multiplication.

$$\vec{q}=q_1+q_2\hat{i}+q_3\hat{j}+q_4\hat{k}=\vec{q}_\psi\vec{q}_\eta\vec{q}_\phi$$

$$=(\cos\frac{\psi}{2}+\sin\frac{\psi}{2}\hat{k})(\cos\frac{\eta}{2}+\sin\frac{\eta}{2}\hat{i})(\cos\frac{\phi}{2}+\sin\frac{\phi}{2}\hat{k}) \tag{36}$$

Note that

$$\hat{i}^2=\hat{j}^2=\hat{k}^2=-1$$

$$\hat{i}\hat{j}=-\hat{j}\hat{i}=\hat{k}$$

$$\hat{j}\hat{k}=-\hat{k}\hat{j}=\hat{i}$$

$$\hat{k}\hat{i}=-\hat{i}\hat{k}=\hat{j}$$

The components of $\vec{q}$ equal

$$q_1=\cos\frac{\psi}{2}\cos\frac{\eta}{2}\cos\frac{\phi}{2}-\sin\frac{\psi}{2}\cos\frac{\eta}{2}\sin\frac{\phi}{2} \tag{37}$$

$$q_2 = \sin\frac{\psi}{2}\sin\frac{\eta}{2}\sin\frac{\phi}{2} + \cos\frac{\psi}{2}\sin\frac{\eta}{2}\cos\frac{\phi}{2} \tag{38}$$

$$q_3 = \sin\frac{\psi}{2}\sin\frac{\eta}{2}\cos\frac{\phi}{2} - \cos\frac{\psi}{2}\sin\frac{\eta}{2}\sin\frac{\phi}{2} \tag{39}$$

$$q_4 = \sin\frac{\psi}{2}\cos\frac{\eta}{2}\cos\frac{\phi}{2} + \cos\frac{\psi}{2}\cos\frac{\eta}{2}\sin\frac{\phi}{2} \tag{40}$$

The time derivatives of the above expressions for q_1, q_2, q_3, and q_4 can be written as follows:

$$\dot{\vec{q}} = \begin{vmatrix} \dot{q}_1 \\ \dot{q}_2 \\ \dot{q}_3 \\ \dot{q}_4 \end{vmatrix} = \frac{1}{2} \begin{vmatrix} a_{1\dot{\psi}} & a_{1\dot{\theta}} & a_{1\dot{\phi}} \\ a_{2\dot{\psi}} & a_{2\dot{\theta}} & a_{2\dot{\phi}} \\ a_{3\dot{\psi}} & a_{3\dot{\theta}} & a_{3\dot{\phi}} \\ a_{4\dot{\psi}} & a_{4\dot{\theta}} & a_{4\dot{\phi}} \end{vmatrix} \begin{vmatrix} \dot{\psi} \\ \dot{\eta} \\ \dot{\phi} \end{vmatrix} \tag{41}$$

where

$$a_{1\dot{\psi}} = -\sin\frac{\psi}{2}\cos\frac{\eta}{2}\cos\frac{\phi}{2} - \cos\frac{\psi}{2}\cos\frac{\eta}{2}\sin\frac{\phi}{2}$$

$$a_{1\dot{\eta}} = \sin\frac{\psi}{2}\sin\frac{\eta}{2}\sin\frac{\phi}{2} - \cos\frac{\psi}{2}\sin\frac{\eta}{2}\cos\frac{\phi}{2}$$

$$a_{1\dot{\phi}} = -\cos\frac{\psi}{2}\cos\frac{\eta}{2}\sin\frac{\phi}{2} - \sin\frac{\psi}{2}\cos\frac{\eta}{2}\cos\frac{\phi}{2}$$

$$a_{2\dot{\psi}} = \cos\frac{\psi}{2}\sin\frac{\eta}{2}\sin\frac{\phi}{2} - \sin\frac{\psi}{2}\sin\frac{\eta}{2}\cos\frac{\phi}{2}$$

$$a_{2\dot{\eta}} = \sin\frac{\psi}{2}\cos\frac{\eta}{2}\sin\frac{\phi}{2} + \cos\frac{\psi}{2}\cos\frac{\eta}{2}\cos\frac{\phi}{2}$$

$$a_{2\dot{\phi}} = \sin\frac{\psi}{2}\sin\frac{\eta}{2}\cos\frac{\phi}{2} - \cos\frac{\psi}{2}\sin\frac{\eta}{2}\sin\frac{\phi}{2}$$

$$a_{3\dot{\psi}} = \cos\frac{\psi}{2}\sin\frac{\eta}{2}\cos\frac{\phi}{2} + \sin\frac{\psi}{2}\sin\frac{\eta}{2}\sin\frac{\phi}{2}$$

$$a_{3\dot{\eta}} = \sin\frac{\psi}{2}\cos\frac{\eta}{2}\cos\frac{\phi}{2} - \cos\frac{\psi}{2}\cos\frac{\eta}{2}\sin\frac{\phi}{2}$$

$$a_{3\dot{\phi}} = -\sin\frac{\psi}{2}\sin\frac{\eta}{2}\sin\frac{\phi}{2} - \cos\frac{\psi}{2}\sin\frac{\eta}{2}\cos\frac{\phi}{2}$$

$$a_{4\dot{\psi}} = \cos\frac{\psi}{2}\cos\frac{\eta}{2}\cos\frac{\phi}{2} - \sin\frac{\psi}{2}\cos\frac{\eta}{2}\sin\frac{\phi}{2}$$

$$a_{4\dot{\eta}} = -\sin\frac{\psi}{2}\sin\frac{\eta}{2}\cos\frac{\phi}{2} - \cos\frac{\psi}{2}\sin\frac{\eta}{2}\sin\frac{\phi}{2}$$

$$a_{4\dot{\phi}} = \cos\frac{\psi}{2}\cos\frac{\eta}{2}\cos\frac{\phi}{2} - \sin\frac{\psi}{2}\cos\frac{\eta}{2}\sin\frac{\phi}{2}$$

By substituting equations 32 into 41 and then simplifing, $\dot{\vec{q}}$ in terms of the body rates ω_x, ω_y, and ω_z equals

$$\dot{\vec{q}} = \begin{vmatrix} \dot{q}_1 \\ \dot{q}_2 \\ \dot{q}_3 \\ \dot{q}_4 \end{vmatrix} = \frac{1}{2} \begin{vmatrix} -q_2 & -q_3 & -q_4 \\ q_1 & -q_4 & q_3 \\ q_4 & q_1 & -q_2 \\ -q_3 & q_2 & q_1 \end{vmatrix} \begin{vmatrix} \omega_x \\ \omega_y \\ \omega_z \end{vmatrix} \tag{42}$$

Using the above relationship, the quaternion rate $\dot{\vec{q}}$ is computed from the sensed body rates ω_x, ω_y, and ω_z. The computed rates $\dot{\vec{q}}$ is then integrated using a numerical integration technique to compute $\vec{q}$. Equation 42 and the equations used to perform this numerical integration are referred to as the quaternion strapdown equations. Assume that the numerical integration technique selected is trapezoidal integration. The resulting expressions for q_1, q_2, q_3, and q_4 are:

$$q_1 = q_{1P} + 0.5[\dot{q}_{1P} + \dot{q}_1]\Delta t \tag{43}$$

$$q_2 = q_{2P} + 0.5[\dot{q}_{2P} + \dot{q}_2]\Delta t \tag{44}$$

$$q_3 = q_{3P} + 0.5[\dot{q}_{3P} + \dot{q}_3]\Delta t \tag{45}$$

$$q_4 = q_{4P} + 0.5[\dot{q}_{4P} + \dot{q}_4]\Delta t \tag{46}$$

q_{1P}, q_{2P}, q_{3P}, and q_{4P} are the previously computed quaternions while $\dot{q}_{1P}$, $\dot{q}_{2P}$, $\dot{q}_{3P}$, and $\dot{q}_{4P}$ are their corresponding previously computed quaternion rates. Δt is the sample period in seconds between numerical integrations.

The numerical integration of $\dot{\vec{q}}$ to obtain $\vec{q}$ must be initialized and occasionally updated to correct for computational errors and the accumulative effects of errors such as rate gyro drift contained in the measured body rates ω_x, ω_y, and ω_z. To perform this initialization or update procedure, the transformation $[\Phi]$

from reference space to body space must be determined. This update procedure is normally performed using star tracker attached to the spacecraft. The star trackers are used to measure in vehicle coordinates the location of two reference stars whose coordinates in the XYZ reference frame are known.

Assume that the locations of two reference stars in the XYZ reference frame are given by the two unit vectors, $\vec{S}_1$ and $\vec{S}_2$ and that their corresponding vehicle coordinates are described by the unit vectors $\vec{S}_1'$ and $\vec{S}_2'$, respectively. In order to compute $[\Phi]$, two additional unit vectors $\vec{S}_{12}$ and $\vec{S}_{12}'$ must be computed. $\vec{S}_{12}$ and $\vec{S}_{12}'$ are computed from $\vec{S}_1$ and $\vec{S}_2$ and $\vec{S}_1'$ and $\vec{S}_2'$, respectively.

$$\vec{S}_{12}=\frac{\vec{S}_1 x \vec{S}_2}{||\vec{S}_1 x \vec{S}_2||} \tag{47}$$

$$\vec{S}_{12}'=\frac{\vec{S}_1' x \vec{S}_2'}{||\vec{S}_1' x \vec{S}_2'||} \tag{48}$$

$||\vec{A}||$ represents the norm of the enclosed vector $\vec{A}$. $\vec{S}_{12}$ and $\vec{S}_{12}'$ are unit vectors that are perpendicular to the planes formed by $\vec{S}_1$ and $\vec{S}_2$ and $\vec{S}_1'$ and $\vec{S}_2'$, respectively. These six unit vectors $\vec{S}_1$, $\vec{S}_2$, $\vec{S}_{12}$, $\vec{S}_1'$, $\vec{S}_2'$, and $\vec{S}_{12}'$ completely specify the transformation $[\Phi]$. To compute $[\Phi]$, the following relationships must be satisfied.

$$\vec{S}_1=[\Phi]\vec{S}_1' \tag{49}$$

$$\vec{S}_2=[\Phi]\vec{S}_2' \tag{50}$$

$$\vec{S}_{12}=[\Phi]\vec{S}_{12}' \tag{51}$$

where

$$[\Phi]=\begin{vmatrix} a_{11} & a_{12} & a_{13} \\ a_{21} & a_{22} & a_{23} \\ a_{31} & a_{32} & a_{33} \end{vmatrix}$$

Assume that the unit vectors $\vec{S}_1$, $\vec{S}_1'$, $\vec{S}_2$, $\vec{S}_2'$, $\vec{S}_{12}$, and $\vec{S}_{12}'$ are

$$\vec{S}_1 = \begin{vmatrix} c_{11} \\ c_{12} \\ c_{13} \end{vmatrix} \qquad \vec{S}_1' = \begin{vmatrix} c_{21} \\ c_{22} \\ c_{23} \end{vmatrix}$$

$$\vec{S}_2 = \begin{vmatrix} d_{11} \\ d_{12} \\ d_{13} \end{vmatrix} \qquad \vec{S}_2' = \begin{vmatrix} d_{21} \\ d_{22} \\ d_{23} \end{vmatrix}$$

$$\vec{S}_{12} = \begin{vmatrix} f_{11} \\ f_{12} \\ f_{13} \end{vmatrix} \qquad \vec{S}_{12}' = \begin{vmatrix} f_{21} \\ f_{22} \\ f_{23} \end{vmatrix}$$

Substitute the above vectors into equations 49 through 51.

$$\vec{S}_1 = [\Phi]\vec{S}_1' = \begin{vmatrix} c_{11} \\ c_{12} \\ c_{13} \end{vmatrix} = \begin{vmatrix} a_{11} & a_{12} & a_{13} \\ a_{21} & a_{22} & a_{23} \\ a_{31} & a_{32} & a_{33} \end{vmatrix} \begin{vmatrix} c_{21} \\ c_{22} \\ c_{23} \end{vmatrix} \tag{52}$$

$$\vec{S}_2 = [\Phi]\vec{S}_2' = \begin{vmatrix} d_{11} \\ d_{12} \\ d_{13} \end{vmatrix} = \begin{vmatrix} a_{11} & a_{12} & a_{13} \\ a_{21} & a_{22} & a_{23} \\ a_{31} & a_{32} & a_{33} \end{vmatrix} \begin{vmatrix} d_{21} \\ d_{22} \\ d_{23} \end{vmatrix} \tag{53}$$

$$\vec{S}_{12} = [\Phi]\vec{S}_{12}' = \begin{vmatrix} f_{11} \\ f_{12} \\ f_{13} \end{vmatrix} = \begin{vmatrix} a_{11} & a_{12} & a_{13} \\ a_{21} & a_{22} & a_{23} \\ a_{31} & a_{32} & a_{33} \end{vmatrix} \begin{vmatrix} f_{21} \\ f_{22} \\ f_{23} \end{vmatrix} \tag{54}$$

Equations 52 through 54 can be rearranged into the following expressions.

$$\begin{vmatrix} c_{11} \\ d_{11} \\ f_{11} \end{vmatrix} = \begin{vmatrix} c_{21} & c_{22} & c_{23} \\ d_{21} & d_{22} & d_{23} \\ f_{21} & f_{22} & f_{23} \end{vmatrix} \begin{vmatrix} a_{11} \\ a_{12} \\ a_{13} \end{vmatrix} \tag{55}$$

$$\begin{vmatrix} c_{12} \\ d_{12} \\ f_{12} \end{vmatrix} = \begin{vmatrix} c_{21} & c_{22} & c_{23} \\ d_{21} & d_{22} & d_{23} \\ f_{21} & f_{22} & f_{23} \end{vmatrix} \begin{vmatrix} a_{21} \\ a_{22} \\ a_{23} \end{vmatrix} \tag{56}$$

$$\begin{vmatrix} c_{13} \\ d_{13} \\ f_{13} \end{vmatrix} = \begin{vmatrix} c_{21} & c_{22} & c_{23} \\ d_{21} & d_{22} & d_{23} \\ f_{21} & f_{22} & f_{23} \end{vmatrix} \begin{vmatrix} a_{31} \\ a_{32} \\ a_{33} \end{vmatrix} \tag{57}$$

Applying Cramer's rule for solving simultaneous algebraic equations, the components of $[\Phi]$, a_{11}, a_{12}, ..., a_{33}, can be computed using equations 55 through 57. Note that the 3 by 3 matrix appearing in each of these equations are identical. The symbol Δ is used to denote the determinant of this matrix. Δ equals

$$\Delta = \det \begin{vmatrix} c_{21} & c_{22} & c_{23} \\ d_{21} & d_{22} & d_{23} \\ f_{21} & f_{22} & f_{23} \end{vmatrix} = c_{21}(d_{22}f_{23} - d_{23}f_{22})$$

$$+ c_{22}(d_{23}f_{23} - d_{21}f_{23}) + c_{23}(d_{21}f_{22} - d_{22}f_{21}) \tag{58}$$

The nine components of $[\Phi]$ in terms of the components of $\vec{S}_1$, $\vec{S}_2$, $\vec{S}_{12}$, $\vec{S}_1{}'$, $\vec{S}_2{}'$, and $\vec{S}_{12}{}'$ equal

$$a_{11}=\frac{\det\begin{vmatrix} c_{11} & c_{22} & c_{23} \\ d_{11} & d_{22} & d_{23} \\ f_{11} & f_{22} & f_{23}\end{vmatrix}}{\Delta}=[c_{11}(d_{22}f_{23}-d_{23}f_{22})$$

$$+c_{22}(d_{23}f_{11}-d_{11}f_{23})+c_{23}(d_{11}f_{22}-d_{22}f_{11})]/\Delta \tag{59}$$

$$a_{12}=\frac{\det\begin{vmatrix} c_{21} & c_{11} & c_{23} \\ d_{21} & d_{11} & d_{23} \\ f_{21} & f_{11} & f_{23}\end{vmatrix}}{\Delta}=[c_{21}(d_{11}f_{23}-d_{23}f_{11})$$

$$+c_{11}(d_{23}f_{21}-d_{21}f_{23})+c_{23}(d_{21}f_{11}-d_{11}f_{21})]/\Delta \tag{60}$$

$$a_{13}=\frac{\det\begin{vmatrix} c_{21} & c_{22} & c_{11} \\ d_{21} & d_{22} & d_{11} \\ f_{21} & f_{22} & f_{11}\end{vmatrix}}{\Delta}=[c_{21}(d_{22}f_{11}-d_{11}f_{22})$$

$$+c_{22}(d_{11}f_{21}-d_{21}f_{11})+c_{11}(d_{21}f_{22}-d_{22}f_{21})]/\Delta \tag{61}$$

$$a_{21}=\frac{\det\begin{vmatrix} c_{12} & c_{22} & c_{23} \\ d_{12} & d_{22} & d_{23} \\ f_{12} & f_{22} & f_{23}\end{vmatrix}}{\Delta}=[c_{12}(d_{22}f_{23}-d_{23}f_{22})$$

$$+c_{22}(d_{23}f_{12}-d_{12}f_{23})+c_{23}(d_{12}f_{22}-d_{22}f_{12})]/\Delta \tag{62}$$

$$a_{22}=\frac{\det\begin{vmatrix} c_{21} & c_{12} & c_{23} \\ d_{21} & d_{12} & d_{23} \\ f_{21} & f_{12} & f_{23}\end{vmatrix}}{\Delta}=[c_{21}(d_{12}f_{23}-d_{23}f_{12})$$

$$+c_{12}(d_{23}f_{21}-d_{21}f_{23})+c_{23}(d_{21}f_{12}-d_{12}f_{21})]/\Delta \tag{63}$$

$$a_{23}=\frac{\det\begin{vmatrix} c_{21} & c_{22} & c_{12} \\ d_{21} & d_{22} & d_{12} \\ f_{21} & f_{22} & f_{12} \end{vmatrix}}{\Delta}=[c_{21}(d_{22}f_{12}-d_{12}f_{22})$$

$$+c_{22}(d_{12}f_{21}-d_{21}f_{12})+c_{12}(d_{21}f_{22}-d_{22}f_{21})]/\Delta \qquad (64)$$

$$a_{31}=\frac{\det\begin{vmatrix} c_{13} & c_{22} & c_{23} \\ d_{13} & d_{22} & d_{23} \\ f_{13} & f_{22} & f_{23} \end{vmatrix}}{\Delta}=[c_{13}(d_{22}f_{23}-d_{23}f_{22})$$

$$+c_{22}(d_{23}f_{13}-d_{13}f_{23})+c_{23}(d_{13}f_{22}-d_{22}f_{13})]/\Delta \qquad (65)$$

$$a_{32}=\frac{\det\begin{vmatrix} c_{21} & c_{13} & c_{23} \\ d_{21} & d_{13} & d_{23} \\ f_{21} & f_{13} & f_{23} \end{vmatrix}}{\Delta}=[c_{21}(d_{13}f_{23}-d_{23}f_{13})$$

$$+c_{13}(d_{23}f_{21}-d_{21}f_{23})+c_{23}(d_{21}f_{13}-d_{13}f_{21})]/\Delta \qquad (66)$$

$$a_{33}=\frac{\det\begin{vmatrix} c_{21} & c_{22} & c_{13} \\ d_{21} & d_{22} & d_{13} \\ f_{21} & f_{22} & f_{13} \end{vmatrix}}{\Delta}=[c_{21}(d_{22}f_{13}-d_{13}f_{22})$$

$$+c_{22}(d_{13}f_{21}-d_{21}f_{13})+c_{13}(d_{21}f_{22}-d_{22}f_{21})]/\Delta \qquad (67)$$

The four quaternions q_1, q_2, q_3, and q_4 can be computed using the components of $[\Phi]$, a_{11}, a_{12}, ..., a_{33} defined in equations 59 through 67. In order to compute q_1, q_2, q_3, and q_4, one needs only to determine the eigenaxis $\vec{E}$ and the rotational displacement

θ about this axis as specified by $[\Phi]$. θ can be computed using the unique property that the trace of $[\Phi]$ equals $1+2\cos\theta$.

$$\text{trace of } [\Phi]=\sum_{i=1}^{3} a_{ii}=1+2\cos\theta \tag{68}$$

θ equals

$$\theta=\cos^{-1}[0.5(a_{11}+a_{22}+a_{33}-1)] \tag{69}$$

The eigenaxis $\vec{E}$ is defined by the three direction cosines, $\cos\alpha$, $\cos\beta$, and $\cos\gamma$. These three direction cosines are designated E_x, E_y, and E_z, respectively. Using equations 17 through 25, it can be shown that E_x, E_y, and E_z equal

$$E_x=\cos\alpha=\frac{a_{32}-a_{23}}{4\cos(\frac{\theta}{2})\sin(\frac{\theta}{2})} \tag{70}$$

$$E_y=\cos\beta=\frac{a_{13}-a_{31}}{4\cos(\frac{\theta}{2})\sin(\frac{\theta}{2})} \tag{71}$$

$$E_z=\cos\gamma=\frac{a_{21}-a_{12}}{4\cos(\frac{\theta}{2})\sin(\frac{\theta}{2})} \tag{72}$$

Using the results of equations 69 through 72, the quaternions q_1, q_2, q_3, and q_4 as a function of the components of $[\Phi]$ equal

$$q_1=\cos(\frac{\theta}{2}) \quad \text{where } \theta=\cos^{-1}[0.5(a_{11}+a_{22}+a_{33}-1)] \tag{73}$$

$$q_2=E_x\sin(\frac{\theta}{2})=\frac{a_{32}-a_{23}}{4q_1} \tag{74}$$

$$q_3=E_y\sin(\frac{\theta}{2})=\frac{a_{13}-a_{31}}{4q_1} \tag{75}$$

$$q_4=E_z\sin(\frac{\theta}{2})=\frac{a_{21}-a_{12}}{4q_1} \tag{76}$$

The quaternion strapdown equations are initialized or updated by substituting the above values of q_1 through q_4 into equation 42 and for those of q_{1P}, q_{2P}, q_{3P}, and q_{4P}, respectively. The affected equations are

$$\begin{vmatrix} \dot{q}_1 \\ \dot{q}_2 \\ \dot{q}_3 \\ \dot{q}_4 \end{vmatrix} = \frac{1}{2} \begin{vmatrix} -q_2 & -q_3 & -q_4 \\ q_1 & -q_4 & q_3 \\ q_4 & q_1 & -q_2 \\ -q_3 & q_2 & q_1 \end{vmatrix} \begin{vmatrix} \omega_x \\ \omega_y \\ \omega_z \end{vmatrix} \tag{42}$$

$$q_1 = q_{1P} + 0.5[\dot{q}_{1P} + \dot{q}_1]\Delta t \tag{43}$$

$$q_2 = q_{2P} + 0.5[\dot{q}_{2P} + \dot{q}_2]\Delta t \tag{44}$$

$$q_3 = q_{3P} + 0.5[\dot{q}_{3P} + \dot{q}_3]\Delta t \tag{45}$$

$$q_4 = q_{4P} + 0.5[\dot{q}_{4P} + \dot{q}_4]\Delta t \tag{46}$$

The above equations 42 through 46 are the quaternion strapdown equations.

B3.2. DETERMINATION OF THREE AXIS ATTITUDE ERROR INFORMATION BY TRACKING TWO GUIDE STARS

The three axis attitude error information needed to stabilize a telescope about its three control axes can be determined by tracking two guide stars. Tracking a single guide star provides only two axis attitude error information, azimuth and elevation. By tracking a second guide star, its roll axis attitude error is also specified.

Assume these are two stars located in the telescope field of view as shown in figure B3-4. Let one star be designated star 1 and the other one, star 2. At time t equal to zero (t=0), the locations of stars 1 and 2 are described in telescope coordinates by the unit vectors $\overline{S}_1$ and $\overline{S}_2$, respectively. Assume that at a later time t_1, the stars 1 and 2 appear to have moved to new locations corresponding to unit vectors $\overline{S}_1'$ and $\overline{S}_2'$, respectively. $\overline{S}_1$, $\overline{S}_2$, $\overline{S}_1'$, and $\overline{S}_2'$ are signals derived from the telescope sensors. Let $\overline{S}_1$ and $\overline{S}_2$, the locations of the two stars at t=0, be used as a reference. The rotational displacement of the telescope is then computed with respect to the telescope attitude described by $\overline{S}_1$ and $\overline{S}_2$. In order to determine the rotational displacement of the telescope at time t_1, two other unit vectors $\overline{S}_{12}$ and $\overline{S}_{12}'$ are needed. $\overline{S}_{12}$ and $\overline{S}_{12}'$ are unit vecotrs corresponding to the cross products of $\overline{S}_1$ and $\overline{S}_2$ and $\overline{S}_1'$ and $\overline{S}_2'$, respectively. $\overline{S}_{12}$ and $\overline{S}_{12}'$ equal

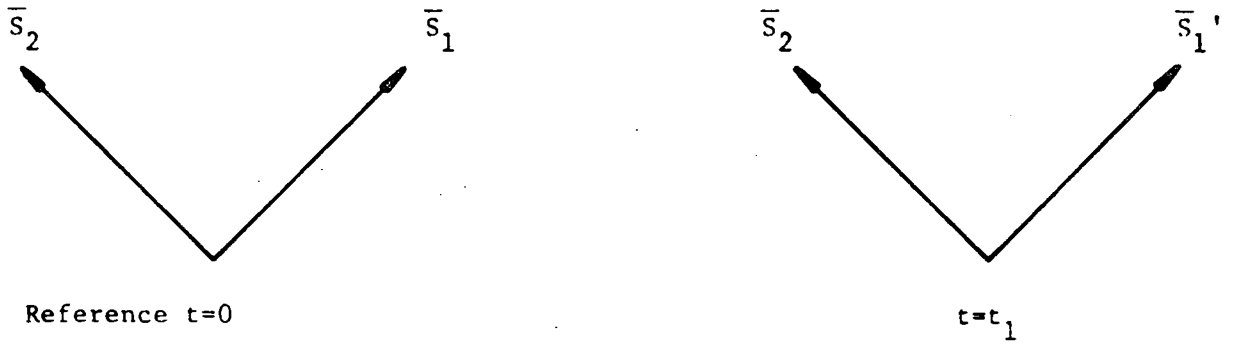

Figure B3-4. Sketch of Locations of Two Guide Stars $\bar{S}_1$ and $\bar{S}_2$ at $t=0$ and $t=t_1$.

$$\bar{S}_{12} = \frac{\bar{S}_1 x \bar{S}_2}{||\bar{S}_1 x \bar{S}_2||} \tag{77}$$

$$\bar{S}_{12}' = \frac{\bar{S}_1' x \bar{S}_2'}{||\bar{S}_1' x \bar{S}_2'||} \tag{78}$$

where $||\bar{S}||$ equals the norm of the vector $\bar{S}$ enclosed.

The apparent rotational motion of the stars can be described by a transformation [T] which is completely defined by the six vectors $\bar{S}_1$, $\bar{S}_2$, $\bar{S}_{12}$, $\bar{S}_1'$, $\bar{S}_2'$, and $\bar{S}_{12}'$. To compute [T], the following conditions must be satisfied.

$$\bar{S}_1' = [T]\bar{S}_1 \tag{79}$$

$$\bar{S}_2' = [T]\bar{S}_2 \tag{80}$$

$$\bar{S}_{12}' = [T]\bar{S}_{12} \tag{81}$$

where

$$[T] = \begin{vmatrix} a_{11} & a_{12} & a_{13} \\ a_{21} & a_{22} & a_{23} \\ a_{31} & a_{32} & a_{33} \end{vmatrix}$$

Assume that the unit vectors $\bar{S}_1$, $\bar{S}_1'$, $\bar{S}_2$, $\bar{S}_2'$, $\bar{S}_{12}$, and $\bar{S}_{12}'$ equal

$$\bar{S}_1 = \begin{vmatrix} c_{11} \\ c_{12} \\ c_{13} \end{vmatrix} \qquad \bar{S}_1' = \begin{vmatrix} c_{21} \\ c_{22} \\ c_{23} \end{vmatrix}$$

$$\bar{S}_2 = \begin{vmatrix} d_{11} \\ d_{12} \\ d_{13} \end{vmatrix} \qquad \bar{S}_2' = \begin{vmatrix} d_{21} \\ d_{22} \\ d_{23} \end{vmatrix}$$

$$\overline{S}_{12} = \begin{vmatrix} f_{11} \\ f_{12} \\ f_{13} \end{vmatrix} \qquad \overline{S}_{12}' = \begin{vmatrix} f_{21} \\ f_{22} \\ f_{23} \end{vmatrix}$$

Substitute the above vectors into equations 79 thru 81.

$$\overline{S}_1' = [T]\overline{S}_1 = \begin{vmatrix} c_{21} \\ c_{22} \\ c_{23} \end{vmatrix} = \begin{vmatrix} a_{11} & a_{12} & a_{13} \\ a_{21} & a_{22} & a_{23} \\ a_{31} & a_{32} & a_{33} \end{vmatrix} \begin{vmatrix} c_{11} \\ c_{12} \\ c_{13} \end{vmatrix} \tag{82}$$

$$\overline{S}_2' = [T]\overline{S}_2 = \begin{vmatrix} d_{21} \\ d_{22} \\ d_{23} \end{vmatrix} = \begin{vmatrix} a_{11} & a_{12} & a_{13} \\ a_{21} & a_{22} & a_{23} \\ a_{31} & a_{32} & a_{33} \end{vmatrix} \begin{vmatrix} d_{11} \\ d_{12} \\ d_{13} \end{vmatrix} \tag{83}$$

$$\overline{S}_{12}' = [T]\overline{S}_{12} = \begin{vmatrix} f_{21} \\ f_{22} \\ f_{23} \end{vmatrix} = \begin{vmatrix} a_{11} & a_{12} & a_{13} \\ a_{21} & a_{22} & a_{23} \\ a_{31} & a_{32} & a_{33} \end{vmatrix} \begin{vmatrix} f_{11} \\ f_{12} \\ f_{13} \end{vmatrix} \tag{84}$$

Equations 82 thru 84 can be arranged into the following expressions.

$$\begin{vmatrix} c_{21} \\ d_{21} \\ f_{21} \end{vmatrix} = \begin{vmatrix} c_{11} & c_{12} & c_{13} \\ d_{11} & d_{12} & d_{13} \\ f_{11} & f_{12} & f_{13} \end{vmatrix} \begin{vmatrix} a_{11} \\ a_{12} \\ a_{13} \end{vmatrix} \tag{85}$$

$$\begin{vmatrix} c_{22} \\ d_{22} \\ f_{22} \end{vmatrix} = \begin{vmatrix} c_{11} & c_{12} & c_{13} \\ d_{11} & d_{12} & d_{13} \\ f_{11} & f_{12} & f_{13} \end{vmatrix} \begin{vmatrix} a_{21} \\ a_{22} \\ a_{23} \end{vmatrix} \tag{86}$$

$$\begin{vmatrix} c_{23} \\ d_{23} \\ f_{23} \end{vmatrix} = \begin{vmatrix} c_{11} & c_{12} & c_{13} \\ d_{11} & d_{12} & d_{13} \\ f_{11} & f_{12} & f_{13} \end{vmatrix} \begin{vmatrix} a_{31} \\ a_{32} \\ a_{33} \end{vmatrix} \tag{87}$$

Using Cramer's rule, the components of the transformation [T], a_{11}, a_{12}, a_{13}, a_{21}, ..., a_{33}, can be computed using equations 85 thru 87. Note that the 3 by 3 matrix appearing in each of these equations are identical. The symbol Δ is used to denote the determinant of this matrix. Δ equals

$$\Delta=\det\begin{vmatrix} c_{11} & c_{12} & c_{13} \\ d_{11} & d_{12} & d_{13} \\ f_{11} & f_{12} & f_{13} \end{vmatrix} = c_{11}(d_{12}f_{13}-d_{13}f_{12})$$

$$+c_{12}(d_{13}f_{11}-d_{11}f_{13})+c_{13}(d_{11}f_{12}-d_{12}f_{11}) \tag{88}$$

The nine components of [T] are

$$a_{11}=\frac{\det\begin{vmatrix} c_{21} & c_{12} & c_{13} \\ d_{21} & d_{12} & d_{13} \\ f_{21} & f_{12} & f_{13} \end{vmatrix}}{\Delta} = [c_{21}(d_{12}f_{13}-d_{13}f_{12})$$

$$+c_{12}(d_{13}f_{21}-d_{21}f_{13})+c_{13}(d_{21}f_{12}-d_{12}f_{21})]/\Delta \tag{89}$$

$$a_{12}=\frac{\det\begin{vmatrix} c_{11} & c_{21} & c_{13} \\ d_{11} & d_{21} & d_{13} \\ f_{11} & f_{21} & f_{13} \end{vmatrix}}{\Delta} = [c_{11}(d_{21}f_{13}-d_{13}f_{21})$$

$$+c_{21}(d_{13}f_{11}-d_{11}f_{13})+c_{13}(d_{11}f_{21}-d_{21}f_{11})]/\Delta \tag{90}$$

$$a_{13}=\frac{\det\begin{vmatrix} c_{11} & c_{12} & c_{21} \\ d_{11} & d_{12} & d_{21} \\ f_{11} & f_{12} & f_{21} \end{vmatrix}}{\Delta} = [c_{11}(d_{12}f_{21}-d_{21}f_{12})$$

$$+c_{12}(d_{21}f_{11}-d_{11}f_{21})+c_{21}(d_{11}f_{12}-d_{12}f_{11})]/\Delta \tag{91}$$

$$a_{21}=\frac{\det\begin{vmatrix} c_{22} & c_{12} & c_{13} \\ d_{22} & d_{12} & d_{13} \\ f_{22} & f_{12} & f_{13} \end{vmatrix}}{\Delta}=[c_{22}(d_{12}f_{13}-d_{13}f_{12})$$

$$+c_{12}(d_{13}f_{22}-d_{22}f_{13})+c_{13}(d_{22}f_{12}-d_{12}f_{22})]/\Delta \qquad (92)$$

$$a_{22}=\frac{\det\begin{vmatrix} c_{11} & c_{22} & c_{13} \\ d_{11} & d_{22} & d_{13} \\ f_{11} & f_{22} & f_{13} \end{vmatrix}}{\Delta}=[c_{11}(d_{22}f_{13}-d_{13}f_{22})$$

$$+c_{22}(d_{13}f_{11}-d_{11}f_{13})+c_{13}(d_{11}f_{22}-d_{22}f_{11})]/\Delta \qquad (93)$$

$$a_{23}=\frac{\det\begin{vmatrix} c_{11} & c_{12} & c_{22} \\ d_{11} & d_{12} & d_{22} \\ f_{11} & f_{12} & f_{22} \end{vmatrix}}{\Delta}=[c_{11}(d_{12}f_{22}-d_{22}f_{12})$$

$$+c_{12}(d_{22}f_{11}-d_{11}f_{22})+c_{22}(d_{11}f_{12}-d_{12}f_{11})]/\Delta \qquad (94)$$

$$a_{31}=\frac{\det\begin{vmatrix} c_{23} & c_{12} & c_{13} \\ d_{23} & d_{12} & d_{13} \\ f_{23} & f_{12} & f_{13} \end{vmatrix}}{\Delta}=[c_{23}(d_{12}f_{13}-d_{13}f_{12})$$

$$+c_{12}(d_{13}f_{23}-d_{23}f_{13})+c_{13}(d_{23}f_{12}-d_{12}f_{23})]/\Delta \qquad (95)$$

$$a_{32}=\frac{\det\begin{vmatrix} c_{11} & c_{23} & c_{13} \\ d_{11} & d_{23} & d_{13} \\ f_{11} & f_{23} & f_{13} \end{vmatrix}}{\Delta}=[c_{11}(d_{23}f_{13}-d_{13}f_{23})$$

$$+c_{23}(d_{13}f_{11}-d_{11}f_{13})+c_{13}(d_{11}f_{23}-d_{23}f_{11})]/\Delta \qquad (96)$$

$$a_{33}=\frac{\det\begin{vmatrix} c_{11} & c_{12} & c_{23} \\ d_{11} & d_{12} & d_{23} \\ f_{11} & f_{12} & f_{23}\end{vmatrix}}{\Delta}=[c_{11}(d_{12}f_{23}-d_{23}f_{12})$$

$$+c_{12}(d_{23}f_{11}-d_{11}f_{23})+c_{23}(d_{11}f_{12}-d_{12}f_{11})]/\Delta \tag{97}$$

Assume that the apparent motion of the stars is due to a single eigenaxis maneuver. Let α, β, and γ be the directional-angles between the eigenaxis and the telescope X, Y, and Z axes, respectively. Let θ be the rotation about this eigenaxis necessary to rotate the stars from its reference location described by $\bar{S}_1$ and $\bar{S}_2$ to its location defined by $\bar{S}_1'$ and $\bar{S}_2'$. This maneuver can be described by the four Euler quaternions q_1, q_2, q_3, and q_4 defined below.

$$q_1=\cos(\frac{\theta}{2}) \tag{98}$$

$$q_2=\cos\alpha\sin(\frac{\theta}{2}) \tag{99}$$

$$q_3=\cos\beta\sin(\frac{\theta}{2}) \tag{100}$$

$$q_4=\cos\gamma\sin(\frac{\theta}{2}) \tag{101}$$

The transformation [T] can be written in terms of α, β, γ, and θ. The components of [T], a_{11}, a_{12}, a_{13}, a_{21}, ..., a_{33}, are

$$a_{11}=1-2\sin^2\alpha\sin^2(\frac{\theta}{2})=q_1^{\,2}+q_2^{\,2}-q_3^{\,2}-q_4^{\,2} \tag{102}$$

$$a_{12}=2\cos\alpha\cos\beta\sin^2(\frac{\theta}{2})-2\cos\gamma\sin\frac{\theta}{2}\cos\frac{\theta}{2} \tag{103}$$

$$=2(q_2q_3-q_1q_4)$$

$$a_{13}=2\cos\alpha\cos\gamma\sin^2(\frac{\theta}{2})+2\cos\beta\sin\frac{\theta}{2}\cos\frac{\theta}{2} \tag{104}$$

$$=2(q_2q_4-q_1q_3)$$

$$a_{21}=2\cos\alpha\cos\beta\sin^2(\frac{\theta}{2})+2\cos\gamma\sin\frac{\theta}{2}\cos\frac{\theta}{2}$$

$$=2(q_2q_3+q_1q_4) \tag{105}$$

$$a_{22}=1-2\sin^2\beta\sin^2(\frac{\theta}{2})=q_1{}^2-q_2{}^2+q_3{}^2-q_4{}^2 \tag{106}$$

$$a_{23}=2\cos\beta\cos\gamma\sin^2(\frac{\theta}{2})-2\cos\alpha\sin\frac{\theta}{2}\cos\frac{\theta}{2}$$

$$=2(q_3q_4-q_1q_2) \tag{107}$$

$$a_{31}=2\cos\alpha\cos\gamma\sin^2(\frac{\theta}{2})-2\cos\beta\sin\frac{\theta}{2}\cos\frac{\theta}{2}$$

$$=2(q_2q_4-q_1q_3) \tag{108}$$

$$a_{32}=2\cos\beta\cos\gamma\sin^2(\frac{\theta}{2})+2\cos\alpha\sin\frac{\theta}{2}\cos\frac{\theta}{2}$$

$$=2(q_1q_2+q_3q_4) \tag{109}$$

$$a_{33}=1-2\sin^2\gamma\sin^2(\frac{\theta}{2})=q_1{}^2-q_2{}^2-q_3{}^2+q_4{}^2 \tag{110}$$

The eigenaxis is defined by the three direction cosines, $\cos\alpha$, $\cos\beta$, and $\cos\gamma$. Let the direction cosines $\cos\alpha$, $\cos\beta$, and $\cos\gamma$ be designated E_x, E_y, and E_z, respectively. These direction cosines can be derived from the transformation [T] as follows.

$$a_{32}-a_{23}=4\cos\alpha\sin\frac{\theta}{2}\cos\frac{\theta}{2}$$

$$E_x=\cos\alpha=\frac{a_{32}-a_{23}}{4\cos\frac{\theta}{2}\sin\frac{\theta}{2}}=\frac{a_{32}-a_{23}}{4q_1\sin\frac{\theta}{2}} \tag{111}$$

$$a_{13}-a_{31}=4\cos\beta\sin\frac{\theta}{2}\cos\frac{\theta}{2}$$

$$E_y=\cos\beta=\frac{a_{13}-a_{31}}{4\cos\frac{\theta}{2}\sin\frac{\theta}{2}}=\frac{a_{13}-a_{31}}{4q_1\sin\frac{\theta}{2}} \tag{112}$$

$$a_{21}-a_{12}=4\cos\gamma\sin\frac{\theta}{2}\cos\frac{\theta}{2}$$

$$E_z=\cos\gamma=\frac{a_{21}-a_{12}}{4\cos\frac{\theta}{2}\sin\frac{\theta}{2}}=\frac{a_{21}-a_{12}}{4q_1\sin\frac{\theta}{2}} \tag{113}$$

The eigenaxis rotation θ can be computed using the property that the trace of [T] equals $1+2\cos\theta$ (reference 1).

$$\text{trace of } [T]=\sum_{i=1}^{3} a_{ii}=1+2\cos\theta \tag{114}$$

$$\cos\theta=\frac{1}{2}(a_{11}+a_{22}+a_{33}-1) \tag{115}$$

$\cos\theta$ can be approximated by the following power series.

$$\cos\theta=1-\frac{\theta^2}{2!}+\frac{\theta^4}{4!}-\frac{\theta^6}{6!}+\ldots \tag{116}$$

The rotation θ corresponds to the telescope attitude error and should be very small if the telescope's fine stabilization system is operating properly. Since θ is small, $\cos\theta$ can be approximated by

$$\cos\theta\simeq 1-\frac{\theta^2}{2} \tag{117}$$

Using equations 113 and 115 θ equals

$$\theta=(3-a_{11}-a_{22}-a_{33})^{1/2} \tag{118}$$

The eigenaxis rotation defined by E_x, E_y, E_z, and θ describes the apparent star motion. But since the stars are inertially fixed, their apparent motion is actually due to the motion of the telescope. The telescope motion is opposite the apparent star motion and can be described by an eigenaxis rotation of θ about an axis defined by $-E_x$, $-E_y$, and $-E_z$.

The telescope eigenaxis direction cosines E_x', E_y', and E_z' are:

$$E_x'=-E_x=\frac{a_{23}-a_{32}}{4q_1\sin\frac{\theta}{2}} \tag{119}$$

$$E_y'=-E_y=\frac{a_{31}-a_{13}}{4q_1\sin\frac{\theta}{2}} \tag{120}$$

$$E_z'=-E_z=\frac{a_{12}-a_{21}}{4q_1\sin\frac{\theta}{2}} \tag{121}$$

The four quaternions q_1, q_2, q_3, and q_4 describing the rotational motion of the telescope are:

$$q_1=\cos\frac{\theta}{2}=\cos[0.5(3-a_{11}-a_{22}-a_{33})^{1/2}] \tag{122}$$

$$q_2=E_x'\sin\frac{\theta}{2}=\frac{a_{23}-a_{32}}{4q_1} \tag{123}$$

$$q_3=E_y'\sin\frac{\theta}{2}=\frac{a_{31}-a_{13}}{4q_1} \tag{124}$$

$$q_4=E_z'\sin\frac{\theta}{2}=\frac{a_{12}-a_{21}}{4q_1} \tag{125}$$

Since θ is small,

$$\sin\frac{\theta}{2}\simeq\frac{\theta}{2} \tag{126}$$

Using equations 123 thru 126, the telescope X, Y, and Z attitude errors θ_x, θ_y, and θ_z, respectively equal

$$\theta_x=2E_x'\frac{\theta}{2}\simeq 2q_2=\frac{a_{23}-a_{32}}{2q_1} \tag{127}$$

$$\theta_y=2E_y'\frac{\theta}{2}\simeq 2q_3=\frac{a_{31}-a_{13}}{2q_1} \tag{128}$$

$$\theta_z=2E_z'\frac{\theta}{2}\simeq 2q_4=\frac{a_{12}-a_{21}}{2q_1} \tag{129}$$

Listed below are the computational requirements and sequence needed to calculate the telescope attitude errors θ_x, θ_y, and θ_z.

a. The unit vectors $\overline{S}_1$, $\overline{S}_2$, and $\overline{S}_{12}$' are derived from the telescope fine attitude error sensor. Initially, these unit vectors are designated $\overline{S}_1$, $\overline{S}_2$, and $\overline{S}_{12}$, are stored, and are used to describe the desired telescope attitude.

b. The components of [T] a_{11}, a_{12}, a_{13}, a_{21}, ..., a_{33} are computed using $\overline{S}_1$, $\overline{S}_2$, and $\overline{S}_{12}$ and their present, corresponding unit vectors $\overline{S}_1'$, $\overline{S}_2'$ and $\overline{S}_{12}'$.

c. Quaternion q_1 is computed using equation 122.

d. The telescope attitude errors θ_x, θ_y, and θ_z are computed using equations 127 thru 129.

B3.3. TELESCOPE POINTING AND STABILIZATION TRADE STUDY

From its stowed position parallel to the floor of the ASM pallet, the telescope complement tube is deployed to a position perpendicular to the floor as shown in figure B3-5. The high energy arrays are similarly stowed and deployed. Hardware commonality between the telescope and the array gimballing system can be realized in this area of experiment mounting and deployment. As shown in the figure, this Deployed Wide Angle Gimbal (DWAG) technique affords hemispherical viewing for the telescope complement and the high energy arrays. To utilize this capability, the telescope and array gimballing systems must be capable of rotational motion of 90 degrees in elevation and 360 degrees in azimuth.

For the candidate telescope fine stabilization systems investigated, the telescope complement center of mass is assumed to be located at the intersection of its three control axes to minimize telescope orbiter disturbance coupling. The payload pointing requirements used in this analysis are listed in table B3-1. Contained in table B3-2 are the estimated stabilization capabilities of the two candidate ASM shuttle orbiter stabilization systems, a CMG system and a low thrust reaction control system (RCS).

The stabilization concepts to be investigated are:

a. Standard telescope mount flexible suspension fine stabilization gimbal system.

b. Standard telescope mount with spherical gas bearing fine stabilization system.

c. Standard telescope mount with coarse external stabilization and image motion compensation (IMC) internal to individual instruments.

d. Wide angle spherical gas bearing mount.

B3.3.1. Standard Telescope Mount - The Deployed Wide Angle Gimbal concept of figure B3-5 is essentially a standard telescope mount approach. Experiment pointing is achieved by 360-degree rotation of the telescope yoke combined with 90-degree telescope tube rotation in elevation to provide hemispherical coverage. For fine stabilization, a secondary three-degree-of-freedom gimbal system at the elevation axis is required, or direct stabilization could be utilized with final image stabilization being achieved internal to the individual experiments where required. If a secondary gimbal system is used, the system could employ flexible suspensions/rolling element bearings or a gas bearing design.

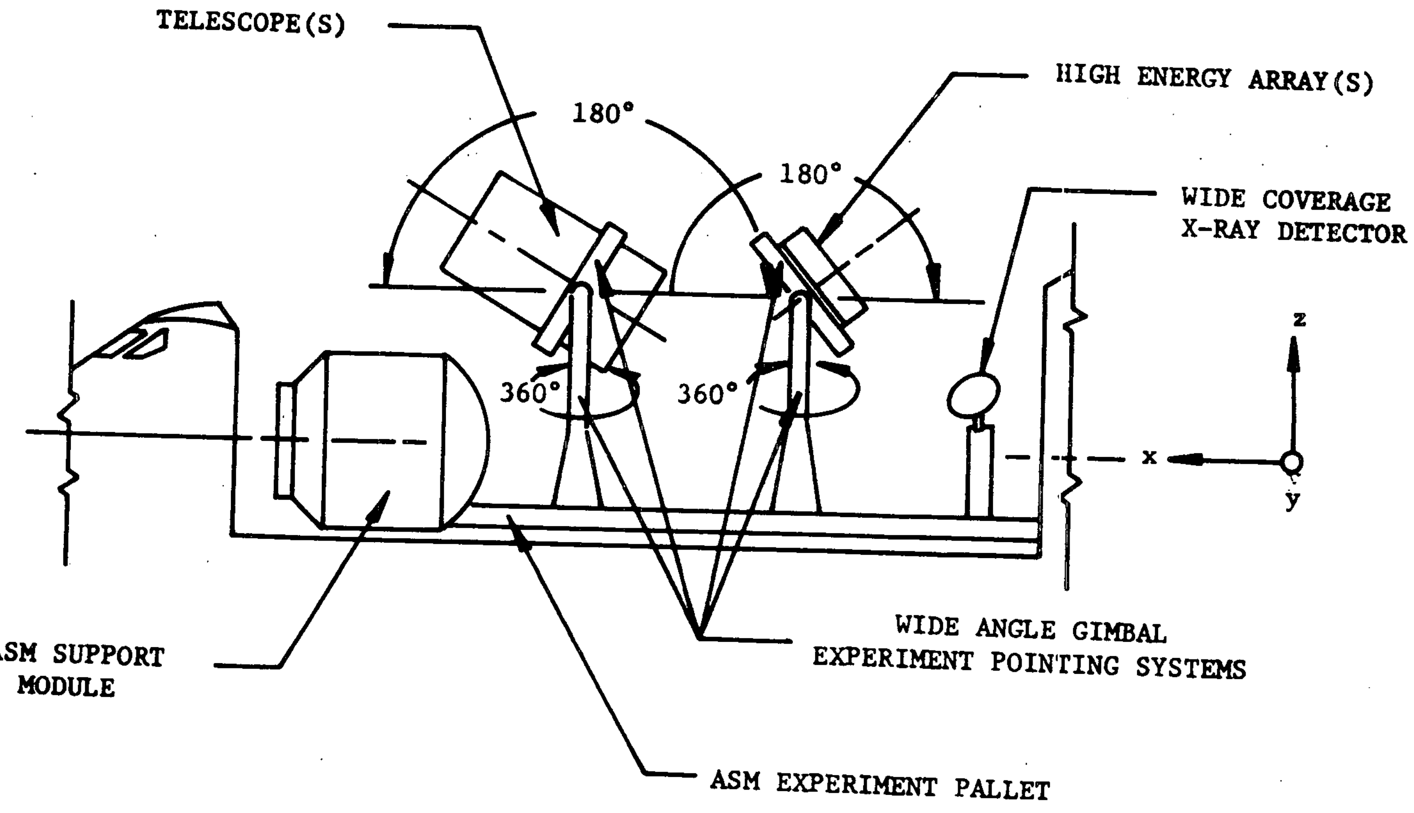

Figure B3-5. ASM Shuttle Orbiter Baseline Experiment Payload

Table B3-1. ASM Telescope and High Energy Array Pointing and Stabilization Requirements

EXPERIMENT	POINTING	STABILIZATION		
		PITCH	YAW	ROLL
Telescope	10 μrad (2 $\widehat{\text{sec}}$)	0.5 μ rad (0.1 $\widehat{\text{sec}}$)	0.5 μrad (0.1 $\widehat{\text{sec}}$)	25 μrad (5 $\widehat{\text{sec}}$)
High Energy Array	0.3 mrad (1 $\widehat{\text{min}}$)	0.3 mrad (1 $\widehat{\text{min}}$)	0.3 mrad (1 $\widehat{\text{min}}$)	0.1 rad (6 deg)

Table B3-2. CMG, RCS Estimated Stability Capabilities

SHUTTLE ORBITER STABILIZATION SYSTEM	CAPABILITY
CMG	0.3 mrad (1 min)
RCS	4 mrad (0.2 deg)

B3.3.2. Flexible Suspension Fine Stabilization - Fine stabilization can be achieved by a secondary gimballing system consisting of an azimuth gimbal, an elevation gimbal and a roll ring for rotational isolation, figure B3-6. The azimuth and elevation gimbal rings would be supported at diametrically opposite points with flexible suspensions. Flexible suspensions support rotation by means of criss-crossed flat springs that flex to allow movement; the action is like a combination spring and bearing. Unloaded, the flexible suspensions have a center seeking feature. Flexible suspensions have no rubbing parts which could produce cold welding, friction, and breakaway torques. Rotational isolation can be achieved with a roll ring with rolling element bearings. In order to utilize flexible suspensions for rotational isolation, it would be necessary to mount the bearing beyond the rear of the tube and thus cantilever the tube from the bearing. This approach would present problems in attaining a rigid system, but would eliminate friction and breakaway torques associated with rolling element bearings. However, roll stabilization is much less critical than azimuth and elevation stabilization, so a rolling element bearing concept appears reasonable for rotation isolation. The concept of utilizing flexible suspensions in a secondary fine stabilization gimbal system is probably adequate based on its present use in the Skylab program.

B3.3.3. Gas Bearing Fine Stabilization - The spherical gas bearing may offer advantages in terms of gimbal simplicity, mechanical rigidity, and near zero friction and breakaway torque. A ball attached to the telescope tube is gas suspended in its mating socket and thus provides two-axis gimballing and rotational isolation in one unit. The escaping support gas raises the potential problem of experiment contamination since gas scavenging would be difficult due to the vacuum of space, and would not be 100 percent efficient. Additionally, implementation is a problem due to telescope tube size, and weight and space restrictions. Three possible bearing locations are shown in figure B3-7: inside the telescope tube at its center of mass, girding the tube at its center of mass, or beyond the tube with appropriate counterweights.

Locating the gas bearing inside the tube, (a) of figure B3-7, would impose design constraints on the Stratoscope III, IR, and PHG telescopes. Their size relative to the telescope complement tube would require that the gas bearing be within the telescope envelope. Packaging of the other experiment clusters would be difficult due to the presence of the bearing within the tube. Also, for these reasons, the system is not flexible regarding future experiments. This approach, therefore, is eliminated.

The second possibility is to locate the gas bearing at the telescope tube center of mass in a girding fashion as a ball/socket configuration, (b) of the figure. Manufacture of a spherical gas bearing of this size ($\approx$100 in. diameter) would require a development program. Fecker Systems Division of Owens-Illinois, builder of the NASA Ames airborne telescope, felt a bearing of this size could be developed. Development would be required since manufacture of a

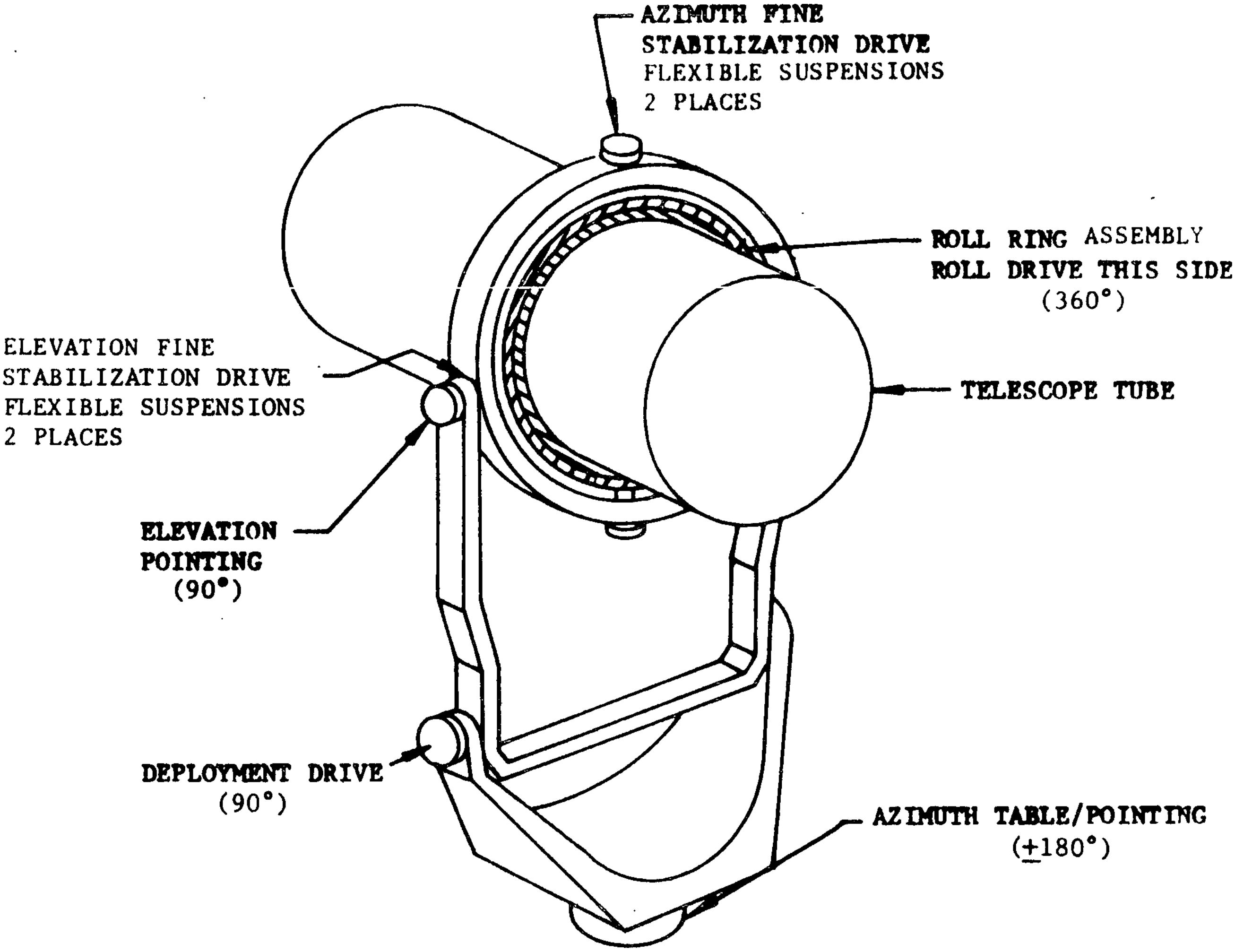

Figure B3-6. Flexible Suspension Gimbal System

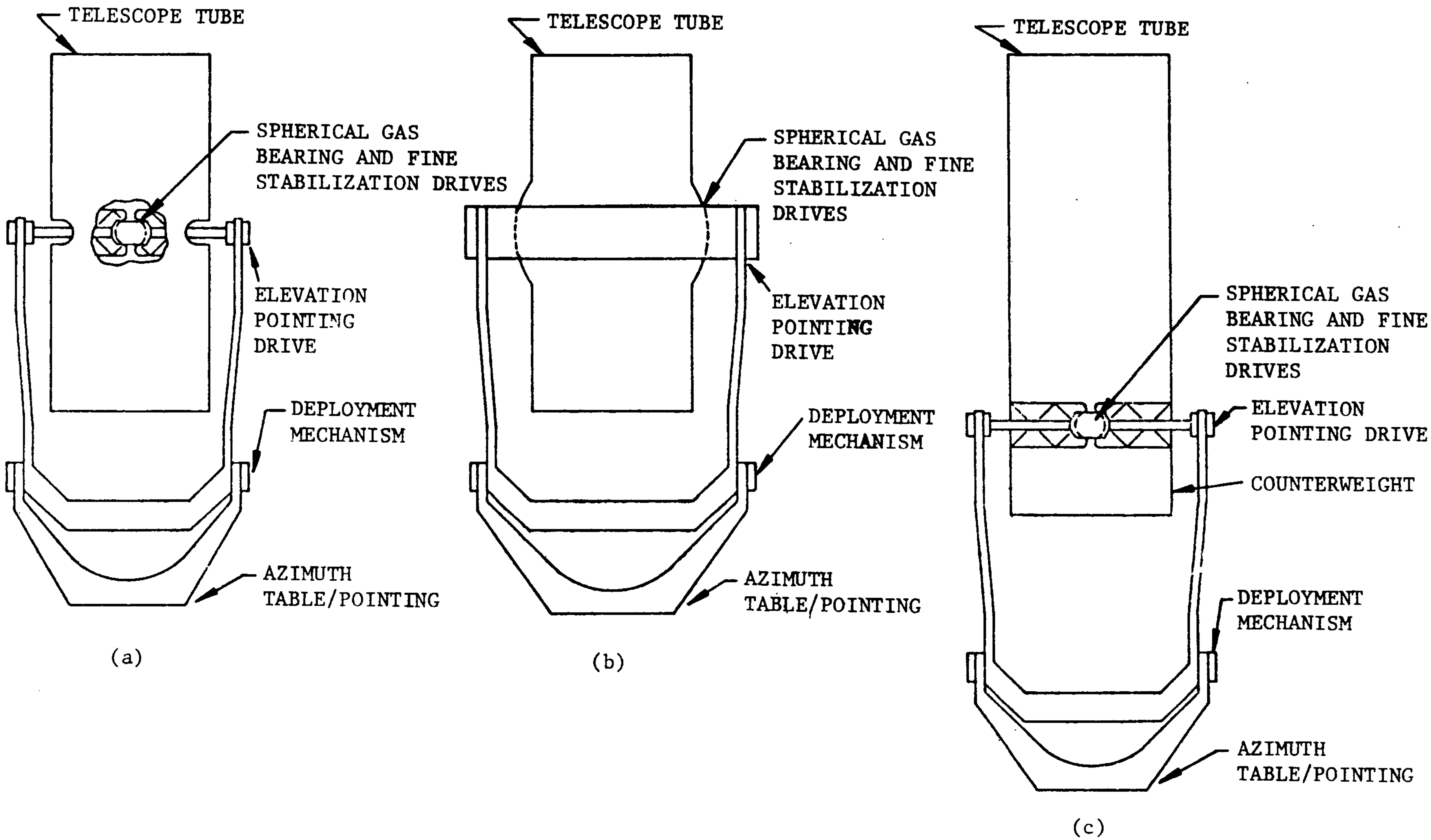

Figure B3-7. Small Angle Spherical Gas Bearing Configurations

100-inch diameter bearing would require extension of present technology beyond that used for the 16-inch diameter Ames telescope bearing; the Ames bearing design can be manufactured in sizes up to 24 inches in diameter. Fecker Systems estimated cost for development and delivery of a 100-inch diameter spherical bearing was approximately $3 million. This concept will be further evaluated.

The third possible location for the spherical bearing is beyond the telescope tube, (c) of the figure. This position would result in a much smaller diameter bearing, which is within the present state of the art. However, this concept has the disadvantage that counterweights would be required to transfer the payload (telescope plus counterweights) center of mass to the bearing area. Due to the shuttle orbiter space limitations, the permissible location of the counterweights would be very near the gas bearing, figure B3-8. The counterweight moment-arm length would be on the order of 0.1 of the telescope tube length as compared to the telescope tube center of mass location of about 0.4 of the telescope length from the telescope end. Therefore, the required counterweight, including any experiment support electronics, would be roughly three to four times the telescope complement weight. The counterweight approach is eliminated due to increased volume, weight requirements, and mounting complexity.

In lieu of a spherical gas bearing, a gas bearing supported gimbal system could be considered, figure B3-9. The gimbal system would be constructed similar to the flexible suspensions gimbal system except gas bearings would be substituted for the suspensions. By comparison, the flexible suspensions and gas bearing have near zero friction and breakaway torque, but the gas bearing gimbal system is more complex due to the gas supply. Compared to the spherical bearing, the gas bearing gimbal system is much more complex and less rigid by virtue of the gimbal and roll ring construction. The gas bearing supported fine stabilization gimbal system therefore will not be considered further.

B3.3.4. <u>Coarse External-Internal IMC Stabilization</u> - Simplification of the gimballing system for the telescope tube can be realized if coarse external, internal IMC stabilization is utilized,

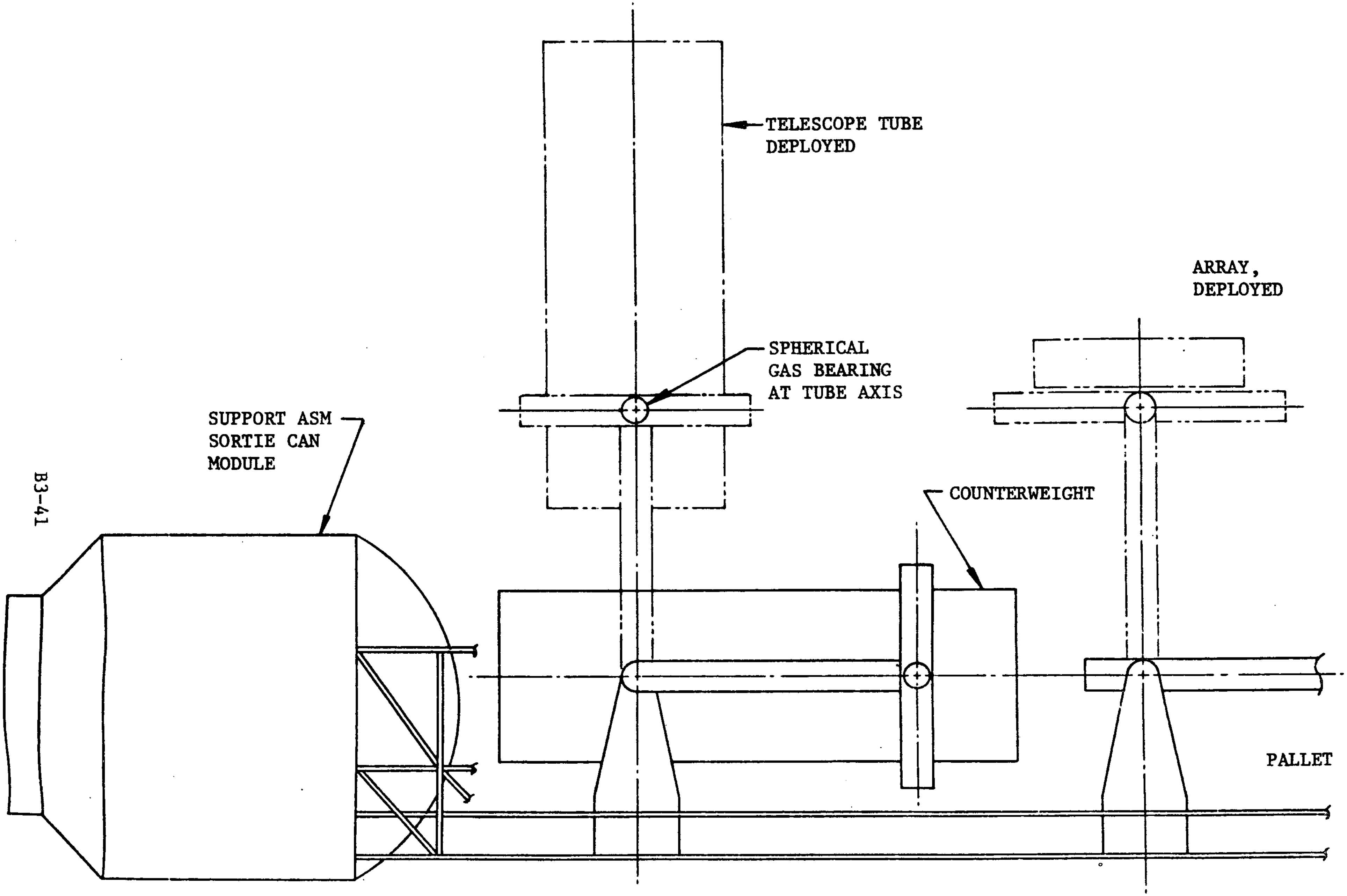

Figure B3-8. Spherical Gas Bearing With Counterweight

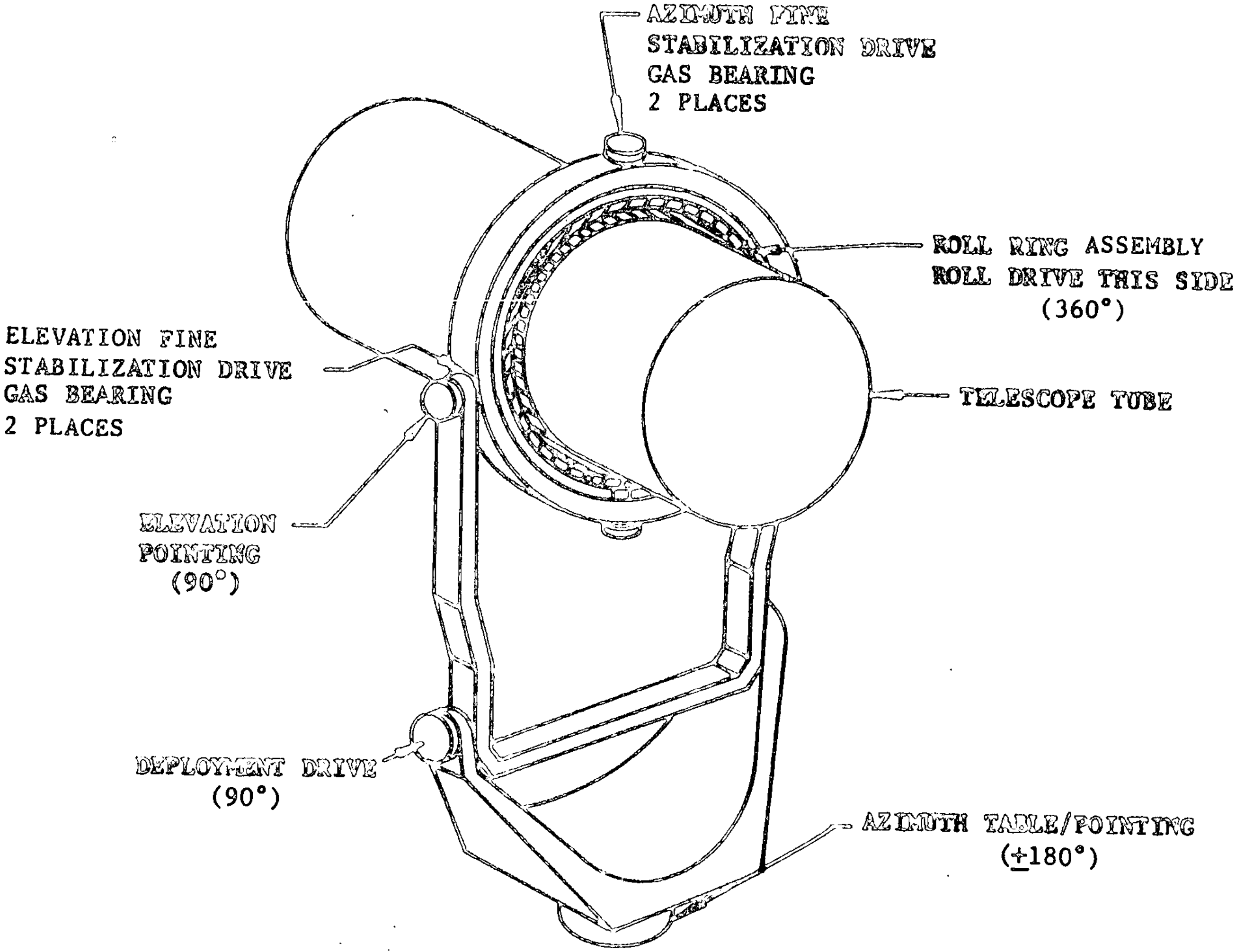

Figure B3-9. Gas Bearing Gimbal System

see figure B3-10. The azimuth and elevation axes, figure B3-5, of the Deployed Wide Angle Gimbal would be coarsely stabilized directly in order to eliminate the azimuth and elevation axes portions of the secondary gimbal system. This approach requires that final stabilization be performed within each experiment. Coarse azimuth and elevation stabilization can probably be achieved to approximately 1 arc-second, IMC internal to the experiments would then provide fine stabilization (0.1 arc-second range) for those experiments requiring this level of stability. A rotational isolation device would still be required; internal vernier rotational stabilization is not recommended since it would be extremely difficult to achieve and could alter image quality.

Although the gimballing system is simplified, the design of individual experiments may become complicated and, in certain instances, very complicated and expensive. Also, any additional experiments with stability requirements finer than 1 arc-second would require an internal IMC with attendant design costs and probably delays, thus reducing the flexibility of the pallet to accommodate a variety of payloads. This concept will be further evaluated.

B3.3.5. Wide Angle Spherical Gas Bearing Mount - Implementation of a wide angle spherical gas bearing involves replacing the azimuth/elevation drives of the Deployed Wide Angle Gimbal with a gas bearing, but retaining the azimuth table and deployment concept. The gas bearing would then be positioned at the elevation axis with, or without, an additional gimballing system for fine stabilization. Physically mounting the bearing is a problem. The three mounting positions available are shown in figure B3-11. Locating the bearing within the tube cavity, (a) of the figure, imposes design restrictions on the large experiments, e.g., for SIII, IR, and PHG (SIII: Stratoscope III; IR: Infrared Telescope; PHG: Photoheliograph), and hampers packaging of other experiment groups. Also, the restricted motion available with this approach severely limits viewing. Similarly, mounting the bearing beyond the tube with the addition of counterweights results in severely restricted motion, (c) of the figure. In addition to the volume penalty, the weight penalty is high due to the moment arm length available and vehicle space limitations, as pointed out previously for the small angle spherical bearing analysis. As the third possibility, the bearing could gird the telescope complement tube at its center of mass, (b) of the figure. As previously stated for the standard telescope mount, a bearing this size is beyond the state of the art and would require development. Also, as can be readily seen, hemispherical coverage is not possible due to interference between the bearing parts at the extremes of rotation in elevation; the azimuth axis presents no problem. The arc of travel in elevation is dependent on the

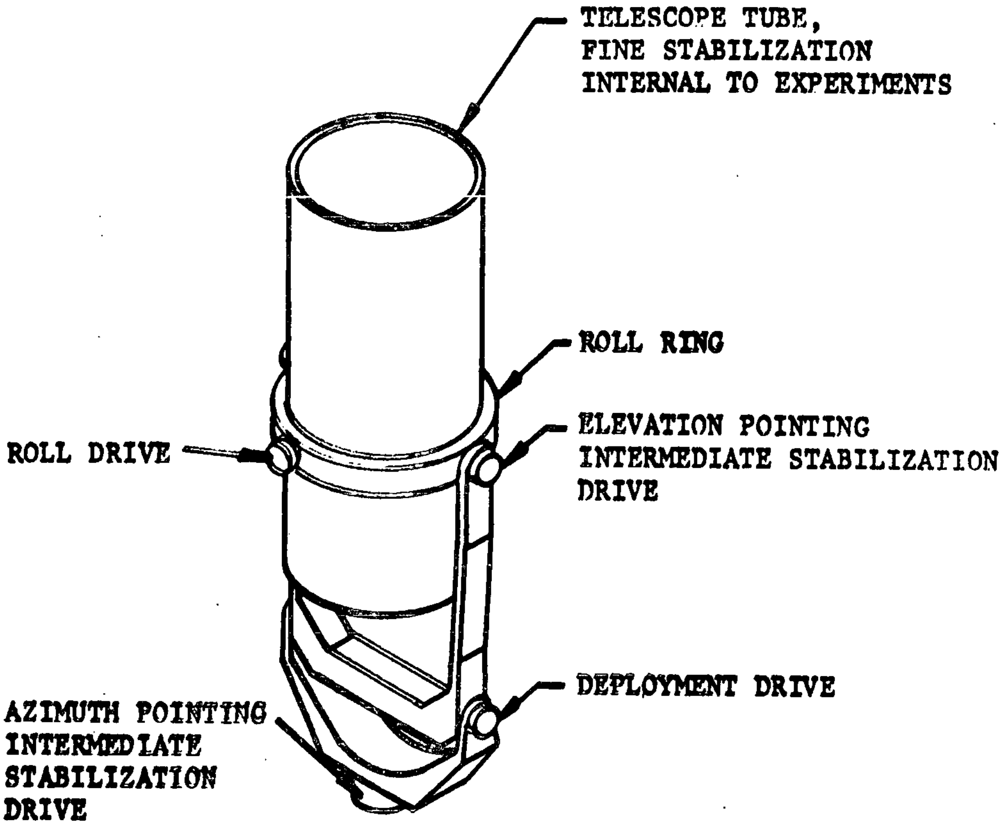

Figure B3-10. Coarse External - Internal IMC System

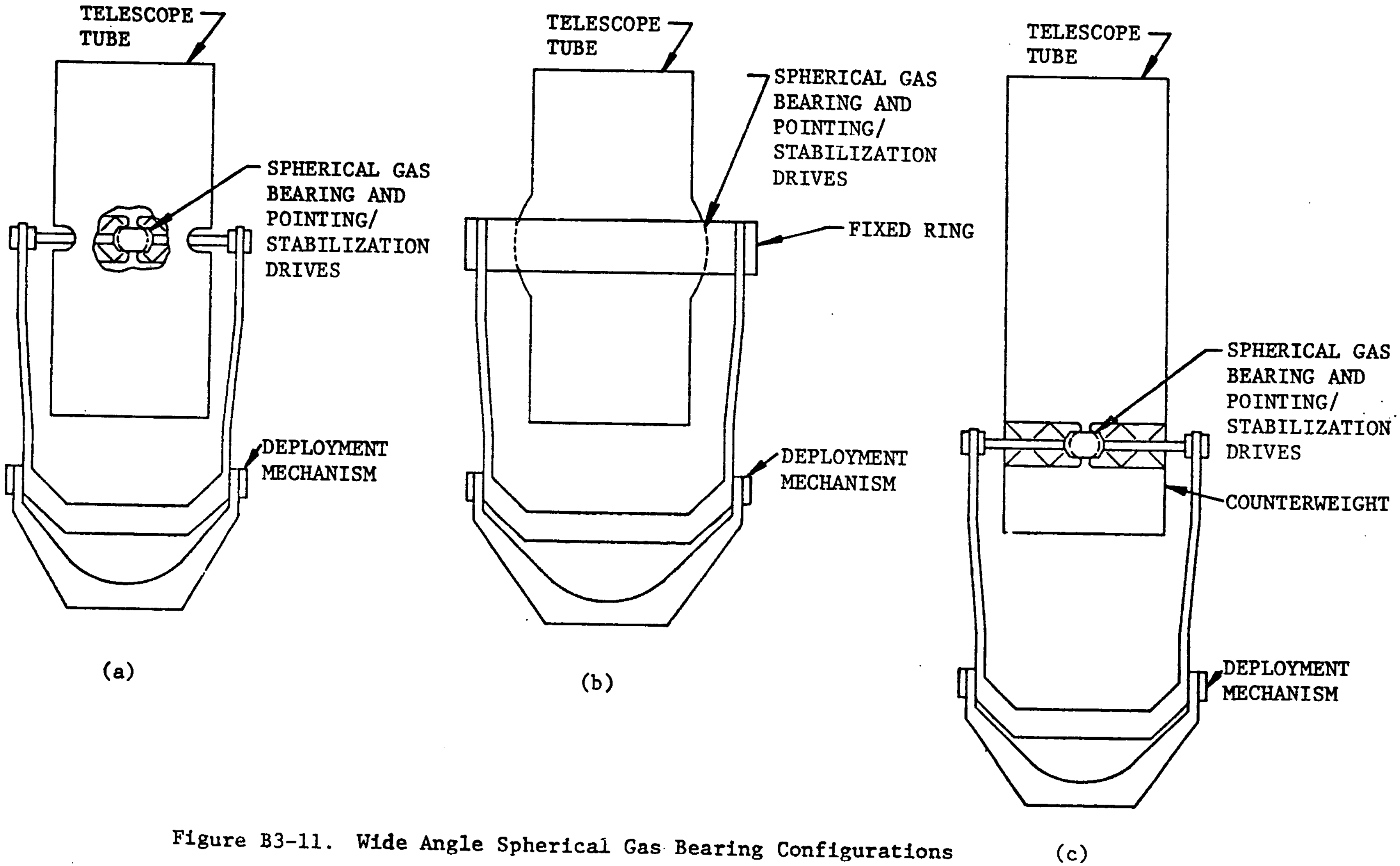

Figure B3-11. Wide Angle Spherical Gas Bearing Configurations

degree of spherical envelopment of the bearing parts and is estimated to be ± 20 degrees. Based on these analyses, the wide angle spherical gas bearing configurations of figure B3-11 are eliminated.

The girded bearing concept, (b) of figure B3-11, may have certain inherent performance advantages which warrant further analyses, of the concept. An alternative configuration, figure B3-12, eliminates the drawback of limited rotation. Two spherical bearing ball/socket segments are mounted on the deployment mechanism at diametrically opposite positions, as opposed to the ring mount concept of (b) in figure B3-11. This concept would permit 180 degrees of rotation in elevation about a prescribed axis. With this motion range, hemispherical coverage is possible when azimuth rotation is performed at the azimuth table. Using the girded-bearing concept, direct stabilization may be possible without the necessity for a secondary gimbal system, which would make the system more rigid and less complex. Available gas bearing pad size, mechanical support, end actuator design, and scavenging are some areas that require further investigation to determine feasibility. Also, the control problem that may occur with two gimbals as the system tracks near zenith will require a solution; perhaps the addition of another gimbal. Because of its potential inherent performance advantages, the system will not be eliminated although feasibility has not been established.

B3.3.6. Tradeoff - The stabilization systems to be further evaluated are:

a. Flexible Suspension Fine Stabilization

b. Small Angle Spherical Gas Bearing Fine Stabilization

c. Coarse External-Internal IMC Stabilization

d. Wide Angle Spherical Gas Bearing Mount

All systems use the Deployed Wide Angle Gimbal as the basic mount. The coarse external-internal IMC stabilization system and the wide angle spherical gas bearing mount require no secondary fine gimbal system except for a rotational isolation device for the IMC system. The remaining two systems include a secondary gimbal system with azimuth, elevation, and roll axes stabilization.

From a subsystem point of view, a cursory look might suggest that coarse external-internal IMC stabilization may be the most favorable. However, its impact upon the overall ASM program warrants closer examination. Image Motion Compensation (IMC)

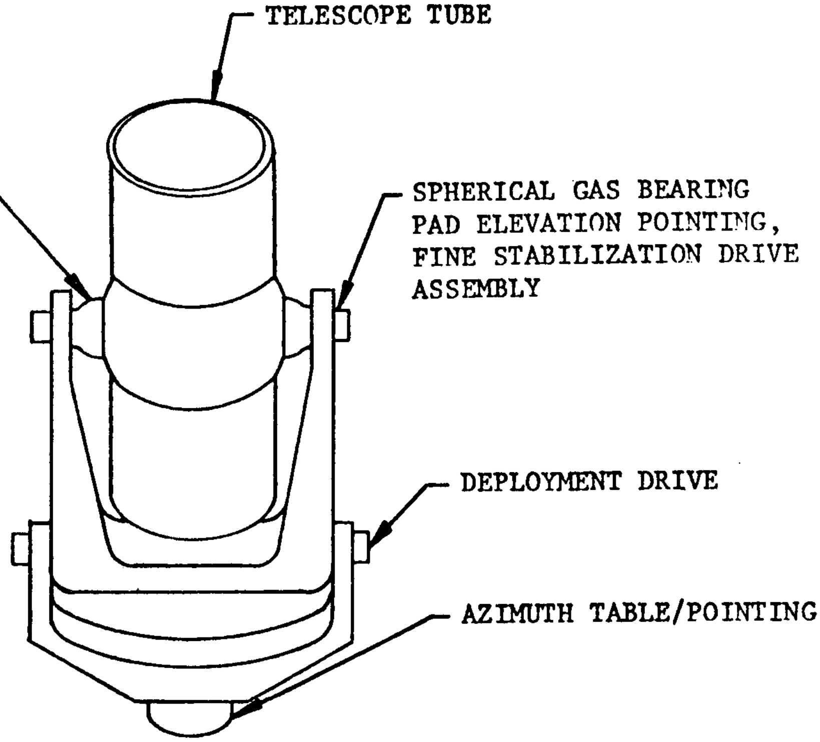

Figure B3-12. Wide Angle Spherical Gas Bearing, Two-Pad Configuration

refers to equipment included in an imaging instrument that is used to correct for improper tracking by the instrument's primary optical axis. Generally it involves the mechanical motion of one component of the optical system (for example, rotation of a folding mirror, or lateral translation of a lens) in such a manner as to null out the signals detected by a "fine pointing error sensor." Image motion compensation is often referred to as involving an "image stabilization system" or an "internal vernier system."

A key element in the IMC system is the fine error sensor. (Development and implementation of the fine error sensor systems will be required regardless of the technique used to achieve the specified stabilization.) The sensor should have rms noise and accuracy performance characteristics at least a factor of two better than the desired image stabilization accuracy. Ideally, this fine error sensor tracks a feature of the image, as formed by the instrument's main optics. If the same image is observed by the primary detector and by the error sensor, instrument flexure problems can be overcome with image motion compensation (loop is closed through the error sensor). If a separate optical system is used for the fine error sensor, it is necessary to carefully adjust the gain of the control signals for the image motion compensation system, to prevent undesired image motion effects due to over- or under-compensation (IMC actuator loop is not closed through the error sensor).

For each type of imaging system, there exists a limited number of good techniques for IMC implementation. The difficulties (and cost) of IMC implementation depend on the characteristics of the individual instrument. The main telescope characteristics that affect IMC design are detailedin table B3-3.

As a general rule, IMC implementation is relatively simple if the telescope has a high f-number (f-25 or higher), a small field of view (θ<1 mrad) and includes a fine error sensor that uses the same image used by the scientific detector, such that the loop can be closed through the error sensor. All of these key characteristics are found in the photoheliograph. Over the entire spectral range of the photoheliograph, the sun is such a bright source that the image must be attenuated before it reaches the detector: no penalty is incurred if part of the telescope's image is split off and routed to the fine error sensor. For the other candidate telescopes, at least one of the simplifying features is not available.

The f-number of the Stratoscope III telescope is f-12, about twice as fast as the f-25 lower limit. While the scientific field of view is only 1.8 mrad, the internal fine pointing error sensor system can only be implemented if the telescope's total available

Table B3-3. Telescope Characteristics That Affect IMC Implementation

INSTRUMENT	ANGULAR RESOLUTION (microradians)	SPECIFIED IMAGE STABILIZATION (microradians)	INSTRUMENT F-NUMBER	INSTRUMENT FIELD OF VIEW (milliradians)	CONTROLLED COMPONENT	INTERNAL FINE ERROR SENSOR FEASIBILITY
PHOTOHELIOGRAPH	0.6	0.5	3.85/50	0.9	Folding mirror	Yes
STRATOSCOPE III	0.5	0.5	2.2/12	1.8	Secondary mirror	Possible
INFRARED TELESCOPE	2	<2.5	1.5/10	1.5	Secondary or folding mirror	Doubtful
XUV SPECTROHELIOGRAPH	3	0.5	12	9	Concave objective grating	No
X-RAY TELESCOPE	2.5	0.5	10	3	Detector at image plane	No

field of view is on the order of 20 mrad (about 1.2 degrees) to insure that sources bright enough for fine tracking will be found within the field of view with high probability. All components of the imaging optical system must be large enough to handle a large image field (about 30-cm diameter) with comparatively fast (f-12) optics. The component currently suggested for mechanical control in an IMC system is the secondary mirror of the Cassegrain optical system. For the Stratoscope III telescope, the secondary mirror must be approximately 40 cm diameter; after allowance for a mounting and support structure, the secondary assembly will have a mass of 40 to 50 kg. Precise positioning of such a massive component with a fast response servo system is not a simple problem. Feasibility of a closed-loop IMC is not yet verified, but seems to be within the current state of technology.

For the infrared telescope, the f-number is even lower, f-10 nominal. The scientific field of view is conveniently small (1.5 mrad). Implementation feasibility of an internal fine error sensor, using the main instrument optics, is doubtful at best. The narrow field of view limits the availability of bright sources. The instrument's operating wavelength range is at considerably longer wavelengths than the sensitive range of the standard optical sensors used for error detection. Therefore, only open-loop IMC appears feasible. It should be emphasized that the low temperature cryogenic environment (20 K) within the instrument is undesirable for accurate mechanical motion and control of an optical component.

The XUV Spectroheliograph's image field is curved, with center of curvature approximately midway between the entrance aperture and the concave imaging grating. The grating is the only optical element available for IMC control; grating rotation will induce some undesirable focus errors, particularly at the ends of the image field. It is deemed impossible to develop an internal fine error sensor using the instrument's main optical train, due to the low level of solar flux in the extreme ultraviolet, the dispersed nature of the images, and the limited availability of distinct solar features in the XUV range sharp enough for precision tracking (these only appear occasionally). Only open-loop IMC can be mechanized.

For the X-Ray Focusing Telescope, it is not possible to use an intermediate optical component to achieve IMC, simply because none can be used. Either the primary objective system or the detector system must be translated laterally to compensate for tracking errors. (An alternative was suggested, involving the transformation of the x-ray image to an electron image on a thin-window photocathode. The electron image could then be stabilized (open loop) using star sensor outputs for control signals. This technique is adequate for an imaging experiment, but is invalid for spectrometric experiments.) Both of these components are massive, and are at opposite ends of the instrument, far removed from the instrument's center of mass. If either of these components is translated, high induced torque levels will develop which will adversely affect

other instruments in the telescope system. The fine error sensor cannot use the telescope image, so that IMC is restricted to open-loop operation. The anticipated flux level is usually too low to allow splitting off any part of it, and only on rare occasions are the solar features sharp enough in this spectral range for good tracking accuracy.

It is recognized that Stratoscope III is a special case, due to the high similarity of the optical configuration with that of the Large Space Telescope (LST). If a design for an IMC system is developed for LST, it can be scaled down and used in the Stratoscope III instrument, thus realizing a substantial cost savings in the overall space astronomy program.

Based on the above discussions, budgetary estimates of the cost of developing and implementing satisfactory IMC systems for the five instruments are shown in table B3-4.

Overall ASM program cost would be increased by at least $6.4 million in order to incorporate the internal IMCs required by the experiments. Also, adding internal IMCs to the experiments would in effect reduce the reliability of the stabilization system since the stabilization system performance is now directly tied to the internal IMC system. Most of the trade-off parameters are summarized in table B3-5. Power consumption is essentially the same for all systems, but the volume and weight data favor the coarse external-internal IMC system, although not by an appreciable margin compared to the flexible suspension system. In view of the high cost of implementation and marginal volume and weight advantages compared to the flexible suspension gimbal, the coarse external-internal IMC is not recommended.

The spherical gas bearing secondary gimbal concept has significant disadvantages in the volume, weight, and cost categories, although not as costly as the coarse external-internal IMC system. It is estimated that gas bearing supports will require about 3 500 lb of gas for a 160 hr mission, without scavenging. Exhaustion as much as 7 lb of gas per hour at low velocities will result in a strong contribution to the gas cloud surrounding the spacecraft. For example, if nitrogen were used, the anticipated cloud might be virtually opaque to radiation in the far ultraviolet and x-ray spectrums. For these reasons, the spherical gas bearing is not recommended as an approach for fine stabilization. However, the spherical gas bearing approach might be subject to future investigation for the system has advantages in that it is more mechanically rigid than a gimbal system and is nearly frictionless, which may be important factors in achieving 0.1 arc-seconds stability. Similarly, the wide-angle spherical gas bearing mount is not recommended, but due to its potential inherent performance advantages might be subject to future investigation at the same time.

Table B3-4. Estimated Cost of Image Motion Compensation Subsystems

INSTRUMENT	COST OF IMC DEVELOPMENT AND IMPLEMENTATION ($K)
PHOTOHELIOGRAPH	200
STRATOSCOPE III	
a. If LST development available	1 000
b. If LST development not available	1 500
INFRARED TELESCOPE	700
XUV SPECTROHELIOGRAPH	1 500
X-RAY TELESCOPE	3 000
	6 400 (or 6 900)

Table B3-5. Estimated Parameters for Candidate Stabilization Systems

STABILIZATION SYSTEM	VOLUME m^3	WEIGHT, kg	POWER, WATTS	COST, $	RELIABILITY MTBF (HR)
Flexible Suspension Secondary Gimbal	2.5	1 360	1 500 peak 500 avg	600 000	15 000
Spherical Gas Bearing Secondary Gimbal	4.8	3 000	1 500 peak 400 avg	3 100 000	20 000
Coarse External IMC Interior	1.8	1 050	1 500 peak 1 500 peak 500 avg	6 880 000*	20 000
Wide Angle Spherical Gas Bearing Mount	4.4	2 800	1 500 peak 400 avg	3 100 000	20 000

*Includes $6 400 000 for internal vernier implementation.

The recommendation for the telescope fine stabilization system is therefore the gimbal/roll ring system utilizing flexible suspensions/rolling element bearings.

As mentioned earlier, the high energy array is deployed and stowed in the same manner as the telescope complement. Depending on whether CMG or RCS is used for orbiter stabilization, two levels of hardware commonality are possible. The azimuth and elevation coarse pointing/deployment hardware would be utilized for both the high energy array and the telescope complement tube. Regardless of orbiter stabilization technique, the telescope complement requires three axis fine stabilization. For the high energy array, the flexible suspension gimbal system without a roll ring would be required for a RCS stabilized orbiter configuration. For a CMG stabilized orbiter, no fine stabilization would be required for the high energy array. The effects on hardware commonality for the telescope and array as a function of orbiter stabilization are shown in table B3-6. These are estimates of the volume, weight, power, cost, and reliability of combined gimbal-experiment systems when used in conjunction with a CMG- or RCS-stabilized orbiter. The differences result from the need for an additional secondary two degree-of-freedom isolation system for the high energy arrays when the orbiter is stabilized by RCS. This additional system is not required for a CMG stabilized shuttle orbiter.

A CMG **shuttle** orbiter stabilization system was selected principally on the basis of experiment contamination. The candidate RCS systems considered are less expensive than a CMG system and their cost savings over a CMG system would more than offset the apparent cost advantage of the CMG system shown in table B3-6. But cost cannot be the only consideration; mission and experiment objectives must take priority. The principal disadvantage of a RCS system and the reason it was not selected is that it is a major source of experiment contamination and thus would interfere with the objectives of the ASM missions. A CMG system by contrast is virtually contamination free and this is the main reason for its selection.

Table B3-6. Telescope/HE Array Estimated Parameters Vs Orbiter Stabilization Technique

COMBINED TELESCOPE AND HIGH ENERGY ARRAY PARAMETERS / ORBITER STABILIZATION	VOLUME m^3	WEIGHT, kg	POWER, WATTS	COST, $	RELIABILITY MTBF (HR)
CMG	3.9	2 300	3 000 peak 500 avg	800 000	15 000 (telescope) 30 000 (array)
RCS	4.8	2 600	3 000 peak 850 avg	1 070 000	15 000 (telescope) 20 000 (array)

B3.4. SELECTED TELESCOPE FINE STABILIZATION SYSTEM DYNAMICS AND PERFORMANCE ANALYSIS

B3.4.1. Telescope Shuttle Orbiter Dynamics - Assume that the ASM telescope complement and the shuttle orbiter are both rigid bodies and that these two bodies are free to rotate with respect to one another. The telescope complement and shuttle orbiter are attached through a set of three degree-of-freedom gimbals. Neglecting the masses and inertias of these gimbals, assume the telescope and shuttle orbiter are attached as shown in figure B3-13 by a hinge point defined by the geometric center of rotation of the gimbals. From the figure, the equations of motion of body 1, the shuttle orbiter, and body 2, the telescope complement are:

body 1

$$\vec{F}_1+\vec{F}_H=m_1\left(\frac{d^2\vec{B}_1}{dt^2}\right)_R \qquad (130)$$

$$J_1\cdot\left(\frac{d\vec{\omega}_1}{dt}\right)_R+\vec{\omega}_1 x J_1\cdot\vec{\omega}_1=\vec{T}_1+\vec{T}_H+\vec{R}_1 x\vec{F}_H \qquad (131)$$

body 2

$$\vec{F}_2-\vec{F}_H=m_2\left(\frac{d^2\vec{B}_2}{dt}\right)_R \qquad (132)$$

$$J_2\cdot\left(\frac{d\vec{\omega}_2}{dt}\right)+\vec{\omega}_2 x J_2\cdot\vec{\omega}_2=\vec{T}_2-\vec{T}_H+\vec{R}_2 x\vec{F}_H \qquad (133)$$

where

$\vec{F}_H$ is the reactive force transmitted through the hinge point acting on body 1.

$\vec{F}_1$, $\vec{F}_2$ are the resultant forces acting on bodies 1 and 2, respectively minus $\vec{F}_H$.

$\vec{T}_H$ is the reactive torque transmitted through the hinge point acting on body 1.

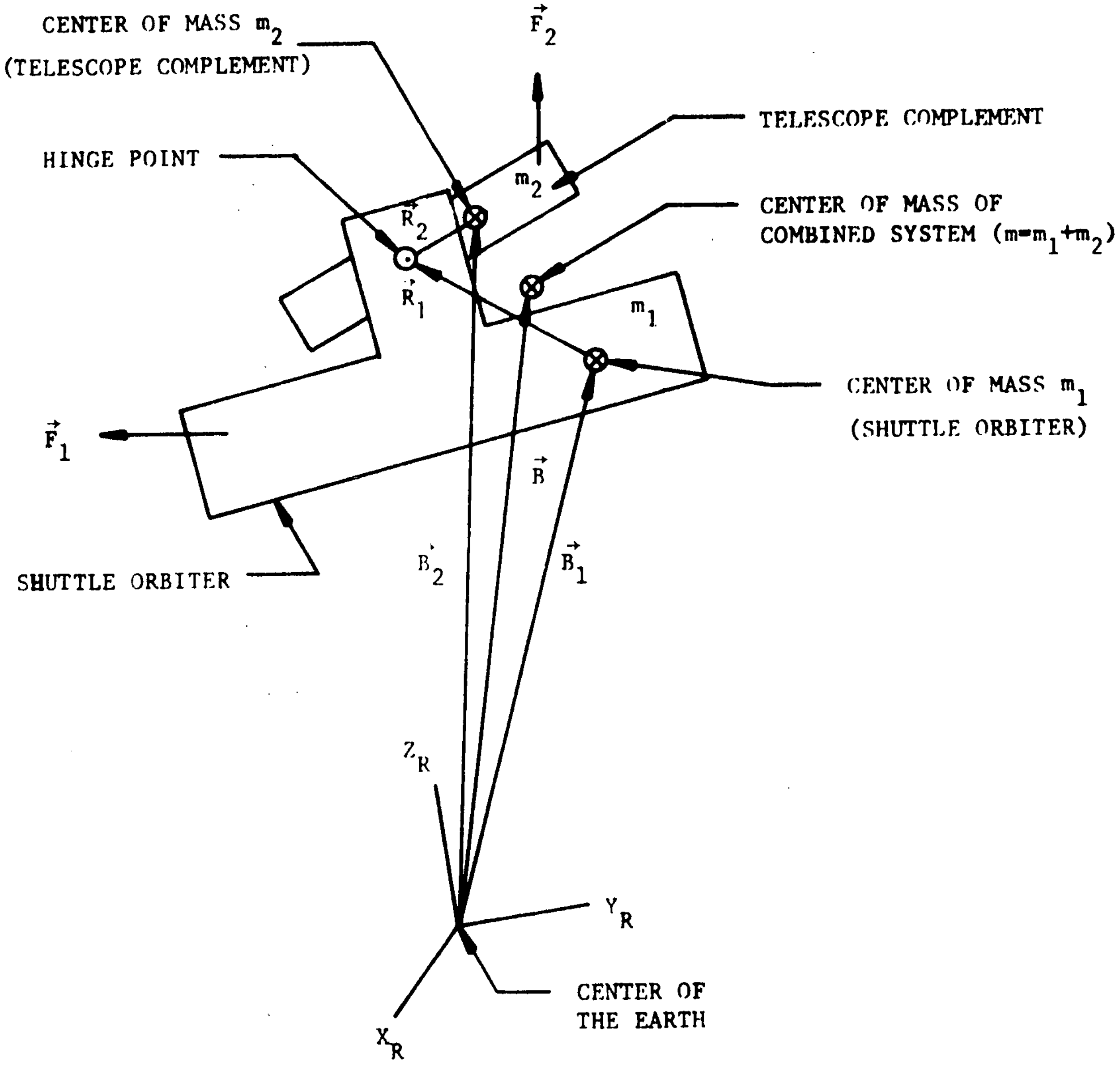

Figure B3-13. Orientation of Body 2 With Respect to Body 1

$\vec{T}_1$, $\vec{T}_2$ are the resultant torques acting on bodies 1 and 2, respectively minus $\vec{T}_H$.

$\vec{\omega}_1$, $\vec{\omega}_2$ are the rotational rates of bodies 1 and 2, respectively. (ω_{1x}, ω_{1y}, ω_{1z}, ω_{2x}, ω_{2y}, ω_{2z})

J_1, J_2 are the inertia tensors of body 1 and 2, respectively. (J_{1x}, J_{1y}, J_{1z}, J_{2x}, J_{2y}, J_{2z})

m_1, m_2 are the masses of bodies 1 and 2, respectively.

$(\frac{d}{dt})_R$, $(\frac{d^2}{dt^2})_R$ are the first and second time derivatives with to the inertial $X_RY_RZ_R$ reference frame, respectively.

Adding equations 130 and 132,

$$\vec{F}_1+\vec{F}_2=m_1(\frac{d^2\vec{B}_1}{dt^2})_R+m_2(\frac{d^2\vec{B}_2}{dt^2})_R=m(\frac{d^2\vec{B}}{dt^2})_R \qquad (134)$$

where

$$m=m_1+m_2$$

Using the geometry shown in figure B3-14 an expression for $\vec{B}_1$ can be written in terms of $\vec{B}$, $\vec{R}_1$, $\vec{R}_2$, m_2 and m as follows:

$$m_1\vec{d}_1=m_2\vec{d}_2 \qquad (135)$$

$\vec{d}_2$ equals

$$\vec{d}_2=\frac{m_1}{m_2}\vec{d}_1 \qquad (136)$$

From figure B3-14,

$$\vec{R}_1-\vec{R}_2=\vec{d}_1+\vec{d}_2 \qquad (137)$$

Substituting equation 136 into 137,

$$\vec{R}_1-\vec{R}_2=(1+\frac{m_1}{m_2})\vec{d}_1=(\frac{m_1+m_2}{m_2})\vec{d}_1=\frac{m}{m_2}\vec{d}_1$$

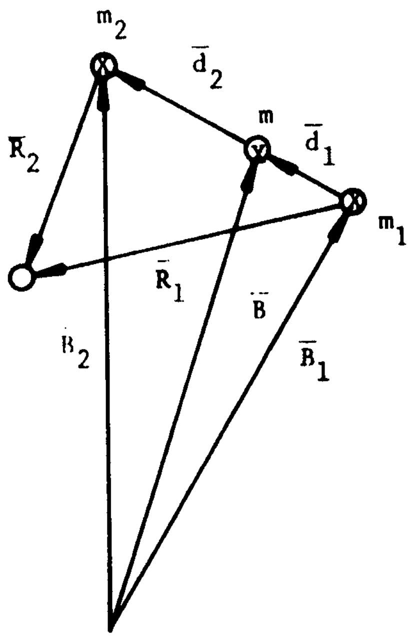

Figure B3-14. Relationship of Center of Masses m_1, m_2, and m With Respect to Hinge Point

$$\vec{d}_1 = \frac{m_2}{m}(\vec{R}_1 - \vec{R}_2) \tag{138}$$

Note that $\vec{B}_1$ equals

$$\vec{B}_1 = \vec{B} - \vec{d}_1 \tag{139}$$

Substituting equation 138 into 139,

$$\vec{B}_1 = \vec{B} - \frac{m_2}{m}(\vec{R}_1 - \vec{R}_2) \tag{140}$$

Substituting equation 140 into 130,

$$\vec{F}_1 + \vec{F}_H = m_1\left(\frac{d^2\vec{B}}{dt^2}\right)_R - \frac{m_1 m_2}{m}\left[\frac{d^2}{dt^2}(\vec{R}_1 - \vec{R}_2)\right]_R \tag{141}$$

Solving for $\vec{F}_H$ using equations 134 and 141,

$$\vec{F}_H = m_1(\vec{F}_1 + \vec{F}_2) - \frac{m_1 m_2}{m}\left[\frac{d^2}{dt^2}(\vec{R}_1 - \vec{R}_2)\right]_R - \vec{F}_1$$

$$= \frac{m_1}{m}\vec{F}_2 - \frac{m_2}{m}\vec{F}_1 - \frac{m_1 m_2}{m}\left[\frac{d^2}{dt^2}(\vec{R}_1 - \vec{R}_2)\right]_R \tag{142}$$

$\left(\frac{d\vec{R}_1}{dt}\right)_R$ and $\left(\frac{d^2\vec{R}_1}{dt^2}\right)_R$ can be written as follows:

$$\left(\frac{d\vec{R}_1}{dt}\right)_R = \vec{\omega}_1 x \vec{R}_1 \tag{143}$$

$$\left(\frac{d^2\vec{R}_1}{dt^2}\right)_R = \frac{d\vec{\omega}_1}{dt} x \vec{R}_1 + \vec{\omega}_1 x \left(\frac{d\vec{R}_1}{dt}\right)_R$$

$$= \frac{d\vec{\omega}_1}{dt} x \vec{R}_1 + \vec{\omega}_1 x (\vec{\omega}_1 x \vec{R}_1) \tag{144}$$

Body 2 can be thought of as a moving part of body 1, therefore, $\vec{R}_2$ is a variable with respect to body 1. Let

$$\vec{\omega} = \vec{\omega}_2 - \vec{\omega}_1 \tag{145}$$

$\vec{\omega}$ is the angular velocity of body 2 with respect to body 1.

$(\frac{d\vec{R}_2}{dt})_R$ and $(\frac{d^2\vec{R}_2}{dt^2})_R$ equal

$$(\frac{d\vec{R}_2}{dt})_R=(\frac{d\vec{R}_2}{dt})_{m1}+\vec{\omega}_1 x\vec{R}_2 \tag{146}$$

$$(\frac{d^2\vec{R}_2}{dt^2})_R=(\frac{d^2\vec{R}_2}{dt^2})_{m1}+\frac{d\vec{\omega}_1}{dt}x\vec{R}_2+\vec{\omega}_1 x(\frac{d\vec{R}_2}{dt})_R \tag{147}$$

where $(\frac{d\vec{R}_2}{dt})_{m1}$ and $(\frac{d^2\vec{R}_2}{dt^2})_{m1}$ are the first and second derivative of $\vec{R}_2$ with respect to body 1, respectively. $(\frac{d\vec{R}_2}{dt})_{m1}$ and $(\frac{d^2\vec{R}_2}{dt^2})_{m2}$ equal

$$(\frac{d\vec{R}_2}{dt})_{m1}=\vec{\omega}x\vec{R}_2 \tag{148}$$

$$\begin{aligned}(\frac{d^2\vec{R}_2}{dt^2})_{m1}&=\frac{d\vec{\omega}}{dt}x\vec{R}_2+\vec{\omega}x(\frac{d\vec{R}_2}{dt})_{m1}\\ &=\frac{d\vec{\omega}}{dt}x\vec{R}_2+\vec{\omega}x(\vec{\omega}x\vec{R}_2)\end{aligned} \tag{149}$$

Substituting equations 148 and 149 into 146 and 147, $(\frac{d\vec{R}_2}{dt})_R$ and $(\frac{d^2\vec{R}}{dt^2})_R$ equal

$$(\frac{d\vec{R}_2}{dt})_R=\vec{\omega}x\vec{R}_2+\vec{\omega}_1 x\vec{R}_2 \tag{150}$$

$$\begin{aligned}(\frac{d^2\vec{R}_2}{dt^2})_R=&\frac{d\vec{\omega}}{dt}x\vec{R}_2+\vec{\omega}x(\vec{\omega}x\vec{R}_2)+\vec{\omega}_1 x(\vec{\omega}x\vec{R}_2)\\ &+\frac{d\vec{\omega}_1}{dt}x\vec{R}_2+2\vec{\omega}_1 x(\vec{\omega}xR_2)\end{aligned} \tag{151}$$

Substitute equations 150 and 151 into equation 142 and let

$$M=\frac{m_1 m_2}{m} \tag{152}$$

$\vec{F}_H$ equals

$$\vec{F}_H = \frac{m_1}{m}\vec{F}_2 - \frac{m_2}{m}\vec{F}_1 - M[\frac{d\vec{\omega}_1}{dt}x\vec{R}_1 + \vec{\omega}_1 x(\vec{\omega}_1 x\vec{R}_1)$$

$$- \frac{d\vec{\omega}}{dt}x\vec{R}_2 - \vec{\omega}x(\vec{\omega}x\vec{R}_2) - \vec{\omega}_1 x(\vec{\omega}x\vec{R}_2)$$

$$- \frac{d\vec{\omega}_1}{dt}x\vec{R}_2 - 2\vec{\omega}_1 x(\vec{\omega}x\vec{R}_2)] \tag{153}$$

Substituting this expression for $\vec{F}_H$ in the two rotational equations of motion 131 and 133,

$$J_1 \cdot \frac{d\vec{\omega}_1}{dt} + \vec{\omega}_1 xJ_1 \cdot \vec{\omega}_1 = \vec{T}_1 + \vec{T}_H + \vec{R}_1 x[\frac{m_1}{m}\vec{F}_2 - \frac{m_2}{m}\vec{F}_1$$

$$-M(\frac{d\vec{\omega}_1}{dt}xR_1) - M\vec{\omega}_1 x(\vec{\omega}_1 x\vec{R}_1) + M(\frac{d\vec{\omega}}{dt}x\vec{R}_2)$$

$$+M\vec{\omega}x(\vec{\omega}x\vec{R}_2) + M\vec{\omega}_1 x(\vec{\omega}_1 x\vec{R}_2) + M(\frac{d\vec{\omega}_1}{dt}x\vec{R}_2)$$

$$-2M\vec{\omega}_1 x(\vec{\omega}x\vec{R}_2)] \tag{154}$$

$$J_2 \cdot \frac{d\vec{\omega}_2}{dt} + \vec{\omega}_2 xJ_2 \cdot \vec{\omega}_2 = \vec{T}_2 - \vec{T}_H - \vec{R}_2 x[\frac{m_1}{m}\vec{F}_2 - \frac{m_2}{m}\vec{F}_1$$

$$-M(\frac{d\vec{\omega}_1}{dt}x\vec{R}_1) - M\vec{\omega}_1 x(\vec{\omega}_1 x\vec{R}_1) + M(\frac{d\vec{\omega}}{dt}x\vec{R}_2)$$

$$+M\vec{\omega}x(\vec{\omega}x\vec{R}_2) + M\vec{\omega}_1 x(\vec{\omega}_1 x\vec{R}_2) + M(\frac{d\vec{\omega}_1}{dt}x\vec{R}_2)$$

$$-2M\vec{\omega}_1 x(\vec{\omega}x\vec{R}_2)] \tag{155}$$

In order to develop a linear model, all terms in the equations that contain products of $\vec{\omega}$, $\vec{\omega}_1$, $\vec{\omega}_2$, $\frac{d\vec{\omega}}{dt}$, $\frac{d\vec{\omega}_1}{dt}$, and $\frac{d\vec{\omega}_2}{dt}$ are eliminated. The resulting linear rotational equations of motion are:

$$J_1 \circ \frac{d\vec{\omega}_1}{dt} = \vec{T}_1 + \vec{T}_H + \frac{m_1}{m}\vec{R}_1 x \vec{F}_2 - \frac{m_2}{m}\vec{R}_1 x \vec{F}_1$$

$$-M[(\vec{R}_1 \circ \vec{R}_1)\frac{d\vec{\omega}_1}{dt} - (\vec{R}_1 \circ \frac{d\vec{\omega}_1}{dt})\vec{R}_1] + M[(\vec{R}_1 \circ \vec{R}_2)\frac{d\vec{\omega}_2}{dt}$$

$$-(\vec{R}_1 \circ \frac{d\vec{\omega}_2}{dt})\vec{R}_2] \tag{156}$$

$$J_2 \circ \frac{d\vec{\omega}_2}{dt} = \vec{T}_2 - \vec{T}_H - \frac{m_1}{m}\vec{R}_2 x \vec{F}_2 + \frac{m_2}{m}\vec{R}_2 x \vec{F}_1$$

$$+M[(\vec{R}_2 \circ \vec{R}_1)\frac{d\vec{\omega}_1}{dt} - (\vec{R}_2 \circ \frac{d\vec{\omega}_1}{dt})\vec{R}_1] - M[(\vec{R}_2 \circ \vec{R}_2)\frac{d\vec{\omega}_2}{dt}$$

$$-(\vec{R}_2 \circ \frac{d\vec{\omega}_2}{dt})\vec{R}_2] \tag{157}$$

Assume that the motion of body 2 does not significantly effect the dynamics of body 1. This assumption is valid since the inertias of the shuttle orbiter, body 1, are much larger than those of the telescope complement, body 2, and also because the relative motion between the orbiter and telescope complement while the telescope complement's fine stabilization system is operating will be small. The motion of body 1 can be thought of as input to the dynamics of body 2. Assume that the reactive torque $\vec{T}_H$ is small ($\vec{T}_H \approx 0$). The torque $\vec{T}_2$ acting on body 2 is assumed to equal

$$\vec{T}_2 = \vec{T}_{2D} - \vec{T}_{2C} \tag{158}$$

where

$\vec{T}_{2D}$ is the resultant disturbance torques acting on body 2. (T_{2Dx}, T_{2Dy}, T_{2Dz})

$\vec{T}_{2C}$ is the fine stabilization control torque acting on body 2. (T_{2Cx}, T_{2Cy}, T_{2Cz})

The three axial rotational equations of motion for body 2 are

$$[J_{2x}+M(R_{2y}{}^2+R_{2z}{}^2)]\frac{d\omega_{2x}}{dt}=T_{Dx}-T_{2Cx}+MR_{2x}R_{2y}\frac{d\omega_{2y}}{dt}$$

$$+MR_{2x}R_{2z}\frac{d\omega_{2z}}{dt} \tag{159}$$

$$[J_{2y}+M(R_{2x}{}^2+R_{2z}{}^2)]\frac{d\omega_{2y}}{dt}=T_{Dy}-T_{2Cy}+MR_{2x}R_{2y}\frac{d\omega_{2x}}{dt}$$

$$+MR_{2x}R_{2z}\frac{d\omega_{2z}}{dt} \tag{160}$$

$$[J_{2z}+M(R_{2x}{}^2+R_{2y}{}^2)]\frac{d\omega_{2z}}{dt}=T_{Dz}-T_{2Cz}+MR_{2x}R_{2z}\frac{d\omega_{2x}}{dt}$$

$$+MR_{2y}R_{2z}\frac{d\omega_{2y}}{dt} \tag{161}$$

where

$$T_{Dx}=T_{2Dx}-\frac{m_1}{m}(R_{2y}F_{2z}-R_{2z}F_{2y})+\frac{m_2}{m}(R_{2y}F_{1z}-R_{2z}F_{1y})$$

$$+M(R_{1y}R_{2y}+R_{1z}R_{2z})\frac{d\omega_{1x}}{dt}-MR_{1x}R_{2y}\frac{d\omega_{1y}}{dt}-MR_{1x}R_{2z}\frac{d\omega_{1z}}{dt}$$

$$T_{Dy}=T_{2Dy}-\frac{m_1}{m}(R_{2z}F_{2x}-R_{2x}F_{2z})+\frac{m_2}{m}(R_{2z}F_{1x}-R_{2x}F_{1z})$$

$$-MR_{1y}R_{2x}\frac{d\omega_{1x}}{dt}+M(R_{1x}R_{2x}+R_{1z}R_{2z})\frac{d\omega_{1y}}{dt}-MR_{1y}R_{2z}\frac{d\omega_{1z}}{dt}$$

$$T_{Dz}=T_{2Dz}-\frac{m_1}{m}(R_{2x}F_{2y}-R_{2y}F_{2x})+\frac{m_2}{m}(R_{2x}F_{1y}-R_{2y}F_{1x})$$

$$-MR_{1z}R_{2x}\frac{d\omega_{1x}}{dt}-MR_{1z}R_{2y}\frac{d\omega_{1y}}{dt}+M(R_{1x}R_{2x}+R_{1y}R_{2y})\frac{d\omega_{1z}}{dt}$$

Figure B3-15 is a block diagram of this system. $H_x(s)$, $H_y(s)$, and $H_z(s)$ are the transfer functions for the X, Y, and Z axis fine stabilization actuators, respectively. ε_x, ε_y, and ε_z are the rotational displacements of the X, Y, and Z axes due to the T_{Dx}, T_{Dy}, and T_{Dz} disturbances.

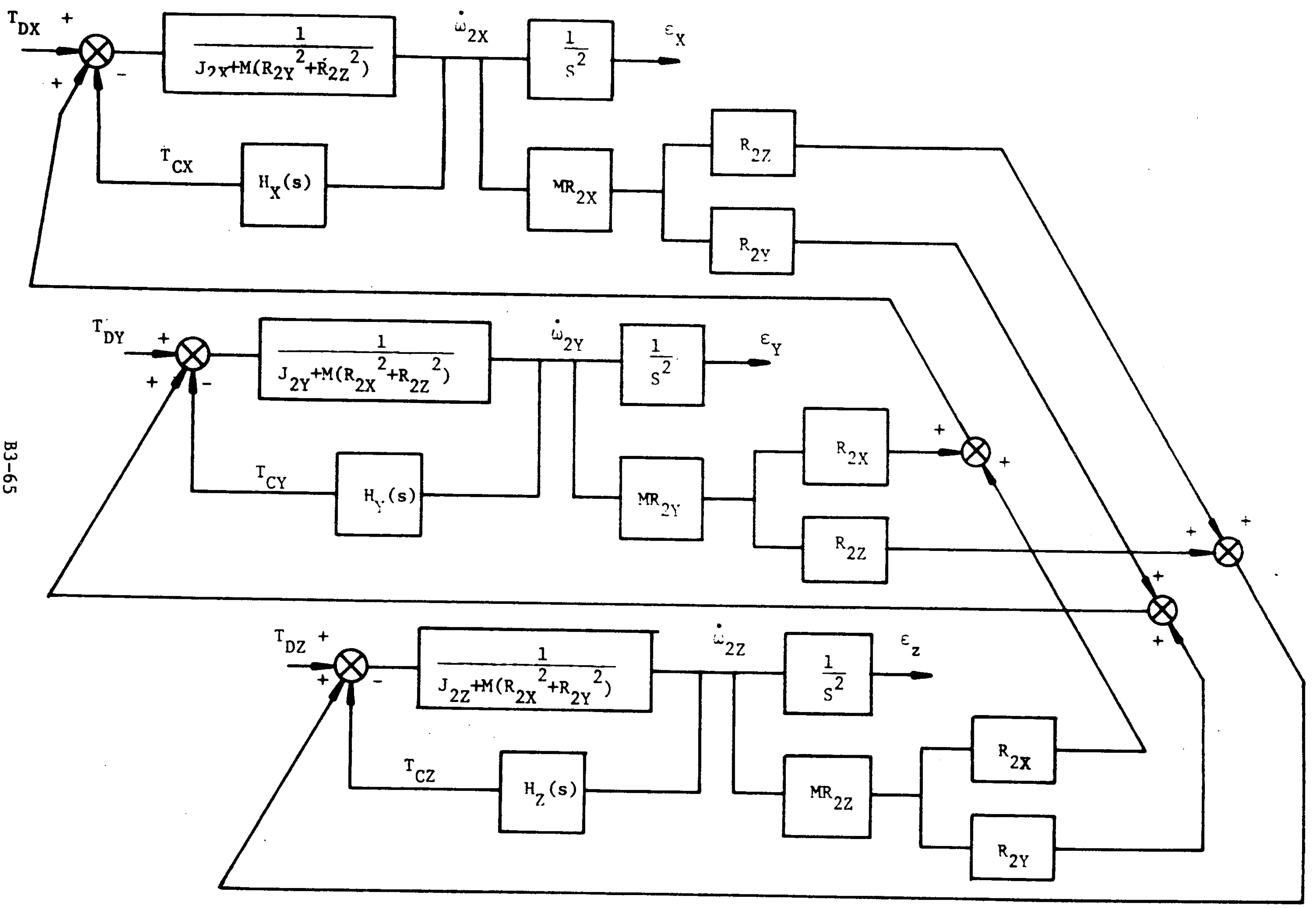

Figure B3-15. Block Diagram of Telescope Fine Stabilization System

The Laplace transforms of ε_x, ε_y, and ε_z as a function of T_{Dx}, T_{Dy}, and T_{Dz} are:

$$\varepsilon_x(s) = \frac{G_x(s)[1-M^2R_{2y}{}^2R_{2z}{}^2G_y(s)G_z(s)]T_{Dx}(s)}{\Delta' s^2} + \frac{MR_{2x}R_{2y}G_x(s)G_y(s)[1+MR_{2z}{}^2G_z(s)]T_{Dy}(s)}{\Delta' s^2} + \frac{MR_{2x}R_{2z}G_x(s)G_z(s)[1+MR_{2y}{}^2G_y(s)]T_{Dz}(s)}{\Delta' s^2} \tag{162}$$

$$\varepsilon_y(s) = \frac{MR_{2x}R_{2y}G_x(s)G_y(s)[1+MR_{2z}{}^2G_z(s)]T_{Dx}(s)}{\Delta' s^2} + \frac{G_y(s)[1-M^2R_{2x}{}^2F_{2z}{}^2G_x(s)G_z(s)]T_{Dy}(s)}{\Delta' s^2} + \frac{MR_{2y}R_{2z}G_y(s)G_z(s)[1+MR_{2x}{}^2G_x(s)]T_{Dz}(s)}{\Delta' s^2} \tag{163}$$

$$\varepsilon_z(s) = \frac{MR_{2x}R_{2z}G_x(s)G_z(s)[1+MR_{2y}{}^2G_y(s)]T_{Dx}(s)}{\Delta' s^2} + \frac{MR_{2y}R_{2z}G_y(s)G_z(s)[1+MR_{2x}{}^2G_x(s)]T_{Dy}(s)}{\Delta' s^2} + \frac{G_z(s)[1-M^2R_{2x}{}^2R_{2y}{}^2G_x(s)G_y(s)]T_{Dz}(s)}{\Delta' s^2} \tag{164}$$

where

$$\Delta' = 1-M^2R_{2x}{}^2R_{2y}{}^2G_x(s)G_y(s)-M^2R_{2x}{}^2R_{2z}{}^2G_x(s)G_y(s)$$
$$-M^2R_{2y}{}^2R_{2z}{}^2G_y(s)G_z(s)-2M^3R_{2x}{}^2R_{2y}{}^2R_{2z}{}^2G_x(s)G_y(s)G_z(s)$$

The transfer functions $G_x(s)$, $G_y(s)$, and $G_z(s)$ contained in the Laplace transforms of ε_x, ε_y, and ε_z are

$$G_x(s)= \frac{1}{J_{2x}+M(R_{2y}^2+R_{2z}^2)+H_x(s)} \tag{165}$$

$$G_y(s)= \frac{1}{J_{2y}+M(R_{2x}^2+R_{2z}^2)+H_y(s)} \tag{166}$$

$$G_z(s)= \frac{1}{J_{2z}+M(R_{2x}^2+R_{2y}^2)+H_z(s)} \tag{167}$$

B3.4.2. Telescope Fine Stabilization Servo Design - The transfer functions $H_x(s)$, $H_y(s)$, and $H_z(s)$ shown in figure B3-15 correspond to the pitch, yaw, and roll telescope fine stabilization actuators, respectively. The telescope fine stabilization system utilizes flex-pivot suspension to stabilize the telescopes in pitch and yaw and a servoed roll ring to isolate the telescopes in roll. In this section, the actuator transfer functions $H_x(s)$, $H_y(s)$, and $H_z(s)$ are derived in order to perform a preliminary performance analysis of the system using the block diagram contained in the figure. Note that $H_x(s)$, $H_y(s)$, and $H_z(s)$ are the transfer functions relating the control torque $\vec{T}_c$ as a function of the telescope rotational acceleration $\dot{\vec{\omega}}$.

$$H_x(s)= \frac{T_{cx}(s)}{\dot{\omega}_x(s)} \tag{168}$$

$$H_y(s)= \frac{T_{cy}(s)}{\dot{\omega}_y(s)} \tag{169}$$

$$H_z(s)= \frac{T_{cz}(s)}{\dot{\omega}_z(s)} \tag{170}$$

Figure B3-16 contains the mechanical networks used in this report to describe the dynamics of the flex-pivot and roll ring systems. The flex-pivots are assumed to be frictionless springs

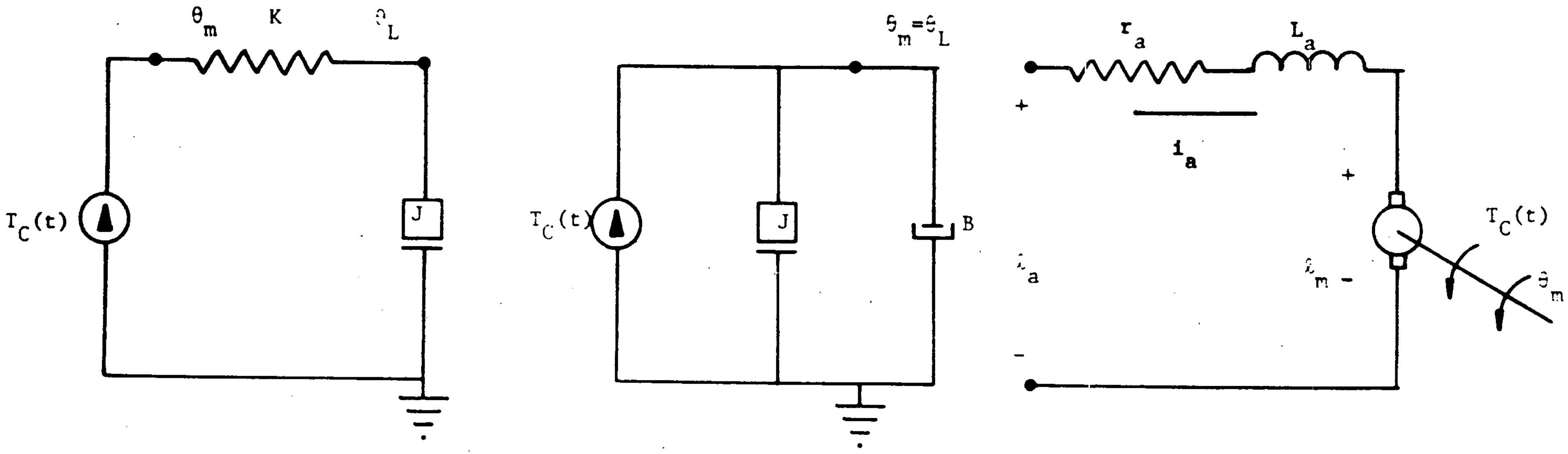

(a) Pitch and Yaw Actuator Model

(b) Roll Actuator Model

(c) DC Motor Electrical Armature Network

SYMBOLS

LOAD:

J - LOAD INERTIA

θ_L - LOAD ANGULAR DISPLACEMENT

K - FLEX-POINT SPRING CONSTANT

B - ROLL RING DAMPING COEFFICIENT

MOTOR:

$T_C(t)$ - MOTOR OUTPUT TORQUE

θ_m - MOTOR ANGULAR DISPLACEMENT

r_a - ARMATURE RESISTANCE

L_a - ARMATURE INDUCTANCE

e_m - MOTOR BACK EMF

e_a - ARMATURE EXCITATION VOLTAGE

i_a - ARMATURE CURRENT

Figure B3-16. Flex-Pivot, Roll Ring, and DC Motor Models

with a rotational spring constant K. The dynamics of the roll ring are modeled by a mechanical rotational damper with a damping coefficient B. This damper describes the damping action of this system due to the friction between its various elements. Also contained in figure B3-16 is the electrical armature winding network describing the dynamics of the DC motor used to drive these three systems.

Assume that the telescope center of mass is located at the intersection of the three control axes; R_{2x}, R_{2y}, and R_{2z} equal zero. The system block diagram of figure B3-15 reduces to the three independent pitch, yaw, and roll block diagrams shown in figure B3-17. This figure is used to determine $H_x(s)$, $H_y(s)$, and $H_z(s)$. Assume that the inertia characteristics of the telescope complement are:

$$J_{2x}=J_{2y}=1\ 900\ \text{kg-m}^2\ (1\ 400\ \text{slug-feet}^2) \tag{171}$$

$$J_{2x}=800\ \text{kg-m}^2\ (600\ \text{slug-feet}^2) \tag{172}$$

B3.4.2.1. DC Motor Dynamics - The output torque of the DC motor $T_c(t)$ is proportional to the armature current i_a.

$$T_c(t)=K_T i_a \tag{173}$$

The loop equation for the armature winding shown in (c) of figure B3-16 is

$$L_a \frac{di_a}{dt} + r_a i_a + 3_m = e_a \tag{174}$$

The back EMF voltage, e_m, is proportional to the motor speed.

$$e_m = K_m \frac{d\theta_m}{dt} \tag{175}$$

Substituting equation 145 into 144.

$$L_a \frac{di_a}{dt} + r_a i_a + K_m \frac{d\theta_m}{dt} = e_a \tag{176}$$

B3.4.2.2. Flex-Pivot Dynamics - Using (a) of figure B3-16, the dynamics of the flex-pivot stabilization system are

$$T_c(t)=K(\theta_m-\theta_L)=J\frac{d^2\theta_L}{dt^2} \tag{177}$$

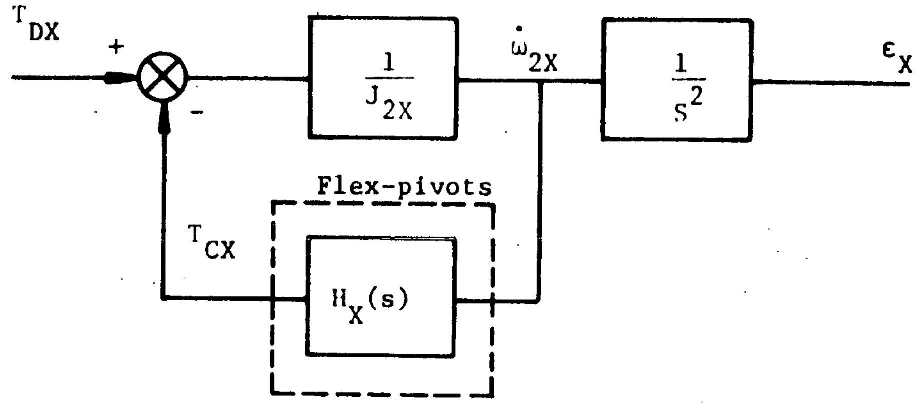

(a) Pitch Axis Control System

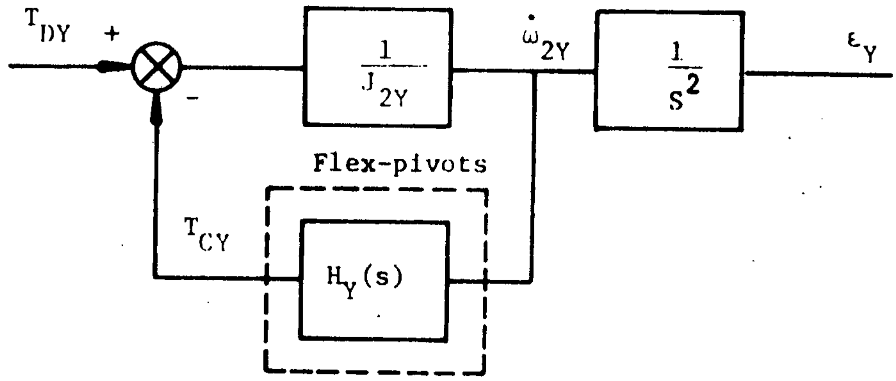

(b) Yaw Axis Control System

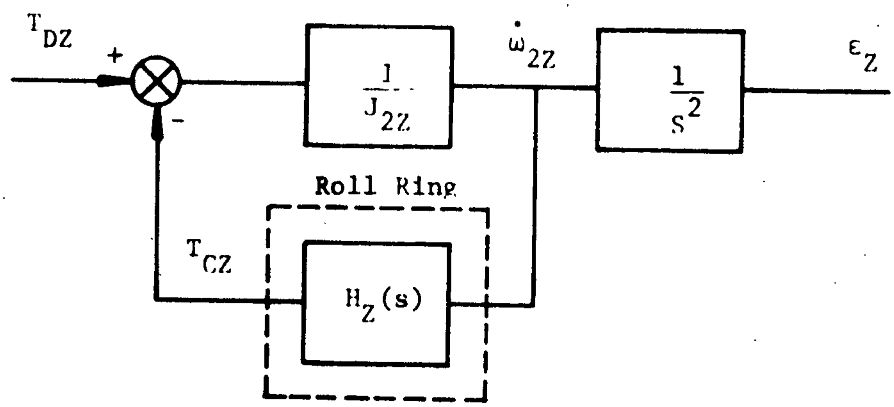

(c) Roll Axis Control System

Figure B3-17. Block Diagram of Telescope Fine Stabilization System With $R_{2X}=R_{2Y}=R_{2Z}=0$

Using equations 173 and 177, i_a and θ_m equal

$$i_a = \frac{J}{K_T} \frac{d^2\theta_L}{dt^2} \tag{178}$$

$$\theta_m = \frac{J}{K} \frac{d^2\theta_2}{dt^2} + \theta_L \tag{179}$$

Substituting equations 178 and 179 into 176,

$$\left(\frac{L_a J}{K_T} + \frac{K_m J}{K}\right)\frac{d^3\theta_L}{dt^3} + \frac{r_a J}{K_T} \frac{d^2\theta_L}{dt^2} + K_m \frac{d\theta_L}{dt} = e_a \tag{180}$$

Assume the armature inductance L_a equals zero,

$$\frac{K_m J}{K} \frac{d^3\theta_L}{dt^3} + \frac{r_a J}{K_T} \frac{d^2\theta_L}{dt^2} + K_m \frac{d\theta_L}{dt} = e_a \tag{181}$$

From equation 181, the Laplace transform of θ_L equals

$$\theta_L(s) = \frac{e_a(s)}{s\left(\frac{K_m J}{K} s^2 + \frac{r_a J}{K_T} + K_m\right)} \tag{182}$$

Assume the armature excitation voltage e_a is proportional to the telescope body rate ω and position ε. The Laplace transform of $e_a(s)$ equals

$$e_a(s) = \frac{K_r \dot{\omega}(s)}{s} + \frac{K_p \dot{\omega}(s)}{s^2} = \frac{K_r\left(s + \frac{K_p}{K_r}\right)\dot{\omega}(s)}{s^2} \tag{183}$$

K_r and K_p are the constant rate and position control gains, respectively. Using equations 177, 182, and 183, the transfer function $\frac{T_c(s)}{\dot{\omega}(s)}$ equals

$$\frac{T_c(s)}{\dot{\omega}(s)} = \frac{\frac{KK_r}{K_m}\left(s + \frac{K_p}{K_r}\right)}{s\left[s^2 + \frac{Kr_a}{K_m K_T} s + \frac{K}{J}\right]} \tag{184}$$

From equation 184 $H_x(s)$ and $H_y(s)$ equal

$$H_x(s)=\frac{T_{cx}(s)}{\dot{\omega}_x(s)}=\frac{\frac{KK_{rx}}{K_m}(s+\frac{K_{px}}{K_{rx}})}{s[s^2+\frac{Kr_a}{K_mK_T}s+\frac{K}{J_{2x}}]} \tag{185}$$

$$H_y(s)=\frac{T_{cy}(s)}{\dot{\omega}_y(s)}=\frac{\frac{KK_{ry}}{K_m}(s+\frac{K_{py}}{K_{ry}})}{s[s^2+\frac{Kr_a}{K_mK_T}s+\frac{K}{J_{2y}}]} \tag{186}$$

K_{px}, K_{rx}, K_{py}, and K_{ry} are the rate and position gains associated with the X and Y axes.

Using figure B3-17, assume the actuation systems $\frac{T_{cx}(s)}{T_{Dx}(s)}$ and $\frac{T_{cy}(s)}{T_{DY}(s)}$ have 5 Hz bandwidths. Since the inertias J_{2x} and J_{2y} are equal and because R_{2x}, R_{2y}, and R_{2z} are assumed to be zero, the transfer functions $G_x(s)$ and $G_y(s)$ are the same. The transfer function $\frac{T_{cx}(s)}{T_{Dx}(s)}$ equals

$$\frac{T_{cx}(s)}{T_{Dx}(s)}=\frac{K'(s+Z)}{S^3+Rs^2+(\frac{K}{J_{2x}}+K')+K'Z} \tag{187}$$

where

$$K'=\frac{KK_{rx}}{K_mJ_{2x}}$$

$$Z=\frac{K_{px}}{K_{rx}}$$

$$R=\frac{Kr_a}{K_mK_T}$$

Let

$$s=j\omega$$

where ω corresponds to the closed loop bandwidth of $\frac{T_{cx}(s)}{T_{Dx}(s)}$ in radians/second. (ω=31.4 radians/second)

$$\frac{T_{cx}(j\omega)}{T_{Dx}(j\omega)} = \frac{K'(j\omega+Z)}{j[(\frac{K}{J_{2x}}+K')\omega-\omega^3]+K'Z-R\omega^2} \tag{188}$$

Since ω corresponds to the bandwidth of $\frac{T_{cx}(s)}{T_{Dx}(s)}$,

$$\left|\frac{T_{cx}(j\omega)}{T_{Dx}(j\omega)}\right|^2=0.5 \tag{189}$$

The following relationship results from equations 188 and 189,

$$(K')^2(Z^2+\omega^2)=0.5[(\frac{K}{J_{2x}}+K')\omega-\omega^3]^2+0.5[K'Z-R\omega^2]^2 \tag{190}$$

The above expression can be written as

$$(K')^2+aK'+b=0 \tag{191}$$

where

$$a=\frac{2(ZR\omega^2-\frac{K}{J}\omega^2+\omega^4)}{Z^2+\omega^2}$$

$$b=\frac{\frac{2K\omega^4}{J_{2x}}-(\frac{K\omega}{J_{2x}})^2-\omega^6-R^2\omega^4}{Z^2+\omega^2}$$

In terms of a and b, K' equals

$$K'=\frac{-a+\sqrt{a^2-4b}}{2} \tag{192}$$

Assume the DC motor and flex-pivots have the following parameters:

DC motor:

r_a=1.5 ohms

K_T=0.52 ft-lb/amp=0.719 N-m/amp

K_m=0.72 volts/(rad/sec)

Flex-pivots:

K=6 N-m/rad

Also assume that the gain ratio Z equals 0.3. For a 5 Hz bandwidth system, ω equals 31.4 radians/second. The resulting values of a, b, and K' are

$$a \cong 2\omega^2 = 1.97\times10^3$$

$$b \cong \omega^4 - R^2\omega^2 = -1.27\times10^6$$

$$K' = 510$$

The rate and position gains K_{rx} and K_{px} equal

$$K_{rx} = \frac{K_m J_{2x} K'}{K} = 1.16\times10^5 \text{ volts/(rad/sec)}$$

$$K_{px} = ZK_{rx} = 3.49\times10^4 \text{ volts/rad}$$

Since $H_x(s)$ and $H_y(s)$ are the same, the rate and position gains K_{ry} and K_{py} for $H_y(s)$ are

$$K_{ry} = K_{rx} = 1.16\times10^5 \text{ volts/(rad/sec)}$$

$$K_{py} = K_{px} = 3.49\times10^4 \text{ volts/rad}$$

The above gains K_{rx}, K_{px}, K_{ry}, and K_{py} completely define the transfer functions $H_x(s)$ and $H_y(s)$.

$$H_x(s) = \frac{\frac{KK_{rx}}{K_m}\left(s+\frac{K_{px}}{K_{rx}}\right)}{s\left[s^2+\frac{Kr_a}{K_mK_T}s+\frac{K}{J_{2x}}\right]} \tag{185}$$

$$H_y(s) = \frac{\frac{KK_{ry}}{K_m}\left(s+\frac{K_{py}}{K_{ry}}\right)}{s\left[s^2+\frac{Kr_a}{K_mK_T}s+\frac{K}{J_{2y}}\right]} \tag{186}$$

For the general case where R_{2x}, R_{2y}, and R_{2z} are not zero, the transfer functions $H_x(s)$ and $H_y(s)$ are

$$H_x(s) = \frac{\frac{KK_{rx}}{K_m}\left(s+\frac{K_{px}}{K_{rx}}\right)}{s\left[s^2+\frac{Kr_a}{K_mK_T}s+\frac{K}{J_{2x}+M(R_{2y}^{\,2}+R_{2z}^{\,2})}\right]} \tag{193}$$

$$H_y(s) = \frac{\frac{KK_{ry}}{K_m}\left(s+\frac{K_{py}}{K_{ry}}\right)}{s\left[s^2+\frac{Kr_a}{K_mK_T}s+\frac{K}{J_{2y}+M(R_{2x}^{\,2}+R_{2z}^{\,2})}\right]} \tag{194}$$

From equations 165 and 166, the transfer functions $G_x(s)$ and $G_y(s)$ are

$$G_x(s) = \frac{s\left[s^2+\frac{Kr_a}{K_mK_T}s+\frac{K}{J_{2x}'}\right]}{J_{2x}'s\left[s^2+\frac{Kr_a}{K_mK_T}s+\frac{K}{J_{2x}'}\right]+\frac{KK_{rx}}{K_m}\left(s+\frac{K_{px}}{K_{rx}}\right)} \tag{195}$$

$$G_y(s) = \frac{s\left[s^2+\frac{Kr_a}{K_mK_T}s+\frac{K}{J_{2y}'}\right]}{J_{2y}'s\left[s^2+\frac{Kr_a}{K_mK_T}s+\frac{K}{J_{2y}'}\right]+\frac{KK_{ry}}{K_m}\left(s+\frac{K_{py}}{K_{ry}}\right)} \tag{196}$$

where

$$J_{2x}'=J_{2x}+M(R_{2y}^2+R_{2z}^2)$$
$$J_{2y}'=J_{2y}+M(R_{2x}^2+R_{2z}^2)$$

B3.4.2.3. Roll-Ring Dynamics - Using (c) of figure B3-16, the dynamics of the roll ring stabilization system are

$$T_c(t)=J\frac{d^2\theta_L}{dt^2}+B\frac{d\theta_L}{dt} \tag{197}$$

Using equations 173 and 196, i_a equals

$$i_a=\frac{J}{K_T}\frac{d^2\theta_L}{dt^2}+\frac{B}{K_T}\frac{d\theta_L}{dt} \tag{198}$$

Note that

$$\theta_m=\theta_L \tag{199}$$

Substituting the above expressions for i_a and θ_m into the DC motor armature loop equation, equation 176

$$\frac{L_aJ}{K_T}\frac{d^3\theta_L}{dt^3}+\left(\frac{L_aB}{K_T}+\frac{r_aJ}{K_T}\right)\frac{d^2\theta_L}{dt^2}+\left(\frac{r_aB}{K_T}+K_m\right)\frac{d\theta_L}{dt}=e_a \tag{200}$$

Assume L_a equals zero.

$$\frac{r_aJ}{K_T}\frac{d^2\theta_L}{dt^2}+\left(\frac{r_aB}{K_T}+K_m\right)\frac{d\theta_L}{dt}=e_a \tag{201}$$

From equation 201, the Laplace transform of θ_L equals

$$\theta_L(s)=\frac{e_a(s)}{s\left[\frac{r_aJ}{K_T}s+\left(\frac{r_aB}{K_T}+K_m\right)\right]} \tag{202}$$

Assume

$$\frac{r_a B}{K_T} = 0.1\ K_m$$

B then equals

$$B = 0.1 \frac{K_m K_T}{r_a} \tag{203}$$

Assume the DC motors that drive the roll ring and flex-pivot system are the same. Substituting the appropriate motor parameters into equation 203, B equals

$$B = 0.0345\ \text{N-m/(rad/sec)}$$

Just as in the flex-pivot case, assume that the armature excitation voltage e_a is proportional to the telescope body rate ω and position ε. $e_a(s)$ equals

$$e_a(s) = \frac{K_r(s + \frac{K_p}{K_r})\dot{\omega}(s)}{s^2} \tag{183}$$

Using equations 183, 197, and 202, the transfer function $\frac{T_c(s)}{\omega(s)}$ equals

$$\frac{T_c(s)}{\dot{\omega}(s)} = \frac{\frac{K_T K_r}{r_a}(s + \frac{B}{J})(s + \frac{K_p}{K_r})}{s^2[s + \frac{K_T}{r_a J}(\frac{r_a B}{K_T} + K_m)]} \tag{204}$$

From equation 204, the transfer function, $H_a(s)$ equals

$$H_z(s) = \frac{T_{cz}(s)}{\dot{\omega}_z(s)} = \frac{\frac{K_T K_{rz}}{r_a}(s + \frac{B}{J_{2z}})(s + \frac{K_p}{K_r})}{s^2[s + \frac{K_T}{r_a J_{2z}}(\frac{r_a B}{K_T} + K_m)]} \tag{205}$$

K_{rz} and K_{pz} are the rate and position gains associated with the Z axis stabilization system.

Assume that the roll actuator system $\frac{T_{cz}(s)}{T_{Dz}(s)}$ has a 2 Hz bandwidth. For R_{2x}, R_{2y}, and R_{2z} equal to zero, $\frac{T_{cz}(s)}{T_{Dz}(s)}$ equals

$$\frac{T_{cz}(s)}{T_{Dz}(s)} = \frac{K'(s+\frac{B}{J_{2z}})(s+Z)}{s^3+(\frac{B}{J_{2z}}+\frac{K_T K_m}{r_a J_{2z}}+K')s^2+K'(\frac{B}{J_{2z}}+Z)s+\frac{K'BZ}{J_{2z}}} \tag{206}$$

where

$$K' = \frac{K_T K_{rz}}{r_a J_{2z}}$$

$$Z = \frac{K_{pz}}{K_{rz}}$$

To compute the gains K_{rz} and K_{pz}, let B equal zero and

$$s=j\omega$$

where ω corresponds to the closed loop bandwidth of $\frac{T_{cz}(s)}{T_{Dz}(s)}$ in radians/second. (ω=12.57 radians/second)

$$\frac{T_{cz}(j\omega)}{T_{Dz}(j\omega)} = \frac{K'(j\omega+Z)}{jK'\omega+(K'z-\omega^2)} \tag{207}$$

Since ω corresponds to the bandwidth of $\frac{T_{cz}(s)}{T_{Dz}(s)}$,

$$\left|\frac{T_{cz}(j\omega)}{T_{Dz}(j\omega)}\right|^2=0.5 \tag{208}$$

The following relationship results from equations 207 and 208,

$$(K')^2 + \frac{2K'Z\omega^2 K'}{Z^2+\omega^2} - \frac{\omega^4}{(Z^2+\omega^2)} = 0 \tag{209}$$

Let Z equal 0.3. K' equals

$$K' = 12.3 \tag{210}$$

The rate and position gains K_{rz} and K_{pz} equal

$$K_{rz} = \frac{K'J_{2z}r_a}{K_T} = 2.05\text{x}10^4 \text{ volts/(rad/sec)}$$

$$K_{pz} = ZK_{rz} = 6.15\text{x}10^3 \text{ volts/rad}$$

The gains K_{rz} and K_{pz} completely define the roll ring transfer function $H_z(s)$.

$$H_z(s) = \frac{\frac{K_T K_{rz}}{r_a}(s+\frac{B}{J_{2z}})(s+\frac{K_{pz}}{K_{rz}})}{s^2[s+\frac{K_T}{r_a J_{2z}}(\frac{r_a B}{K_T}+K_m)]} \tag{205}$$

For the general case where R_{2x}, R_{2y}, and R_{2z} are not zero, the transfer function $H_z(s)$ equals

$$H_z(s) = \frac{\frac{K_T K_{rz}}{r_a}(s+\frac{B}{J_{2z}+M(R_{2x}^2+R_{2y}^2)})(s+\frac{K_{pz}}{K_{rz}})}{s^2[s+\frac{K_T}{r_a[J_{2z}+M(R_{2x}^2+R_{2y}^2)]}(\frac{r_a B}{K_T}+K_m)]} \tag{211}$$

Using equation 167, $G_z(s)$ equals

$$G_z(s) = \frac{s^2[s+\frac{K_T}{r_a J_{2z}'}(\frac{r_a B}{K_T}+K_m)]}{J_{2z}'s^2[s+\frac{K_T}{r_z J_{2z}'}(\frac{r_a B}{K_T}+K_m)] + \frac{K_T K_{rz}}{r_a}(s+\frac{B}{J_{2z}'})(s+\frac{K_{pz}}{K_{rz}})} \tag{212}$$

where

$$J_{2z}' = J_{2z} + M(R_{2x}^2 + R_{2y}^2)$$

B3.4.3. <u>Telescope Fine Stabilization System Performance Analysis</u> - The linear dynamics of the telescope fine stabilization system were derived in section B3.4.1. Figure B3-15 is the resultant block diagram of this linear model. This model is used to determine the gross stabilization capabilities of this system and to determine the effects of the telescope center of mass being offset from the intersection of the three stabilization control axes. The results of this analysis should not be considered to demonstrate the feasibility of this system. To demonstrate the feasibility of this system, a more detailed model would be required. This new model should include (1) the nonlinear cross-coupling terms deleted from the model shown in figure B3-15, (2) a CMG orbiter stabilization system with a detailed nonlinear CMG model, (3) all analog to digital (A/D) and all digital to analog (D/A) interfaces, (4) the bending modes associated with the telescope complement and the shuttle orbiter, (5) more detailed fine stabilization actuator models including such nonlinearities as flex-pivot hysteresis characteristics, and (6) a detailed disturbance model including shuttle orbiter induced disturbances plus those generated by the telescopes themself.

Using the model derived in this report, the Laplace transforms of ε_x, ε_y, and ε_z, the rotational displacement of the telescope X, Y, and Z axes, as a function of the three disturbance torques T_{Dx}, T_{Dy}, and T_{Dz} are given in equations 162 thru 164.

$$\begin{aligned} \varepsilon_x(s) = {} & \frac{G_x(s)\left[1 - M^2 R_{2y}^2 R_{2z}^2 G_y(s) G_z(s)\right] T_{Dx}(s)}{\Delta' s^2} \\ & + \frac{M R_{2x} R_{2y} G_x(s) G_y(s)\left[1 + M R_{2z}^2 G_z(s)\right] T_{Dy}(s)}{\Delta' s^2} \\ & + \frac{M R_{2x} R_{2z} G_x(s) G_z(s)\left[1 + M R_{2y}^2 G_y(s)\right] T_{Dz}(s)}{\Delta' s^2} \end{aligned} \qquad (162)$$

$$\varepsilon_y(s)= \frac{MR_{2x}R_{2y}G_x(s)G_y(s)[1+MR_{2z}{}^2G_z(s)]T_{Dx}(s)}{\Delta' s^2}$$

$$+\frac{G_y(s)[1-M^2R_{2x}{}^2R_{2z}{}^2G_x(s)G_z(s)]T_{Dy}(s)}{\Delta' s^2}$$

$$+\frac{MR_{2y}R_{2z}G_y(s)G_z(s)[1+MR_{2x}{}^2G_x(s)]T_{Dz}(s)}{\Delta' s^2} \qquad (163)$$

$$\varepsilon_z(s)= \frac{MR_{2x}R_{2z}G_x(s)G_z(s)[1+MR_{2y}{}^2G_y(s)]T_{Dx}(s)}{\Delta' s^2}$$

$$+\frac{MR_{2y}R_{2z}G_y(s)G_z(s)[1+MR_{2x}{}^2G_x(s)]T_{Dy}(s)}{\Delta' s^2}$$

$$+\frac{G_z(s)[1-M^2R_{2x}{}^2R_{2y}{}^2G_x(s)G_y(s)]T_{Dz}(s)}{\Delta' s^2} \qquad (164)$$

where

$$\Delta'=1-M^2R_{2x}{}^2R_{2y}{}^2G_x(s)G_y(s)-M^2R_{2x}{}^2R_{2z}{}^2G_x(s)G_y(s)$$

$$-M^2R_{2y}{}^2R_{2z}{}^2G_y(s)G_z(s)-2M^3R_{2x}{}^2R_{2y}{}^2R_{2z}{}^2G_x(s)G_y(s)G_z(s)$$

The transfer functions $G_x(s)$, $G_y(s)$, and $G_z(s)$ are given in equations 195, 196, and 212.

$$G_x(s)= \frac{s[s^2+\frac{Kr_a}{K_mK_T}s+\frac{K}{J_{2x}{}'}]}{J_{2x}{}'s[s^2+\frac{Kr_a}{K_mK_T}s+\frac{K}{J_{2x}{}'}]+\frac{KK_{rx}}{K_m}(s+\frac{K_{px}}{K_{rx}})} \qquad (165)$$

$$G_y(s)= \frac{s[s^2+\frac{Kr_a}{K_mK_T}s+\frac{K}{J_{2y}{}'}]}{J_{2y}{}'s[s^2+\frac{Kr_a}{K_mK_T}s+\frac{K}{J_{2y}{}'}]+\frac{KK_{ry}}{K_m}(s+\frac{K_{py}}{K_{ry}})} \qquad (166)$$

$$G_z(s)=\frac{s^2\left[s+\frac{K_T}{r_aJ_{2z}'}\left(\frac{r_aB}{K_T}+K_m\right)\right]}{J_{2z}'s^2\left[s+\frac{K_T}{r_aJ_{2z}'}\left(\frac{r_aB}{K_T}+K_m\right)\right]+\frac{K_TK_{rz}}{r_a}\left(s+\frac{B}{J_{2z}'}\right)\left(s+\frac{K_{pz}}{K_{rz}}\right)} \tag{212}$$

where

$$J_{2x}'=J_{2x}+M(R_{2y}^2+R_{2z}^2)$$

$$J_{2y}'=J_{2y}+M(R_{2x}^2+R_{2z}^2)$$

$$J_{2z}'=J_{2z}+M(R_{2x}^2+R_{2y}^2)$$

The torque disturbance T_{Dx}, T_{Dy}, and T_{Dz} are

$$\begin{aligned}T_{Dx}=T_{2Dx}&-\frac{m_1}{m}(R_{2y}F_{2z}-R_{2z}F_{2y})+\frac{m_2}{m}(R_{2y}F_{1z}-R_{2z}F_{1y})\\&+M(R_{1y}R_{2y}+R_{1z}R_{2z})\frac{d\omega_{1x}}{dt}-MR_{1x}R_{2y}\frac{d\omega_{1y}}{dt}\\&-MR_{1x}R_{2z}\frac{d\omega_{1z}}{dt}\end{aligned} \tag{213}$$

$$\begin{aligned}T_{Dy}=T_{2Dy}&-\frac{m_1}{m}(R_{2z}F_{2x}-R_{2x}F_{2z})+\frac{m_2}{m}(R_{2z}F_{1x}-R_{2x}F_{1z})\\&-MR_{1y}R_{2x}\frac{d\omega_{1x}}{dt}+M(R_{1x}R_{2x}+R_{1z}R_{2z})\frac{d\omega_{1y}}{dt}\\&-MR_{1y}R_{2z}\frac{d\omega_{1z}}{dt}\end{aligned} \tag{214}$$

$$\begin{aligned}T_{Dz}=T_{2Dz}&-\frac{m_1}{m}(R_{2x}F_{2y}-R_{2y}F_{2x})+\frac{m_2}{m}(R_{2x}F_{1y}-R_{2y}F_{1x})\\&-MR_{1z}R_{2x}\frac{d\omega_{1x}}{dt}-MR_{1z}R_{2y}\frac{d\omega_{1y}}{dt}\\&+M(R_{1x}R_{2x}+R_{1y}R_{2y})\frac{d\omega_{1z}}{dt}\end{aligned} \tag{215}$$

Contained in table B3-7 are the telescope fine stabilization linear model parameters.

The Laplace transforms $\varepsilon_x(s)$, $\varepsilon_y(s)$, and $\varepsilon_z(s)$ can be approximated as follows:

$$\varepsilon_x(s)=\frac{G_x(s)}{s^2}T_{Dx}(s) \tag{216}$$

$$\varepsilon_y(s)=\frac{G_y(s)}{s^2}T_{Dy}(s) \tag{217}$$

$$\varepsilon_z(s)=\frac{G_z(s)}{s^2}T_{Dz}(s) \tag{218}$$

The effect of telescope center of mass offset from the hinge point described by R_{2x}, R_{2y}, and R_{2z} does not significantly affect the transfer functions $\frac{\varepsilon_x(s)}{\vec{T}_D(s)}$, $\frac{\varepsilon_y(s)}{\vec{T}_D(s)}$, and $\frac{\varepsilon_z(s)}{\vec{T}_D(s)}$ as long as the magnitude of $\vec{R}_2$ is small.

B3.4.4. Experiment Mass Motion Disturbance - Assume that the experiment mass motion disturbance T_D shown in figure B3-18 is applied to both the X and Y telescope fine stabilization control axes ($T_{2Dx}=T_{2Dy}=T_D$). T_D is a projected worst case experiment mass motion disturbance torque. The Fourier transform of T_D equals

$$
\begin{aligned}
T_D(\omega) &= \int_0^{0.2} T_D(t)e^{-j\omega t}dt \\
&= \frac{1.10\sin(0.025\omega)\cos(0.175\omega)}{\omega} \\
&- \frac{0.37\sin(0.075\omega)\cos(0.075\omega)}{\omega} \\
&+j\left[\frac{0.37\sin^2(0.075\omega)}{\omega}\right. \\
&\left.\frac{1.10\sin(0.025\omega)\sin(0.175\omega)}{\omega}\right]
\end{aligned} \tag{219}
$$

Table B3-7. Telescope Fine Stabilization Model Parameters

Mass and Telescope Inertia Properties

Shuttle Orbiter mass, $m_1=91\times10^3$ kg

Telescope Complement mass, $m_2=1.8\times10^3$ kg

Combined System mass, $m=92.8\times10^3$ kg

$J_{2x}=J_{2y}=1\ 900$ kg-m^2 (1 400 slug-ft^2)

$J_{2z}=800$ kg-m^2 (600 slug-ft^2)

DC Motor Parameters

$K_T=0.52$ ft-lb/amp$=0.719$ N-m/amp

$K_m=0.72$ volts/(rad/sec)

$r_a=1.5$ ohms

Flex-Pivot Spring Constant, $K=6$ N-m/rad

Roll Ring Damping Coefficient, $B=0.0345$ N-m/(rad/sec)

Actuator Rate and Position Gains

$K_{rx}=K_{ry}=1.16\times10^5$ volts/(rad/sec)

$K_{rz}=2.05\times10^4$ volts/(rad/sec)

$K_{pz}=K_{py}=3.49\times10^4$ volts/rad

$K_{pz}=6.15\times10^3$ volts/rad

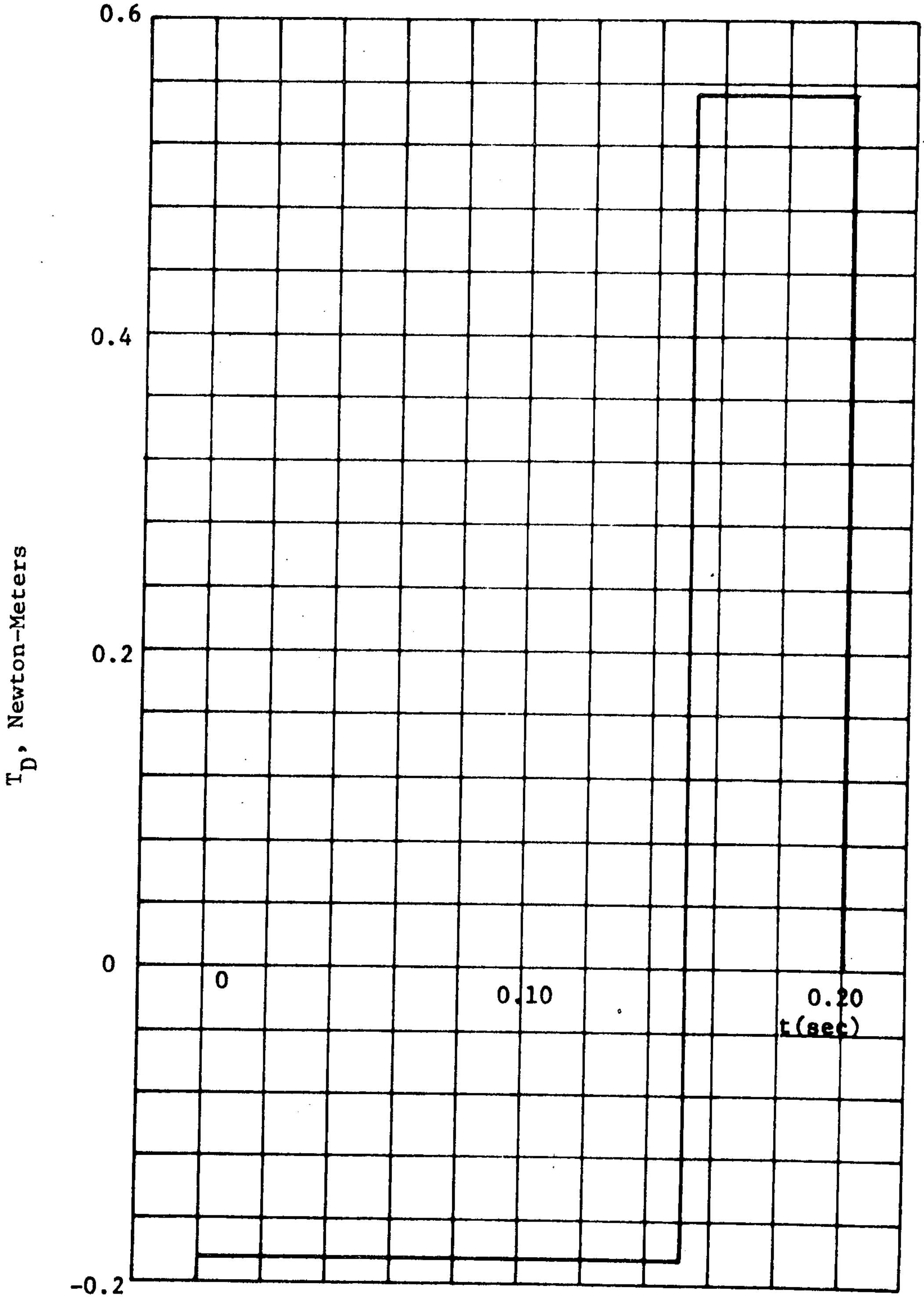

Figure B3-18. Experiment Mass Motion Disturbance Torque T_D

Plotted in figure B3-19 is $T_D(\omega)$. Assume that $T_D(t)$ is periodic with a period of T seconds. This periodic disturbance $T_D'(t)$ can be written as the following Fourier series

$$T_D'(t) = \sum_{n=-\infty}^{\infty} \alpha_n e^{jn\omega_o T}$$

$$= 2\sum_{n=0}^{\infty} |\alpha_n| \cos(n\omega_o t + \phi_n) \tag{220}$$

where

$$\omega_o = \frac{\pi}{T}$$

$$\alpha_n = \frac{T_D(n\omega_o)}{2T} = |\alpha_n| e^{-j\phi_n}$$

Assume the period of the disturbance $T_D'(t)$ is one second (T=1 sec). Table B3-8 contains the rms stability ε_x, ε_y, and ε_z due to this disturbance $T_D'(t)$ being applied to both the X and Y telescope control axes. The desired telescope rms stability about the X and Y telescope axes is 0.5 μrad (0.1 sec). Note that the computed rms stability about these axes due to $T_D'(t)$ is approximately 0.2 μrad (0.04 sec). Although this stability is within the desired stability of the system, it does not demonstrate the feasibility of this system, it only demonstrates that this system may be feasible.

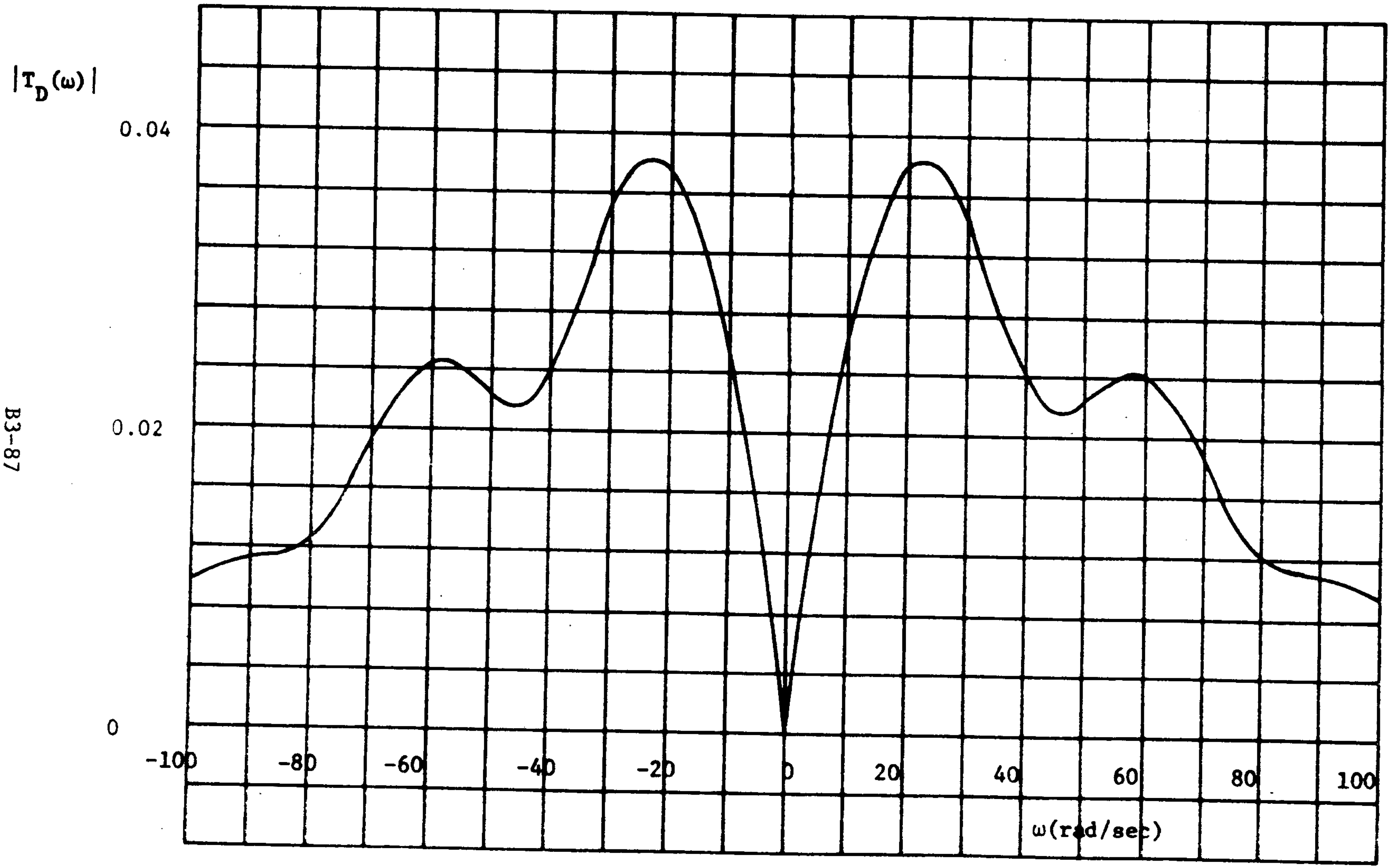

Figure B3-19. Fourier Transform of $T_D(t)$

Table B3-8. RMS Stability of ε_x, ε_y, and ε_z Due to the Telescope Mass Motion Disturbance $T_D'(t)$, $T_{Dx}=T_{Dy}=T_D'(t)$

Harmonic n	$n\omega_o$ rad/sec	$2\lvert\alpha_n\rvert$ rad	RMS Stability ($\times10^{-6}$ rad) ε_x	ε_y	ε_z
0	0	0	0	0	0
1	6.28	0.017	0.035	0.035	~0
2	12.57	0.027	0.043	0.043	~0
3	18.85	0.034	0.054	0.054	~0
4	25.1	0.034	0.038	0.038	~0
5	31.4	0.033	0.020	0.020	~0
6	37.6	0.026	0.009	0.009	~0
7	43.9	0.022	0.005	0.005	~0
8	50.2	0.023	0.004	0.004	~0
9	56.5	0.024	0.003	0.003	~0
10	62.8	0.023	0.002	0.002	~0
TOTAL			0.213	0.213	~0

B3.4.5. <u>Telescope Shuttle Orbiter Coupling Disturbance</u> - Note that all but one term in each of the telescope disturbance torque equations T_{Dx}, T_{Dy}, and T_{Dz}, equations 213 thru 215, are proportional to the components of the telescope center of mass offset vector, $\vec{R}_2$. For the model derived in this report, if $\vec{R}_2$ is a null vector, no disturbance originating from the shuttle orbiter due to $\vec{F}_1$ and $\frac{d\vec{\omega}_1}{dt}$ is transmitted through the hinge.

Assume that the only disturbance torques acting on the telescope complement originate from the shuttle orbiter. The resultant telescope disturbance torques T_{Dx}, T_{Dy}, and T_{Dz} due to the orbiter's translational force $\vec{F}_1$ and rotational acceleration $\frac{d\vec{\omega}_1}{dt}$ are:

$$T_{Dx}(\vec{F}_1, \frac{d\vec{\omega}_1}{dt}) = \frac{m_2}{m}(R_{2y}F_{1z}-R_{2z}F_{1y}) +M(R_{1y}R_{2y}+R_{1z}R_{2z})\frac{d\omega_{1x}}{dt} -MR_{1x}R_{2y}\frac{d\omega_{1y}}{dt} -MR_{1x}R_{2z}\frac{d\omega_{1z}}{dt} \qquad (221)$$

$$T_{Dy}(\vec{F}_1, \frac{d\vec{\omega}_1}{dt}) = \frac{m_2}{m}(R_{2z}F_{1x}-R_{2x}F_{1z}) -MR_{1y}R_{2x}\frac{d\omega_{1x}}{dt} +M(R_{1x}R_{2x}+R_{1z}R_{2z})\frac{d\omega_{1y}}{dt} -MR_{1y}R_{2z}\frac{d\omega_{1z}}{dt} \qquad (222)$$

$$T_{Dz}(\vec{F}_1, \frac{d\vec{\omega}_1}{dt}) = \frac{m_2}{m}(R_{2x}F_{1y}-R_{2y}F_{1x}) -MR_{1z}R_{2x}\frac{d\omega_{1x}}{dt} -MR_{1z}R_{2y}\frac{d\omega_{1y}}{dt} +M(R_{1x}R_{2x}+R_{1y}R_{2y})\frac{d\omega_{1z}}{dt} \qquad (223)$$

Assume that the modified ACPS system described in appendix A1, section A1.1, is used to stabilize the shuttle orbiter. The modified ACPS thruster characteristics are listed in table B3-9. When one of the ACPS pitch, yaw, or roll thrusters is fired, both an orbiter rotational acceleration $\frac{d\vec{\omega}_1}{dt}$ and a translational force $\vec{F}_1$ is produced. The resultant rotational acceleration $\frac{d\vec{\omega}_1}{dt}$ and translational force $\vec{F}_1$ are pulses with a pulse width equal to the thruster pulse duration, t_f, therefore, the disturbance torques T_{Dx}, T_{Dy}, and T_{Dz} are also similar pulses. The magnitude of $\frac{d\vec{\omega}_1}{dt}$ and $\vec{F}_1$ due to firing a pitch, yaw, and roll ACPS thruster are:

Pitch control thruster:

$$\frac{d\omega_{1x}}{dt} = \frac{d\omega_{1z}}{dt} = 0$$

$$\frac{d\omega_{1y}}{dt} = \frac{F\ell_y}{I_{yy}} = 2.41 \times 10^{-3} \text{ rad/sec (0.138 deg/sec)}$$

$$F_{1x} = F = 1.8 \times 10^3 \text{ newtons (400 lbf)}$$

$$F_{1y} = F_{1z} = 0$$

Yaw control thruster:

$$\frac{d\omega_{1x}}{dt} = \frac{d\omega_{1y}}{dt} = 0$$

$$\frac{d\omega_{1z}}{dt} = \frac{F\ell_z}{2I_{zz}} = 2.32 \times 10^{-3} \text{ rad/sec (0.133 deg/sec)}$$

$$F_{1x} = F = 1.8 \times 10^3 \text{ newtons (400 lbf)}$$

$$F_{1y} = F_{1z} = 0$$

Table B3-9. Modified ACPS Thruster Characteristics

Shuttle Orbiter Inertias:

$I_{xx}=1.41\times10^6$ kg-m^2(1.04×10^6 slug-ft^2)

$I_{yy}=8.22\times10^6$ kg-m^2(6.05×10^6 slug-ft^2)

$I_{zz}=8.55\times10^6$ kg-m^2(6.30×10^6 slug-ft^2)

$I_{xy}=I_{xz}=I_{yz}=0$

Engine Thrust Level: $F=1.8\times10^3$ newton (400 lbf)

Engine Thrust Pulse Duration: $t_f=0.1$ sec

Vehicle Control Moment Arms:

pitch (Y_v axis): $\ell_y=11$m(36 ft)

yaw (Z_v axis: $\ell_z=22$m(72 ft)

roll (X_v axis): $\ell_x=22$m(72 ft)

pitch coupling moment arm: $\ell_{CM}=11$m(36 ft)

Roll control thruster:

$$\frac{d\omega_{1x}}{dt} = \frac{F\ell_x}{2I_{xx}} = 1.41\text{x}10^{-2} \text{ rad/sec } (0.804 \text{ deg/sec})$$

$$\frac{d\omega_{1y}}{dt} = \frac{F\ell_{CM}}{I_{yy}} = 2.41\text{x}10^{-3} \text{ rad/sec } (0.138 \text{ deg/sec})$$

$$F_{1x} = F_{1y} = 0$$

$$= F = 1.8\text{x}10^{3} \text{ newtons } (400 \text{ lbf})$$

Assume that the center of mass of the telescope is offset from the telescope hinge point along the telescope centerline ($R_{2x}=R_{2y}=0$, $R_{2z}\neq 0$). The location of the telescope hinge point is described with respect to the shuttle orbiter center of mass by the vector $\vec{R}_1$. The components of $\vec{R}_1$ are approximately: $R_{1x}=-2.9$ meters, $R_{1y}=0$, and $R_{1z}=2.9$ meters. Figure B3-20 is a plot of the magnitudes of T_{Dx}, T_{Dy}, and T_{Dz} as a function of R_{2z} due to firing a pitch ACPS thruster. Figures B3-21 and B3-22 are similar plots due to firing a yaw and a roll ACPS thrusters, respectively.

Note from figures B3-20 thru B3-22 that a small center of mass offset, R_{2z}, can produce a rather large disturbance torque. This large disturbance torque due to firing the large ACPS thrusters will significantly disturb the telescope fine stabilization system, thus making it either impossible, or much more difficult, for this stabilization system to meet it' desired stability goals.

The conclusions of this analysis are (1) the center of mass of the telescope complement should be carefully mounted as close as possible to the center of rotation of the telescope fine stabilization system and (2) the shuttle orbiter stabilization system should be designed so that it will not generate any large shuttle orbiter rotational accelerations or translational forces during the ASM telescope experimentation periods. These above recommendations are designed to minimize the disturbance coupling between the shuttle orbiter and the ASM telescopes.

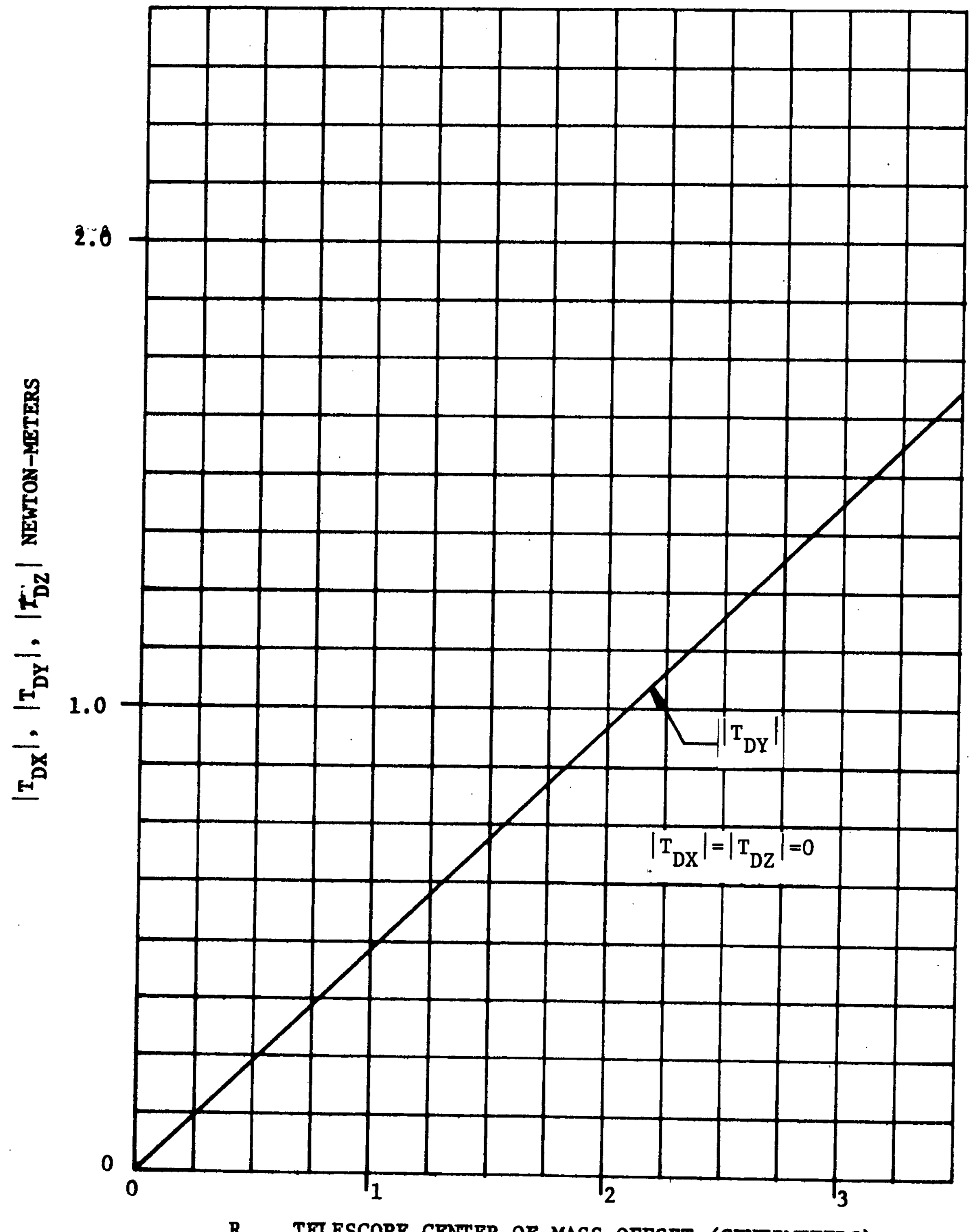

Figure B3-20. T_{DX}, T_{DY}, T_{DZ} As A Function Of Telescope Center Of Mass Offset Due To Firing One Pitch ACPS Thruster

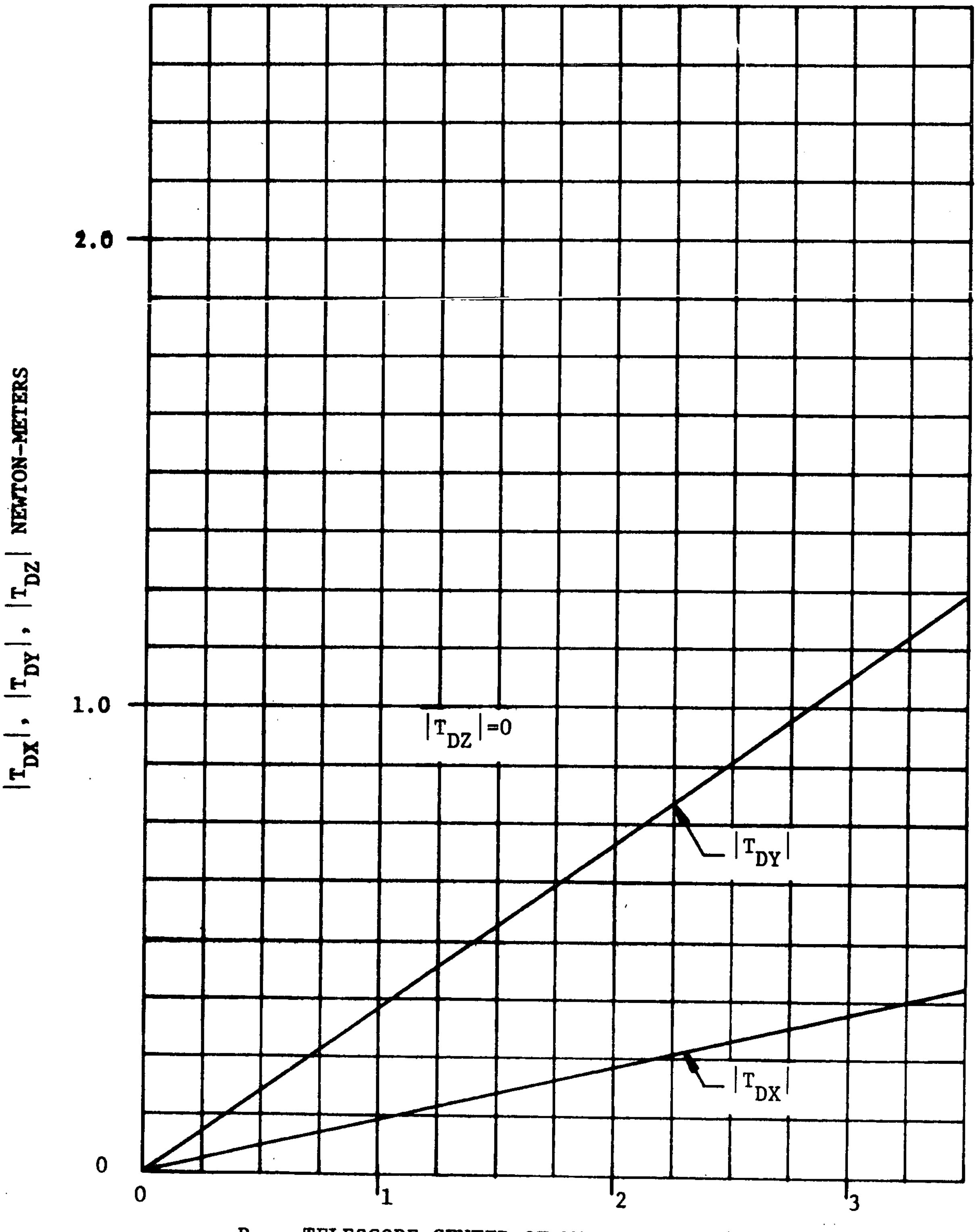

Figure B3-21. T_{DX}, T_{DY}, T_{DZ} As A Function Of Telescope Center Of Mass Offset Due To Firing One Yaw ACPS Thruster

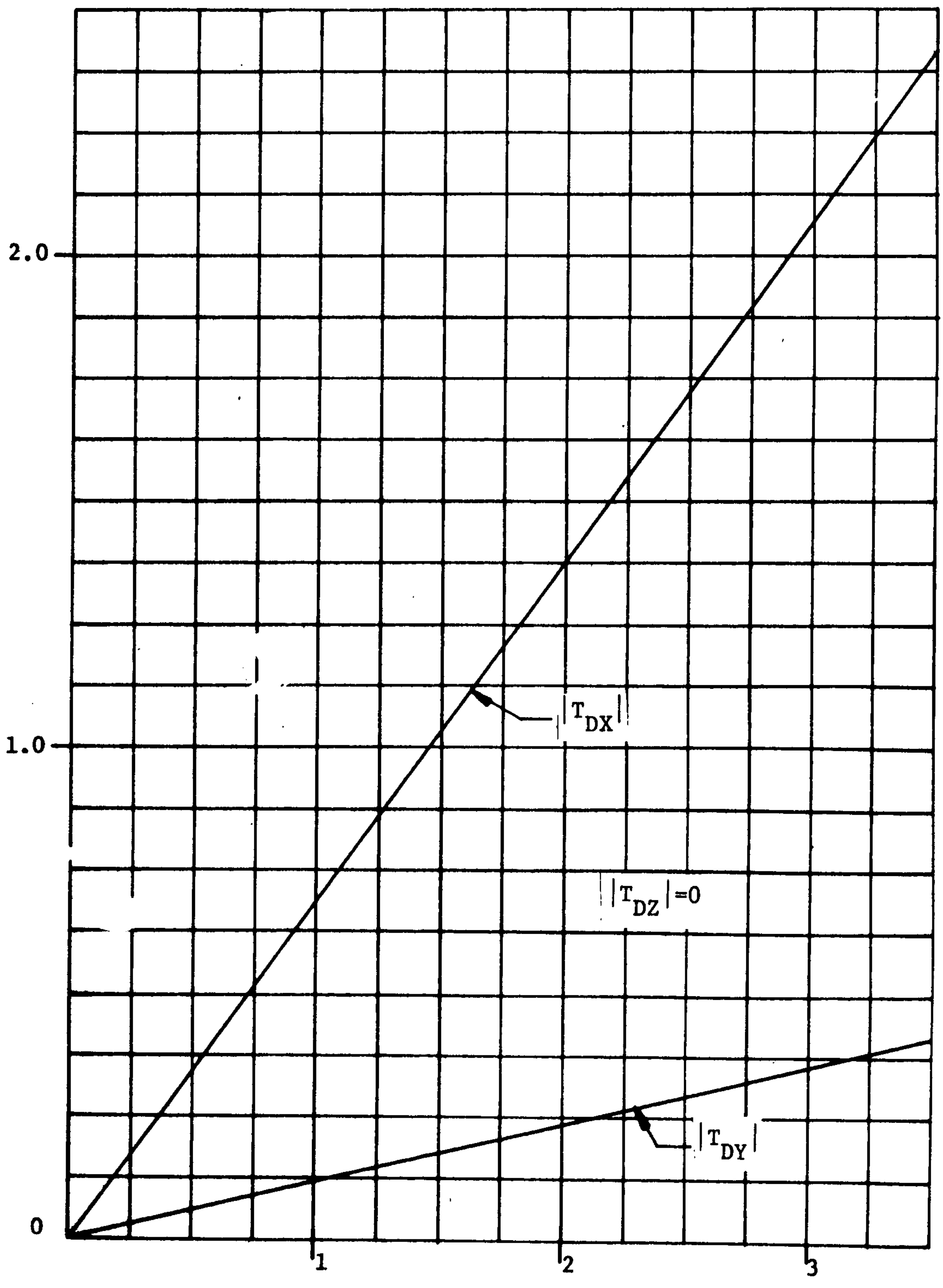

Figure B3-22. T_{DX}, T_{DY}, T_{DZ} As A Function Of Telescope Center Of Mass Offset Due To Firing One Roll AGCS Thruster

B3.5 REFERENCES

1. Goldstein, Herbert, Classical Mechanics, Addison-Wesley, 1959.

2. Whittaker, E. T., A Treatise on the Analytical Dynamics of Particles and Rigid Bodies, Cambridge University Press, 1961.

3. Papoulis, Athanasios, The Fourier Integral and Its Applications, McGraw-Hill, 1962.

APPENDIX C1

MASS PROPERTIES - SYSTEM

DETAILED MASS PROPERTIES

OF

SOLAR PAYLOAD

ASTRONOMY SORTIE MISSIONS AUG 25 1972
COMMON SORTIE LAB AND PALLET

DESCRIPTION	WEIGHT (POUNDS)	CENTER OF GRAVITY X (IN)	Y	Z	RADIUS OF GYRATION KX (IN)	KY	KZ
PALLET STRUCTURE	3050.00	443.9	0.	-37.3	47.5	153.2	159.9
CMG 1	420.00	355.0	0.	-62.0	12.2	12.2	12.2
CMG 2	420.00	405.0	0.	-62.0	12.2	12.2	12.2
CMG 3	420.00	460.0	0.	-62.0	12.2	12.2	12.2
SHUTTLE IMU	15.00	360.0	-0.	-45.0	3.5	2.5	2.5
SUPPORTS CMG 1	30.00	355.0	0.	-60.0	13.0	13.0	13.0
SUPPORTS CMG 2	30.00	405.0	0.	-60.0	13.0	13.0	13.0
SUPPORT CMG 3	30.00	460.0	0.	-60.0	13.0	13.0	13.0
SUPPORTS IMU	2.00	360.0	0.	-41.0	2.5	2.5	2.5
CONTROL + INPUT BOX	20.00	360.0	-30.0	-45.0	3.0	5.0	5.0
INVERTER 1 + HEATER + SUPT	57.00	315.0	10.0	-82.0	6.6	8.5	8.5
INVERTER 2 + HEATER + SUPT	57.00	405.0	35.0	-82.0	6.6	8.5	8.5
INVERTER 3 + HEATER + SUPT	57.00	495.0	10.0	-82.0	6.6	8.5	8.5
CABLING	15.00	405.0	0.	-90.0	1.0	40.0	40.0
STABILIZATION SYSTEM	1573.00	405.4	1.6	-63.9	15.8	49.2	49.3
FWD AZIMUTH TABLE	289.00	270.0	0.	-57.0	14.2	13.6	12.6
FWD AZIMUTH YOKE	396.00	270.0	0.	-14.4	38.5	35.9	27.6
FWD AZIMUTH POINTING ACT	35.00	270.0	0.	-71.0	4.0	4.0	3.0
FWD DEPLOYMENT YOKE	194.00	313.0	0.	26.0	66.3	40.3	77.4
FWD DEPLOYMENT ACTUATOR +Y	30.00	400.0	72.0	26.0	4.0	2.8	4.0
FWD DEPLOYMENT ACTUATOR -Y	30.00	400.0	-72.0	26.0	4.0	2.8	4.0
FWD DEPLOYMENT LOCK +Y	44.00	531.0	58.8	10.0	20.5	3.0	20.5
FWD DEPLOYMENT LOCK -Y	44.00	531.0	-58.8	10.0	20.5	3.0	20.5
FWD COMMON MOUNT	1062.00	315.1	0.	-16.2	55.3	109.2	110.0
AFT AZIMUTH TABLE	289.00	515.0	0.	-51.0	14.2	13.6	12.6
AFT AZIMUTH YOKE	396.00	515.0	0.	-14.4	38.5	35.9	27.6
AFT AZIMUTH POINTING ACT	35.00	270.0	0.	-71.0	4.0	4.0	3.0

ASTRONOMY SORTIE MISSIONS AUG 25 1972
COMMON SORTIE LAB AND PALLET

DESCRIPTION	WEIGHT (POUNDS)	CENTER OF GRAVITY X (IN)	Y	Z	RADIUS OF GYRATION KX (IN)	KY	KZ
AFT DEPLOYMENT YOKE	194.00	558.0	0.	25.0	66.3	40.3	77.4
AFT DEPLOYMENT ACTUATOR +Y	30.00	645.0	72.0	25.0	4.0	2.8	4.0
AFT DEPLOYMENT ACTUATOR -Y	30.00	645.0	-72.0	25.0	4.0	2.8	4.0
AFT DEPLOYMENT LOCK +Y	44.00	386.0	58.8	10.0	20.5	3.0	20.5
AFT DEPLOYMENT LOCK -Y	44.00	386.0	-58.8	10.0	20.5	3.0	20.5
AFT COMMON MOUNT	1062.00	511.4	0.	-14.5	54.2	79.9	81.7
ORDNANCE PACKAGE	20.00	360.0	-20.0	-50.0	3.0	5.0	5.0
COMMON MOUNT SYSTEM	2144.00	412.8	-.2	-15.7	54.6	136.6	137.4
CONTROL + JUNCT BOX FWD	20.00	310.0	40.0	-43.0	3.0	5.0	5.0
CONTROL + JUNCT BOX MID	20.00	495.0	30.0	-43.0	3.0	5.0	5.0
INTERFACE JUNCTION BOX	10.00	280.0	-70.0	-30.0	4.0	6.0	6.0
CABLING POWER	25.00	420.0	35.0	-39.0	15.0	150.0	150.0
CABLING DATA	20.00	420.0	35.0	-39.0	15.0	150.0	150.0
ELECTRICAL + DATA SYSTEM	95.00	397.9	23.9	-39.7	34.3	126.5	130.5
THERMAL INSULATION	130.00	400.0	0.	-55.0	45.0	65.0	55.0
COMMON SORTIE PALLET	7002.00	424.3	.6	-37.0	48.2	132.0	134.6
SORTIE LAB 186 IN LONG	12688.00	90.0	0.	0.	77.0	68.0	68.0

ASTRONOMY SORTIE MISSIONS AUG 25 1972
COMMON SORTIE LAB AND PALLET

GRAND TOTAL

WEIGHT 19690.00 LBS

MASS 50.99868 LB-SEC2/IN

CENTER OF GRAVITY
X = 208.87 IN
Y = .22 IN
Z = -13.17 IN

RADIUS OF GYRATION
KX = 70.44 IN
KY = 187.34 IN
KZ = 187.16 IN

MOMENT OF INERTIA
IX = 21088 SLUG-FT2
IY = 149152 SLUG-FT2
IZ = 148876 SLUG-FT2

PRODUCT OF INERTIA
PXY = 216 SLUG-FT2
PXZ = -11435 SLUG-FT2
PYZ = -55 SLUG-FT2

MOMENT OF INERTIA
IX = 253053 LB-SEC2-IN
IY = 1789813 LB-SEC2-IN
IZ = 1786513 LB-SEC2-IN

PRODUCT OF INERTIA
PXY = 2588 LB-SEC2-IN
PXZ = -137218 LB-SEC2-IN
PYZ = -654 LB-SEC2-IN

ASTRONOMY SORTIE MISSIONS AUG 25 1972
SOLAR PAYLOADS (PAYLOAD 1-2)

DESCRIPTION	WEIGHT (POUNDS)	CENTER OF GRAVITY X (IN)	Y (IN)	Z (IN)	RADIUS OF GYRATION KX (IN)	KY (IN)	KZ (IN)
FWD INNER ROLL RING	210.00	400.0	0.	25.0	44.0	31.1	31.1
FWD OUTER ROLL RING	306.00	400.0	0.	26.0	49.5	35.0	35.0
FWD GIMBAL RING	235.00	400.0	0.	25.0	54.3	38.4	38.4
FWD ELEV POINT/STAB ACT +Y	62.00	400.0	63.0	25.0	4.0	3.0	4.0
FWD ELEV POINT/STAB ACT -Y	62.00	400.0	-63.0	25.0	4.0	3.0	4.0
FWD AZM STAB ACTUATOR +Z	35.00	400.0	0.	85.0	4.0	4.0	3.0
FWD AZM STAB ACTUATOR -Z	35.00	400.0	0.	-33.0	4.0	4.0	3.0
FWD ROLL ACTUATOR	19.00	410.0	47.0	26.0	3.0	3.0	2.0
FWD GIMBAL LOCK +Y	38.00	390.0	47.0	26.0	10.0	10.0	10.0
FWD GIMBAL LOCK -Y	38.00	390.0	-47.0	25.0	10.0	10.0	10.0
FWD YOKE LOCK FITT(GIMBAL)	32.00	372.0	0.	25.0	59.3	21.7	52.0
FWD PIONT+CONTROL PLAT	67.00	417.0	0.	26.0	43.0	30.0	30.0
FORWARD GIMBAL	1139.00	399.7	.8	25.0	51.7	33.9	40.6
FWD STAR TRACKER 1	25.00	417.0	-10.0	78.0	4.8	4.8	4.8
FWD STAR TRACKER 2	25.00	417.0	-20.0	76.0	4.8	4.8	4.8
FWD STAR TRACKER 3	25.00	411.0	12.0	75.0	4.8	4.8	4.8
FWD STAR TRACKER 4	25.00	423.0	12.0	75.0	4.8	4.8	4.8
FWD STAR TRACKER IMU	15.00	425.0	8.0	-24.0	2.5	2.5	2.5
FWD STAR TRACKER ELECTRONIC	32.00	426.0	-6.0	-19.0	4.0	3.0	3.0
FWD CABLING	5.00	420.0	0.	26.0	43.0	30.0	30.0
FWD REFERENCE SYSTEM	152.00	419.8	-1.5	44.8	47.1	45.5	14.7
FWD GIMBAL INSTALLATION	1291.00	402.1	.5	29.2	51.5	36.5	39.0
XUV SUG + X-RAY + CORONO	4337.00	398.2	-2.7	27.4	31.0	59.3	59.7
AFT INNER ROLL RING	210.00	545.0	0.	25.0	44.0	31.1	31.1
AFT OUTER ROLL RING	306.00	645.0	0.	25.0	49.5	35.0	35.0
AFT GIMBAL RING	235.00	545.0	0.	25.0	54.3	38.4	38.4

ASTRONOMY SORTIE MISSIONS AUG 25 1972
SOLAR PAYLOADS (PAYLOAD 1-2)

DESCRIPTION	WEIGHT (POUNDS)	CENTER OF GRAVITY X	Y (IN)	Z	RADIUS OF GYRATION KX	KY (IN)	KZ
AFT ELEV POINT/STAB ACT +Y	62.00	545.0	63.0	26.0	4.0	3.0	4.0
AFT ELEV POINT/STAB ACT -Y	62.00	545.0	-63.0	26.0	4.0	3.0	4.0
AFT AZM STAB ACT +Y	35.00	545.0	0.	85.0	4.0	4.0	3.0
AFT AZM STAB ACT -Y	35.00	645.0	0.	-33.0	4.0	4.0	3.0
AFT ROLL ACT	19.00	655.0	47.0	26.0	3.0	3.0	2.0
AFT GIMBAL LOCK +Y	38.00	535.0	47.0	26.0	10.0	10.0	10.0
AFT GIMBAL LOCK -Y	38.00	535.0	-47.0	26.0	10.0	10.0	10.0
AFT YOKE LOCK FITT (GIMBAL)	32.00	517.0	0.	26.0	59.3	21.7	62.0
AFT POINT + CONTROL PLAT	67.00	562.0	0.	25.0	43.0	30.0	30.0
AFT GIMBAL	1139.00	644.7	.8	26.0	51.7	33.9	40.6
AFT STAR TRACKER 1	25.00	562.0	-10.0	78.0	4.8	4.8	4.8
AFT STAR TRACKER 2	25.00	562.0	-20.0	75.0	4.8	4.8	4.8
AFT STAR TRACKER 3	25.00	556.0	12.0	75.0	4.8	4.8	4.8
AFT STAR TRACKER 4	25.00	568.0	12.0	75.0	4.8	4.8	4.8
AFT TELESCOPE IMU	15.00	570.0	8.0	-24.0	2.5	2.5	2.5
AFT STAR TRACKER ELECTRONIC	32.00	571.0	-6.0	-19.0	4.0	3.0	3.0
AFT CABLING	5.00	565.0	0.	26.0	43.0	30.0	30.0
AFT REFERENCE SYSTEM	152.00	564.8	-1.5	44.8	47.1	45.5	14.7
AFT GIMBAL INSTALLATION	1291.00	547.1	.5	28.2	51.5	36.5	39.0
PHOTOHELIOGRAPH	2200.00	542.3	.3	26.4	21.7	61.4	59.8
SOLAR PAYLOAD UNIQUE ITEMS	9119.00	492.9	-1.1	27.4	36.4	130.9	131.0

ASTRONOMY SORTIE MISSIONS AUG 25 1972
SOLAR PAYLOADS (PAYLOAD 1-2)

GRAND TOTAL

WEIGHT	28809.00 LBS	MASS	74.61763 LB-SEC2/IN

CENTER OF GRAVITY		RADIUS OF GYRATION	
X =	298.77 IN	KX =	64.55 IN
Y =	-.13 IN	KY =	217.30 IN
Z =	-.33 IN	KZ =	216.40 IN

MOMENT OF INERTIA		PRODUCT OF INERTIA	
IX=	25911 SLUG-FT2	PXY=	-6 SLUG-FT2
IY=	293603 SLUG-FT2	PXZ=	4013 SLUG-FT2
IZ=	291181 SLUG-FT2	PYZ=	-128 SLUG-FT2

MOMENT OF INERTIA		PRODUCT OF INERTIA	
IX=	310929 LB-SEC2-IN	PXY=	-67 LB-SEC2-IN
IY=	3523233 LB-SEC2-IN	PXZ=	48154 LB-SEC2-IN
IZ=	3494175 LB-SEC2-IN	PYZ=	-1533 LB-SEC2-IN

MASS PROPERTIES SUMMARY

Stratoscope III Payloads:	3AB, 3AC, 3AD, 3AE
IR Telescope Payloads:	4AB, 4AC, 4AD, 4AE

ASTRONOMY SORTIE MISSIONS AUG 25 1972
ARRAY PAYLOAD COMMON ITEMS

DESCRIPTION	WEIGHT (POUNDS)	CENTER OF GRAVITY X (IN)	CENTER OF GRAVITY Y (IN)	CENTER OF GRAVITY Z (IN)	RADIUS OF GYRATION KX (IN)	RADIUS OF GYRATION KY (IN)	RADIUS OF GYRATION KZ (IN)
COMMON SORTIE LAB + PALLET	19690.00	208.9	.2	-13.2	70.4	187.3	187.2
FWD GIMBAL INSTALLATION	1291.00	402.1	.5	28.2	51.5	36.5	39.0
AFT ELEV PIONT ACTUATOR +Y	35.00	545.0	63.0	25.0	4.0	3.0	4.0
AFT ELEV PIONT ACTUATOR -Y	35.00	545.0	-63.0	25.0	4.0	3.0	4.0
AFT LAUNCH LOCKS (ARRAY) +Y	37.00	635.0	47.0	25.0	10.0	10.0	10.0
AFT LAUNCH LOCKS (ARRAY) -Y	37.00	635.0	-47.0	25.0	10.0	10.0	10.0
AFT YOKE LOCK FITT (ARRAY)	32.00	521.0	0.	25.0	59.3	18.1	50.8

ASTRONOMY SORTIE MISSIONS AUG 25 1972
ARRAY PAYLOAD COMMON ITEMS

GRAND TOTAL

WEIGHT 21157.00 LBS

MASS 54.79833 LB-SEC2/IN

CENTER OF GRAVITY
X = 224.25 IN
Y = .22 IN
Z = -10.35 IN

RADIUS OF GYRATION
KX = 70.07 IN
KY = 190.80 IN
KZ = 190.52 IN

MOMENT OF INERTIA
IX= 22422 SLUG-FT2
IY= 166238 SLUG-FT2
IZ= 165751 SLUG-FT2

PRODUCT OF INERTIA
PXY= 12 SLUG-FT2
PXZ= 2666 SLUG-FT2
PYZ= 3 SLUG-FT2

MOMENT OF INERTIA
IX= 269069 LB-SEC2-IN
IY= 1994851 LB-SEC2-IN
IZ= 1989010 LB-SEC2-IN

PRODUCT OF INERTIA
PXY= 141 LB-SEC2-IN
PXZ= 31986 LB-SEC2-IN
PYZ= 35 LB-SEC2-IN

ASTRONOMY SORTIE MISSION STRATOSCOPE III PAYLOADS
WITH ARRAY GROUP AB (PAYLOAD 3AB)

GRAND TOTAL

WEIGHT 27280.50 LBS

MASS 70.65869 LB-SEC2/IN

CENTER OF GRAVITY

X =	284.83	IN
Y =	.13	IN
Z =	-3.53	IN

RADIUS OF GYRATION

KX =	65.27	IN
KY =	212.78	IN
KZ =	212.16	IN

MOMENT OF INERTIA

IX=	25082	SLUG-FT2
IY=	265591	SLUG-FT2
IZ=	265042	SLUG-FT2

PRODUCT OF INERTIA

PXY=	-129	SLUG-FT2
PXZ=	9454	SLUG-FT2
PYZ=	-7	SLUG-FT2

MOMENT OF INERTIA

IX=	300983	LB-SEC2-IN
IY=	3199097	LB-SEC2-IN
IZ=	3180507	LB-SEC2-IN

PRODUCT OF INERTIA

PXY=	-1547	LB-SEC2-IN
PXZ=	113448	LB-SEC2-IN
PYZ=	-83	LB-SEC2-IN

ASTRONOMY SORTIE MISSION STRATOSCOPE III PAYLOADS
WITH ARRAY GROUP AC (PAYLOAD 3AC)

GRAND TOTAL

WEIGHT 30191.00 LBS

MASS 78.13712 LB-SEC2/IN

CENTER OF GRAVITY

X =	317.74	IN
Y =	.13	IN
Z =	.11	IN

RADIUS OF GYRATION

KX =	63.95	IN
KY =	226.52	IN
KZ =	225.50	IN

MOMENT OF INERTIA

IX=	26648	SLUG-FT2
IY=	334352	SLUG-FT2
IZ=	331359	SLUG-FT2

PRODUCT OF INERTIA

PXY=	-140	SLUG-FT2
PXZ=	16788	SLUG-FT2
PYZ=	-9	SLUG-FT2

MOMENT OF INERTIA

IX=	319771	LB-SEC2-IN
IY=	4012224	LB-SEC2-IN
IZ=	3976305	LB-SEC2-IN

PRODUCT OF INERTIA

PXY=	-1681	LB-SEC2-IN
PXZ=	201456	LB-SEC2-IN
PYZ=	-110	LB-SEC2-IN

ASTRONOMY SORTIE MISSION STRATOSCOPE III PAYLOADS
WITH ARRAY GROUP AD (PAYLOAD 3AD)

GRAND TOTAL

WEIGHT	27351.00 LBS	MASS	70.84129 LB-SEC2/IN
CENTER OF GRAVITY		RADIUS OF GYRATION	
X =	285.55 IN	KX =	65.19 IN
Y =	.11 IN	KY =	213.12 IN
Z =	-3.46 IN	KZ =	212.48 IN
MOMENT OF INERTIA		PRODUCT OF INERTIA	
IX=	25085 SLUG-FT2	PXY=	-171 SLUG-FT2
IY=	268124 SLUG-FT2	PXZ=	9596 SLUG-FT2
IZ=	266521 SLUG-FT2	PYZ=	-10 SLUG-FT2
MOMENT OF INERTIA		PRODUCT OF INERTIA	
IX=	301022 LB-SEC2-IN	PXY=	-2051 LB-SEC2-IN
IY=	3217482 LB-SEC2-IN	PXZ=	115152 LB-SEC2-IN
IZ=	3198255 LB-SEC2-IN	PYZ=	-126 LB-SEC2-IN

ASTRONOMY SORTIE MISSION STRATOSCOPE III PAYLOADS
WITH ARRAY GROUP AE (PAYLOAD 3AE)

GRAND TOTAL

WEIGHT	27793.00 LBS	MASS	71.98610 LB-SEC2/IN

CENTER OF GRAVITY		RADIUS OF GYRATION	
X =	290.86 IN	KX =	65.04 IN
Y =	-.20 IN	KY =	215.43 IN
Z =	-3.00 IN	KZ =	214.79 IN

MOMENT OF INERTIA		PRODUCT OF INERTIA	
IX=	25375 SLUG-FT2	PXY=	-810 SLUG-FT2
IY=	278399 SLUG-FT2	PXZ=	10477 SLUG-FT2
IZ=	276742 SLUG-FT2	PYZ=	-65 SLUG-FT2

MOMENT OF INERTIA		PRODUCT OF INERTIA	
IX=	304495 LB-SEC2-IN	PXY=	-9721 LB-SEC2-IN
IY=	3340791 LB-SEC2-IN	PXZ=	125720 LB-SEC2-IN
IZ=	3320905 LB-SEC2-IN	PYZ=	-775 LB-SEC2-IN

ASTRONOMY SORTIE MISSION IR PAYLOADS
WITH ARRAY GROUP AB (PAYLOAD 4AB)

DESCRIPTION	WEIGHT (POUNDS)	CENTER OF GRAVITY X (IN)	Y	Z	RADIUS OF GYRATION KX (IN)	KY	KZ
IR TELESCOPE ASSEM	4383.00	400.5	0.	25.0	34.0	43.4	43.4
BORE SIGHTED STAR TRACKER	25.00	391.0	-18.0	60.0	4.8	4.8	4.8
STAR TRACKER ELECTRONICS	10.00	420.0	-6.0	-13.0	1.0	1.0	1.0
OPTICAL TELE + IMAGE TUBE	106.00	382.0	18.0	60.0	2.4	10.8	10.8
IR TELESCOPE + AUX UNITS	4524.00	400.1	.3	25.9	34.2	43.3	43.0
ARRAY GROUP A	962.00	597.9	-.4	-12.1	52.7	36.5	44.6
ARRAYGROUP B	1210.50	639.9	-.5	25.0	40.5	30.2	30.2

ASTRONOMY SORTIE MISSION IR PAYLOADS
WITH ARRAY GROUP AB (PAYLOAD 4AB)

GRAND TOTAL

WEIGHT	27853.50 LBS	MASS	72.14280 LB-SEC2/IN

CENTER OF GRAVITY		RADIUS OF GYRATION	
X =	287.22 IN	KX =	65.66 IN
Y =	.18 IN	KY =	211.13 IN
Z =	-2.78 IN	KZ =	210.45 IN

MOMENT OF INERTIA		PRODUCT OF INERTIA	
IX=	25922 SLUG-FT2	PXY=	-104 SLUG-FT2
IY=	267998 SLUG-FT2	PXZ=	9950 SLUG-FT2
IZ=	266265 SLUG-FT2	PYZ=	12 SLUG-FT2

MOMENT OF INERTIA		PRODUCT OF INERTIA	
IX=	311069 LB-SEC2-IN	PXY=	-1242 LB-SEC2-IN
IY=	3215975 LB-SEC2-IN	PXZ=	119399 LB-SEC2-IN
IZ=	3195186 LB-SEC2-IN	PYZ=	149 LB-SEC2-IN

ASTRONOMY SORTIE MISSION IR PAYLOADS
WITH ARRAY GROUP AC (PAYLOAD 4AC)

GRAND TOTAL

WEIGHT 30764.00 LBS   MASS 79.68123 LB-SEC2/IN

CENTER OF GRAVITY		RADIUS OF GYRATION	
X =	319.29 IN	KX =	64.23 IN
Y =	.17 IN	KY =	224.59 IN
Z =	.72 IN	KZ =	223.53 IN

MOMENT OF INERTIA		PRODUCT OF INERTIA	
IX=	27392 SLUG-FT2	PXY=	-124 SLUG-FT2
IY=	334934 SLUG-FT2	PXZ=	17102 SLUG-FT2
IZ=	331788 SLUG-FT2	PYZ=	9 SLUG-FT2

MOMENT OF INERTIA		PRODUCT OF INERTIA	
IX=	328703 LB-SEC2-IN	PXY=	-1486 LB-SEC2-IN
IY=	4019207 LB-SEC2-IN	PXZ=	205228 LB-SEC2-IN
IZ=	3981451 LB-SEC2-IN	PYZ=	111 LB-SEC2-IN

ASTRONOMY SORTIE MISSION IR PAYLOADS
WITH ARRAY GROUP AD (PAYLOAD 4AD)

GRAND TOTAL

WEIGHT	27924.00 LBS	MASS	72.32541 LB-SEC2/IN

CENTER OF GRAVITY		RADIUS OF GYRATION	
X =	288.02 IN	KX =	65.50 IN
Y =	.15 IN	KY =	211.46 IN
Z =	-2.71 IN	KZ =	210.76 IN

MOMENT OF INERTIA		PRODUCT OF INERTIA	
IX=	25859 SLUG-FT2	PXY=	-145 SLUG-FT2
IY=	269507 SLUG-FT2	PXZ=	10087 SLUG-FT2
IZ=	267722 SLUG-FT2	PYZ=	9 SLUG-FT2

MOMENT OF INERTIA		PRODUCT OF INERTIA	
IX=	310310 LB-SEC2-IN	PXY=	-1745 LB-SEC2-IN
IY=	3234080 LB-SEC2-IN	PXZ=	121048 LB-SEC2-IN
IZ=	3212659 LB-SEC2-IN	PYZ=	108 LB-SEC2-IN

ASTRONOMY SORTIE MISSION IR PAYLOADS
WITH ARRAY GROUP AE (PAYLOAD 4AE)

GRAND TOTAL

WEIGHT	28366.00 LBS	MASS	73.47022 LB-SEC2/IN

CENTER OF GRAVITY		RADIUS OF GYRATION	
X =	293.09 IN	KX =	65.35 IN
Y =	-.15 IN	KY =	213.71 IN
Z =	-2.27 IN	KZ =	213.01 IN

MOMENT OF INERTIA		PRODUCT OF INERTIA	
IX=	26145 SLUG-FT2	PXY=	-782 SLUG-FT2
IY=	279636 SLUG-FT2	PXZ=	10939 SLUG-FT2
IZ=	277801 SLUG-FT2	PYZ=	-44 SLUG-FT2

MOMENT OF INERTIA		PRODUCT OF INERTIA	
IX=	313739 LB-SEC2-IN	PXY=	-9383 LB-SEC2-IN
IY=	3355637 LB-SEC2-IN	PXZ=	131268 LB-SEC2-IN
IZ=	3333609 LB-SEC2-IN	PYZ=	-527 LB-SEC2-IN

MASS PROPERTIES OF GIMBALLED MASSES

GIMBAL PLANE REFERENCE

Axis	Forward	Aft
x	400	645
y	0	0
z	26	26

PHOTOHELIOGRAPH ON AFT GIMBAL
MASS DRIVEN BY ROLL ACTUATOR

GRAND TOTAL

WEIGHT 2705.00 LBS

MASS 7.00617 LB-SEC2/IN

CENTER OF GRAVITY

X =	544.05	IN
Y =	.15	IN
Z =	27.38	IN

RADIUS OF GYRATION

KX =	28.05	IN
KY =	57.77	IN
KZ =	55.86	IN

MOMENT OF INERTIA

IX=	459	SLUG-FT2
IY=	1949	SLUG-FT2
IZ=	1822	SLUG-FT2

PRODUCT OF INERTIA

PXY=	-1	SLUG-FT2
PXZ=	7	SLUG-FT2
PYZ=	-1	SLUG-FT2

MOMENT OF INERTIA

IX=	5513	LB-SEC2-IN
IY=	23385	LB-SEC2-IN
IZ=	21859	LB-SEC2-IN

PRODUCT OF INERTIA

PXY=	-15	LB-SEC2-IN
PXZ=	80	LB-SEC2-IN
PYZ=	-15	LB-SEC2-IN

PHOTOHELOGRAPH ON AFT GIMBAL
MASS DRIVEN BY AZIMUTH STABILIZATION ACTUATORS

GRAND TOTAL

WEIGHT	3030.00 LBS	MASS	7.84794 LB-SEC2/IN

CENTER OF GRAVITY		RADIUS OF GYRATION	
X =	644.22 IN	KX =	31.05 IN
Y =	.44 IN	KY =	55.72 IN
Z =	27.23 IN	KZ =	54.07 IN

MOMENT OF INERTIA		PRODUCT OF INERTIA	
IX=	630 SLUG-FT2	PXY=	1 SLUG-FT2
IY=	2030 SLUG-FT2	PXZ=	7 SLUG-FT2
IZ=	1912 SLUG-FT2	PYZ=	-1 SLUG-FT2

MOMENT OF INERTIA		PRODUCT OF INERTIA	
IX=	7564 LB-SEC2-IN	PXY=	9 LB-SEC2-IN
IY=	24365 LB-SEC2-IN	PXZ=	78 LB-SEC2-IN
IZ=	22944 LB-SEC2-IN	PYZ=	-17 LB-SEC2-IN

PHOTOHELOGRAPH ON AFT GIMBAL
MASS DRIVEN BY ELEVATION POINTING + STABILIZATION ACTUATORS

GRAND TOTAL

WEIGHT	3335.00 LBS	MASS	8.63792 LB-SEC2/IN
CENTER OF GRAVITY		**RADIUS OF GYRATION**	
X =	644.29 IN	KX =	34.02 IN
Y =	.41 IN	KY =	54.76 IN
Z =	27.12 IN	KZ =	52.54 IN
MOMENT OF INERTIA		**PRODUCT OF INERTIA**	
IX=	833 SLUG-FT2	PXY=	1 SLUG-FT2
IY=	2158 SLUG-FT2	PXZ=	6 SLUG-FT2
IZ=	1987 SLUG-FT2	PYZ=	-1 SLUG-FT2
MOMENT OF INERTIA		**PRODUCT OF INERTIA**	
IX=	9994 LB-SEC2-IN	PXY=	9 LB-SEC2-IN
IY=	25893 LB-SEC2-IN	PXZ=	78 LB-SEC2-IN
IZ=	23844 LB-SEC2-IN	PYZ=	-17 LB-SEC2-IN

XUV SHG + X-RAY + CORONOGRAPH ON FWD GIMBAL
MASS DRIVEN BY ROLL ACTUATOR

GRAND TOTAL

WEIGHT	4842.00 LBS	MASS	12.54117 LB-SEC2/IN

CENTER OF GRAVITY		RADIUS OF GYRATION	
X =	399.09 IN	KX =	32.96 IN
Y =	-2.45 IN	KY =	57.45 IN
Z =	27.84 IN	KZ =	57.53 IN

MOMENT OF INERTIA		PRODUCT OF INERTIA	
IX=	1135 SLUG-FT2	PXY=	1 SLUG-FT2
IY=	3449 SLUG-FT2	PXZ=	6 SLUG-FT2
IZ=	3460 SLUG-FT2	PYZ=	0 SLUG-FT2

MOMENT OF INERTIA		PRODUCT OF INERTIA	
IX=	13622 LB-SEC2-IN	PXY=	15 LB-SEC2-IN
IY=	41388 LB-SEC2-IN	PXZ=	70 LB-SEC2-IN
IZ=	41514 LB-SEC2-IN	PYZ=	1 LB-SEC2-IN

XUV SHG + X-RAY + CORONOGRAPH ON FWD GIMBAL
MASS DRIVEN BY AZIMUTH STABILIZATION ACTUATORS

GRAND TOTAL

WEIGHT 5167.00 LBS

MASS 13.38295 LB-SEC2/IN

CENTER OF GRAVITY		RADIUS OF GYRATION	
X =	399.18 IN	KX =	34.24 IN
Y =	-2.14 IN	KY =	56.27 IN
Z =	27.73 IN	KZ =	56.43 IN

MOMENT OF INERTIA		PRODUCT OF INERTIA	
IX=	1308 SLUG-FT2	PXY=	4 SLUG-FT2
IY=	3531 SLUG-FT2	PXZ=	6 SLUG-FT2
IZ=	3551 SLUG-FT2	PYZ=	-1 SLUG-FT2

MOMENT OF INERTIA		PRODUCT OF INERTIA	
IX=	15691 LB-SEC2-IN	PXY=	43 LB-SEC2-IN
IY=	42368 LB-SEC2-IN	PXZ=	67 LB-SEC2-IN
IZ=	42615 LB-SEC2-IN	PYZ=	-7 LB-SEC2-IN

XUV SHG + X-RAY + CORONOGRAPH ON FWD GIMBAL
MASS DRIVEN BY ELEVATION POINTING + STABILIZATION ACTUATORS

GRAND TOTAL

WEIGHT	5472.00 LBS	MASS	14.17292 LB-SEC2/IN

CENTER OF GRAVITY		**RADIUS OF GYRATION**	
X =	399.23 IN	KX =	35.76 IN
Y =	-2.02 IN	KY =	55.66 IN
Z =	27.63 IN	KZ =	55.41 IN

MOMENT OF INERTIA		**PRODUCT OF INERTIA**	
IX=	1510 SLUG-FT2	PXY=	4 SLUG-FT2
IY=	3659 SLUG-FT2	PXZ=	6 SLUG-FT2
IZ=	3627 SLUG-FT2	PYZ=	-1 SLUG-FT2

MOMENT OF INERTIA		**PRODUCT OF INERTIA**	
IX=	18125 LB-SEC2-IN	PXY=	44 LB-SEC2-IN
IY=	43902 LB-SEC2-IN	PXZ=	66 LB-SEC2-IN
IZ=	43519 LB-SEC2-IN	PYZ=	-10 LB-SEC2-IN

STRATOSCOPE III ON FWD GIMBAL
MASS DRIVEN BY ROLL ACTUATOR

GRAND TOTAL

WEIGHT 4456.00 LBS

MASS 11.54140 LB-SEC2/IN

CENTER OF GRAVITY

X =	400.67	IN
Y =	-.05	IN
Z =	26.64	IN

RADIUS OF GYRATION

KX =	26.81	IN
KY =	49.68	IN
KZ =	49.31	IN

MOMENT OF INERTIA

IX=	691	SLUG-FT2
IY=	2374	SLUG-FT2
IZ=	2339	SLUG-FT2

PRODUCT OF INERTIA

PXY=	-1	SLUG-FT2
PXZ=	6	SLUG-FT2
PYZ=	-1	SLUG-FT2

MOMENT OF INERTIA

IX=	8298	LB-SEC2-IN
IY=	28488	LB-SEC2-IN
IZ=	28059	LB-SEC2-IN

PRODUCT OF INERTIA

PXY=	-11	LB-SEC2-IN
PXZ=	72	LB-SEC2-IN
PYZ=	-14	LB-SEC2-IN

STRATOSCOPE III ON FWD GIMBAL
MASS DRIVEN BY AZIMUTH STABILIZATION ACTUATORS

GRAND TOTAL

WEIGHT	4781.00 LBS	MASS	12.38317 LB-SEC2/IN

CENTER OF GRAVITY		RADIUS OF GYRATION	
X =	400.67 IN	KX =	28.91 IN
Y =	.14 IN	KY =	48.78 IN
Z =	26.60 IN	KZ =	48.51 IN

MOMENT OF INERTIA		PRODUCT OF INERTIA	
IX=	862 SLUG-FT2	PXY=	1 SLUG-FT2
IY=	2455 SLUG-FT2	PXZ=	6 SLUG-FT2
IZ=	2429 SLUG-FT2	PYZ=	-1 SLUG-FT2

MOMENT OF INERTIA		PRODUCT OF INERTIA	
IX=	10349 LB-SEC2-IN	PXY=	10 LB-SEC2-IN
IY=	29465 LB-SEC2-IN	PXZ=	72 LB-SEC2-IN
IZ=	29143 LB-SEC2-IN	PYZ=	-15 LB-SEC2-IN

STRATOSCOPE III ON FWD GIMBAL
MASS DRIVEN BY ELEVATION POINTING + STABILIZATION ACTUATORS

GRAND TOTAL

WEIGHT	5086.00 LBS	MASS	13.17315 LB-SEC2/IN

CENTER OF GRAVITY		RADIUS OF GYRATION	
X =	400.63 IN	KX =	31.15 IN
Y =	.13 IN	KY =	48.51 IN
Z =	26.56 IN	KZ =	47.76 IN

MOMENT OF INERTIA		PRODUCT OF INERTIA	
IX=	1065 SLUG-FT2	PXY=	1 SLUG-FT2
IY=	2583 SLUG-FT2	PXZ=	6 SLUG-FT2
IZ=	2504 SLUG-FT2	PYZ=	-1 SLUG-FT2

MOMENT OF INERTIA		PRODUCT OF INERTIA	
IX=	12778 LB-SEC2-IN	PXY=	10 LB-SEC2-IN
IY=	30997 LB-SEC2-IN	PXZ=	72 LB-SEC2-IN
IZ=	30042 LB-SEC2-IN	PYZ=	-15 LB-SEC2-IN

IR TELESCOPE ON FORWARD GIMBAL
MASS DRIVEN BY ROLL ACTUATOR

GRAND TOTAL

WEIGHT	5029.00 LBS	MASS	13.02551 LB-SEC2/IN

CENTER OF GRAVITY		RADIUS OF GYRATION	
X =	400.72 IN	KX =	35.59 IN
Y =	.23 IN	KY =	42.76 IN
Z =	27.36 IN	KZ =	42.09 IN

MOMENT OF INERTIA		PRODUCT OF INERTIA	
IX=	1375 SLUG-FT2	PXY=	-8 SLUG-FT2
IY=	1985 SLUG-FT2	PXZ=	-12 SLUG-FT2
IZ=	1923 SLUG-FT2	PYZ=	10 SLUG-FT2

MOMENT OF INERTIA		PRODUCT OF INERTIA	
IX=	16499 LB-SEC2-IN	PXY=	-96 LB-SEC2-IN
IY=	23818 LB-SEC2-IN	PXZ=	-147 LB-SEC2-IN
IZ=	23074 LB-SEC2-IN	PYZ=	117 LB-SEC2-IN

IR TELESCOPE ON FORWARD GIMBAL
MASS DRIVEN BY AZIMUTH STABILIZATION ACTUATORS

GRAND TOTAL

WEIGHT 5354.00 LBS

MASS 13.86729 LB-SEC2/IN

CENTER OF GRAVITY

X =	400.72	IN
Y =	.39	IN
Z =	27.28	IN

RADIUS OF GYRATION

KX =	36.57	IN
KY =	42.29	IN
KZ =	41.74	IN

MOMENT OF INERTIA

IX=	1546	SLUG-FT2
IY=	2065	SLUG-FT2
IZ=	2013	SLUG-FT2

PRODUCT OF INERTIA

PXY=	-6	SLUG-FT2
PXZ=	-12	SLUG-FT2
PYZ=	10	SLUG-FT2

MOMENT OF INERTIA

IX=	18550	LB-SEC2-IN
IY=	24796	LB-SEC2-IN
IZ=	24157	LB-SEC2-IN

PRODUCT OF INERTIA

PXY=	-74	LB-SEC2-IN
PXZ=	-147	LB-SEC2-IN
PYZ=	115	LB-SEC2-IN

IR TELESCOPE ON FORWARD GIMBAL
MASS DRIVEN BY ELEVATION POINTING + STABILIZATION ACTUATORS

GRAND TOTAL

WEIGHT 5659.00 LBS

MASS 14.65727 LB-SEC2/IN

CENTER OF GRAVITY

X =	400.68	IN
Y =	.37	IN
Z =	27.21	IN

RADIUS OF GYRATION

KX =	37.83	IN
KY =	42.38	IN
KZ =	41.35	IN

MOMENT OF INERTIA

IX=	1748	SLUG-FT2
IY=	2194	SLUG-FT2
IZ=	2088	SLUG-FT2

PRODUCT OF INERTIA

PXY=	-6	SLUG-FT2
PXZ=	-12	SLUG-FT2
PYZ=	10	SLUG-FT2

MOMENT OF INERTIA

IX=	20980	LB-SEC2-IN
IY=	26329	LB-SEC2-IN
IZ=	25056	LB-SEC2-IN

PRODUCT OF INERTIA

PXY=	-74	LB-SEC2-IN
PXZ=	-146	LB-SEC2-IN
PYZ=	115	LB-SEC2-IN

APPENDIX C2

MASS PROPERTIES - TELESCOPE AND ARRAY GROUPS

PHOTOHELIOGRAPH
SOLAR GROUP
    XUV SPECTROHELIOGRAPH
    X-RAY TELESCOPE
    CORONAGRAPHS
    MONITORS
STRATOSCOPE III
IR TELESCOPE
ARRAY GROUP A
ARRAY GROUP B
ARRAY GROUP C
ARRAY GROUP D
ARRAY GROUP E

MASS PROPERTIES DATA
TELESCOPE GROUP 1 - PHOTOHELIOGRAPH

ITEM	WT. (LBS)	X (IN)	Y (IN)	Z (IN)	Iox (LB IN^2)	Ioy (LB IN^2)	Ioz (LB IN^2)
TELESCOPE							
PRIMARY MIRROR	475	50	0	0	105,000	52,500	52,500
MOUNT & BULKHEAD	80	60	0	0	23,100	11,550	11,550
TRUSS SHELL ETC	750	-25	0	0	43,200	2,220,000	2,220,000
SECONDARY MIRROR	30	-105	0	0	374	1,390	1,390
SEC. MIRROR SUPP.	20	-107	0	0	38,000	19,000	19,000
TRUNION RING	20	0	0	0	11,520	5,760	5,760
DOORS	50	-120	0	0	14,400	7,200	7,200
INSTRUMENT INST.							
HOUSING	295	-20	0	35	62,000	820,000	900,000
FOLDING MIRROR	25	-95	0	15	10,000	500	500
BEAM SPLITTER	40	38	0	35	85,000	1,700	85,000
FILTERS	20	30	0	0	250	320	320
IMAGE DISECTOR	25	20	3	38	310	420	310
VIDICON DETECTOR	25	20	-3	38	310	420	310
SPECTOGRAPH	115	-65	10	38	7,000	180,000	180,000
H-ALPHA CAMERA	25	54	-14	38	310	420	310
BROADBAND CAMERA	25	54	-7	38	310	420	310
UNIVERSAL CAMERA	25	54	3	38	310	420	310
ELECTRONICS	155	-16	0	33	4,200	33,600	35,200

		INERTIA POUNDS IN^2	SLUG FT^2	RADIUS OF GYRATION
WEIGHT 2,200				
X C.G. -5.7	Iox	1,039,784.4	224.4	Kx 21.7
Y C.G. .3	Ioy	8,307,761.1	1793.1	Ky 61.4
Z C.G. 11.9	Ioz	7,874,075.3	1699.5	Kz 59.8

MASS PROPERTIES DATA

TELESCOPE GROUP 2 - XUV SHG + X-RAY + CORONAGRAPHS

ITEM	WT. (LBS)	X (IN)	Y (IN)	Z (IN)	Iox (LB IN^2)	Ioy (LB IN^2)	Ioz (LB IN^2)
STRUCTURE							
CYLINDER	668	-30	0	0	1,090,000	2,540,000	2,540,000
FRONT RING	16	-125	0	0	26,000	13,000	13,000
AFT RING	11	65	0	0	17,800	8,900	8,900
CENTER FRAME	73	-37	0	0	164,000	86,500	86,500
AFT BULKHEAD	64	65	0	0	56,300	28,150	28,150
FRONT BULK & DOORS	103	-126	0	0	91,000	45,500	45,500
VERTICAL PARTITION	138	-30	3.5	0	71,600	487,000	413,000
DIAGONAL PARTITION	84	-30	-17.5	5	16,100	256,000	250,000
ATTACHING FITTINGS	18	-25	0	0	3,330	1,665	1,665
INNER & OUTER CORONAGRAPHS							
IC	530	-46	-29	2	17,000	750,000	750,000
OC	351	-63	-13.5	-21	35,100	276,000	276,000
FILM CAMERA	22	22	-29	2	366	300	300
FILM CAMERA	22	-8	-13.5	-21	366	300	300
XUV SHG							
INSTRUMENT	945	4	21	0	230,000	1,590,000	1,510,000
FILM CAMERA	22	-61	21	-10	366	300	300
COLLECTING OPTICS	33	55	21	11.5	500	300	300
ELECTRONICS	10	52	21	-20	100	100	100
X-RAY TELESCOPE							
TELESCOPE	450	-10	-12	20.5	230,000	1,590,000	1,510,000
GRATING	25	-60	-12	20.5	800	400	400
FILM CAMERA	40	45	-12	20.5	700	600	600
CRYSTAL SPECTROMETER	40	45	-12	20.5	700	600	600
PROPORTIONAL COUNTER	15	40	-12	20.5	220	220	220
PM DETECTOR	20	-80	-12	20.5	300	300	300
H-ALPHA SLIT	10	20	-12	20.5	150	150	150
ELECTRONICS	50	55	-6	-30.0	1,000	1,000	1,000
SUPPORT UNITS							
H-ALPHA TELESCOPE	124	-82	11	30	3,100	37,200	37,200
XRT MONITOR	100	-94	-6	35	1,800	19,000	19,000

WEIGHT ______

X C.G. ______

Y C.G. ______

Z C.G. ______

INERTIA

POUNDS IN^2

Iox ______

Ioy ______

Ioz ______

SLUG FT^2

______

______

______

RADIUS OF GYRATION

Kx ______

Ky ______

Kz ______

MASS PROPERTIES DATA

TELESCOPE GROUP 2 - XUV SHG + X-RAY + CORONAGRAPHS

ITEM	WT. (LBS)	X (IN)	Y (IN)	Z (IN)	Iox (LB IN^2)	Ioy (LB IN^2)	Ioz (LB IN^2)
FINE SUN SENSOR	23	-119	-22	-8	400	300	300
FINE S. S. CONTROL	31	57	-12	-25	500	400	400
CORRELATION TRACKER	120	-85	-34	-8	2,200	43,600	43,600
XUV MONITOR	100	-34	12	-30	1,700	26,000	26,000
XUV MONITOR	24	57	-12	-20	400	400	400
CORONAGRAPH MOUNT	20	-53	-22	-8	4,000	2,000	2,000
MISC CABLING	15	5	0	0	12,000	16,000	16,000

INERTIA

WEIGHT	4,337		POUNDS IN^2	SLUG FT^2		RADIUS OF GYRATION	
X C.G.	-26.8	Iox	4,171,562	900.4	Kx	31.0	
Y C.G.	- 2.7	Ioy	15,291,680	3,300.6	Ky	59.3	
Z C.G.	1.4	Ioz	15,480,526	3,341.3	Kz	59.7	

MASS PROPERTIES DATA

TELESCOPE GROUP 3 - STRATOSCOPE III

ITEM	WT. (LBS)	X (IN)	Y (IN)	Z (IN)	Iox (LB IN^2)	Ioy (LB IN^2)	Ioz (LB IN^2)
CYLINDER	785	-54	0	0	870,000	1,090,000	1,090,000
PRIMARY MIRROR	473	-7	0	0	167,000	85,000	85,000
PRIMARY MIRROR MOUNT	126	-3	0	0	102,000	51,000	51,000
CENTER BAFFLE	17	-28	0	0	515	1,480	1,480
SEC. MIRROR ASSEM	40	-103	0	0	1,620	1,700	1,700
SEC. MIRROR SUPP.	25	-100	0	0	7,800	2,800	2,800
EXTENDABLE SHIELD	164	-123	0	0	224,000	250,000	250,000
INSTRUMENT COMP	596	18	0	0	430,000	400,000	400,000
PRIMARY REF. RING	110	0	0	0	106,000	53,000	53,000
DOOR & MECHANISM	74	-104	0	0	35,600	17,800	17,800
INSTRUMENTS	1541	35	0	0	111,000	52,000	52,000

C.G FOR EXTENDED SUN SHIELD

RETRACTED MOMENT	-4.1	X	3951	=	-16,199
SHIELD SHIFT	-67	X	164	=	-10,988
DOOR SHIFT	-10	X	74	=	740
					-27,827
C.G. EXTENDED	-27,827		3,951	=	-7.0

INERTIA

			POUNDS IN^2	SLUG FT^2	RADIUS OF GYRATION	
WEIGHT	3,951					
X C.G.	-4.1	Iox	2,109,535	455.3	Kx	23.1
Y C.G.	0	Ioy	10,300,300	2223.2	Ky	51.0
Z C.G.	0	Ioz	10,300,300	2223.2	Kz	51.0

MASS PROPERTIES DATA

TELESCOPE GROUP 4 - IR TELESCOPE

ITEM	WT. (LBS)	X (IN)	Y (IN)	Z (IN)	Iox (LB IN^2)	Ioy (LB IN^2)	Ioz (LB IN^2)
AFT TANK & BULKHEAD	293	50	0	0	1,075,000	536,000	536,000
INSTRUMENT	229	34	0	0	11,450	11,900	11,900
MECHANISM	50	32	-12	0	3,200	30,400	30,400
MIDDLE BULKHEAD	100	22	0	0	364,000	182,000	182,000
PRIMARY MIRROR	665	13.7	0	0	1,470,000	735,000	735,000
CYLINDER	2169	-11.2	0	0	1,353,000	3,320,000	3,320,000
AFT RING FRAMES	19	47	0	0	11,900	5,950	5,950
SPLICE FRAME	43	22	0	0	27,900	13,950	13,950
FWD RING FRAME	22	-41.5	0	0	13,800	6,900	6,900
FRONT FRAME	25	-73	0	0	15,600	7,800	7,800
LONGERONS	14	-11.5	0	0	8,700	12,550	12,550
INSULATION SUPPORT	45	-53.5	0	0	49,000	33,000	33,000
AFT SUPPORT RING	150	0	0	0	240,000	120,000	120,000
FWD SUPPORT RING	80	-42	0	0	81,600	40,800	40,800
FWD. SUPPORT TUBES	120	-21	0	0	26,000	28,520	28,520
SHUTTER DOOR	30	-60	0	0	8,600	4,300	4,300
TOWER & MECH	10	-55	0	0	45	270	270
COVER DOOR	49	-82	0	0	19,300	9,650	9,650
METEROID CYLINDER	112	-10	0	0	191,000	270,000	270,000
METEROID BULKHEAD	18	58	0	0	15,900	7,950	7,950
METEROID FRAME TIE-IN	30	0	0	0	53,000	26,500	26,500
METEROID FRAME BULK	15	58	0	0	26,500	13,250	13,250

	INERTIA POUNDS IN^2	SLUG FT^2	RADIUS OF GYRATION
WEIGHT ______			
X C.G. ______	Iox ______	______	Kx ______
Y C.G. ______	Ioy ______	______	Ky ______
Z C.G. ______	Ioz ______	______	Kz ______

MASS PROPERTIES DATA
TELESCOPE GROUP 4 - IR TELESCOPE

ITEM	WT. (LBS)	X (IN)	Y (IN)	Z (IN)	Iox ($LB\ IN^2$)	Ioy ($LB\ IN^2$)	Ioz ($LB\ IN^2$)
SECONDARY MIRROR	38	-42	0	0	300	300	300
INSTRUMENT COOLING	135	34	0	0	6,750	7,000	7,000
HELIUM	22	34	0	0	1,000	1,000	1,000

		INERTIA			
		POUNDS IN^2	SLUG FT^2		RADIUS OF GYRATION
WEIGHT	4,383				
X C.G.	.5	Iox 5,087,711	10981	Kx	34.0
Y C.G.	0	Ioy 8,280,480	1787.2	Ky	43.4
Z C.G.	0	Ioz 8,276,877	1786.5	Kz	43.4

MASS PROPERTIES DATA
ARRAY GROUP A - WIDE COVERAGE X-RAY

ITEM	WT. (LBS)	X (IN)	Y (IN)	Z (IN)	Iox (LB IN^2)	Ioy (LB IN^2)	Ioz (LB IN^2)
ARRAY ASSEM. (1)	253	-20	41.5	31	168,000	168,000	168,000
ARRAY ASSEM. (2)	253	-20	-41.5	31	168,000	168,000	168,000
DEPLOYMENT MECH (1)	170	0	41.5	-22	71,000	71,000	3,060
DEPLOYMENT MECH (2)	170	0	-41.5	-22	71,000	71,000	3,060
CENTRAL DATA PROCESSOR	55	-10	0	-34	1,320	1,320	6,250
CONTROL & DATA PACKAGE	20	-10	-20	-36	180	180	500
PROTON FLUX DET. (1)	18	-23	20	8	200	100	100
PROTON FLUX DET. (2)	18	-23	-20	8	200	100	100
CABLING	5	-5	0	-40	2,500	100	2,500

	INERTIA POUNDS IN^2	INERTIA SLUG FT^2	RADIUS OF GYRATION
WEIGHT 962			
X C.G. -12.1	Iox 2,678,466	578.1	Kx 52.7
Y C.G. - .4	Ioy 1,282,821	276.8	Ky 36.5
Z C.G. 5.9	Ioz 1,917,039	413.7	Kz 44.6

MASS PROPERTIES DATA

ARRAY GROUP B - NARROW BAND SPECTROMETER/POLARIMETER

ITEM	WT. (LBS)	X (IN)	Y (IN)	Z (IN)	Iox (LB IN^2)	Ioy (LB IN^2)	Ioz (LB IN^2)
SUPPORT FRAME	420	0	0	0	990,000	536,000	465,000
DETECTOR 1	59.5	-12	33	33	4,280	4,120	4,120
DETECTOR 2	59.5	-12	0	33	4,280	4,120	4,120
DETECTOR 3	59.5	-12	-33	33	4,280	4,120	4,120
DETECTOR 4	59.5	-12	33	0	4,280	4,120	4,120
DETECTOR 5	59.5	-12	0	0	4,280	4,120	4,120
DETECTOR 6	59.5	-12	-33	0	4,280	4,120	4,120
DETECTOR 7	59.5	-12	33	-33	4,280	4,120	4,120
DETECTOR 8	59.5	-12	0	-33	4,280	4,120	4,120
DETECTOR 9	59.5	-12	-33	-33	4,280	4,120	4,120
CENTRAL DATA PROCESSOR	110	10	0	0	15,800	17,750	17,750
CONTROL & DATA PACKAGE	20	5	30	0	500	180	180
ASPECT SENSOR	25	-10	-52	0	125	8,000	8,000
THERMAL CONTROL	50	-16	0	0	41,000	25,000	25,000
CABLING	30	3	0	0	24,500	12,100	12,100
MISC ATTACHMENTS ETC	20	0	0	0	16,500	8,100	8,100

		INERTIA		
WEIGHT 1210.5	POUNDS IN^2	SLUG FT^2		RADIUS OF GYRATION
X C.G. - 5.1	Iox 1,989,685	429.4	Kx	40.5
Y C.G. - .5	Ioy 1,105,552	238.6	Ky	30.2
Z C.G. 0	Ioz 1,107,217	238.9	Kz	30.2

MASS PROPERTIES DATA

ARRAY GROUP C - GAMA RAY SPECTROMETER & LOW BACKGROUND GAMA RAY DETECTOR

ITEM	WT. (LBS)	X (IN)	Y (IN)	Z (IN)	Iox (LB IN^2)	Ioy (LB IN^2)	Ioz (LB IN^2)
SUPPORT FRAME	420	0	0	0	990,000	536,000	465,000
LOW BACKGROUND DETECTOR							
DETECTOR 1	500	-14	16	0	30,300	23,200	23,200
DETECTOR 2	500	-14	-16	0	30,300	23,200	23,200
DETECTOR 3	500	-14	16	-32	30,300	23,200	23,200
DETECTOR 4	500	-14	-16	-32	30,300	23,200	23,200
DETECTOR SUPP.	176	-6	0	-20	106,000	60,000	60,000
ELECTRONICS	22	6	0	-20	530	530	530
NARROW BAND SPECTROMETER							
SPECTROMETER	264	-34	0	44	2,080	3,240	3,240
CRYOGENIC REFRIGERATOR	22	- 7	0	44	395	460	460
PROTECTIVE CYLINDER	687	-27	0	44	90,000	75,000	75,000
PROTECTIVE LID & MECH	169	-42	0	44	17,750	9,800	9,800
SPECT/REFRIG ATTACH.	9	-21	0	44	300	250	250
DEPLOYMENT MECHANISM	150	26	0	44	670	27,800	27,800
SUPPORT BASE	35	- 9	0	44	440	228	228
ELECTRONICS	22	6	0	30	530	530	530
CONTROL & DATA PACKAGE	20	5	30	0	500	180	180
ASPECT SENSOR	25	-10	-52	0	125	8,000	8,000
THERMAL CONTROL	50	-16	0	0	41,000	25,000	25,000
CABLING	30	3	0	0	24,500	12,100	12,100
MISC ATTACHMENTS ETC.	20	0	0	0	16,500	8,100	8,100

		INERTIA POUNDS IN^2	SLUG FT^2	RADIUS OF GYRATION
WEIGHT 4121				
X C.G. -14.8	Iox	5,552,183	1198.3	Kx 36.7
Y C.G. - .1	Ioy	5,127,681	1106.7	Ky 35.2
Z C.G. 5.8	Ioz	2,111,981	455.8	Kz 22.6

MASS PROPERTIES DATA

ARRAY GROUP D - LARGE MODULATION COLLIMATOR

ITEM	**WT. (LBS)**	**X (IN)**	Y (IN)	Z (IN)	Iox (LB IN^2)	Ioy (LB IN^2)	Ioz (LB IN^2)
SUPPORT FRAME	420	0	0	0	990,000	536,000	465,000
5 ARRAYS	660	-13.5	0	0	765,000	519,000	293,000
CENTRAL PROCESSOR	55	9	0	0	6,250	1,320	1,320
GAS SUPPLY	11	7	-45	0	150	150	150
CONTROL & DATA PACKAGE	20	5	30	0	500	180	180
ASPECT SENSOR	25	-10	-52	0	125	8,000	8,000
THERMAL CONTROL	50	-16	0	0	41,000	25,000	25,000
CABLING	20	3	0	0	16,500	8,100	8,100
MISC. ATTACHMENT ETC.	20	0	0	0	16,500	8,100	8,100

		INERTIA		
		POUNDS IN^2	**SLUG FT^2**	**RADIUS OF GYRATION**
WEIGHT 1281				
X C.G. -7.2	**Iox**	1,942,785	419.3	**Kx** 38.9
Y C.G. - .9	**Ioy**	1,180,633	254.8	**Ky** 30.3
Z C.G. 0	**Ioz**	990,393	213.7	**Kz** 27.8

MASS PROPERTIES DATA

ARRAY GROUP E - LARGE AREA X-RAY DETECTOR + COLLIMATED PLANE CRYSTAL SPECTROMETER

ITEM	WT. (LBS)	X (IN)	Y (IN)	Z (IN)	Iox ($LB\ IN^2$)	Ioy ($LB\ IN^2$)	Ioz ($LB\ IN^2$)
SUPPORT FRAME	420	0	0	0	990,000	536,000	465,000
X-RAY DETECTORS							
4 DETECTORS	352	-12	24	0	329,000	274,000	78,500
1 DETECTOR	88	-12	-24	48	21,200	7,250	19,600
1 DETECTOR	88	-12	-24	-48	21,200	7,250	19,600
CENTRAL PROCESSOR	55	9	0	0	6,250	1,320	1,320
CRYSTAL SPECTROMETER							
3 SPECTROMETERS	560	-30	-24	0	355,000	373,000	242,000
ELECTRONICS	15	6	0	-30	250	160	160
CONTROL & DATA PACKAGE	20	5	30	0	500	180	180
ASPECT SENSOR	25	-10	-52	0	125	8,000	8,000
THERMAL CONTROL	50	-16	0	0	41,000	25,000	25,000
CABLING	30	3	0	0	24,500	12,100	12,100
MISC. ATTACHMENT ETC.	20	0	0	0	16,500	8,100	8,100

		INERTIA POUNDS IN^2	INERTIA SLUG FT^2		RADIUS OF GYRATION
WEIGHT	1723				
X C.G.	-13.5	Iox 2,879,632	621.5	Kx	40.8
Y C.G.	- 5.7	Ioy 1,954,250	421.8	Ky	33.6
Z C.G.	- .2	Ioz 1,817,784	392.3	Kz	32.4